

# **ASSESSMENT OF NUCLEAR REPROGRAMMING ACTIVITY IN MAMMALIAN ES CELLS**

A thesis submitted for the degree of Doctor of Philosophy  
in the University of Edinburgh



**Stephen Sullivan M.Sc.**

Department of Gene Expression & Development,  
Roslin Institute (Edinburgh), Midlothian EH25 9PS, UK

September 2003



## Contents

- [i] Contents **i**
- [ii] Index of tables and figures **ix**
- [iii] Declaration **xvii**
- [iv] Dedication **xii**
- [v] Acknowledgements **xii**
- [vi] Abstract **xviii**
- [vii] Abbreviations **xx**

### [1] Introduction **1**

- [1.1] Background **1**
- [1.2] Cell differentiation, mammalian embryonic development, and nuclear reprogramming **3**
- [1.3] The cell cycle **5**
- [1.4] The differentiated state of the mammalian somatic cell is plastic **10**
- [1.5] Self-renewing pluripotent cells: ES, EG and EC cells **12**
  - [1.5.1] Teratocarcinomas and murine embryonal carcinoma cells **12**
  - [1.5.2] Origins and characteristics of murine embryonic stem and germ cells **13**
  - [1.5.3] Propagation and differentiation of murine ES cells **14**
  - [1.5.4] Isolation, propagation and characterisation of human ES cells **15**
- [1.6] The maintenance of pluripotency and the *Oct-4* gene **16**
- [1.7] Nuclear reprogramming in development and pathology **22**
  - [1.7.1] Genomic imprinting in mammalian development **23**
  - [1.7.2] X-chromosome inactivation in mammalian development **26**
  - [1.7.3] Telomere maintenance in mammalian development **27**
- [1.8] Artificially induced nuclear reprogramming **29**
  - [1.8.1] Nuclear Transfer **30**
  - [1.8.2] Cytoplasmic injections and incubations **32**
  - [1.8.3] Cell fusion and hybridisation **33**



- [1.8.3.1] Changes in gene expression and phenotype  
in cell hybrids 37
- [1.8.3.2] Pluripotent stem cell hybrids 39
- [1.8.3.3] Inter-species cell hybrids 41
- [1.8.3.4] Spontaneous cell fusion and the overestimation  
of adult stem cell plasticity 41
- [1.9] Heat shock 42
  - [1.9.1] Heat shock proteins 44
- [1.10] Chromatin Structure 46
  - [1.10.1] Lower Order Chromatin Structure 46
    - [1.10.1.1] Nucleoplasmin 47
    - [1.10.1.2] Linker histones and histone switching  
during development 49
  - [1.10.2] Higher orders of chromatin structure 50
- [1.11] Nuclear Reprogramming and associated chromatin modification 51
  - [1.11.1] DNA methylation 52
  - [1.11.2] Genomic imprinting 55
  - [1.11.3] X chromosome inactivation 57
  - [1.11.4] Telomere maintenance and telomerase activity 58
  - [1.11.5] Histone modifications 58
  - [1.11.6] Chromatin remodelling complexes 60
- [1.12] Summary 60
- [1.13] Objectives 61
- [2] Materials and Methods 62
  - [2.1] Cell culture 62
    - [2.1.1] Routine culture conditions 62
      - [2.1.1.1] Murine ES and EC cells 62
      - [2.1.1.2] Human ES cells 62
    - [2.1.2] Transfection 66

- [2.1.2.1] Transfection of murine ES cells and human EC cells 66
- [2.1.2.1] Transfection of human ES cells 67
- [2.1.3] Cell lines 67
- [2.2] Cell fusion and hybridisation 68
  - [2.2.1] Electrofusion 68
  - [2.2.2] Polyethylene Glycol (PEG) mediated cell fusion 70
  - [2.2.3] Sendai virus mediated cell fusion 70
  - [2.2.4] Selecting for cell hybrids 73
  - [2.2.5] Measuring heterokaryon formation 77
  - [2.2.6] Calculation of hybridisation frequency 83
- [2.3] Cytogenetic analysis 85
  - [2.3.1] Giemsa staining 85
  - [2.3.2] Mitotic spreads 85
  - [2.3.3] G-banding and karyotyping 86
  - [2.3.4] Fluorescence *in situ* hybridisation 86
  - [2.3.5] Propidium iodide staining and associated FACS analysis 87
  - [2.3.5] PCNA staining 88
- [2.4] Phenotypic analysis 89
  - [2.4.1] Alkaline phosphatase 89
  - [2.4.2] *In vitro* differentiation of murine clones 90
  - [2.4.3] Immunostaining 90
  - [2.4.4] *In vivo* differentiation 91
  - [2.4.5] *LacZ* staining 94
- [2.5] Manipulation and analysis of DNA 94
  - [2.5.1] Extraction of mammalian genomic DNA 94
  - [2.5.2] Extraction of plasmid DNA from bacteria 95
  - [2.5.3] DNA purification 96
  - [2.5.4] DNA quantitation 97
  - [2.5.5] DNA analysis and manipulation 97
    - [2.5.5.1] Restriction analysis of DNA 97



**[3.4] Conclusions 127****[4] Characterisation of murine hybrid cells 128****[4.1] Introduction 128****[4.2] Objectives 128****[4.3] Results and Discussion 129**

**[4.3.1]** Clonal lines are all hybrids displaying a subtetraploid chromosome number **129**

**[4.3.2]** The somatically-derived transgenic *Oct-4* promoter is silent in thymocytes but is reactivated after fusion with HM-1 cells **132**

**[4.3.3]** Hybrid lines display strong tissue non-specific alkaline phosphatase activity **134**

**[4.3.4]** Hybrid lines display cell surface marker expression profiles similar to HM-1 cells **136**

**[4.3.5]** Hybrid lines generate tumours in SCID mice that contain cells representing all three embryonic germ layers **138**

**[4.3.6]** Hybrid lines can be differentiated *in vitro* into cells representing all three embryonic germ layers **141**

**[4.4] Conclusions 144****[5] The effect of heat shock on nuclear reprogramming 145****[5.1] Introduction 145****[5.2] Objective 145****[5.3] Results and discussion 146**

**[5.3.1]** Thymocytes are heat shocked when incubated at 42°C for 10 minutes **146**

**[5.3.2]** Heat shocking thymocytes increases the hybrid colony yield **147**

**[5.3.3]** Heat shocking thymocytes does not affect cell viability of electropulsed mixtures of cells but does increase heterokaryon formation **150**

**[5.3.4]** Heat shocking thymocytes prior to fusion does not affect hybridisation frequencies **154**

**[5.3.4]** Heat shocking cells after fusion does not increase hybridisation frequency **155**

**[5.4]** Conclusions **157**

**[6] The effect of ES cell confluence and passage number on the murine cell hybrid system 158**

**[6.1]** Introduction **158**

**[6.2]** Objectives **159**

**[6.3]** Results and discussion **160**

**[6.3.1]** HM-1 cell seeding densities, that yield cultures at different ranges of confluence, were identified empirically **160**

**[6.3.2]** HM-1 cell confluence affects hybrid colony yield **160**

**[6.3.3]** HM-1 cell confluence does not affect heterokaryon formation or cell viability **163**

**[6.3.4]** HM-1 cell confluence affects hybridisation **167**

**[6.3.5]** 90-100% confluent ES cells display the highest hybridisation frequencies **168**

**[6.3.6]** Confluence of HM-1 cells affect their cell cycle characteristics **168**

**[6.3.7]** HM-1 cell confluence affects the induction of heat shock protein Hsp72 **174**

**[6.3.8]** Confluence does not affect HM-1 cell size **176**

**[6.3.9]** HM-1 cell passage number affects hybrid colony yield **177**

**[6.4]** Conclusions **181**

- [7] The effect of serum starvation and quiescence on the murine cell hybrid system 183**
- [7.1] Introduction 183**
  - [7.2] Objectives 184**
  - [7.3] Results and discussion 184**
    - [7.3.1] Serum starvation of primary embryonic fibroblasts renders them quiescent 184**
    - [7.3.2] Serum starvation of primary embryonic fibroblasts increases hybrid colony yield 188**
    - [7.3.3] Serum starvation of fibroblasts does not affect cell viability of electropulsed cells but does decrease heterokaryon formation 191**
    - [7.3.4] Serum starvation of fibroblasts increases hybridisation frequency 195**
    - [7.3.5] Serum starvation of fibroblasts strongly induces expression of Hsp72 196**
    - [7.3.6] Hybrid colony yield remains elevated after serum reactivation of fibroblasts 197**
  - [7.4] Conclusion 199**
- [8] The effect of *Xenopus* nucleoplasmin expression on the murine cell hybrid system 200**
- [8.1] Introduction 200**
    - [8.1.1] *Xenopus* nucleoplasmin and reprogramming 200**
    - [8.1.2] Tet-On system for inducible transgene expression 201**
    - [8.1.3] Recombinase-mediated cassette exchange (RCME) 203**
  - [8.2] Objectives 207**
  - [8.3] Results and discussion 208**
    - [8.3.1] Expression strategies for investigating the effect of *Xenopus* nucleoplasmin on the murine hybrid system 208**

**[8.3.2]** Constitutive expression of *Xenopus* nucleoplasmin affects HM-1 cell viability **211**

**[8.3.3]** Transient nucleoplasmin expression affects the viability of TNG-8 cells and causes a decrease in hybrid colony yield **213**

**[8.4]** Conclusion **217**

**[9] Generation of hybrids from human ES/EC cells 218**

**[9.1]** Introduction **218**

**[9.2]** Objectives **219**

**[9.3]** Results and Discussion **219**

**[9.3.1]** Development of selection regimes to isolate human cell hybrids **219**

**[9.3.2]** Attempts to generate cell hybrids from human ES cells and EC cells failed **222**

**[9.3.3]** Under a range of conditions human ES cells are less fusable than their murine counterparts **225**

**[9.3.4]** Growing cells on matrigel does not decrease their ability to fuse **226**

**[9.3.5]** H9 cell fusion increases 5 fold after hyaluronidase treatment **231**

**[9.4]** Conclusions **234**

**[10] Conclusions 235**

**[11] Bibliography 244**

**[12] Appendices 276**

**[12.1]** Media and stock solutions **276**

**[12.1.1]** Tissue culture stock solutions **276**

**[12.1.2]** Routine culture media **276**

- [12.1.3] Karyotyping 277
- [12.1.4] Genomic DNA extraction 278
- [12.1.5] Extraction of plasmid DNA from bacteria 278
- [12.1.6] DNA purification 278
- [12.1.7] RNA purification 278
- [12.1.8] Western blotting 279
- [12.1.9] Immunostaining for FACS analysis 279
- [12.1.10] Propidium iodide staining 280
- [12.1.11] FISH analysis 280
- [12.1.12] *LacZ* staining 281
- [12.2] Optimising instrument electronics for FACS analysis 282
- [12.3] Cloning strategies used for plasmid construction 285
- [12.4] Antibodies 287

## [ii] Index of Figures and Tables

### [1] Introduction 1

- Fig 1.1** Reprogramming human somatic cells could revolutionise cell replacement therapy in humans 2
- Fig 1.2** A schematic view of one cell cycle, with associated stages and major checkpoints 5
- Fig 1.3** Typical histogram from FACS analysis of a somatic cell population stained with propidium iodide 6
- Fig 1.4** Cdk activity and the cell cycle 9
- Fig 1.5** Cyclin and MPF levels fluctuate during the cell cycle 9
- Fig 1.6** Early embryonic development in the mouse 18
- Fig 1.7** Regulatory elements involved in *Oct-4* expression 19
- Fig 1.8** Mutual exclusion model of mammalian gene imprinting 25
- Fig 1.9** Artificial methods of nuclear reprogramming 29
- Fig 1.10** Generating heterokaryons and cell hybrids by cell fusion 33



- Fig 1.11** Trypsin or hyaluronidase both allow enzymatic disaggregation of adherent cells **36**
- Fig 1.12** Lower order chromatin structure **47**
- Fig 1.13** Proposed pathway of nucleosome assembly in *Xenopus* eggs **48**

## [2] Materials and methods **62**

- Fig 2.1** Schematic showing electrofusion and selection for ES x somatic cell hybrids **73**
- Fig 2.2** Fluorescence of HM-1 cells stained with seven different concentrations of either CMFDA or CMTMR **78**
- Fig 2.3** Fluorescence of murine thymocytes stained with five different concentrations of either CMFDA or CMTMR **79**
- Fig 2.4** Fluorescence of H9 cells stained with five different concentrations of either CMFDA or CMTMR **80**
- Fig 2.5** Fluorescence of murine primary embryonic fibroblasts stained with five different concentrations of either CMFDA or CMTMR **80**

**Table 2.1** Summary of selection regimes used to isolate hybrid colonies **76**

**Table 2.2** Protocol used to automatically embed tumour sections in paraffin **92**

## [3] Generation of cell hybrids from murine ES cells **109**

- Fig 3.1** Puromycin kill curve for primary embryonic fibroblasts **109**
- Fig 3.2** G418 kill curve for primary embryonic fibroblasts **111**
- Fig 3.3** Electrofusion of HM-1 cells generated viable homokaryons **115**
- Fig 3.4** Electrofusion of HM-1 cells and CBA<sup>Octneo/Octneo</sup> thymocytes generates viable heterokaryons **118**
- Fig 3.5** Colonies are reproducibly generated under single and double selection for hybrids generated from heterokaryons **118**

- Fig 3.6** All colonies derived from selection plates displayed a murine ES cell morphology **120**
- Table 3.1** Colonies are generated by electropulsing HM-1 cells and thymocytes and selecting for hybrids generated from heterokaryons **116**
- Table 3.2** Hybrids can be generated from electrofusions of HM-1 cells and CBA<sup>Octneo/Octneo</sup> primary embryonic fibroblasts **121**
- Table 3.3** Colonies could be generated from thymocytes but not from splenocytes using either electropulsing or PEG exposure to induce fusion **122**
- Table 3.4** Voltage affects hybrid colony yield from electropulsed cells **123**
- Table 3.5** Hybrid colony yield is affected by gap distance **124**
- Table 3.6** Hybrid colony yield is affected by chamber volume **125**
- Table 3.7** Polarisation of the electrofusion chamber did not increase hybrid colony yield **126**

#### **[4] Characterisation of murine hybrid cells 128**

- Fig 4.1** Clones are hybrid cells **130**
- Fig 4.2** DNA rearrangement of the Tcr $\gamma$  gene in TESH-1 cells shows that these cells are derived from adult thymocytes **133**
- Fig 4.3** A somatically-derived transgenic Oct-4 promoter is reactivated in hybrid cells **133**
- Fig 4.4** Cell hybrid lines displayed alkaline phosphatase activity **135**
- Fig 4.5** TESH-1 cells express the undifferentiated cell marker SSEA-1 but not SSEA-4 or the thymocyte specific marker CD90 **137**
- Fig 4.6** Hybrid cells and HM-1 cells generate benign tumours when injected into SCID mice **139**

- Fig 4.7** *In vivo* differentiation in SCID mice shows that hybrid cells have similar potential to HM-1 cells **140**
- Fig 4.8** *In vitro* differentiation shows that hybrid cells have similar potential to HM-1 cells **143**

**[5] The effect of heat shock on phenotypic ES cell hybridisation 123**

- Fig 5.1** Increased expression of heat shock protein Hsp72 in murine thymocytes exposed to hyperthermia **147**
- Fig 5.2** Heat shocking thymocytes increases hybrid colony yield **149**
- Fig 5.3** Heat shocking thymocytes does not affect electropulsed cell viability **149**
- Fig 5.4** The effect of heat shock on heterokaryon formation was assessed using 2-dye FACS analysis **152**
- Fig 5.5** Heat shocking thymocytes increases heterokaryon formation **153**
- Fig 5.6** Heat shocking thymocytes did not affect hybridisation frequency **154**
- Fig 5.7** Heat shocking, at various time points after electrofusion, does not increase hybridisation frequency **156**
- Table 5.1** Heat shocking thymocytes prior to fusion with ES cells increases hybrid colony yield **148**

**[6] The effect of ES cell confluence and passage number on phenotypic ES cell hybridisation 158**

- Fig 6.1** ES cell confluence affects hybrid colony yield **161**
- Fig 6.2** Confluence of HM-1 cells affect hybrid colony yield **162**
- Fig 6.3** Two-dye FACS analysis to assess the effect of ES cell confluence on heterokaryon formation **164**
- Fig 6.4** HM-1 cell confluence does not affect heterokaryon formation **165**

- Fig 6.5** HM-1 cell confluence does not affect the viability of electropulsed cell mixtures **166**
- Fig 6.6** HM-1 cell confluence affects hybridisation frequency **167**
- Fig 6.7** Confluence affects the cell cycle characteristics of HM-1 cells **169**
- Fig 6.8** HM-1 cell confluence affects the mean percentage of HM-1 cells lying within each FACS gate **171**
- Fig 6.9** HM-1 cell confluence affects the induction of Hsp72 **175**
- Fig 6.10** HM-1 cell size does not change at different levels of confluence **177**
- Fig 6.11** HM-1<sup>puro</sup> passage number affects hybrid colony yield **178**
- Fig 6.12** Loss of reprogramming activity correlates with the loss of euploidy with HM-1<sup>puro</sup> cells **180**
- Table 6.1** HM-1 cell confluence affects the percentage of HM-1 cells lying within the G1, S, and G2/M gates **170**

**[7] The effect of serum starvation and quiescence on phenotypic ES cell hybridisation 183**

- Fig 7.1** Primary embryonic fibroblasts cease proliferation under low serum conditions but resume when normal serum conditions are re-introduced **185**
- Fig 7.2** The percentage of primary embryonic fibroblasts expressing proliferating cell nuclear antigen (PCNA) decrease under low serum conditions but returns to initial levels when normal serum conditions are restored **185**
- Fig 7.3** Serum starvation of primary embryonic fibroblasts affects their cell cycle characteristics **187**
- Fig 7.4** Morphological changes in control, serum starved and serum reactivated primary embryonic fibroblasts **188**

- Fig 7.5** Identification of an appropriate PEF plating density for subsequent fusion experiments **189**
- Fig 7.6** Serum starvation of PEFs increases hybrid colony yield **190**
- Fig 7.7** Serum starvation of primary embryonic fibroblasts does not affect viability of electropulsed cell mixtures **192**
- Fig 7.8** Two-dye FACS analysis to assess the effect of serum starving fibroblasts on heterokaryon formation **193**
- Fig 7.9** Serum starving fibroblasts decreases heterokaryon formation **194**
- Fig 7.10** Serum starvation increases ES cell hybridisation **195**
- Fig 7.11** Serum starvation induces expression of Hsp72 **196**
- Fig 7.12** Hybrid colony yield remains elevated after serum reactivation **198**

**[8] The effect of *Xenopus* nucleoplasmin expression in the mouse hybrid system**

- Fig 8.1** Using the Tet-On system to transiently express a *Xenopus* nucleoplasmin and a *LacZ* reporter in murine cells **203**
- Fig 8.2** Sequence and structure of incompatible loxP sites **205**
- Fig 8.3** Use of recombinase-mediated cassette exchange (RCME) to insert other genes besides nucleoplasmin into sites permissible for Tet inducible transgene expression **207**
- Fig 8.4** Description of plasmids pSV40NPM, pTNG and pTetNPM **209**
- Fig 8.5** Strategies for *Xenopus* nucleoplasmin expression in the mouse hybrid system **210**
- Fig 8.6** Constitutive expression of *Xenopus* nucleoplasmin expression in the mouse hybrid system **212**
- Fig 8.7** Exposure of transfected TNG-8 cells to doxycycline induced expression of  $\beta$ -galactosidase **213**
- Fig 8.8** TNG-8 cell viability to affected by nucleoplasmin expression induced by exposing the cells to 1.0 $\mu$ M doxycycline for

1 hour **215**

**Table 8.1** Transient nucleoplasmin expression in murine ES cells prior to fusion with thymocytes decreases hybrid colony yield **216**

**[9] Attempts to generate cell hybrids from human ES and EC cells 218**

- Fig 9.1** Aneuploid NTERA2 nuclei frequently have abnormally replicated segments of the X-chromosome **220**
- Fig 9.2** G418 kill curves for NTERA2 and NCCIT cells **221**
- Fig 9.3** Puromycin kill curve for NTERA cells **221**
- Fig 9.4** Duration of PEF exposure affects viability of H9, Socs2 and TG11.nR cells **224**
- Fig 9.5** Assessment of H9 homokaryon formation using 2-dye FACS analysis **225**
- Fig 9.6** Optimisation of electrofusion conditions for H9 homokaryon formation using 2-dye FACS analysis **225**
- Fig 9.7** Two-dye FACS analysis shows that H9 cells fuse at a lower frequency than HM-1 cells when Sendai virus is used as a fusagen **229**
- Fig 9.8** The effect of matrigel on HM-1 homokaryon formation is assessed using 2-dye FACS analysis **230**
- Fig 9.9** Hyaluronidase breaks down the hyaluronan-based extracellular matrix of H9 cells **233**
- Fig 9.10** Hyaluronidase treatment increases H9 homokaryon formation **234**


**[12] Appendices 275**

- Fig 12.1** Forward (FSC) Amp gain, Side Scatter (SSC) Voltage adjustment allows gating of live cells from dead cells **281**

- Fig 12.2** Forward Scatter (FSC) adjustment of the fluorescence detectors **282**
- Fig 12.3** Compensation prevents spectral overlap, allowing CMTMR stained cells to be distinguished from CMFDA stained cells **283**
- Fig 12.4** Construction of pSV40NPM **284**
- Fig 12.5** Construction of plasmid pTetNPM **285**

**[ii] Declaration**

I hereby declare that this submission is my own work and that, to the best of my knowledge and belief, it contains no material previously published or written by another person nor material which to a substantial extent has been accepted for the award of any other degree or diploma of the university or other institute of higher learning, except where due acknowledgment has been made in the text.

  
Stephen Sullivan M.Sc.

2003

**[iii] Dedication**

This thesis is dedicated to the memory of my father Dr. John D. Sullivan F.R.C.P.I., F.R.C., PSYCH., D.P.M. and to my mother Kathleen Sullivan B.A.. I could not have asked for more supportive parents.

**[iv] Acknowledgements**

I would like to thank the following people for their assistance and advice: Dr. Jim McWhir, Prof. Martin Hooper, Dr. Ed Gallagher, Dr. Alison Thomson, Judy Fletcher, Tricia Ferrier, Susan Craigmile, Dr. Virginie Sottile, Davina Wojtacha, Peter Lodge, Zoë Hewitt, Dr. Steve Pells, Dr. Margot Marques, Dr. Helen Priddle, Yasmin Babaie, Claire Neill, Marjorie Ritchie, Tim King, Dr. Sarah Howie, William Richie, Laura Dick, and Prof. Ian Wilmut.

I also would like thank the following for their support: Kieran O’Riordan, Diarmuid Lenihan, Peter Curley, Salva Diez, Juan Emilio Valles, Alex Lebad, Matias Maistrello, Maria Ibiricu, Vanessa Lopez, Jose Carlos de Luna, Amparo Ortiz, Pilar Corez, Daniella Samti, Adam Wentzell, Katherine O’Kellylynch, Christine Hickey, and John D. Sullivan Jnr.



**[v] Abstract**

The cloning of Dolly the sheep and other mammals via nuclear transfer showed that the adult somatic nucleus could have its developmental potential restored. This restoration is the result of heritable epigenetic modifications made by nuclear reprogramming mechanisms. Little is known about factors affecting such nuclear reprogramming and even less about the mechanisms responsible.

A murine cell hybrid system was established and optimised to study nuclear reprogramming of somatic cells via fusion with embryonic stem cells. The system generated hybrid clones which displayed an ES phenotype and in which the somatic *Oct-4* promoter had been reactivated. These cell lines expressed alkaline phosphatase activity and undifferentiated cell marker SSEA-4 but not markers associated with differentiated cells (SSEA-1 and CD90). These lines were pluripotent, demonstrating the ability to form the three embryonic lineages both *in vivo* and *in vitro*.

This system was used to investigate whether several treatments (all either known or expected to perturb global gene expression patterns) affected nuclear reprogramming. Moderate heat shocking of thymocytes prior to fusion with ES cells resulted in increased reprogrammed hybridisation frequencies but as fusion was also increased it was impossible to verify whether an increase in nuclear reprogramming was partly responsible. Serum starvation of primary embryonic fibroblasts significantly increased nuclear reprogramming, as did ES cell confluence. ES cells were found to lose their capacity to reprogram as they reached high passage numbers. Constitutive or transient expression of nucleoplasmin in HM-1 cells did not increase reprogramming but instead to cell death.

Attempts were made to generate hybrids from human ES cells, but no hybrids were successfully generated. This was at least partly due to human ES cells being more difficult to fuse with other cells even using a range of different fusagens. Finally it was found that treating human ES cells with hyaluronidase prior to electropulsing resulted in 5x more heterokarionformation indicating that the ECM of these cells had prevented fusion.

Much remains to be learnt about the mechanisms underpinning reprogramming.

**[vi] Abbreviations**

**ATCC** American tissue culture collection

**APase** alkaline phosphatase

**BCA** bicinchonic acid

**BSA** bovine serum albumin

**cDNA** complementary DNA

**conc** concentrated

**CMFDA** 5-chloromethylfluorescein diacetate

**CMTMR** (5-(and-6)-(((4-chloromethyl)benzoyl)amino) tetramethylrhodamine)

**CNS** central nervous system

**Cre** Cre recombinase

**d** distilled

**DAPI** 4',6'-diamidino-2-phenylindole hydrochloride

**DCC** dextran coated charcoal

**DE** distal enhancer

**DEPC** diethyl pyrocarbonate

**DMF** dimethylformamide

**Dil** Dilute

**DPX** synthetic resin made from distyrene, tricresyl phosphate and xylene

**ECM** extracellular matrix

**EGTA** ethyleneglycol-bis (aminoethyl ether)

**FACS** fluorescence activated cell sorting

**FCS** fetal calf serum

**g** gram

**g** acceleration due to gravity

**FESH** fibroblast x ES cell hybrid

**hEC** human embryonal carcinoma

**hES** human embryonic stem

**HM-1** a HPRT deficient murine ES cell line

**hr** hour

**HPRT** hypoxanthine guanine phosphoribosyl transferase  
**HRP** horseradish peroxidase  
**H&E** haematoxylin and eosin  
**ICM** inner cell mass  
**LB** Luria-Bertani bacterial medium  
**LIF** leukaemia inhibitory factor  
**LOS** large offspring syndrome  
**E** embryonic stage  
**G** gauge (needle size)  
**mag** magnification  
**min** minute  
**MCS** multiple cloning site  
**mEC** murine embryonal carcinoma  
**mES** murine embryonic stem  
**MOPS** 3-Morpholinopropanesulfonic acid  
**NEAA** non-essential amino acids  
**NPM** xenopus nucleoplasmin  
**OD** optical density  
**PBS** phosphate buffered saline  
**PCA** Paraffin Cleaning Agent  
**PE** Proximal Enhancer  
**PEG** PolyEthylene Glycol  
**PEF** Primary Embryonic Fibroblast  
**PHF** Primary Human Fibroblast  
**PGC** Primordial Germ Cell  
**PSC** Pluripotent Stem Cell  
**PVA** polyvinyl alcohol  
**RA** all trans-Retinoic Acid  
**R1** a murine ES cell line  
**RMCE** Recombinase-Mediated Cassette Exchange

**RT** Room Temperature or reverse transcriptase  
**RT-PCR** reverse transcriptase polymerase chain reaction  
**SCID** Severe Combined Immunodeficient  
**SSC** standard sodium citrate  
**SDS** sodium dodecyl sulphate  
**TCA** trichloroacetic acid  
**TEMED** N,N,N',N'-Tetramethyl-Ethylenediamine  
**TESH** Thymocyte x ES cell Hybrid  
**TNAP** Tissue non-specific alkaline phosphatase  
**Tris** 2-amino-2-(hydroxymethyl)-1,3-propanediol  
**Tween 20** polyoxyethylenesorbitan monolaurate  
**V** volts  
**v/v** volume per volume  
**w/w** weight per weight  
**°C** degrees Celsius

# [1] Introduction

## [1.1] Background

Traditional models of mammalian cell commitment are based on the assumption that as a cell becomes specialised, irreversible changes occur in the nucleus altering the cell's potential to give rise to other cell types [McGrath & Solter 1984]. However this paradigm does not extend to the experimental situation where the nucleus is transplanted into a foreign cytoplasm. Wilmot *et al.* (1997) produced a viable mammal by fusing an adult differentiated somatic nucleus to an enucleated oocyte. Such fusion caused changes that restored nuclear potency to the extent that the nucleus could direct the development of a viable mammal. Nuclear reprogramming is the process underlying this restoration of developmental potential. Induction of this process has been demonstrated many times in somatic cells from nine mammalian species [Wilmot *et al.* 1997] [Wakayama *et al.* 1998][Kato *et al.* 1998][Bagiuisi *et al.* 1999][Campbell *et al.* 2000][Chesne *et al.* 2002][Gomez *et al.* 2003][Polejaeva *et al.* 2003][Vogel *et al.* 2003].

Frustratingly, the mechanism by which a somatic nucleus may be reprogrammed remains unknown, although such a mechanism almost certainly involves both structural [Kikyo *et al.* 2000] and chemical changes [Monk *et al.* 1987] to chromatin.

Pluripotent stem cells (PSCs) possess the capacity to generate, not only identical daughter cells, but also daughter cells fated to become other cell types [Smith 1998]. It may be possible that human somatic cells can be reprogrammed to generate PSCs. If successful, this strategy would provide a potentially endless source of cells for biological research as well as medical applications (e.g. cell replacement therapy [Brüstle *et al.* 1999], toxicity assessment, drug testing and possible even gene therapy [Smith 1998]). **Fig 1.1** illustrates how identification of reprogramming molecules and mechanisms could facilitate cell replacement therapy in humans.

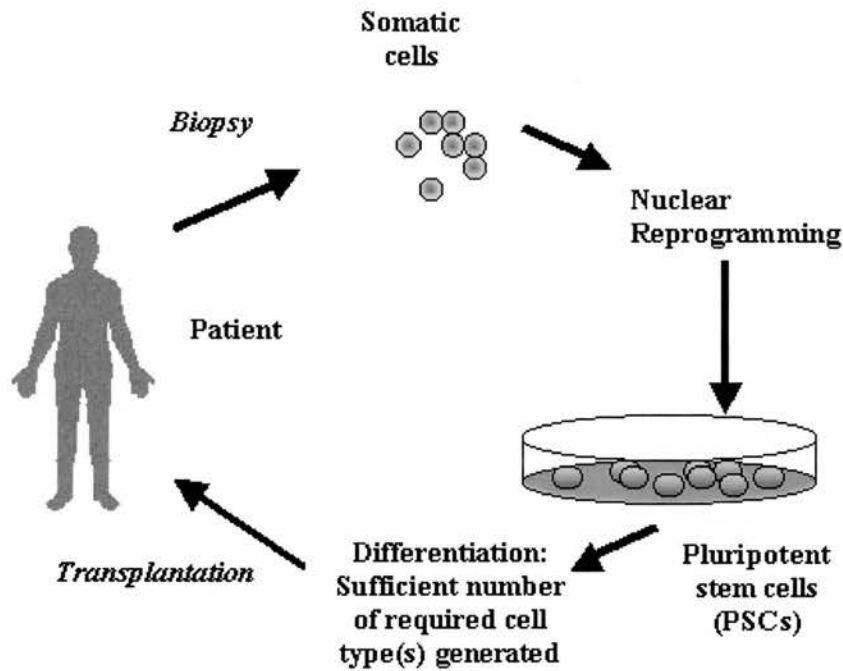


**Fig 1.1 Reprogramming human somatic cells could revolutionise cell replacement therapy in humans**

Once the mechanism by which epigenetic reprogramming is understood, human somatic cells extracted from the patient could be induced to dedifferentiate into pluripotent stem cells (PSCs). PSCs could then be expanded in culture and induced to redifferentiate into the cell type(s) required by the patient. Differentiated cells could then be transplanted into the patient without risk of immunorejection.

Mammalian embryonic development will be outlined in the next section to put definitions of nuclear reprogramming and pluripotent stem cells into context.

## **[1.2] Cell Differentiation, Mammalian Embryonic Development, and Nuclear Reprogramming**

Cell differentiation is the process by which a cell becomes specialised to perform specific biological functions [reviewed in Gurdon 1968]. The process is associated with a decline in the range of cell types that that cell is capable of generating [Gurdon 1968]. It had been initially thought that as cells differentiated that hereditary material no longer required were cast off or permanently inactivated [Weismann 1893]. 50 years ago however, Briggs and King transferred differentiated nuclei from blastula cells to enucleated eggs of *Rana pipiens*. These reconstructed cells went on to generate normal hatched embryos. Gurdon later showed that somatic nuclei could even direct development so that adult frogs were generated [Gurdon 1962]. These observations showed that Weismann's paradigm was incorrect and nuclei of differentiated cells contain the same genetic material as those of undifferentiated cells [Briggs & King 1952]. The current paradigm for how cell differentiation occurs involves the assembly of condensed chromosomal structures [reviewed in Kass & Wolffe 1998]. Such structures, formed via interactions between DNA and protein, are thought to compartmentalise chromatin into functional domains and, in some unknown way, stably maintain the differentiated state even when the cell divides. If this is true, reprogramming the cell to restore developmental potential will involve the disassembly of such chromosomal structures. Indeed this is a premise upon which work described in several chapters of this thesis are based. Heat shock, cell cycle stage and nuclear chaperone activity are all chromatin-structure altering phenomena and their effects on nuclear reprogramming are investigated in this work.

In mammalian development, differentiation first occurs after fertilisation in the preimplantation embryo. After the zygote has undergone several cell divisions, the embryo consists of a population of cells called blastomeres, which are totipotent, i.e. capable of generating any cell type. As the embryo develops, the outer layer of cells of the embryo (the trophoctoderm) becomes morphologically distinct from the inner cell



mass (ICM). Cells of the trophoctoderm and ICM have different developmental potentials e.g. cells of the ICM have the potential to form all the cells of the embryo, whereas the trophoctoderm cells have not, instead differentiating into extra-embryonic cell types that will form the placenta.

Differentiation of cells is found to be highly stable. The only stage during which normal mammalian cells seem to dedifferentiate naturally is after fertilisation. The sperm and oocyte, both highly differentiated cells with condensed chromatin structure, fuse to produce a zygote. Within the zygote, changes lead to the reversion to a totipotent cellular state. Although the mechanism responsible is unknown, two events correlate with this dedifferentiation: chromatin structure becomes less dense (protamines are removed from sperm-derived chromatin by nuclear chaperone nucleoplasmin and replaced by oocyte-derived histones [Perreault 1992] and methylated haploid parental genomes are demethylated [Barton *et al.* 2001]). Later sections of this chapter will discuss these two events in more detail: **Subsection [1.10.2]** discusses protamine removal from sperm chromatin by nuclear chaperone nucleoplasmin and **Subsection [1.11.1]** gives more detail on DNA methylation after fertilisation.

The processes responsible for the epigenetic changes that lead to dedifferentiation are referred to as nuclear reprogramming mechanisms. Throughout this thesis the term “nuclear reprogramming” will refer to “the process by which a specialised nucleus re-acquires developmental potential” [Singh 2000]. This definition includes complete reprogramming to a totipotent state (verifiable only by generation of viable offspring via nuclear transfer) and also partial reprogramming where only pluripotency is restored.

It has been suggested that the cell cycle stage (the status of a cell with regards to cell division) affects nuclear reprogramming of somatic cells [Wilmut *et al.* 1998]. This theory and evidence on which it is based are discussed in detail in **Subsection [1.8.1]**. Before this however, the basic features of eukaryotic cell cycle will be discussed.

### [1.3] The cell cycle

Cell division is the result of several events that occur within a cell since its previous division. These events are strictly regulated and collectively form a process known as the cell cycle [Murray & Hunt (1993) reviews the cell cycle and how it is regulated]. The cell cycle is divided into two main phases: M phase, where the cell undergoes mitosis, and interphase, where the cell is not visibly dividing. Interphase is itself broken down into three smaller phases (G1, S, and G2). During G1 phase of the cycle, the cell makes the decision whether or not to become committed to undergoing another full cell cycle. During S phase, DNA replication occurs in the nucleus of the cell. During G2 phase DNA synthesis ceases and mitosis occurs. The phases of the cell cycle are shown in **Figure 1.2**.

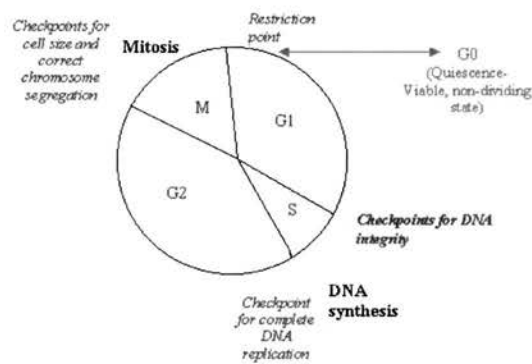


**Figure 1.2 A schematic view of one cell cycle with associated stages and major checkpoints.**

Several distinguishable phases occur within a cell prior to it completing cell division. These include S phase, where the cell is actively replicating DNA in its nucleus, M phase where the cell is actively undergoing cell division and the “gap” or G phases. G1 is the gap after mitosis before DNA replication starts and G2 is the gap after DNA synthesis is complete before mitosis and cell division. Quiescence or G0 is a state cells are in when they leave the cell cycle, while still retaining the ability to return to it after additional signals, such as peptide growth factors, are present.

Also indicated are points in the cell cycle where various surveillance systems determine whether progress to the next stage of the cell cycle can proceed without damaging the cell. These points are termed checkpoints. Further details regarding these are mentioned in the text.

Progression through the cycle is carefully regulated. Checkpoints are points along the cycle where progression can be safely arrested while certain conditions can be checked. There are several checkpoints along the eukaryotic somatic cell cycle, the major one being the restriction point checkpoint, which occurs in the G1 phase of the cell cycle. At this checkpoint, the cell either becomes committed to undergoing another cell cycle or else refrains from doing so. Factors such as nutrient supply and cell mass are important in determining whether a cell passes through this checkpoint of the cell cycle. Cells may leave the cell cycle and stop dividing while still retaining the ability to re-enter the cell cycle given the appropriate biochemical cues. Such cells are said to be quiescent or in G0 phase. Cells in this state, while not preparing for cell division, are however viable. Many cells *in vivo* that are poised to differentiate are quiescent. Fibroblasts in culture can be induced into quiescence by feeding the cells with medium containing low levels of serum or essential growth factors.

The cell cycle stage of a cell can be identified by measuring its DNA content [Krishan 1975]. Using fluorescent activated cell sorter (FACS) analysis, propidium iodide stained cells with different amounts of DNA can be distinguished. The DNA complement of cells provides information as to which stage of the cell cycle they are in. This is explained in **Fig 1.3**.

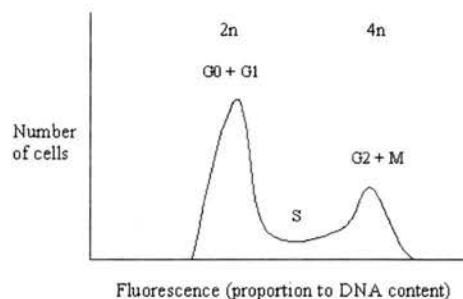


**Fig 1.3 Typical histogram from FACS analysis of a somatic cell population stained with propidium iodide**

In G1, somatic cells have a diploid complement of chromosomes. During S phase they have an increasingly greater amount of DNA due to its synthesis. From the beginning of G2 until mitosis, cells normally have a 4n complement of chromosomes. At cell division, two daughter cells with separate nuclei are formed giving two diploid cells.

The mechanisms underpinning the regulation of cells progressing through the cell cycle are highly complex and only partially understood. Protein phosphorylation/dephosphorylation is an integral part of regulation at several checkpoints [as reviewed by Hartwell 1995].

The mechanism regulating the triggering of mitosis is the best understood to date. Experiments involving cell fusion highlighted that a factor was responsible for inducing mitosis [Johnson & Game 1970][Rao & Johnson 1970]. Behaviour of the nuclei in the binucleated cells resulting from fusion, termed heterokaryons, was studied. When cells in G1, S, or G2 phases are fused with M phase cells, in the resultant heterokaryon both nuclei undergo mitosis. This showed that a factor was present in the cytoplasm of the M phase cell induced the nucleus originating from the other cell to undergo mitosis. Subsequently it was discovered that small amounts of cytoplasm from *Xenopus* eggs could induce G2 arrested *Xenopus* oocytes to start dividing [Masui & Markert 1971]. In 1988 Lohka *et al.* purified and characterised this factor, now called **M-phase promoting factor** or MPF.

MPF induces nuclear membrane breakdown within cells [Masui & Markert 1971], as well as triggering nuclear membrane breakdown, chromatin condensation and spindle fibre formation in cell free systems [Lohka *et al.* 1984]. The factor is a dimer of two proteins: a catalytic kinase subunit and a regulatory cyclin subunit [Pines 1993][Gautier *et al.* 1990][Draetta *et al.* 1989]. Dimerisation of the two subunits activates the phosphorylation activity of the kinase, and it phosphorylates a range of proteins which in turn trigger mitosis [Murray *et al.* 1989]. Similar mechanisms act at other checkpoints (see **Fig 1.4**)

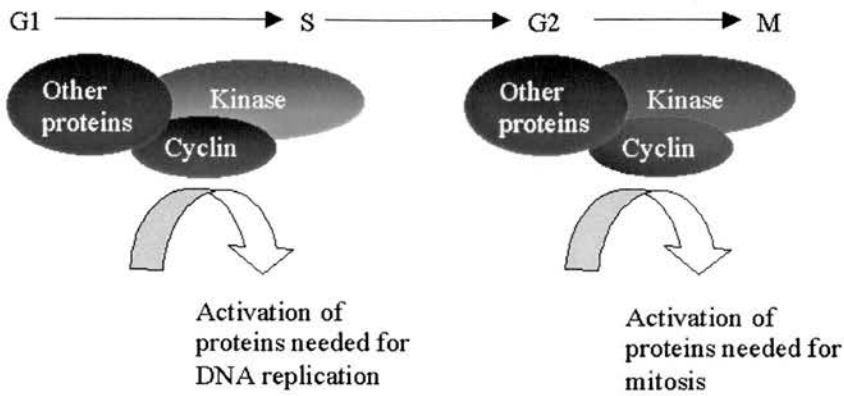


**Fig 1.4 Cdk activity and the cell cycle.**

At the major checkpoints of the cell cycle, the phosphorylation status of critical proteins determines progression. A particular class of protein kinases, termed cyclin dependent kinases (cdk), is responsible for these phosphorylations. A cdk is composed of a catalytic kinase subunit, a cyclin and other proteins. By phosphorylating critical proteins, cdks allow progression through the cell cycle. The diagram shows the two major checkpoints of the eukaryotic somatic cell cycle: the DNA synthesis (G1/S) checkpoint and the mitosis (restriction point) checkpoint. Cdk activity allows phosphorylation of critical proteins and progression through the cell cycle.

Cyclins are a family of proteins whose expression varies as the cell cycle progresses: they are synthesised throughout the cell cycle but are degraded at the end of mitosis (See **Figure 1.5**).

**Proliferating cell nuclear antigen (PCNA, also cyclin)** is a 36kD nuclear protein which has been demonstrated to be a co-factor for DNA polymerase  $\delta$  [Bravo *et al.* 1987] and is essential for the synthesis of DNA during the S phase of cell division. PCNA is detectable immunocytochemically only in S phase and may be used as a naturally occurring marker for cell proliferation [Galand & Degraef 1989][Thaete *et al.* 1989]. Based on fixation procedures two forms of PCNA can be visualised in cultured cells [Bravo & MacDonald-Bravo 1987].

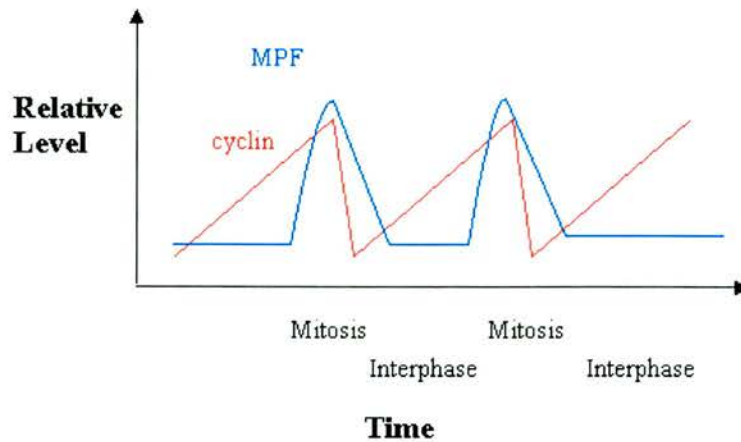


**Fig 1.5 Cyclin and MPF levels fluctuate during the cell cycle**

This simplified graph shows relative levels of MPF (blue) and cyclin (red) as they change during the lifetime of the cell. MPF kinase activity is required to initiate mitosis while proteolysis of cyclin proteins triggers the cell to exit mitosis. [Modified from Murray & Hunt 1993].

In mammals, many cyclin families exist, however only two have been linked to the regulation of mitotic onset: the A and B cyclin families [Pagano *et al.* 1992][Girard *et al.* 1991]. These families show weak sequence homology to each other and have different patterns of gene expression but both can bind to the kinase protein and activate its catalytic activity [Pagano *et al.* 1992] [Draetta *et al.* 1988]. The significance of having two cyclin families and any different effects they have on the catalytic subunit substrate specificity remains unclear. However it is known that cyclins are necessary for the M phase-specific activity of the kinases [Pagano *et al.* 1992][Girard *et al.* 1991]. A and B cyclins share a sequence near the N-terminal domain, termed a “cyclin destruction box”. When this sequence is deleted, resultant mutant cyclins are not targeted for proteolysis at the appropriate part of M-phase [Murray *et al.* 1989]. When no destruction of cyclins occurs, the M-phase kinases remain active and the cell is unable to exit mitosis [Murray *et al.* 1989].



Finally, much work has focused on identifying proteins phosphorylated by M-phase kinases, in order to try and further elucidate the M-phase pathway. Interestingly *in vitro* studies have shown linker histone protein H1 to be a target for M-phase kinase activity [Lohka *et al.* 1988]. It is easy to envisage a system whereby the phosphorylation status of H1 is linked to the changes in chromatin structure occurring during the cell cycle for two reasons:

- (a) the phosphorylation status of H1 predictably changes during the cell cycle (2 phosphate groups are added during S phase and 4 phosphate groups are added during mitosis) and
- (b) H1 is one of four histone proteins around which DNA winds to form nucleosomes, the building block of chromatin [Lohka *et al.* 1988] (See **Section [1.10]** for discussion on histone H1 and nucleosomal structure).

Having briefly outlined some aspects of the eukaryotic cell cycle, the discussion again returns to cell differentiation, and the overturning of dogma stating the differentiated state of the mammalian somatic cell is irreversible.

Chromatin condensation has been observed in chromosomes in hybrid cells produced by fusing cells in different stages of the cell cycle [Johnson & Rao 1971]. The molecular basis for such changes is unknown despite the biochemistry of histones and other chromatin associated proteins having been intensely studied. At present, this field is still lacking an *in vitro* system that can reproduce chromatin condensation. More on chromatin structure and nuclear reprogramming is detailed in **Section [1.10]**.

#### **[1.4] Differentiated state of the mammalian somatic cell is plastic**

It has been known for 37 years that the nuclei of amphibian differentiated cells could be reprogrammed to pluripotency by nuclear transfer [Gurdon & Uehlinger 1966]. For a long time this technique was applied unsuccessfully to mammalian somatic cells, until in 1981 Illmensee & Hoppe reported the cloning of mice by injecting donor nuclei

from ICM cells into enucleated zygotes. Attempts to repeat this work failed [McGrath & Solter 1984][Tsunoda *et al.* 1987], and after allegations from his own staff, Illmensee was charged with scientific fraud. Tsunoda & Kato (1993) tried to clone mice by transferring nuclei from Embryonic Stem cells to enucleated zygotes and also failed. McGrath and Solter (1983) did generate live mice when they injected a zygote donor nucleus into a enucleated zygote, but they could not obtain any successful development when they used donor cell nuclei from later developmental stages. The reason for these failures is now understood: oocytes have a greater nuclear reprogramming activity than zygotes [Gurdon & Byrne 2003]. Despite previous successful amphibian experiments using oocytes, early nuclear transfer experiments in the mammal used zygotes as nuclear donors.

More recently however, several observations have shown that a mammalian somatic cell's differentiated state may indeed be reprogrammed to reacquire developmental potential. These cases fall into two groups, in the first group the nuclei are reprogrammed when exposed to a foreign cytoplasm:

- a) Nuclei of somatic cells taken from adult mammals are capable of directing normal development following fusion with enucleated oocytes [Wilmot *et al.* 1997].
- b) Fusion of murine Embryonic Germ (mEG) [Tada *et al.* 1997] or murine Embryonic Stem (mES) cells with thymocytes [Tada *et al.* 2001][Gallagher & McWhir, Unpublished data] or splenocytes [Matveeva *et al.* 1998] produces hybrid cells where the epigenetic status of the somatic nucleus is thought to be heritably altered. Tada *et al.* (1997) showed that the DNA methylation patterns of the hybrid nucleus are different from those of the unfused somatic nucleus indicating that pluripotent stem cells may carry reprogramming activity.

The second group contains other cases where exposure to foreign cytoplasm is not apparent, but evidence for somatic cell plasticity still exists:

- (c) Adult haematopoietic stem cells, when injected into early embryos are assimilated into chimeric haematopoietic system and are reprogrammed to



express the embryonic repertoire of gene expression in haematopoiesis [Geiger *et al.* 1998].

(d) After transplantation into irradiated hosts, cells from the central nervous system can contribute to haematopoiesis [Bjornson *et al.* 1999].

Mammalian cells known as pluripotent embryonic cells, give rise to all embryonic cell types and may be grown *in vitro* indefinitely in a primitive undifferentiated state [As reviewed by Smith 2001]. Such cells have become a powerful tool in every aspect of mammalian developmental biology and medicine and are essential to the work done in this thesis. The history, function, development and potential of these cells will now be discussed.

## **[1.5] Self-renewing pluripotent cells in mammals: ES, EG and EC cells**

### **[1.5.1] Teratocarcinomas and murine embryonal carcinoma cells**

Kleinsmith and Pierce (1964) discovered that cells other than the zygote could give rise to several cell types comprising all three embryonic germ layers. This group isolated an undifferentiated pluripotent cell type, known as the Embryonal Carcinoma (EC) cell, from murine teratocarcinomas (malignant germ cell tumours that displayed chaotic, unregulated differentiation of cells). Murine EC cells were found to be immortal and could be expanded in culture [Hogan 1976], which allowed their characterisation. Clonally derived and expanded murine EC cells possess the capacity to differentiate and produce derivatives of all three primary germ layers both *in vitro* [Martin & Evans 1975] [Finch & Ephrussi 1967] and after injection into adult mice [Kleinsmith & Pierce 1964]. Even more intriguingly, when reintroduced back into the developing embryo, it was found that some murine EC cell lines could contribute to embryogenesis and participate in the formation of a range of tissues to the extent that viable chimeric animals could be produced [Brinster 1974]. Most EC cell lines however did not display this differential potential either *in vitro* or *in vivo* and contributed poorly to chimeras [Smith 2001]. It was also observed that EC cells were almost always aneuploid [Smith 2001].

Thus, EC cells gave rise to the concept of a self-renewing pluripotent stem cell. Soon however the therapeutic potential of EC cells and their value as a model for mammalian development was questioned as the cells were derived from malignant tumours and displayed karyotypic abnormalities. Researchers sought to isolate a pluripotent cell type with a stable, normal karyotype that could be maintained and expanded in culture.

### **[1.5.2] Origins and characteristics of murine embryonic stem and germ cells**

It was noted that teratocarcinomas develop from ectopically transplanted blastocysts and spontaneously from Primordial Germ Cells in some mouse tissue strains, and it was hypothesised that progeny of PGCs and blastocyst cells could also be pluripotent. This proved to be true and two additional murine pluripotent cell types, termed Embryonic Germ (EG) [Matsui *et al.* 1992] and Embryonic Stem (ES) cells [Evans & Kaufman 1981][Martin 1981], were isolated from primordial germ cell and blastocyst explants respectively.

Murine ES and EG cells were found to have similar properties to EC cells:

- (a) they are derived from pluripotent cell populations;
- (b) they are immortal and can be propagated indefinitely in an undifferentiated state given correct culture conditions;
- (c) homogeneous populations of these cells are capable of spontaneously differentiating into cell types associated with all three primary germ layers of the embryo;
- (d) they are tumorigenic when injected into adult mice.

Thus researchers had achieved their aim of isolating self-renewing pluripotent stem cells that were derived from non-transformed tissue and were karyotypically stable.

Murine ES cells can generate all cell types of the foetus including the germline [Bradley *et al.* 1984][Nagy *et al.* 1991]. Whether they are actually totipotent like the zygote remains in question, as murine ES cells contribute poorly to extra-embryonic

tissues and no reports of spontaneous differentiation to trophoblast cells have been reported. Despite this, murine ES cells can participate fully and consistently into embryogenesis when returned into an early embryo, even after they have been genetically manipulated. Using either blastocyst injection or morula aggregation, chimeric offspring have been generated where the ES cells give rise to all cell types of the foetus, including functional gametes [Bradley *et al.* 1984]. Mouse ES cells have been used to introduce gene knock-outs and other precise genomic modifications into the mouse germ line via homologous recombination in order to study the function of specific genes [as reviewed by Babinet & Cohen-Tannoudji 2001]. Thus ES cells have become a very important and commonly used tool for engineering the mouse genome. Such ES cell-based technology would prove useful for genetic engineering in many other vertebrate species but as yet proven ES cells colonising the germ line have only been established for mouse [Evans & Kaufman 1981][Martin 1981]. Failure of traditional isolation methods to generate ES cells in other species has fuelled the desire to create them *in vitro* via nuclear reprogramming of somatic cells.

### **[1.5.3] Propagation and differentiation of murine ES cells**

Observations were made initially with murine EC [Martin & Evans 1975], ES [Evans & Kaufman 1981][Martin 1981] and EG [Matsui *et al.* 1992] cells that cells grew better and maintained their pluripotent state longer when co-cultured with fibroblasts. It was reasoned that such cells provide essential nutrients and growth factors and were called “feeder” cells.

Coculture with feeder cells was initially thought to be necessary to maintain murine ES cells in an undifferentiated state. In 1987 however, Smith & Hooper showed that feeder-conditioned medium was sufficient and physical contact with the feeders was not required. It was reasoned that the feeders secreted a factor that suppressed differentiation in mES cells. This factor, a cytokine called leukaemia inhibitory factor (LIF), was subsequently identified [Williams *et al.* 1988][Smith *et al.* 1988]. Murine ES cells are now routinely cultured in LIF-supplemented medium (See **Subsection [2.1.1.1]**)

for details). If LIF is removed from the culture medium, ES cells rapidly differentiate [Williams *et al.* 1988]. Upon withdrawal of both LIF and stromal contact, ES cells readily form spherical cellular aggregates of differentiated cell types called embryoid bodies. The formation of such bodies is characteristic of the ES cell phenotype.

#### **[1.5.4] Isolation, culture and characterisation of human ES cells**

Human ES cell (hES) lines have now been isolated in several laboratories throughout the world [Thomson *et al.* 1998][Reubinoff *et al.* 2000][Richards *et al.* 2002][Amit & Itskovitz-Eldor. 2002][Amit *et al.* 2000]. At the present time, a relatively small number of ES cell lines has been completely characterised but enough work has been done to show that human ES cells are different from their murine counterparts in several ways:

- (a) human ES cells differentiate into cells of extra-embryonic tissues. Two laboratories have reported that differentiated cells secrete chorionic gonadotrophin, a hormone only secreted by extra-embryonic tissues [Reubinoff *et al.* 2000][Thomson *et al.* 1998]. Xu *et al.* (2002) has now shown hES cells can be differentiated into trophoblast cells in the presence of growth factor BMP-4. In contrast, mES cells rarely differentiate into extra-embryonic cell lineages and there is no report of wild type mES cells forming trophoblast cells. See **Section [1.6]** for more on how trophoblast cells were derived from transgenically manipulated mES cells.
- (b) hES cells express a different array of cell markers to mES cells [as reviewed by Carpenter *et al.* 2003]. For example, undifferentiated mES cells express the SSEA-1 epitope in the undifferentiated state and the SSEA-4 epitope when they differentiate into some cell types (primitive endoderm), whereas human ES cells express the two epitopes in a reciprocal fashion [Thomson *et al.* 1998][See **Section 2.1.1** for further details. Human ES cells bear a much closer resemblance to human EC lines, like NTERA2, in terms of marker expression [Henderson *et al.* 2002].
- (c) Differentiation of hES cells is not suppressed in LIF-supplemented medium. Reubinoff *et al.* 2000 reported that LIF had no effect on growth or differentiation

of established hES lines. Again this is reminiscent of hEC lines [Henderson *et al.* 2002].

- (d) hES cells self renewal requires feeders or bFGF-supplemented, feeder-conditioned medium [Lebkowshi *et al.* 2001][Amit & Itskovitz-Eldor 2002].

There are some limitations and frustrations currently associated with human ES cell research. For ethical reasons, one cannot truly verify that these lines are human embryonic stem cells (i.e. that they are capable of contributing to all cells of the conceptus including the germ-line) as this would require generating a chimeric human. There is also significant variability displayed between currently available lines: there have been many reports of spontaneous differentiation and cell death during routine culture; some lines lack the ability to form embryoid bodies [Reubinoff *et al.* 2000]; and some lack the ability to grow in feeder-conditioned medium. The extent to which this variability between lines is caused by intrinsic factors related to the cells (eg. genetic background of the cells or their epigenetic status) or just purely technical differences such as variations in blastocyst quality and/or suboptimal isolation/expansion conditions, will presumably not be known for some time to come.

Despite these challenges, the potential of human ES cells both for treatment of human disease and for studying early human embryonic development continues to strongly motivate researchers in the field (See **Fig 1.1**). Technical difficulties are gradually being surmounted: hES cells can now be efficiently cloned from single cells [Amit *et al.* 2000]; conditions for efficiently transfecting these cells have been identified [Smith-Arica *et al.* 2003][Zwaka & Thomson 2003]; and gene targeting has been demonstrated [Zwaka & Thomson 2003].

### **[1.6] The maintenance of pluripotency and the *Oct-4* gene**

Although the differentiated state of mammalian somatic cells is now known to be reversible [Evidence for this is reviewed in **Section 1.9**], the mechanisms by which developmental potential can be artificially reinstated have yet to be elucidated. In mouse and human cells, maintenance of the pluripotent state of cells is dependent on the

expression of the *Oct-4* gene. The expression patterns and regulation of this gene will now be discussed.

Expression of *Oct-4* is required to maintain murine embryonic stem and germ cells in a pluripotent state. This gene is expressed in cells from the Inner Cell Mass, Primordial Germ Cells (PGC), Embryonic Germ (EG), Embryonic Stem (ES) and Embryonal Carcinoma (EC) cells of the mouse. It encodes a POU transcription factor that binds a specific octomeric sequence of DNA (ATGCAAAT) [Herr *et al.* 1988].

*Oct-4* was initially identified as a DNA binding activity in extracts from ES and EC cells [Lenardo *et al.* 1989][Schöler *et al.* 1989]. It is known to interact with a range of other transcription factors to alter gene activity important to early embryonic development e.g.  $\alpha$ , $\beta$  HMG, Sox-2, FGF-4, Osteopontin, Rex-1, UTF-1 [Reviewed by Pesce & Schöler 2000].

*Oct-4* expression is stringently regulated both temporally and spatially during early murine embryogenesis. **Fig 1.6** shows a simplified schematic of the main steps in early mouse embryonic development where changes in *Oct-4* expression occur. Low concentrations of the *Oct-4* transcription factor are found in the oocyte and the zygote and in all cells of the early embryo for the first two divisions [Palmieri *et al.* 1994]. At the 8-cell stage, however, an increase of *Oct-4* expression occurs and high concentrations of the transcription factor are observed in all nuclei until the compaction of the morula [Yeom *et al.* 1991].

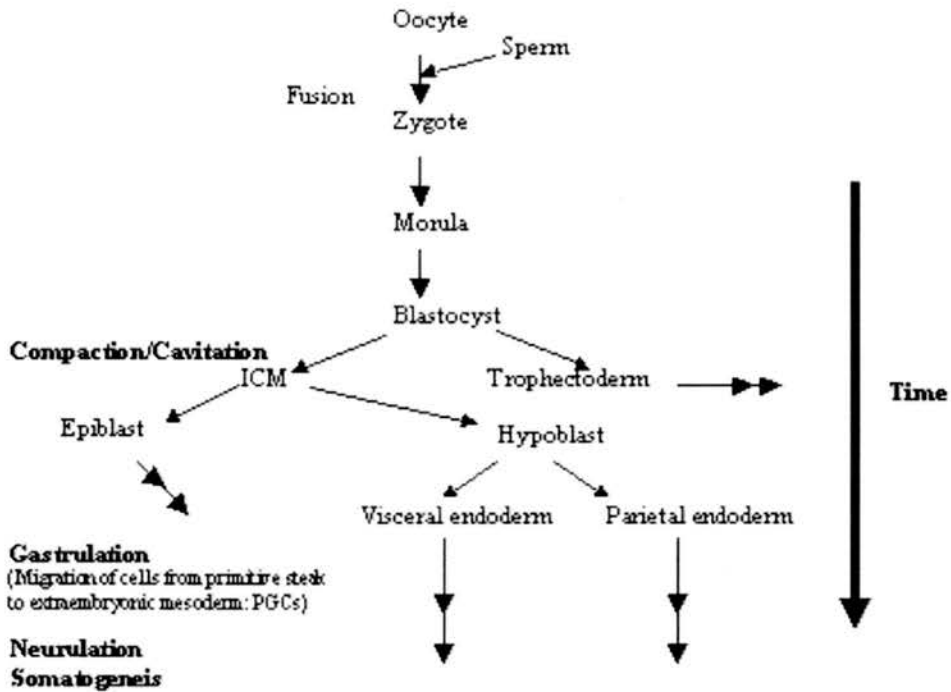


**Fig 1.6 Early embryonic development in the mouse**

The mouse embryo is the embryo of choice for the study of mammalian development. Not only has the embryology of the mouse been studied extensively, but mouse genetics and genetic manipulation are readily conducted. Early murine embryonic development can be divided into five stages: fertilisation (where egg and sperm fuse); cleavage (where the zygote rapidly divides forming a morula and later a blastocyst); gastrulation (where the three germ layers [ectoderm, mesoderm and endoderm] are formed); neurulation (where the nervous system begins to develop); and somatogenesis (where further differentiation of cells into many somatic cell types occurs). Double arrows indicate continued development has been omitted for clarity.

*Oct-4* expression then becomes confined to cells of the Inner Cell Mass (ICM) and is down regulated in the trophectoderm [Palmieri *et al.* 1994]. After implantation, *Oct-4* is highly expressed in the epiblast (also referred to as the primitive ectoderm) [Yeom *et al.* 1996]. Furthermore, during gastrulation *Oct-4* expression decreases dramatically in all cells but the primordial germ cells (PGCs) [Ginsberg *et al.* 1990]. It is suspected that unidentified intracellular signals within the embryo initiate the



repression of *Oct-4* expression and that PGCs are the only cells to maintain high *Oct-4* expression after gastrulation due to their absence from the embryo at this developmental stage.

In mouse embryos where *Oct-4* expression has been silenced, the ICM fails to form after 3.5 days of gestation, causing death of the embryos [Nichols *et al.* 1998]. Without the normal levels of the Oct-4 transcription factor, cells of the morula differentiate into the trophectodermal lineage, and compartmental isolation of pluripotent stem cells of the blastocyst does not occur [Nichols *et al.* 1998]. Niwa *et al.* 2000 has shown that when *Oct-4* is over-expressed in mouse ES cells, the cells differentiate into primitive endoderm and mesoderm.

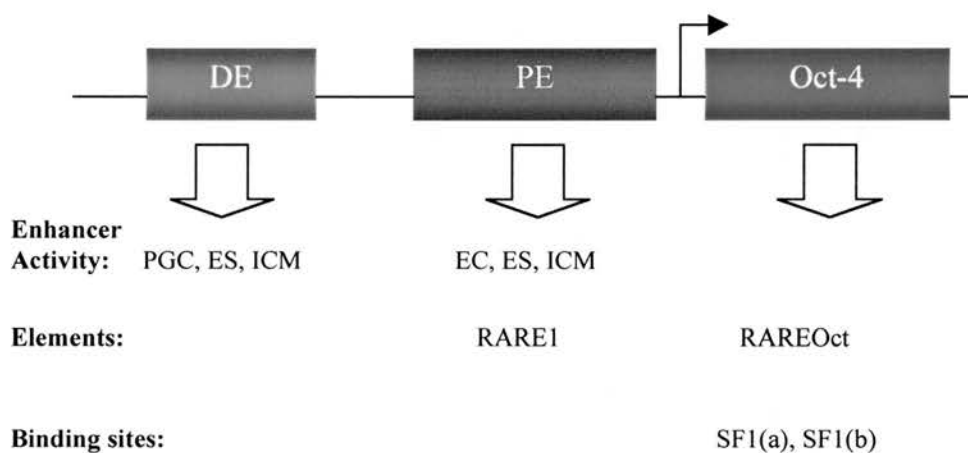


**Fig 1.7 Regulatory elements involved in *Oct-4* expression**

Distal and proximal enhancer elements lie upstream of the promoter. The distal enhancer is active in PGCs while the proximal enhancer is active in EC cells, and both enhancers are active in cells from the ICM and ES cells. Both the proximal enhancer and promoter contain sequences important for retinoic acid induced differentiation (RARE1 and RAREOct). Within RAREOct, there are two binding sites for transcription factor SP1, a possible regulator of Oct-4 activity in EC cells.

The mechanism responsible for regulating *Oct-4* expression has been partially elucidated using Oct-4/lacZ transgenes [Yeom *et al.* 1996]. As **Fig 1.7** shows, two



regulatory elements, the “distal” and “proximal” enhancers, are found upstream of the *Oct-4* gene. Experiments using transgenic mice containing Oct-4 reporter constructs showed that the distal enhancer is active in PGCs and some ES cell lines, while the proximal enhancer is active in ES and EC cells (EG cells were not tested) [Yeom *et al.* 1996]. Both enhancers are active in cells from the ICM. Other work suggests that the distal enhancer may not be required for *Oct-4* promoter activity in ES cells. McWhir *et al.* (1996) used pOctneo1, a plasmid containing a sequence including only the *Oct-4* promoter and the proximal enhancer, to successfully isolate embryonic stem cells from refractory genotypes while killing differentiated cells in drug selection. This selective ablation strategy relies on Oct-4 promoter activity driving the drug resistance gene and suggests that the promoter can promote the necessary expression of the *neo* gene without the distal enhancer.

All developmental models of how Oct-4 acts as a molecular switch activating and repressing gene expression have until recently been binary e.g. “the totipotent cycle” model [as discussed in Pesce *et al.* 1998, Pesce *et al.* 1999]. The model states that either an ES cell expresses Oct-4 above a certain level and retains its totipotent state, or else the level of expression is below the threshold and the cell differentiates [As reviewed by Brehm *et al.* (1998)]. Now it is thought that Oct-4 is involved in three, and not two, distinct developmental fates of ES cells [Niwa *et al.* 2000] [Pesce & Schöler 2001]. Niwa *et al.* (2000) generated transgenic ES lines where the expression of *Oct-4* is controlled by addition or withdrawal of the antibiotic, tetracycline (tetracycline-mediated regulation of gene expression is discussed in **Chapter [8]**). These researchers report outcomes predicted by the totipotent cycle, namely *Oct-4* expression below a certain threshold results in differentiation into trophectoderm, and if it is just above then the cell maintains an ES phenotype. Interestingly, they also reported that when *Oct-4* is expressed at an even higher level above the threshold, differentiation into primitive endoderm and mesoderm occurs [Niwa *et al.* 2000].

The mechanism behind such regulation of cell fate has yet to be elucidated, although Oct-4 is known to regulate expression and repression of many genes involved in development [Ben-Shushan *et al.* 1998][Pesce *et al.* 1998].

All-trans retinoic acid induces murine EC and ES cells to differentiate [Barkai *et al.* 1986]. This chemical is used to investigate *in vitro* differentiation in cell hybrids from murine and human cells in this thesis. Much work has been done to elucidate the underlying mechanism of this process with the hope of finding out more about how the differentiation is regulated.

PGCs, ES, EG and EC cells as well as cells from the ICM strongly express *Oct-4*. In experiments where ES and EC cells are induced to differentiate, expression of *Oct-4* is switched off rapidly [Okamoto *et al.* 1990][Rosner *et al.* 1990][Schöler *et al.* 1990].

All-trans retinoic acid (RA) induces murine EC and ES cells to differentiate while concomitantly down-regulating *Oct-4* expression [Strickland & Mahdavi 1978] [Strickland *et al.* 1980]. The study of RA induced EC differentiation has revealed that differentiation may be induced by one of two *cis*-acting mechanisms. One involves the binding of transcription factors to the Retinoic Acid Regulatory Element 1 (RARE1) within the *Oct-4* promoter causing down regulation of Oct-4 [Schoorlemmer *et al.* 1994] and the other results in *Oct-4* enhancer deactivation after nuclear factors bind to a sequence which lies outside the promoter (RAREOct) [Pikarsky *et al.* 1994]. It is possible that both repression pathways are differentially used at various developmental stages to regulate *Oct-4* expression.

Studies have shown that certain transcription factors, termed SF1 proteins, play a part in up-regulating Oct-4 expression in EC cells [Barnea *et al.* 2000]. Two distinct SF1 binding sites, SF1(a) and SF1(b), have been located within the RAREOct sequence located within the *Oct-4* promoter (See **Fig 1.7**). Previously ligands responsible for down-regulation of *Oct-4* promoter activity (eg. COUP-TF1, ARP-1, heterodimers of retinoic acid receptor and ryanodine receptor) have been found in the same region. It has been shown that SF1 and retinoic acid receptor (RAR) function cooperatively to

transactivate the *Oct-4* promoter and that both SF1 and Oct-4 expression are down regulated in EC cells treated with RA. It is now hypothesised that SF-1 positively regulates *Oct-4* in EC cells [Strickland & Mahdavi 1978][Strickland & Mahdavi 1980].

### **[1.7] Nuclear Reprogramming in Development and Pathology**

One example of nuclear reprogramming which occurs naturally during mammalian embryo development is observed in the zygote [Schultz *et al.* 1999]. The mammalian sperm and oocyte (both highly differentiated cell-types) fuse to generate the zygote, a cell which is then capable of generating totipotent daughter cells [Kelly 1977]. Nuclear reprogramming also occurs during the generation of teratocarcinomas. Such tumours are thought to arise from germ cells that have undergone dedifferentiation to a pluripotent state [Damjanov 1983]. Thus teratocarcinomas can be thought of as the result of inappropriate nuclear reprogramming. These tumours can also be produced experimentally by injection of ES or EG cells into ectopic sites of a syngeneic animal. In non-transformed somatic cells, once the differentiation programme of a cell has started, the process is normally irreversible. However, this program may be reversed artificially.

Certain developmental processes remodel chromatin. Some of these do not alter developmental potential but are required for normal development. Three such phenomena, genomic imprinting, X-chromosome inactivation and telomere maintenance are essential to normal development. These processes are coupled with differentiation and change epigenetic patterns that alter the capacity for gene expression. Imprinting and X-chromosome inactivation will be discussed here in the context of normal development. Later these phenomena will be readdressed in the context of the experimental induction of nuclear reprogramming (**Section [1.11]**).

### [1.7.1] Genomic Imprinting in Mammalian Development

Imprinting is an epigenetic mechanism regulating expression or repression of some genes according to their parental origin [McGrath & Solter 1984]. This phenomenon has been reported in mammals, seed plants and some insect species [Reik & Surani 1989]. In mammals, the majority of imprinted genes, for which a function has been identified, code for proteins involved in embryonic development [as reviewed by Tilghman 1999]. Mammalian imprinted genes are often expressed in the placenta, the primary tissue regulating transfer of nutrients from mother to embryo [Tilghman 1999].

As with nuclear reprogramming, the mechanism by which imprinting takes place is poorly understood, although it is observed to be associated with methylation of specific DNA sequences and changes in chromatin structure.

Methylation of specific DNA sequences is involved in the mechanism by which mammalian genes are imprinted. Normal imprinting of several genes (*H19*, *Igf2*, *Igf2r*, and *Snrpn*) is disrupted in methyltransferase-deficient mice [Li *et al.* 1993]. Specific CpG islands, where allelic differences in methylation occur, are found in all imprinted genes studied to date [Sherman & Pillus 1997]. Such CpG islands are termed 'Differentially Methylated Regions' (DMRs). However, imprinting is possible without DNA methylation in *Drosophila* [Bishop & Jackson 1996] suggesting that imprinting is not necessarily the result of gene methylation in all species where imprinting occurs.

The functional significance of methylation in imprinting has been assessed via two strategies: (a) insertion into nuclei of transgenes containing sequences known to affect imprinting and (b) investigation of changes of imprinting when partial deletions of Differentially Methylated Regions of DNA (DMRs) are introduced using homologous recombination in ES cells. To date, these strategies have failed to clarify the relationship between methylation and imprinting.

In addition to CpG island methylation, chromosomal structure has also been shown to affect imprinting. Shibata *et al.* (1996) showed that imprinting in mice is dependent on chromatin structure in experiments characterising the activity of the

imprinted gene *U2af1-rsl*. Analysis of DNaseI hypersensitivity of the *U2af1-rsl*'s promoter showed an open chromatin confirmation only on the unmethylated, expressed paternal allele [Shibata *et al.* 1996].

Imprinting is regulated by both *cis*- and *trans*- acting elements [Reik & Surani 1989]. *Cis*-acting elements such as Differentially Methylated Regions (DMRs) are reported to be requirements for imprinting in a variety of mammals [Feinberg *et al.* 1980] and it has become clear that both local and regional chromosomal elements interact. *Trans* acting factors, such as DNA methylase, are implicated in experiments where the activity of specific transactivating factors appears to be diluted when additional imprinted genes are introduced. For example, when researchers introduced plasmids containing the imprinted gene *Igf2* into cells already containing this gene in its genome methylation states of both introduced transgenic and endogenous copies of the gene were reduced [Sun *et al.* 1997]. Introduction of plasmids containing another imprinted gene, *U2af bp-rs1*, into imprinted male cells also caused a reduction in the methylation of genomic copies of the gene [Hatada & Mukai 1997]. Methylase activity is unchanged with the introduction of DMR containing transgenes, but the methylation states of endogenous sequences are altered. It is thought that methylation status may be dependent on the equilibrium of various competing factors acting at the same genes [Reik & Walter 1998].

Models currently postulated to explain the imprinting mechanism support observations that methylation and chromatin structure affect imprinting, but are based on several unproved assumptions, for example the most popular model “mutual exclusion” [Feil & Khosla 1999] **Fig 1.8** (overleaf), is based on at least three assumptions:

- (a) Methylation is a causal element in imprinting.
- (b) Specific proteins interact with genes on the basis of methylation status of DMRs associated with the genes.
- (c) Such methylation-state sensitive proteins modify chromatin structure thus regulating gene activity.



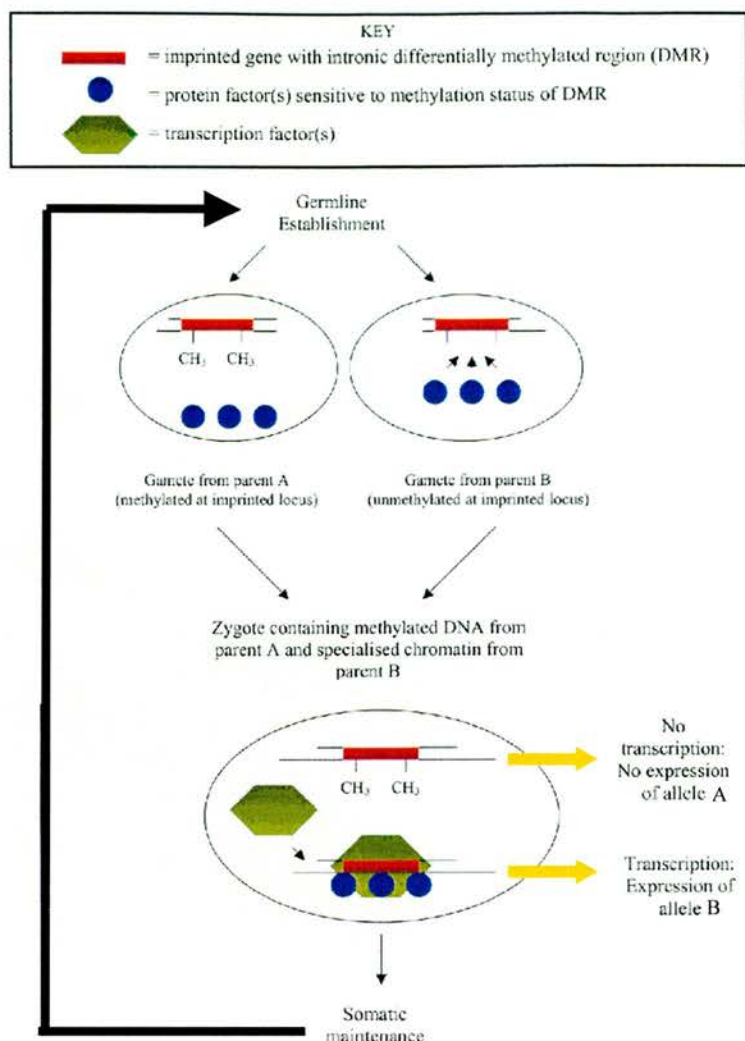


**Figure 1.8 Mutual exclusion model of mammalian gene imprinting**

Modified from Feil & Khosla (1999), the diagram illustrates the simplest scenario where one differentially methylated region (DMR) is contained within the imprinted locus e.g. intronic DMRs of murine *H19* and *Igf2* genes. According to the model, the methylation state of DMRs associated with imprinted loci determine whether specific protein factors interact with the DNA. Such interactions lead to changes in chromatin structure allowing the differential expression of one parental allele. The diagram shows a case where methylation of the DMR allows methylation-sensitive proteins to interact with DNA. These proteins alter chromatin structure to allow interaction with one or more transcription factors. This allows transcription i.e. allele B is transcribed. Allele A is not expressed as the DMR from parent B is not methylated and no changes in chromatin structure occur.

Another theory suggests that RNA encoded by regions adjacent to DMRs might be involved in the imprinting mechanism [Wutz *et al.* 1997]. This idea is based on the observation that DMRs in mammals are sometimes found to overlap with regions which generate non-coding or missense RNAs [Wutz *et al.* 1997][Moore *et al.* 1997]. This theory also assumes that methylation is a causal element in imprinting.

### [1.7.2] X-chromosome Inactivation in Mammalian Development

In somatic cells of normal female mammals, one of the two X-chromosomes is programmed to remain transcriptionally silent and not to respond to signals eliciting transcription in the other, active X chromosome. As a result, XX females and XY males effectively have equal doses of X-linked gene products in their cells. The process by which one X chromosome is programmed to remain transcriptionally silent is termed X-chromosome inactivation.

At the beginning of embryonic development in the mouse and human, both X-chromosomes are in the active state, and their differentiation into active and inactive forms occurs at the blastocyst stage in the trophectoderm and primitive endoderm lineages. The paternally derived X-chromosome is preferentially inactivated in these cells (imprinted XCI). Later in development, XCI is also initiated in cells of the primitive ectoderm. These cells will give rise to the embryo proper, and, in contrast to earlier XCI, both paternally derived and maternally derived X-chromosomes stand an equal chance of being inactivated (random XCI).

The X chromosome to be inactivated translates a non-coding RNA from the *Xist* (*X inactive specific transcript*) gene and this RNA coats the chromosome and is necessary and sufficient for inactivation of the chromosome [Lee and Jaenisch 1986]. Once initiation of XCI has occurred, the same X-chromosome remains inactive in all the mitotic descendants of each cell during the lifetime of the mammal. The inactivated X-chromosome (Xi) displays several features not associated with the active chromosome: overall transcriptional inactivation except for *Xist* and a small number of X-linked genes [Graves & Gartler 1986]; heterochromatic condensation during interphase [Barr &

Bertram 1949]; late chromatin replication [Takagi & Oshimura 1973]; histone H3/H4 hypoacetylation [Jeppesen & Turner 1993]; specific histone methylation (MeK9H3) [Boggs et al. 2002]; variant histone macroH2A incorporation [Mermoud *et al.* 1999]; and DNA methylation of CpG islands [Monk 1986]. The mechanism by which *Xist* RNA stably prevents transcription from the inactivated chromosome is unknown and effort is currently being focused on this area.

### **[1.7.3] Telomere maintenance in Mammalian Development**

Another form of nuclear programming involves the maintenance of the ends of chromosomes. As a stem cell differentiates, the resultant progeny down-regulate the expression of enzymes required for the maintenance of chromosomal ends. This down-regulation prevents the cell from replicating indefinitely and can be viewed as programming a cell to senesce after a given number of cell divisions [Olovnikov 1973] [Harley 1991].

Telomeres are structures formed by multiple DNA sequences found at the ends of eukaryotic chromosomes that serve to stabilise the ends on linear DNA and allow DNA replication. Conventional DNA polymerases cannot replicate the extreme 5' ends of chromosomes because removal of the most terminal RNA primer in the lagging strand leaves a small region of uncopied DNA [Levy *et al.* 1992]. Thus, over time in the absence of a specialist mechanism, chromosomes shorten until a stage is reached that too much DNA has been removed and the cell senesces. There is however a mechanism in mammalian cells that can prevent this scenario occurring, allowing certain cells to replicate indefinitely. This mechanism involves ribonucleoprotein enzymes called telomerases that add DNA repeat sequences to G-rich sequences within the telomere. Such replenishment is carefully regulated and the result is telomeric length is maintained through rounds of DNA replication.

In addition to stabilising chromosome ends, telomeres also have other less well defined functions: they prevent the potentially detrimental recombination of



chromosome ends and broken DNA strands [Lo *et al.* 2002]; and they are involved in chromosome pairing during meiosis [Scherthan *et al.* 1996].

Normal somatic cells do not display telomerase activity and consequently have a finite number of times they can replicate their DNA *in vitro* before senescing [Harley *et al.* 1991]. In contrast other normal cell types (*i.e.* stem cells and germ cells) display telomerase activity and possess an increased capacity to replicate [Hiyama *et al.* 1995]. When stem cells differentiate, their telomerase activity declines and their replicative capacity is decreased. This drop in telomerase activity is due to decreased transcription of the TERT gene that codes for the catalytic subunits of telomerase [Mattson *et al.* 2000].

## [1.8] Artificially Induced Nuclear Reprogramming

Induction of nuclear reprogramming in differentiated somatic cells could provide isogenic replacement cells to treat a variety of diseases [See Fig 1.1]. Using nuclear transfer [Campbell *et al.* 1996], cell fusion [Tada *et al.* 1997], or exposure to cellular extract [Håkelién *et al.* 2002] it is possible to artificially and heritably alter a cell's capacity for gene expression by altering the nucleus's epigenetic state. These techniques may be termed "artificial methods of nuclear reprogramming" [Fig 1.9].

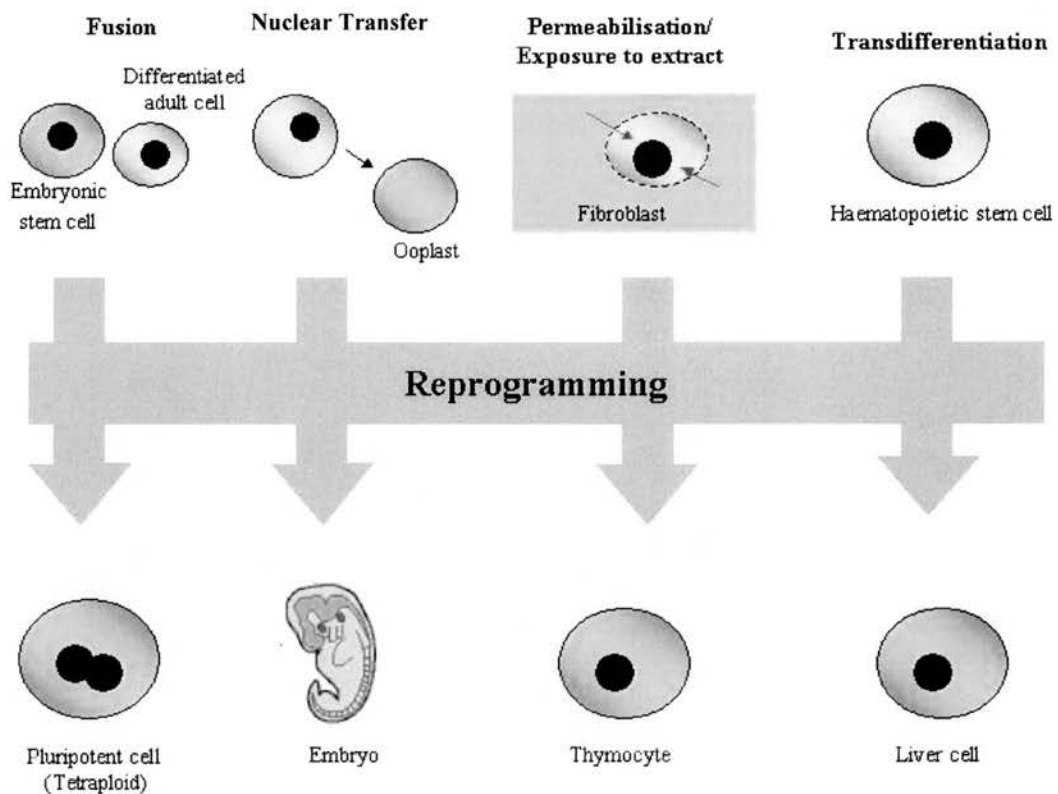


**Fig 1.9 Artificial methods of nuclear reprogramming:** cell fusion [Tada *et al.* 1997], cloning via nuclear transfer [Hochedlinger & Jaenisch 2002] [Campbell *et al.* 1996], permeabilisation & exposure to cellular extracts [Håkelién *et al.* 2002], and transdifferentiation [Theise *et al.* 2000].

### [1.8.1] Nuclear Transfer

Spemann (1938) originally suggested transplantation of nuclei between cells as a technique to study the role of genetic material in cellular differentiation. Nuclei from fully differentiated mammalian somatic cells can now be fully reprogrammed, with totipotency restored, using nuclear transfer [Wilmot *et al.* 1997]. The technique has generated viable animals using eight mammalian species to date: sheep [Wilmot *et al.* 1997], mouse [Wakayama *et al.* 1998], cow [Kato *et al.* 1998], pig [Campbell *et al.* 2000], goat [Bagiuisi *et al.* 1999], rabbit [Chesne *et al.* 2002], cat [Gomez *et al.* 2003], horse [Galli *et al.* 2003] and rat [Vogel *et al.* 2003]. The nuclei of these offspring contain genomes of identical sequence to that of the nuclear donor. This represents total nuclear reprogramming of the somatic nuclei as the totipotent state is restored. Otherwise viable offspring could not be generated [Campbell *et al.* 1999].

It is often overlooked in the literature that nuclear transfer allows only the nuclear genome to be exactly duplicated in another organism. It does not create exact genetic replicas of the organism from which the nucleus was taken. Factors like mitochondrial DNA [Takeda *et al.* 1999], chromatin conformation and other subtle epigenetic factors such as methylation / acetylation patterns [Campbell 1999] will vary from that of the original donor animal due to the cytoplasmic contribution of the ooplast as well as possible effects inadvertently caused by the procedure itself.

Successful reprogramming of somatic nuclei by placing them in enucleated oocytes is perhaps not surprising. As previously discussed in **Section [1.2]**, a mechanism for the removal of epigenetic modifications (excluding gametic imprints) exists in the zygote. The oocyte and sperm are both highly specialised differentiated cells, and removal of their epigenetic patterns is essential to allow development of pluripotent cells from the ICM. It has been speculated that a similar mechanism can reprogramme a somatic nucleus when it is transplanted to an ooplast [Surani 1999].

Much remains to be learnt about how somatic nuclei are reprogrammed after being transferred into ooplasts. Thus, at present, the only unequivocal manner in which one can identify total nuclear reprogramming is to attempt to derive viable offspring from a reconstituted embryo. The production of “Dolly”, the first viable mammal derived from a reprogrammed adult somatic cell, has illustrated that the

nuclear genome may be completely reprogrammed and totipotency of the nucleus can be restored.

Many factors are probably responsible for the successful application of the nuclear transfer technique to reprogramming mammalian nuclei. Some of these have been identified: structural integrity of the nuclear membrane [Blow & Laskey 1988], quality and copy number of donor genetic material, chromatin conformation, histone composition, methylation and acetylation patterns [Reviewed by Campbell (1999)]. Other important variables determining success include the level of M-phase Promoting Factor (MPF) and the cell cycle stage of the donor nucleus and recipient oocyte. It has been suggested that frequency of live offspring generation from reconstructed embryos made by nuclear transfer is improved by placing the donor nuclei into a quiescent state prior to transfer [Campbell 1996, Campbell *et al.* 1999]. It is thought that synchronisation of cell cycle stage in the oocyte using serum starvation minimises chromosomal damage and promotes generation of reconstructed embryos that divide to produce normal diploid daughter cells [Campbell 1999]. The successful production of Dolly, the first viable animal to be generated by nuclear transfer, used a nucleus from a cultured adult differentiated somatic cell which had been serum starved into quiescence [Wilmut *et al.* 1997]. When a cell enters quiescence the histone composition of chromatin [Khochbin & Wolffe 1994][Dimitrov & Wolffe 1996] and the sub-nuclear distribution of chromatin structural proteins is altered. Pallante (2002) suggests that some aspect of these changes make the nuclei of quiescent cells more amenable to being reprogrammed.

Whether quiescence is actually required for nuclear reprogramming to take place is contentious. Wakayama *et al.* (1998) used mouse cumulus cells, a naturally quiescent cell population, as nuclear donating cells in successful nuclear transfer experiments into mouse ooplasts. Kato *et al.* (1998) generated viable calves via nuclear transfer in experiments that also used cumulus cells as nuclear donors. In both of these experiments, the cell cycle stage of the nuclear donors was controlled although the formal possibility that animals can be generated using non-quiescent cells as nuclear donors cannot be dismissed. Other researchers claim successful generation of offspring using nuclei derived from non-quiescent cells [Cibelli *et al.* 1998]. Also the formal possibility that transferred nuclei transferred in Wakayama's

and Kato's experiments were non-quiescent cannot be eliminated. The controversy surrounding the role of quiescence is discussed in more detail in **Chapter 7**.

Experiments by Rideout *et al.* (2000) show that the number of live mice generated from cells reprogrammed via nuclear transfer is dependent on the genetics of the mouse from which the nuclear donor cell is taken. Nuclear transfer experiments using ES cell nuclei from inbred 129/SvJae mice fail to produce any offspring, whereas when nuclei from ES cells derived from mice born of 129/SvJae and C57BL/6 matings were used up to 3% of reconstructed embryos reaching blastocyst stage generated viable offspring. It may be that the use of inbred animals as nuclear donors introduces a reprogramming barrier not present in the outbred strains. Investigating why this occurs might elucidate more about mechanisms involved in nuclear reprogramming.

### **[1.8.2] Cytoplasmic injections and incubations**

Experiments in which *Xenopus* ooplasm was injected into *Xenopus* terminally quiescent erythrocytes have initiated DNA replication and cell division [Gurdon 1966]. Recent experiments have shown that this re-entry into the cell cycle was concomitant with removal of linker histones H1 and H1<sup>0</sup> from erythrocytes chromatin by nucleoplasmin [Lu & Leno 1999] (See **Subsection [1.10.3]** and **Subsection [1.11.2]** for more on linker histones and nucleoplasmin respectively). This constitutes an example of nuclear reprogramming.

Håkelién *et al.* (2002) permeabilised and incubated human fibroblasts in a cytoplasmic extract derived from primary human thymocytes. They reported that such incubation altered the gene expression of fibroblasts such that fibroblast specific genes were silenced and T cell specific genes were expressed. The ATPase activity of chromatin remodelling complex, BAF, increased when the fibroblasts were incubated in extract, suggesting that chromatin remodelling may be taking place. Acetylation of H4 histones (See **Subsection [1.11.1]** for how histone modification alters gene expression) at the IL2 promoter was observed, further suggesting chromatin remodelling. Then they permeabilised and incubated fibroblasts in neural precursor extract and observed that the fibroblasts began to extend neuronal-like outgrowths and express neurofilament protein. This also suggests nuclear

reprogramming but the extent to which such phenotypic changes persist is as yet unknown.

Alteration of gene expression and phenotype has also been extensively studied in heterokaryons and cell hybrids generated from the fusion of mammalian cells.

### [1.8.3] Cell fusion and hybridisation

Mammalian cell fusion, pioneered by Barski in the 1940s, has been used to illuminate many cellular processes involving cytoplasmic-nuclear interactions in the mammalian system [Ying *et al.* 2002]. When cells are fused they generate heterokaryons, membrane enclosed bodies where two or more nuclei share the same cytoplasm. A small proportion of heterokaryons undergo mitosis in such a fashion that chromosomes from both nuclei become contained in the same nucleus of the daughter cell. Such a daughter cell is called a cell hybrid (See **Fig 1.10**).

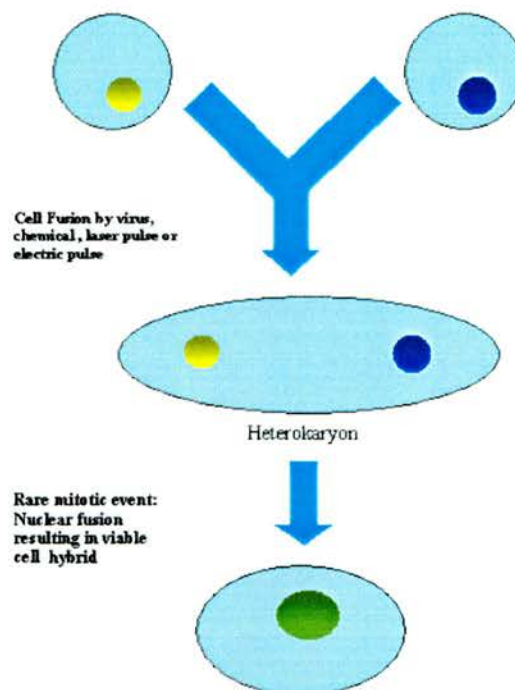


**Fig 1.10 Generating heterokaryons and cell hybrids by cell fusion**

After the heterokaryon undergoes mitosis, a hybrid cell can be produced if the separate nuclear envelopes break down and the chromosomes from the donor species come together to form a single large nucleus [Ekker *et al.* 1999].



Such cell hybrids (also called hybrid cells) are usually karyotypically unstable and tend to lose chromosomes from one of the two parental species. In addition, chromosomal elements are often translocated or inserted into chromosomes from the other parent cell [Ekker *et al.* 1996].

There are numerous methods for fusing cells and microcells. These may be classified into four groups based on the nature of the fusagen:

- (i) Virally mediated fusion e.g. Sendai Virus [Homma & Tashiro 1979][Harris & Watkins 1965],
- (ii) Chemical mediated fusion. The most commonly used chemical fusagen is Polyethylene Glycol (PEG) [Shirahata *et al.* 1998][Vienken *et al.* 1982] [Pentecorvo 1975],
- (iii) Electrofusion [Finaz *et al.* 1984].
- (iv) Laser mediated fusion [Itagaki *et al.* 1997].

Electrofusion is frequently the preferred method of fusion not only because the conditions can be more finely controlled and duplicated but also because reports have cited it as the most efficient method of fusion [Scott-Taylor *et al.* 2000][Finaz *et al.* 1984]. Finaz *et al.* (1984) reported electrofusion to be more than 100x more efficient than the PEG technique at fusing rodent somatic cells.

Parameters for optimising cell electrofusion efficiency can be categorised into two groups, those altering the immediate electromagnetic environment of the cell membranes and those that do not. Strength and duration of electric pulse applied are generally regarded as the most important electromagnetic variables for maximising cell fusion [Scott-Taylor *et al.* 2000]. Polarisation of the electrofusion chamber (by coating one electrode of the cuvette with a thin layer of wax) and application of a low DC electric field in parallel to the AC exponential have been found to increase cell fusion efficiency while not affecting cell viability [Scott-Taylor *et al.* 2000]. Fusion factors not related to the electromagnetic environment of the cell membranes include conductivity, osmolarity, cell ratio and possibly cell-cell contact [Zimmerman *et al.* 1975]. The assumption that cells need to be in contact with each other, at the time an electric pulse is applied, to induce cell fusion has been refuted by data presented by several researchers [Scott-Taylor *et al.* 2000][Teisse & Rols 1986][Sowers 1986]. Application of an electric pulse to cells not in close proximity

and then subsequent centrifugation can generate significant numbers of cell hybrids [Teisse & Rols 1986]. It has been shown that electropulsed cells have a higher fusion rate when centrifuged up to 40 minutes after the application of a single high intensity pulse [Sowers 1986]. This is, perhaps, surprising given lipid bilayers in an aqueous environment reform in a matter of micro- or milliseconds when electric pulses are applied [Benz & Zimmerman 1981]. This rapid reformation occurs due to the hydrophobic nature of hydrocarbon moieties of phospholipid membranes. The “long-lived fusogenic state” may be the result of an alternative electropermeable lipid conformation transiently adopted. Cholesterol and protein content of membranes are thought to affect the duration with which membranes remain susceptible to fusion with membranes from neighbouring cells [Sowers *et al.* 1986].

Viral entry into a host cell and cellular secretory release are the two biological processes where membrane fusion have been best studied. A great deal less is known about the mechanisms responsible for cell membrane-cell membrane fusion [Shemer and Podbilewicz 2003]. There are two contrasting paradigms explaining how cell membranes fuse: the *proximity model* holds that the major factor required for membrane fusion is that the two membranes must be in close proximity and that membranes fuse in a more or less non-specific manner; whereas the *specificity model* holds that the presence of docking proteins in the membrane is the major determinant governing cell fusion [Jahn & Grubmuller 2002]. This second model is clearly important for natural syncytia formation of specialised cells such as myoblasts but it is unclear if docking proteins play a role in the fusion of other cell types.

Empirically, it has been noticed with many cells types that factors such as cell size, cell type, osmotic pressures acting against the membrane, and the extracellular matrices of cells affect cell fusion. The extracellular matrices of cells and how they can be removed will now be discussed.

*In vivo*, cells are embedded in an endogenous extracellular matrix called ground substance. This is secreted by the cells themselves and interaction between



the cells and the matrix is an important factor in the regulation of cell behavior such as cell proliferation and differentiation [Huang & Ingber 1999]. The main components of ground substance are extracellular proteins (eg. laminin, collagen) and polysaccharides (eg. hyaluronan). When culturing adherent cells, enzymes like trypsin and hyaluronidase (see **Fig 1.11**) are used to disaggregate cells as well as dislodging the cells from the underlying matrix.

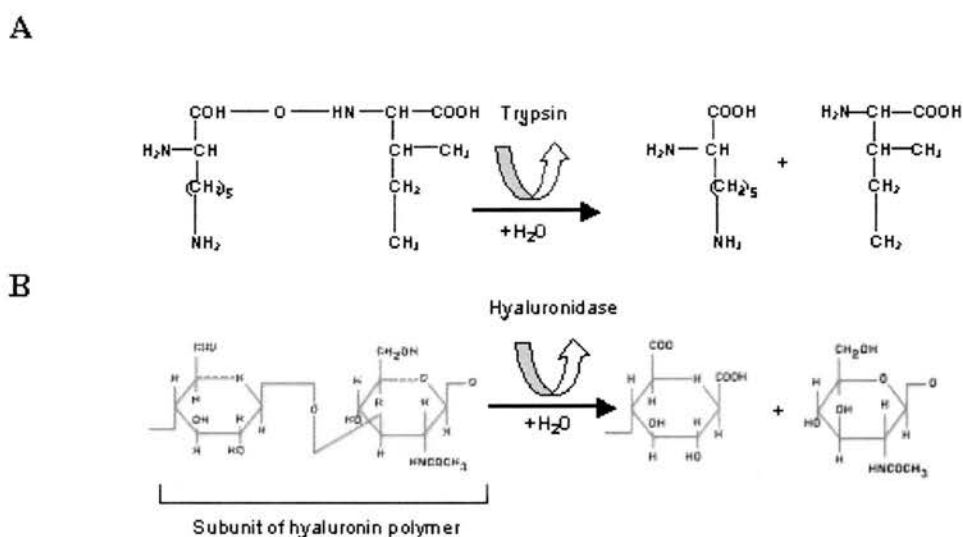


**Fig 1.11 Trypsin or hyaluronidase both allow enzymatic disaggregation of adherent cells**

Trypsin disaggregates adherent cells in culture as it breaks down membrane associated proteins. Hyaluronidase breaks down the polysaccharide which is a component of the extra cellular matrix and is frequently used in medicine to increase the absorption and diffusion of drugs as well as preventing cancerous cells from metastasing. In nuclear transfer work, it is used to remove cumulus cells from oocytes. **Panel A** Trypsin hydrolyses peptide bonds on the carboxyl side of the amino acids arginine and lysine. **Panel B** Hyaluronidase hydrolyses the 1,4-linkages between N-acetyl-beta-D-glucosamine and D-glucuronate residues of the hyaluronate subunits of the polymer hyaluronan. Each hylauronate subunit consists of a uronic acid and an amino sugar linked together by alternating beta-1,4 and beta-1,3 glycosidic bonds.

### Artificial extracellular matrices

Many adherent cells grown in culture fail to secrete an adequate extracellular matrix that will perpetuate appropriate growth and differentiation. To deal with this problem, culture vessels may be coated with artificial matrices prior to being seeded with cells. Two commonly used solutions used to treat culture vessels in this manner

are gelatin (consisting mainly of denatured collagen) and matrigel (a mixture of mainly laminin, collagen IV, nidogen/enactin and proteoglycans).

The section dealing with cell hybridisation has been divided into four subsections for clarity. The sections deal with different types of cell hybrids and discuss how nuclear reprogramming is illustrated.

### **[1.8.3.1] Changes in phenotype and gene expression in cell hybrids**

Aspects of how cell-specific phenotypes are initiated and maintained can be examined using heterokaryons and cell hybrids as model systems. Monoclonal antibodies can be used to study gene expression at the single cell level or in mass cultures at a biochemical and molecular level. Regulatory mechanisms governing cell fate and differentiation have been partially elucidated by studying differences among cell types in the frequency, kinetics, and patterns of gene expression. The results of both strategies applied to heterokaryons and cell hybrids show that the expression of genes in the nuclei of differentiated cells is remarkably plastic and susceptible to modulation by the cytoplasm [Boshart *et al.* 1993].

Isolation of genetically stable cell hybrids can be achieved using selection for transgenes integrated in, or against mutations occurring in, only one of the parental cell types.

Generation of cell hybrids has elucidated three principles of cell differentiation [Review by Boshart *et al.* 1993]:

1. Trans-acting factors that regulate gene expression are involved in cell differentiation.
2. The maintenance of the differentiated state of a cell is a continuing process requiring a constant supply of transcription factors. This can be reversed by cell hybridisation.
3. Regulatory mechanisms repress as well as activate cell specific gene expression.

In intertypic somatic hybrids, genes associated with specialised function are often shut down. Such repression is termed “extinction” [Davidson *et al.* 1974]. One interesting example of hybridisation provided the first direct evidence that telomere

length determines proliferative capacity in human cells [Wright *et al.* 1996]. Extinction of the telomerase gene in hybrids of normal diploid fibroblasts and immortal cell lines had previously been observed [Berry *et al.* 1994]. In immortal cell lines, the ends of the chromosomes (telomeres) are constitutively replenished by the ribonucleoprotein enzyme telomerase [Counter *et al.* 1992] while in somatic cell types, telomere length is found to shorten with age [Lindsey *et al.* 1991][Vaziri *et al.* 1994]. Cell hybrids of immortal and somatic cells are found to have limited life-span and this is due to the extinction of the telomerase gene [Wright *et al.* 1996] [See **Subsection [1.7.3]** for more details of telomeres and telomerases]. Treating these cell hybrids with specific oligonucleotides results in telomere elongation. It is thought telomere elongation reduces the probability of DNAses cutting into essential regulatory and expressed sequences in chromosomal DNA and so extends the life span of the hybrids [Wright *et al.* 1996]. [See **Subsection [1.7.3]** for an explanation of the problem of terminal replication of linear DNA].

It was observed that activation of cell-type specific gene expression can also occur when different cell types are fused [Reviewed by Baron *et al.* 1996]. However gene repression is far more commonly observed than activation [Baron *et al.* 1996]. An interesting example of activation involves fusing erythroid cells at different developmental stages [Broyles *et al.* 1999]. The phenotype of hybrid cells involves the retention of specific chromosomes [Weiss *et al.* 1971] and is dependent on the number of copies of chromosomes retained. For example in hepatoma x fibroblast hybrids possessing only one hepatic chromosome set, the hepatic phenotype is not observed; if however the hybrid contains two sets of hepatic chromosomes, it is. Clearly a delicate equilibrium between positive and negative trans-acting factors mediates hybrid phenotype [Peterson & Weiss 1972]. It is interesting to juxtapose these data with similar findings from imprinting experiments injecting transgenes containing differentially methylated regions (DMRs) [Reik *et al.* 1999]. Introduction of such genes alters the methylation status of the chromosomal DNA also indicating a trans-acting mechanism with a delicate equilibrium [Reik *et al.* 1999].

The characteristics of cell hybrids generated from somatic cells and pluripotent embryonic cells will now be summarised.

### [1.8.3.2] Pluripotent stem cell hybrids

The literature concerning cell hybrids generated by fusions of EC cells and somatic cells offers no clear pattern of extinction and activation of cell-specific genes. Some researchers state that the EC phenotype is dominant in EC cell x somatic cell hybrids [Takagi *et al.* 1983], whereas EC specific genes are shown to be repressed by others [Shimazaki *et al.* 1993][Ben-Shushan *et al.* 1993][Rousett *et al.* 1979]. This is not merely due to differences in selection regime and it has been assumed that this is due to the genomic variance between EC cell lines. It is hoped that EG, ES and EC fusions with somatic cells could give rise to pluripotent stem cell populations eliminating the need for continued isolation of such cells from embryos. This would greatly decrease the demand for foetal and embryonic material in scientific research. The genetic abnormality of EC cells will however seriously limit their use in any new therapy involving nuclear reprogramming.

Another interesting example of nuclear reprogramming in EC x somatic cell hybrids is associated with the reversible repression of the *Oct-4* gene. *Oct-4*, as previously discussed, is involved in the maintenance of pluripotency in ES, EG and EC cells (see **Section [1.5]**). In fusions between EC cells, where *Oct-4* is expressed, and normal differentiating fibroblasts, where it is not, the extinction of *Oct-4* coincides with differentiation of the cell hybrid clones. Introduction of *Oct-4* transactivating elements (chimeric proteins derived from fusion of the transactivating domain of *Oct-4* and the DNA binding domain of GAL4) into the hybrid cells is found to elicit phenotypic changes associated with dedifferentiation [Shimazaki *et al.* 1993]. This observation is consistent with the theory that *Oct-4* is involved in the maintenance of the pluripotent state in EC cells.

Fewer publications refer to cell hybrids generated from EG cells. EG cells display a dominant demethylating effect on somatic chromosomal DNA when fused with lymphocytes. This includes effects on both imprinted and non-imprinted genes [Tada *et al.* 1997]. Germ cells have a strong demethylase activity while lacking factors that protect specific regions from demethylation [Weiss *et al.* 1996]. The link between methylation and change in phenotype has been observed but it is not known

how important methylation status is to the nuclear reprogramming mechanism. *Trans*-acting cytoplasmic and possibly nuclear factors are known to be involved however.

Also reported in EG x somatic cell hybrids is the reactivation of the maternally silent *Peg* allele (*Peg/Mest* is an imprinted gene that is paternally expressed during development), and extensive demethylation of the inactive X chromosome derived from the somatic nucleus [Tada *et al.* 1997]. These epigenetic changes along with maternal *Peg* allele activation show chromatin remodelling but do not further elucidate how nuclear reprogramming may occur.

ES and EG cells are both pluripotent, but they differ in one important respect: parental imprints are maintained in ES cells while erased in EG cells. Surani (1999) suggests that in similar experiments involving hybrids between somatic cells and ES cells, the imprints may not be erased as they are in the presence of ES cells. Tada *et al.* 2001 generated hybrids generated from ES and somatic cells that were still able to contribute to the three embryonic germ layers. Aberrant DNA methylation patterns were found at imprinted loci in these hybrids highlighting that correct expression of imprinted genes is not required for reprogramming of somatic nuclei to pluripotency.

### **[1.8.3.3] Interspecies cell hybrids**

Cells more similar in terms of histology and species have a higher efficiency of *in vitro* hybridisation than those that are not closely related in experiments using PEG as a fusagen [Hart 1983]. However, Siroky & Cervenka (1990) report no such decrease between different mammalian cell types (CHO, HeLa, mouse melanoma cells and human skin fibroblasts) with electrofusion.

The preparation of monoclonal antibodies is the main practical use of trans-species hybridisation [Shirahata *et al.* 1998]. Many different types of chromosome rearrangements are seen in trans-species somatic hybrids. Fluorescence *in situ* hybridisation (FISH) and polymerase chain reaction (PCR) are techniques commonly used to identify integrated chromosomal elements [Boshart *et al.* 1993].

#### **[1.8.3.4] Spontaneous cell fusion and the overestimation of adult stem cell plasticity**

Cell fusion *in vivo* may also explain the apparent plasticity of adult stem cells. Neural, hematopoietic, or mesenchymal stem cells have been reported to give rise to developmentally unrelated tissues [Morrison *et al.* 2001]. Data from coculture experiments have been interpreted to show myocytes can transdifferentiate into adipocytes [Hu *et al.* 1995], pancreatic cells into hepatocytes [Shen *et al.* 2001], keratocytes into fibroblasts [Funderburgh *et al.* 2001] and endothelial cells into cardiomyocytes [Condorelli *et al.* 2001]. It is possible that these data may be explained by spontaneous cell fusion as has been reported elsewhere [Pells *et al.* 2002][Ying *et al.* 2002][Terada *et al.* 2002]. A more recent report by Ianus *et al.* 2003 shows transdifferentiation of bone marrow cells into glucose-competent pancreatic endocrine cells where cell fusion is not thought to have occurred based on results with a Cre-LoxP GFP reporter system. Transdifferentiation and spontaneous fusion may not be mutually exclusive and the spontaneous fusion data does not reduce the prospect of adult stem cells being valuable for therapeutic purposes.



## [1.9] Heat Shock

Major changes in chromatin structure and gene expression patterns are induced when cells are temporarily placed in a moderately hyperthermic environment. Unlike imprinting and X-chromosome inactivation, the effects of this treatment on gene expression do not persist throughout the life time of the cell and are relatively short lived (typically several hours).

Cells transiently exposed to a temperature a few degrees above physiological optimum undergo a process termed a **heat shock response**. The heat shock response entails major changes in gene expression [Csermely *et al.* 1994] and chromatin structure [Iliakis & Pantelias 1989]. The heat shocked cells' capacity to condense chromatin were decreased (when these cells were fused to interphase cells containing factors that normally elicit rapid chromatin condensation, they did not do so) [Iliakis & Pantelias 1989]. Additionally changes in both the pattern of gene transcription and the way mRNAs were recognised for translation resulted in major changes in gene expression [Craig 1986]. When heat shocked, a cell displays a general increase in proteolysis, the strong inhibition of most genes expressed before the heat-shock, and the induction of genes coding for evolutionarily conserved polypeptides termed "heat-shock proteins" (**Hsps**). The induction of hsps is rapidly initiated but is generally short lived in the absence of a continuing stress: hsp synthesis is normally repressed minutes after induction [As reviewed by Mathew *et al.* 2000].

The heat shock response was initially observed by Ritossa (1962). Upon increasing the ambient temperature from 20°C to 37°C, Ritossa reported several new puffs appearing in the polytene chromosomes of *Drosophila*. These were sites of vigorous RNA transcription with some of the RNA synthesised being translated into heat shock proteins. Since this discovery, the heat shock response has been found in all organisms tested including mammals [Craig 1986]. A lot of study has been devoted to this process in order to learn more about the regulation of gene expression [as reviewed by Mathew *et al.* 2000]. This process is termed "heat shock response" only for historical reasons and is more accurately termed the stress response because

other stressors (i.e anoxia, ethanol, arsensite, heavy metals, amino acid analogues [Munro & Pelham 1985], puromycin [Hightower 1980], cell confluence [Watanabe *et al.* 1995] and deprivation of cell nutrients [Neuer *et al.* 2000] can also induce the process.

Several observations suggest that the heat shock response is of fundamental biological importance: the heat shock response is observed in all organisms in which it has been sought, from archebacteria to humans [Craig 1986]; genes coding for heat shock proteins show highest degree of sequence conservation of any genetic system known [Lindquist *et al.* 1988] and heat shock proteins are the first major products of zygotic transcription in mouse embryos [Bensuade *et al.* 1983]. However the physiological role of the heat shock response is still unknown despite the expression levels and structure of heat shock proteins being well characterised. A long held assumption is that the Hsps serve to protect cells from toxic effects of stresses. There is indirect evidence to support this view:

- (a) The induction of Hsps is extremely rapid and this suggests the role of such proteins in an emergency response [Lindquist & Craig 1988].
- (b) The temperature required to induce Hsp synthesis in an organism is related to those experienced in the organism's natural environment. For example in thermophilic bacteria growing optimally at 50°C, the Hsp induction temperature is 60°C [Daniels *et al.* 1985], while in arctic fish living at 0°C, very closely related proteins are induced at 5-10°C [Lindquist & Craig 1988]. Mammals induce heat shock protein expression typically between 39-44°C [Li & Laszlo 1985]
- (c) The correlation between Hsp synthesis and an acquired thermotolerance was initially observed in Chinese hamster fibroblasts [Li & Werb 1982] and has since been shown in many species including human and mouse [Reviewed in Lindquist & Craig 1988]. The papers cited in this review show that cells or organisms are killed rapidly when shifted from their normal growth temperature to a much higher temperature, whereas they are killed much more slowly by the same stress if they are exposed to a mild heat stress beforehand. The assumption many make on the basis of these data is that heat shock protein synthesis, induced by



exposure to a moderate stress, confer the ability to better deal with additional more severe stress. However much data refutes this simple hypothesis: thermotolerance does not always correlate with synthesis of heat shock proteins, and attempts to identify the role of any one hsp in thermotolerance have failed.

### **[1.9.1] Heat shock proteins**

Heat shock proteins are highly conserved polypeptides that are expressed immediately after cells have been moderately shocked. Heat shock proteins have been extensively characterised and are grouped into superfamilies based on their approximate molecular weight: hsp90s, hsp70s and so called “small” hsps. Some are involved in protein-protein interactions. In mammals, hsp90s are generally associated with protein assembly and disassembly, hsp70s have been shown *in vivo* to remove clathrin from coated vesicles [Ungewickell *et al.* 1985][Chappell *et al.* 1986]. It is thought that heat inducible proteins, such as hsp72, are involved with reassembling structures damaged by hyperthermia or other stresses.

The mechanism by which expression of heat shock proteins is induced after stress involves specific DNA sequences called ‘heat shock elements’. These elements are found within the promoters of heat shock genes. In eukaryotes, heat shock elements are found upstream of the TATA box, constituting contiguous arrays of the 5-bp sequence NGAAN present in both orientations [Sorger 1991].

Some heat shock proteins have a role in the cell cycle [See **Section [1.3]**]. Members of the Hsp90 and Hsp70 families show elevated levels in proliferating mammalian cells and a cell cycle-dependent expression [Helmbrecht 2000]. They have been shown to interact with cell cycle factors Cdk4, Wee-1, pRb, p53, p27/Kip1 and are involved in the nuclear localisation of regulatory proteins. Small hsps and their state of phosphorylation and oligomerization also seem to be involved in cell proliferation and differentiation [Helmbrecht *et al.* 2000].

The interaction between heat shock proteins and chromatin structure seems to be bidirectional: the chromatin structure affects hsp expression and this affects

chromatin structure. Hsp90 interacts with histones [Schneider *et al.* 1999] and also induces the condensation of chromatin [Csermely *et al.* 1994].

The synthesis of heat shock proteins can have deleterious effects if expressed at the wrong developmental time e.g. if in the mammalian embryo heat shock protein expression is induced during neural tube development, developmental abnormalities of the forebrain and eye can occur [Walsh *et al.* 1991] [Englen & Finnell 1991].

## [1.10] Chromatin structure

In eukaryotes, genomic DNA is packaged into a highly organised protein containing structure. Chromatin is the term used to describe this DNA-protein complex. It is thought that restoration of totipotency to a cell is mediated in part by changes in chromatin composition and structure [Clarke *et al.* 1998].

Genomic DNA from eukaryotic cells is packaged with histones (basic highly conserved proteins) and also other proteins into chromatin, compacting DNA some 10,000-fold [as reviewed by Zlatanova & Leuba (2003)]. Such condensation of DNA changes accessibility to the nuclear machinery that drives processes such as replication, transcription or DNA repair. Based on historical staining methods chromatin is generally subdivided into highly condensed heterochromatin, which is generally associated with genes that are not expressed, and more diffuse euchromatin, which is generally associated with genes that are.

Chromatin is highly dynamic during development and differentiation. Chromatin not only acts as a DNA packaging element but also as a controller of genetic information either presenting an accessible nucleosome structure or by organising distinct higher order structures that prevent accessibility to underlying DNA. Nuclear reprogramming mechanisms are thought to induce dedifferentiation by stably and safely deconstructing such repressive chromatin conformations [as reviewed by Wade & Kikyo (2002)].

### [1.10.1] Lower order chromatin structure

#### *Nucleosomes*

Decondensed chromatin viewed in the electron microscope looks like ‘beads on a string’. The string is the DNA helix and the beads are DNA protein complexes known as nucleosomes [See **Fig 1.12** overleaf]. Nucleosomes are the fundamental structural unit of chromatin and these assemblages are all composed of histones, other associated proteins and DNA. A nucleosome consists of approximately 1.8 turns of DNA wound around a core particle of histone proteins. The core particle is a

roughly heart-shaped octamer of 4 types of histones: two each of the H2A, H2B, H3, and H4 proteins. These core histones are small ( $M_r$  11,000-15,000) basic proteins that are highly conserved during evolution. Core histones bind DNA very tightly. The N-terminal tails of core histones modulate DNA accessibility within the nucleosome and also affect inter-filament interactions resulting in structural and functional changes within chromatin [Zheng & Hayes 2003]. More will be discussed about posttranslational modifications of core histone tails in **Subsection [1.11.5]**.

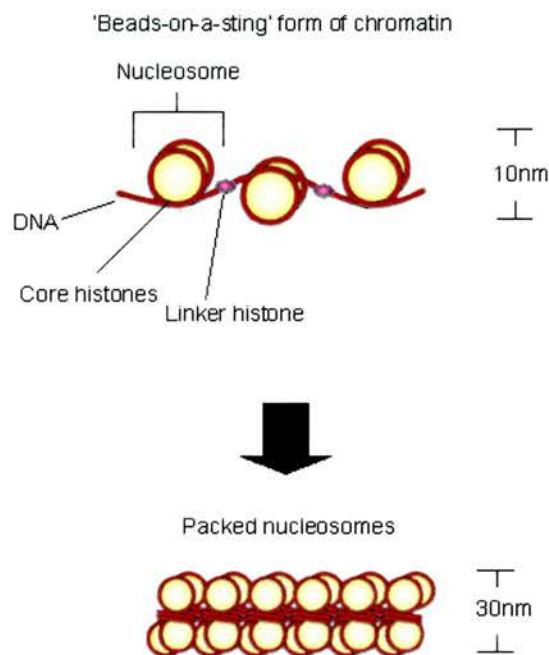


**Fig 1.12 Lower order chromatin structure**

Chromatin is composed of DNA specifically packaged as DNA protein complexes known as nucleosomes. The 10 nm fibre composed of DNA wound around histone cores. The DNA wound around the histone core is termed 'nucleosomal DNA', whereas the DNA that stretches between nucleosomes is termed 'linker DNA'. Histones that bind linker DNA are termed 'linker histones'. 10 nm fibres are tightly wound together to form a 30 nm fibre.

### [1.10.1.1] Nucleoplasmin

Nucleoplasmin is a thermostable histone-binding protein [Laskey *et al.* 1978] consisting of over 200 amino acid residues [Dingwall *et al.* 1987]. It was initially identified in the nuclei of oocytes and eggs from *Xenopus laevis* [Laskey *et al.* 1978], where it constitutes 9-10% of the total protein produced [Krohne & Franke 1980].

Nucleoplasmin has several cellular functions. It was the first protein to be termed a “molecular chaperone” [Laskey *et al.* 1978]. Nucleoplasmin binds histones, shielding their positive charges, preventing non-specific histone-histone interactions thereby facilitating nucleosome assembly [Laskey *et al.* 1978]. Nucleoplasmin is found complexed with histones *in vivo* [Dilworth *et al.* 1987] and is required for nucleosome assembly *in vitro* where it assembles nucleosomes on naked DNA [Earnshaw *et al.* 1980]. As **Fig 1.13** outlines, nucleoplasmin and another molecular chaperone, N1, are thought to assemble nucleosomes in the amphibian system where they mediate DNA binding to core histones.

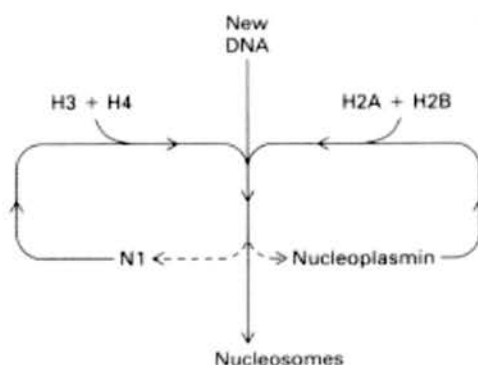


**Figure 1.13 Proposed pathway of nucleosome assembly in *Xenopus* eggs.** Both N1 and nucleoplasmin are acidic proteins that have been shown to associate with histones as indicated [Adapted from Dilworth *et al.* 1987 *Cell* 51:1009].

Nucleoplasmin is also involved in the decompaction of sperm DNA at fertilisation. It binds and removes sperm basic proteins, called protamines, from DNA-protamine complexes in sperm [Iwata *et al.* 1999]. It also replaces these basic proteins with histones [Leno *et al.* 1996]. As is the case with the histones, nucleoplasmin is thought to bind specifically to the protamine via its polyglutamic acid tract.

Nucleoplasmin is known to play an important role in the transfer of proteins into the nucleus [Dingwall & Laskey 1986]. It is associated with ribonucleoproteins. Based on this observation, it has been suggested that this protein may also have a role in post transcriptional events [Moreau *et al.* 1986].

### [1.10.1.2] Linker histones and histone switching during development

Linker histones, also called H1 histones, bind both intra-nucleosomal DNA [See Fig 1.12] and core histone tails [Hill 2001][Kornberg & Lorch 1999]. The bonds between linker histones and linker DNA are weaker than corresponding interactions between core histones and nucleosomal DNA. Genes coding for linker histones also display a lot more sequence variability than highly conserved genes coding for core histones [Kornberg & Lorch 1999].

Interestingly, during development of many non-mammalian organisms, the species of linker histones associated with DNA reproducibly changes during development. There are embryonic and somatic species of linker histones that are found in chromatin at the embryonic and more developed stages of development respectively. When associated with chromatin, linker histones influence the accessibility of regulatory factors to the DNA and play an important role in controlling gene expression [Clarke *et al.* 1998][Alami *et al.* 2003]. The presence of stage-specific linker histone subtypes in non-mammalian oocyte and embryos, together with their role in regulating chromatin structure and gene expression suggest that linker histones may play a role in nuclear reprogramming in these species [Fu *et al.* 2003].

Linker histones are less well characterised in mammals and their roles in chromatin structure and regulation of gene expression are at present unclear. Six linker histone subtypes have been identified in mammalian chromatin [Wang *et al.* 1997][Parseghian and Hamkalo 2001]. These have been divided into two groups: somatic linker histones (H1a-e) and the embryonic linker histone H1<sup>o</sup>. Somatic linker histones are found in chromatin of oocytes and somatic cells, they share a highly conserved globular domain and mRNA coding for these histones fluctuates during the cell cycle, rising sharply during S phase. In contrast, embryonic linker histone H1<sup>o</sup> is expressed highly only in oocytes and some non-dividing cells. It's abundance in embryonic cells decreases rapidly after the zygote begins to divide [Fu *et al.* 2003]. H1<sup>o</sup> has a larger configuration than somatic linker histones and lacks their conserved globular domain. Furthermore, the mRNA coding for it maintains a constant level throughout the cell cycle.



It is now clear that, as in non-mammalian species, linker histone complement in mammalian chromosomes changes during late oogenesis and early embryogenesis [Fu *et al.* 2003]. Unclear however is why, assuming linker histones are important to chromatin conformation and gene expression in mammalian cells, mice lacking somatic linker histones (H1c, H1d or H1e) [Fan *et al.* 2001] or even the embryonic linker histone H1<sup>o</sup> [Sirotkin *et al.* 1995] do not display any phenotypic abnormalities. Also at present unclear is whether mammalian somatic linker histone subtypes are functionally different to each other. It is known that different subtypes bind to different locations in the chromatin but as yet differences in the effects they cause have not been observed [Khochbin 2001]. Further characterisation of mammalian linker histone subtypes and variants of subtypes and investigation into the changing chromatin complement of such proteins during development will help clarify their role in differentiation and nuclear reprogramming in mammalian cells.

### **[1.10.2] Higher orders of chromatin structure**

#### *Chromatin folding*

Most of the chromatin in the nucleus is in the form of 30 nm filaments [See **Fig 1.12**]. The exact structure of 30 nm filaments is still being elucidated although it is known formation of these filaments is highly dependent on H1 being present and is influenced by the N terminal histone tail domains of core histones. The actual location of linker histones within the 30 nm fibre has yet to be identified [as reviewed by Zlatanova & Leuba 2003].

#### *Chromatin loops*

Little is known about additional levels of chromatin organisation beyond 10 nm and 30 nm filaments though much evidence exists to support the idea that interphase chromosomes are composed of loops of chromatin filament. The loops are attached to the nuclear skeleton at their bases and project into the interior of the nucleus [Zlatanova & Leuba 2003].



### *Higher levels of chromatin structure*

Very little is known about chromatin structure above the loop level. It appears such higher levels of chromatin organisation do not need to be maintained for complete reprogramming to occur, at least in sheep: Loi *et al.* 2002 transferred nuclei from severely heat shocked (75°C, 15 min) sheep granulosa cells to enucleated oocytes and the reconstructed embryos developed to live offspring with an efficiency higher than non-heat shocked controls. Studies using mammalian somatic nuclei show high-order chromatin structure to have been destroyed in nuclei from cells heat shocked to this extent [Balbi *et al.* 1989][Shih & Lake 1972]. Also mouse sperm nuclei in which all elements of chromatin structure are lost except the DNA loop anchored in the nuclear matrix were able to generate live offspring when injected into oocytes [Ward *et al.* 1999].

### **[1.11] Nuclear reprogramming and associated chromatin modification**

Nuclear reprogramming involves introducing heritable, but reversible changes in gene expression without altering the DNA sequence, resulting in a restoration of developmental potential. Such reprogramming affects the local structure, composition and remodelling of chromatin that regulates the transcriptional competence of genes and controls the accessibility of regulatory factors to DNA. Cloned animals frequently show epigenetic abnormalities while the sequence of their genomic DNA remains unaltered from that of the donor nuclei [as reviewed by Shi *et al.* 2003]. Complete establishment, maintenance and resetting of epigenetic states are thought to be vital for successful reprogramming. Epigenetic modifications such as DNA methylation, genomic imprinting, X-chromosome inactivation, chromatin remodelling, histone modification, and telomere maintenance are all likely to be associated with the mechanism responsible for nuclear reprogramming [Shi *et al.* 2003].

How epigenetic modifications regulate gene expression is still unclear and much remains to be learnt about how epigenetic modifications are initiated, what their



consequences are, and whether they have a role to play in the restoration of developmental potential. Such epigenetic modifications and why they might be important to nuclear reprogramming will now be reviewed.

### [1.11.1] DNA Methylation

DNA methylation is the best studied epigenetic modification likely to play a part in nuclear reprogramming in mammals. During development it plays an essential role in the determination of cell fate and cell type-specific gene expression by transcriptional repression [Holliday & Pugh 1975][Riggs 1975]. Methylation of DNA takes place at CpG dinucleotides. Small regions in the genome with unusually high cytosine and guanine nucleotide content relative to the rest of the genome are referred to as CpG islands. In the human genome 29,000 of the conservatively estimated 40,000 genes have associated CpG islands, which are generally unmethylated in normal tissues. In contrast, CpG islands associated with imprinted genes, X-linked genes in females, germ line-specific and tissue specific-genes are normally methylated [Shi *et al.* 2003].

The formation of a covalent bond between a methyl group and a cytosine moiety within a CpG dinucleotide is catalysed by cytosine methyltransferases (Dnmts). Dnmt1 is found to be responsible for the maintenance of DNA methylation patterns where Dnmt3a and Dnmt3b are required for *de novo* methylation of DNA. Targeted disruption of these enzymes alters DNA methylation patterns and has profound biological consequences: *Dnmt1* knockout mouse embryos die at mid-gestation [Li *et al.* 1992]. Mouse ES cells lacking *Dnmt1* exhibit increased mutation rates of both the endogenous *hprt* gene and a viral thymidine kinase transgene indicating greater genomic instability [Chen *et al.* 1998]. Overexpression of Dnmt1 leads to loss of imprinting and embryonic lethality [Biniszkiwicz *et al.* 2002] *Dnmt3a* and *Dnmt3b* knockouts also exhibit embryonic lethality in mice [Okano *et al.* 1999]. Other studies, using an inhibitor of DNA methylation, 5-azacytidine, showed an increase in rat embryonic abnormalities during gestation in a dose dependent manner [Doerksen and Trasler 1996]. Taken together these observations

show DNA methylation is necessary for appropriate gene expression and normal development.

During normal mouse embryonic development, there are two times where the genome is globally demethylated and then remethylated, one occurs during the development of germ cells [Lee *et al.* 2002][Hajkova *et al.* 2002] and the other happens shortly after fertilisation [Monk *et al.* 1987][Santos *et al.* 2002]. During germ cell development, genome-wide demethylation leads to mitotic arrest of male and female primordial germ cells (PGCs). *De novo* methylation is initiated before birth in the male germ line, whereas it occurs after birth with the female [Hajkova *et al.* 2002]. During gametogenesis, both the oocyte and sperm genomes become heavily methylated and consequently cease gene transcription. Prior to fertilisation, the sperm genome is tightly packed with small proteins called protamines, whereas the oocyte genome is packaged with histones in nucleosomes as outlined in **Subsection [1.10.1]** [Perreault 1992]. When the egg and sperm fuse, the sperm DNA is exposed to oocyte cytoplasm and is rapidly remodeled. Protamines are quickly removed, by the nuclear chaperone nucleoplasmin (See **Subsection [1.10.1.1]**), and replaced with histones and sperm genome-wide demethylation ensues before the zygote divides [Oswald *et al.* 2000]. In contrast, demethylation of the oocyte genome occurs much more slowly due to the failure to demethylate DNA. By the morula stage, both sperm and oocyte genomes are hypomethylated [Mayer *et al.* 2000]. Genome-wide *de novo* methylation occurs at the blastocyst stage, especially in cells contained within the inner cell mass (ICM) [Dean & Ferguson-Smith 2001]. By gastrulation there is an almost uniform methylation pattern between homologous chromosomes, with the exception of imprinted genes which display different allelic methylation states depending on whether they were derived from the maternal or paternal genome [Surani 2001].

The degree of genomic methylation varies depending on cell lineage. Most somatic cells are heavily methylated, although trophoblast derived lineages that contribute to placental formation as well as the yolk sac are undermethylated [Reik *et al.* 2001]. Little is known about what the post-zygotic demethylation and remethylation waves do biologically or the reason for differences in DNA methylation patterns exhibited by the parental genomes immediately after

fertilisation. Oswald *et al.* 2000 suggest that such changes in methylation are needed to reprogram the highly differentiated gametic genomes so that totipotency is restored and both paternal and maternal genomes can direct normal development.

The timing and cell-type specificity of post fertilisation global DNA remethylation varies with species of mammal: *eg.* extensive genome wide methylation is observed both in the ICM and trophectoderm in the 8-16 cell stage of bovine embryonic development whereas in mouse embryos equivalent methylation is only observed approximately four cell divisions later and then only in cells of the ICM [Dean *et al.* 2001].

Incomplete and abnormal DNA methylation have frequently been observed in cloned animals. The methylation status in preimplantation cloned embryos, especially at repeat sequences, closely resembles that of the donor cell genome, indicating incomplete removal of methylation patterns.

Differential biparental genomic demethylation does not occur in NT reconstructed embryos. The genome from the donor nucleus is packaged with histones (not protamines) and when exposed to ooplasm shows the same slow decline in genome wide methylation as seen in the maternal haploid genome during normal development.

Cloned animals generated by nuclear transfer often express abnormal methylation patterns. No active demethylation was observed in cloned bovine embryos generated by Bourc'his & Viegas-Peguignot (2001) and transferred nuclei maintained methylation patterns associated with somatic nuclei. Furthermore, premature *de novo* methylation was observed in a large proportion of nuclei post transplantation to enucleated oocytes. During normal bovine embryonic development, *de novo* methylation occurs at the 8-16 cell stage but in the reconstructed embryos, it was observed at the 4-8 cell stage [Dean *et al.* 2001].

In the mouse, aberrant genome-wide DNA methylation patterns in 2 cell stage embryos correlate well with the failure to develop to the blastocyst stage and may also contribute to embryonic lethality later in the pregnancy [Shi & Haaf 2002]. The fact that cows and sheep have a longer period than the mouse before *de novo* methylation begins may explain the apparent differences in cloning efficiencies between murine and bovine species [Shi *et al.* 2003]. *De novo* methylation in normal

cow and sheep embryos does not start naturally until the 8-16 cell stage whereas in mouse embryos it starts at the two cell stage. Passive removal of methylation patterns would seem more probable as the start of *de novo* methylation occurs later in development in these species.

Oocytes and fertilized eggs express different Dmnts (cytosine methyltransferases) and Dmnt-associated factors eg. Dmnt1o, a oocyte-specific form of Dmnt1, is not found in fertilized eggs [Ratnam *et al.* 2002] and Dnmt3L, a Dmnt like factor which is associated with Dmnt3a and Dmnt3b is found expressed in fertilized eggs but not oocytes [Bourc'his *et al.* 2002]. It has been speculated that these differences may underly the aberrant DNA methylation patterns in reconstructed embryos. If this were confirmed, Dnmt1o, Dnmt3L as well as other differentially expressed factors may be used as markers for nuclear reprogramming [Shi *et al.* 2003].

### **[1.11.2] Genomic Imprinting**

Genomic imprinting is an epigenetic mechanism that controls the expression of an allele on the basis of its parternal origin (i.e. whether it was derived from the maternal genome in the egg or the paternal genome in the sperm). As a result of imprinting, mammalian paternal and maternal genomes are non-equivalent and for normal development to ensue both parental genomes must be present. Parthenogenic embryos where only the maternal genome is represented only develop to the blastocyst stage [as reviewed by Renard *et al.* 1988].

In nuclear transfer experiments, where imprints were removed from the paternal genome prior to transfer, the resultant reconstructed embryos have abnormalities associated with extraembryonic tissues whereas when maternal imprints are removed the embryo appears abnormal. This suggests paternal genome has more influence on extra embryonic development and the maternal genome has greater affect on the development of the embryo proper. Imprinting also affects other processes important to reproduction including energy metabolism, lactation and parental behaviour to offspring [Lefebvre *et al.* 1998]

Imprinted genes display differential DNA methylation and, as previously outlined, such epigenetic modification is known to play a role in the repression of gene expression. Many imprinted genes are found clustered in groups that display different DNA methylation profiles from the rest of the genome, consequently these loci are termed differentially methylated regions or DMRs [Tilghman *et al.* 1999][Reik *et al.* 2001]. While DNA methylation is generally associated with the repression of gene expression, Surani (2001) states that the relationship between imprinted genes and methylation is more complex: methylation of DMRs can be required for the expression of imprinted genes. An example of this is the imprinted *Igf2/H19* locus on mouse chromosome 7. Methylation of the DMR upstream of *H19* prevents a regulatory factor CTCF from binding the parental insulator, making the *Igf2* promoter accessible to enhancer elements that are shared by *H19* and *Igf2*, allowing the expression of *Igf2* [Bell & Felsenfeld 2000][Hark *et al.* 2000].

During early mammalian development, the global epigenetic state of the genome undergoes extensive change, however the epigenetic state of imprinted genes appears to remain relatively stable. Initiation of imprints occurs in primordial germ cells, diploid cells that produce gametes. During PGC migration to the genital ridge a wave of global DNA demethylation occurs at the same time as imprint erasure [Kafri *et al.* 1992][Hajkova *et al.* 2002] and it is suspected that DNA methylation plays a role in the re-introduction of imprints during gametogenesis. After imprints have been established in the germline, the parental genomes are not equivalent with the maternal genome displaying methylation at many of its imprinted loci while the paternal genome displays a reciprocal pattern. Such epigenetic differences are then maintained during normal development from fertilisation through to adulthood. Erasure and resetting of genomic imprints is important for the removal of aberrant epigenetic modification that occurred during the lifespan of the previous generation [Surani 1999].

Interestingly, the phenotypes of some cloned animals mirror those of animals in which imprinted genes have been mutated [Wang *et al.* 1994][Ludwig *et al.* 1996]. It is speculated that imprinting may be disturbed during the nuclear transfer process and that this accounts for frequent instances of failure to generate viable offspring.



Unlike PGCs, imprints can neither be initiated nor deleted in the mature oocyte, so the genomic imprints cannot be altered by simply exposing chromatin to oocyte cytoplasm [Surani *et al.* 1986]. From this one might expect that transfer of a nucleus into an oocyte would not affect somatic genomic imprints but there are exceptions [Solter *et al.* 2000] where imprints have been erased and this leads to abnormal growth in both the embryo and associated extra-embryonic tissues.

Loss of appropriate imprinting patterns is commonly observed in cloned embryos and newborn animals [as reviewed by Shi *et al.* 2003]. This is thought to occur because (a) the DMRs of imprinted genes are not properly protected from genome-wide demethylation which occurs after nuclear transfer; and (b) reconstructed embryos do not lose and reinitiate their imprints, as occurs in PGCs, so any errors acquired during the lifetime of the somatic nucleus persist in the reconstructed embryo [Hajkova *et al.* 2002].

There is no clear correlation between abnormal expression of any of the 54 imprinted genes identified in mice and the appearance of aberrant development in cloned embryos [Shi *et al.* 2003].

*In vitro* culture and manipulation of cells disrupts imprinted gene expression but such treatment is not the sole reason for it. In sheep and cattle, large offspring syndrome (LOS) could arise as a consequence of embryo culture, where DMR2 methylation and *Igf2r* expression are affected by components of serum [Young *et al.* 2001]. The imprinting status of *H19* in mouse embryos is also affected by culture conditions [Doherty *et al.* 2000]. The length of *in vitro* culture of mouse ES cells is correlated with the frequency of imprinting errors [Dean *et al.* 1998].

### **[1.11.3] X Chromosome Inactivation**

Abnormal XCI is observed in embryos generated by parthenogenesis and also in those reconstructed using nuclear transfer [as reviewed by Shi *et al.* 2003]. Parthenogenic embryos have two maternally derived X-chromosomes and both remain activated in associated extraembryonic cells. It seems some imprinting mechanism makes maternally-derived X chromosomes resistant to being inactivated [Tada & Takagi 1992]. During somatic nuclear transfer, the nucleus to be fused with



the ooplasts contains one inactive and one active X chromosome. However after transfer, some researchers have reported aberrant reactivation of X-chromosomes in reconstructed bovine embryos [Wrenzycki *et al.* 2002]. Xue *et al.* 2002 reported the aberrant expression of 9 X-linked genes in several dead bovine calf clones. Differences in which parental X chromosome was inactivated in placental cells was reported between these calves and calves which survived.

#### **[1.11.4] Telomere maintenance and telomerase activity**

Perhaps surprisingly, there are many reports showing telomere lengths are maintained or lengthened after nuclear transfer [Betts *et al.* 2001]. Lanza *et al.* 2000 used nearly senescent bovine fetal cells as nuclear donors and reported the telomere length restored or in some cases elongated in the cloned animals. Wakayama *et al.* (2000) serially re-cloned cloned mice for up to 6 generations and reported no decrease in telomere length. Thus, while telomere length can be a contributory factor to the death of clones, it is not the only factor [Tian *et al.* 2000]. The generation of larger numbers of cloned animals that display a developmentally normal lifespan suggests telomere length is commonly restored by nuclear transfer at least using certain cell types [Yanagimachi 2002]. How telomerase activity is reinitiated after nuclear transfer is, however, poorly understood.

The stage at which high telomerase activity is observed in reconstructed bovine embryos after nuclear transfer is significantly delayed compared to normal development. Control embryos generated by IVF display high telomerase activity at the 8-16 cell stage whereas in cloned embryos comparable activity was only observed at the blastocyst stage [Betts & King 1999].

#### **[1.11.5] Histone modifications**

Acetylation, methylation, phosphorylation, ADP-ribosylation and ubiquitination of the N-terminal tails of core histones have been linked to changes in high-order chromatin structure [Turner 2002]. Such epigenetic modifications are thought to be important in altering the accessibility of regulatory factors to DNA and

affecting gene transcription. It has been hypothesized that combinations of these epigenetic modifications regulate gene expression in a consistent manner and therefore comprise a “histone code” [Turner 2000].

Of the histone modifications mentioned, histone acetylation is the best studied. Histone acetylation generates a more open chromatin structure that generally correlates with transcriptional activation, whereas histone deacetylation is generally associated with repression of transcription. Deacetylated histone tails bind repressor proteins, whereas acetylated tails bind bromodomain motifs of certain regulatory factors that promote changes in chromatin structure and transcriptional activation [Winston and Allis 1999]. Histone acetylation, at particular regions within the genome, is controlled by the activities of histone acetyltransferases (HATs) and deacetylases (HDACs). Interestingly, Dnmts and HDACs have been found in the same protein complexes indicating that DNA methylation and histone deacetylation are linked in the mechanism responsible for transcription repression.

Histone acetylation of a locus is not always sufficient to induce transcription but it does facilitate such induction by reducing folding of nucleosomal fibres [Wolffe and Matzke 1999]. It is thought that histone acetylation acts in conjunction with chromatin remodeling mechanisms to facilitate gene expression. Such complexes weaken histone-DNA interactions and increase the accessibility of nucleosomal DNA to regulatory factors (See **Subsection [2.11.6]**).

Histone methylation occurs on the arginine and lysine residues. Certain lysine residues at specific positions in the N-terminal tails of histones H3 and H4 are thought to be important for gene repression. For example, methylation of Lys9 of histone H3 (MeK9H3) forms a binding site for heterochromatin protein 1, a protein commonly found in heterochromatin and inactivated chromatin of Xi [Bannister *et al.* 2001][Cowell *et al.* 2002]. The exact mechanism by which this could initiate repression of gene expression is, as yet, not understood. In contrast to histone acetylation and phosphorylation, some histone methylation at lysine residues appears to be a stable epigenetic modification, though the biological consequences are

unclear. Some of the enzymes responsible for methylation of histone tails, HMTases, have been identified in mouse and human [Kouzarides 2002].

#### **[1.11.6] Chromatin remodeling complexes**

In addition to covalent modification to the N-terminal tails of core histones, chromatin structure can be altered in a regulated manner by protein complexes, so called chromatin remodeling complexes, that utilize energy derived from ATP hydrolysis. These complexes change the position and/or structure of nucleosomes such that the accessibility to nucleosomal DNA is enhanced [Kingston & Narlikar 1999].

Deletion or mutation of components of chromatin remodeling complexes can cause death or developmental aberrations in mammals. Murine embryos deficient in either SNF5 (commonly found in chromatin remodeling complexes) or Brg1 die before implantation [Müller & Leutz 2001]. Mice with mutations in Brm are viable and fertile, but exhibit 10-15% increase in bodyweight over their wildtype littermates [Reyes *et al.* 1998].

Chromatin remodeling complexes are involved in many processes beside gene transcription which include: DNA replication; DNA recombination; DNA repair and cellular differentiation [Längst & Becker 2001].

#### **[1.12] Summary**

Nuclear reprogramming may be defined as the process by which a cell reacquires developmental potential [Singh 2000]. Cell hybridisation and nuclear transfer have demonstrated that a mammalian somatic cell's differentiated state may be reprogrammed. The factors responsible for nuclear reprogramming are currently being sought. Nuclear reprogramming involves chemical and structural chromatin changes. When mechanisms by which mammalian cells can be reprogrammed are elucidated, resultant technologies will be of profound benefit to science and medicine.

**[1.13] Objectives**

- 1) To generate and optimise a system for generating cell hybrids from murine ES cells and somatic cells.
- 2) To characterise resultant hybrid lines and assess whether nuclear reprogramming has taken place.
- 3) To investigate the effect of heat shock on the murine cell hybrid system.
- 4) To investigate the effect of ES cell confluence and passage number on the murine cell hybrid system.
- 5) To investigate the effect of quiescence on the murine cell hybrid system.
- 6) To investigate the effect of *Xenopus* nucleoplasmin on the murine cell hybrid system.
- 7) To generate cell hybrids from human ES and EC cells.

## **[2] Materials and Methods**

Protocols for generating solutions and media used here are listed separately in the appendices (**Section [12-1]**). All reagents were sourced from Sigma-Aldrich, Inc. ([www.sigma-aldrich.com](http://www.sigma-aldrich.com)) unless otherwise stated.

### **[2.1] Cell Culture**

#### **[2.1.1] Routine Culture Conditions**

##### **[2.1.1.1] Murine ES cells and EC cells**

#### **Culture of murine ES/EC cells with Leukemia Inhibitory Factor (LIF)-supplemented medium**

Cells were grown at 37°C (5% CO<sub>2</sub>) on 0.1% gelatin-treated tissue culture flasks (Iwaki, [www.iwaki.com](http://www.iwaki.com)) and fed daily with murine ES medium. All media were stored at 4°C when not in use. Media older than 2 weeks were discarded.

#### **Disaggregation of murine cells**

To disaggregate cells, medium was aspirated from the flask and the cells were washed with 1x **Phosphate Buffered Saline (PBS)**. **Trypsin/EGTA** disaggregation solution (**TEG**) was then added until the surface of the flask was completely covered. The flask was then incubated at 37°C for 2-3 minutes. Cells were then detached by slapping the flask. 5 ml of medium were added to inhibit further trypsin activity and pipetted up and down several times to obtain a single-cell suspension. The resultant suspension were then transferred to 15 ml Falcon tubes and centrifuged at 3,000g for 5 minutes. The supernatant was discarded and the pellet of cells was resuspended in fresh medium and plated out or treated as required.

## **Freezing and resuscitation of cells**

A similar freezing procedure was used for all cell types in this study. 2x freezing mix was made by mixing 15 ml of culture medium, 5ml dimethyl sulfoxide DMSO (Sigma) and 5ml of foetal calf serum [or 5 ml Knockout SR serum replacement (Life Technologies) for human ES cell lines]. This solution was filtered and stored at  $-20^{\circ}\text{C}$  when not in use. When cells were to be placed in cryostasis, they were disaggregated, resuspended in medium ( $1-5 \times 10^7$  cells / ml) and placed on ice. One volume of ice-cold freezing mix was added and the suspension was gently mixed and aliquoted into pre-cooled cryovials. The cryovials were stored at  $-80^{\circ}\text{C}$  for two days and were then placed into liquid nitrogen.

To resuscitate the cells, cryovials were placed in a water bath ( $37^{\circ}\text{C}$ ) until thawed. Five milliliters of complete medium were added to the contents of a vial in a 15 ml Falcon tube, and then centrifuged at  $3,000\text{ g}$  for 5 minutes. Supernatant was discarded and pellets resuspended in medium for plating out.

### **[2.1.1.2] Human ES cells**

Human ES cells were cultured using medium conditioned by murine primary embryonic fibroblasts (PEF) in a manner similar to Xu *et al.* 2001.

### **Derivation of primary embryonic fibroblasts from mid-gestation murine fetuses**

Primary Embryonic Fibroblasts (PEFs) were derived from day 13.5 murine fetuses as follows: The uterine horns of a pregnant CBA female mouse were removed on the thirteenth or fourteenth day of pregnancy. Fetuses were liberated from the uterine horns. Each fetus was then dissected such that the placenta, membranes and the soft red tissue (liver, heart and other viscera) was also removed. The dissected fetuses were then separately vortexed in TEG until the solution went cloudy with disaggregated cells. TEG

was then neutralised with Primary Embryonic Fibroblast (PEF) medium [See **Section [13.1]** for details of media and solution preparation]. Large clumps of cellular debris were allowed sediment out and after 4 minutes the cells in suspension were removed. The cells were spun down (3,000 g, 5 min) and resuspended in PEF medium before being used to seed flasks (1 embryo was normally used to seed one 75 cm<sup>2</sup> flask).

### **Routine culture of PEF feeders**

Murine primary embryonic fibroblasts were used as feeders for the human ES cells. When being resuscitated or expanded, these cells were grown at 37°C (5% CO<sub>2</sub>) on tissue culture plastic flasks (Iwaki, [www.iwaki.com](http://www.iwaki.com)) and fed daily with complete PEF medium. Prior to using them to condition medium, the cells were washed for times with 1x **H**epes **B**uffered **S**aline (HBS) to remove serum that would induce human ES cell differentiation.

### **Conditioning of human ES cell medium with PEF feeders**

When culturing human ES cells, the requirement for feeder cells could not be replaced with LIF supplemented medium (as is the case with murine ES cells). It was necessary to condition human ES medium using murine primary PEFs prior to its use on the cells. PEFs provided the necessary growth factors for successful culture of the human ES cells.

PEFs were grown at 37°C (5% CO<sub>2</sub>) on tissue culture flasks (Iwaki) and fed human ES medium. Human ES medium was conditioned on feeders for 24-48 hour prior to feeding human ES cells. All conditioned medium was filtered and 4 ng / ml fresh human recombinant basic fibroblast growth factor was added directly to the medium before feeding human ES cells. Flasks with dead PEFs (seen as either adherent or floating circular refractile cells) were not used as feeders. Typically, PEFs could be passaged four times before significant levels of cell death were seen.



### **Culture in conditioned human ES medium**

Human ES cells were cultured on GFR matrigel (Becton Dickinson, [www.bectondickinson.com](http://www.bectondickinson.com)) a matrix of laminin, collagen IV and heparin sulphate. Aliquots of matrigel were thawed overnight on ice and diluted 1:100 with cold **Knockout Delbeccos Modified Essential Medium (KO DMEM)**. Flasks were then coated with this solution and the matrigel was left to polymerize for at least 1 hour at 37°C. Flasks were then washed with 1x HBS to remove any excess matrigel. Human ES cells were grown at 37°C (5 % CO<sub>2</sub>) on matrigel treated tissue culture flasks and fed daily with murine embryonic fibroblast (MEF) conditioned human ES medium.

### **Disaggregation of human ES cells**

The protocol for disaggregating human ES cells is similar to that previously described for murine cells (See **Subsection [2.1.1.1]**), although there are the following differences:

- 1) 1xHBS, instead of 1xPBS, was used to wash the cells. The cells will “round up” and lower plating efficiencies will be observed if PBS is used.
- 2) Human ES cells lyse and clump together if overexposed to TEG. The cells need to be closely monitored under the microscope and the duration of TEG exposure minimised to prevent this occurring. Human ES cells grown on matrigel are less easily detached than murine cells, thus vigorous slapping of the flask is required to detach the cells after TEG has been added.
- 3) As human ES medium lacks serum protein and thus trypsin inhibitors, it is necessary to add more medium to dilute the trypsin activity and prevent cell lysis (typically 10 ml hES medium per 1 ml of TEG was added prior to centrifugation).

## **[2.1.2] Transfection**

Transfection is the genetic modification of cultured animal cells by the uptake of DNA from the culture medium. This process was used throughout this work mainly to generate selectable cell lines.

### **[2.1.2.1] Transfection of murine ES cells and human EC cells**

#### **Lipofection**

Transfection was performed using the Effectene kit (Qiagen). For transfection of 40-80% confluent cell cultures in 60 mm dishes, best results were observed using the following proportion of reaction components: ~2 µg of DNA in up to 150 µl of EC buffer; 16 µl of Enhancer solution and 20 µl of Effectene reagent.

#### **Electroporation**

Mouse ES cells were passaged 24 hr prior to transfection so that one 80% confluent 175 cm<sup>2</sup> flask was available for each electroporation on the day of the experiment. The medium was changed 2 hours prior to the electroporation to maximize the number of dividing cells and correspondingly the transfection efficiency. The cells were harvested with TEG. 60 mg linearised, EtOH precipitated DNA was used for each stable transfection experiment. This DNA was resuspended in 200 µl 1xHBS. DNA was resuspended using a pipette as vortexing might cause shearing of the DNA. The cells were resuspended in 10ml mES medium, counted and pelleted.  $10^7$  cells were resuspended in 800µl of 1xHBS. The cells were mixed thoroughly with DNA and the suspension was placed in an electroporation cuvette with a 0.4 cm electrode gap. Using a genepulser (BIORAD, [www.biorad.com](http://www.biorad.com)), a pulse of 800 V, 3 µF was applied. The recorded time constant should lie within a range from 0.1 to 0.19. The pulsed cells were left in the cuvette at room temperature for 15-20 minutes before transferring them to 5ml of ES medium. The cells were then seeded at  $5 \times 10^6$  cells/15 cm plates. Forty eight hours

after electroporation, selection media was applied to the plates and colonies of stably transfected clones were picked when they had grown to the appropriate size (this typically takes 10-14 days).

### [2.1.2.2] Transfection of human ES cells

Transfection of hES cells was performed using the Lipofectamine 2000 kit (Invitrogen) following the manufacturer's instructions. H9 cells were plated at  $1 \times 10^5$  per well of 6 well plate (at passage 55) forty eight hours later transfected using Lipofectamine 2000 (life technologies).

### [2.1.3] Cell lines

Cell lines used but not derived in this work:

Cell line	Genotype	Source
HM-1 (mES)	HPRT <sup>-</sup>	Dr. Jim McWhir
TNG-8 (mES)	HPRT <sup>-</sup> , neo <sup>R</sup> , GFP <sup>+</sup> , rtTA <sup>+</sup> HM-1 subclone	Dr. Edward Gallagher
Socs2 (mES)	HPRT <sup>-</sup> neo <sup>R</sup>	Dr. Jim McWhir
NCCIT (hEC)	Wild type	ATCC
NTERA2 (hEC)	Wild type	ATCC
TG11.nR (hEC)	HPRT <sup>-</sup> , neo <sup>R</sup> NTERA2 subclone	Prof. Peter Andrews, University of Sheffield
H9 (hES)	Wild type	Geron Corporation
H1 (hES)	Wild type	Geron Corporation

## [2.2] Cell fusion and hybridisation

### [2.2.1] Electrofusion

Electrofusion is the induction of cell fusion by the administration of an electric pulse (or pulses) to a cellular suspension. The electrofusion protocol described was the amalgamation of ideas from several sources, with the principal influence being the work of Tada *et al.* (1997) and unpublished experiments by the student and Drs. Gallagher and McWhir.

Experiments where reprogramming of the *Oct4* locus was investigated used somatic cells derived from CBA <sup>*Octneo/Octneo*</sup> mice [McWhir *et al.* 1996]. This transgenic line was generated by pronuclear injection of p*Octneo1* into F1 (CBA X C57BL/6) embryos. The p*Octneo1* plasmid contains a 1.9kb sequence 5' of the *Oct4* coding sequence (containing the *Oct4* promoter and proximal enhancer) linked to the bacterial neomycin cassette. Embryos with a genetic background which was 87.5% CBA, 12.5% C57BL/6 were obtained by mating homozygous p*Octneo1* males with CBA females. The HM-1 ES cell line was used in most murine cell fusion experiments. This line was derived from hypoxanthine phosphoribosyltransferase (HPRT) deficient strain 129/Ola mice [Magin *et al.* 1992] (**Subsection [2.2.4]** discusses HPRT and HAT selection). The protocol for fusions using CBA <sup>*Octneo/Octneo*</sup> mice and G418 and HAT double selection is now outlined:

Thymocytes were obtained from female CBA <sup>*Octneo/Octneo*</sup> mice at age 6-7 weeks. Mice were dissected and the thymocytes removed and placed in 1x PBS. They were chopped into small chunks with fine dissecting scissors and passed several times through an 18-gauge needle to give a partial single cell suspension. The crude cellular suspension was allowed to settle for 5 minutes. The supernatant was gently taken off without disturbing the clumps of tissue at the bottom of the tube. The resultant single

cell suspension was washed three times with 1x PBS (spun at 3,000 g for 5 minutes each time).

The ES cells were then disaggregated, rendered into single cell suspension and washed three times with PBS. Aliquots of  $1 \times 10^7$  HM-1 cells and  $5 \times 10^7$  thymocytes were made and mixed. The cells were then spun down (3000 g, 5 min) and resuspended in 400  $\mu$ l of freshly made electrofusion buffer (0.3M D-Mannitol titrated to 280 milliosmoles (mOs) using 0.1mM  $\text{MgSO}_4$ ).

Prior to electropulsing, the cell mixture was centrifuged in a 0.2 cm cuvette at 1,000g for 5 minutes inside 50 ml Falcon tubes cushioned with tissue paper. The cells were then electropulsed (standard conditions 300 V, 25  $\mu$ F) using a Biorad genepulser. Cuvettes were left to sit at room temperature for 15-20 min prior to removing and plating the cells. Each single fusion experiment was plated onto five 100 cm plates with ES cell medium. After 48 hours selection was applied, 1xHAT and 150  $\mu$ g / ml G418 (double selection) or 1xHAT selection (single selection).

During the course of work described in this thesis, breeding problems with the CBA<sup>Octneo/Octneo</sup> line were encountered. This resulted in CBA wild type mice and HAT selection only being used in most of the fusion experiments.

### **Heat shocking cells**

If thymocytes were to be heat-shocked prior to electropulsing and seeding, 1xPBS washed cells were resuspended in 0.5 ml 42°C PBS and placed immediately in a 42°C water bath for 10 minutes. The cells were then counted, divided into  $5 \times 10^7$  cell aliquots, and mixed with  $1 \times 10^7$  ES cells. Controls for pre-fusion heat shock experiments were treated in the same manner except the PBS was not preheated and the cells were left at 37°C for 10 minutes while the other cells were being heat-shocked. For post-fusion heat shock experiments where the cells have already been pulsed and seeded, the cells were heat shocked by removing the medium at the appropriate time point and replaced with preheated PBS (42°C) and placed in a 42°C incubator for 10 minutes. The PBS was then removed and fresh 37°C ES medium was then applied.

### [2.2.2] Polyethylene Glycol (PEG) Mediated Cell Fusion

PolyEthylene Glycol (PEG), a chemical that perturbs membrane structure, was also used to induce cell fusion. The PEG fusion protocol outlined here is based on a similar one by Matveeva *et al.* (1998):

Murine ES cells were fused with somatic cells (either) thymocytes or splenocytes as follows:

A suspension of  $5 \times 10^7$  somatic cells was added to a T175 flask already seeded with a 90-100% confluent monolayer of ES (or EC) cells and allowed to attach. The cell mixture was treated with a 45% polyethylene glycol MW 1,450 (Sigma) in full growth medium plus 10% DMSO for 1-4 min [Davidson and Gerald (1976)]. The cells were then thoroughly washed with 1xPBS and left overnight in complete growth medium. The cells were then transferred to dishes containing selection media. Viable colonies were harvested 9-15 days after fusion. **Subsection [2.2.4]** discusses the selection used.

Human ES cells were fused with other cell types in a similar manner. The only differences were that PEG solution and selection media were made up using conditioned human ES medium (and not murine ES medium) and 1xHBS (not 1xPBS) was used to wash away the PEG solution.

### [2.2.3] Sendai Virus Mediated Cell Fusion

Sendai virus has been used to induce cell fusion [Harris *et al.* 1965]. Such cell fusion has been found to be dependent on the expression of two viral proteins: the haemagglutinin neuraminidase (HN) protein which is thought to be required for close contact between the membranes being fused, and the F glycoprotein which is necessary to disrupt membrane structure and induce membrane fusion [Bousse *et al.* 1994].

This virus is extremely contagious in mice, where it can cause epithelial hyperplasia, squamous metaplasia and syncytial cell formation. Therefore the virus was completely inactivated prior to its use as a cell fusagen. This was done using  $\beta$  propiolactone (BPL – Sigma), a chemical that destroys viral RNA [Neff & Enders 1967]. Such treatment, unlike other inactivation treatments such as UV exposure, does not reduce the virus's ability to induce cell fusion.

BPL-inactivated Sendai virus was kindly supplied by Prof. Ian Wilmut and Bill Richie (Roslin Institute). This stock had been generated by inoculating day 9 hens' eggs with the active virus and removing the virus-rich allantoic fluid from the eggs after 72hr at 37°C. This fluid was centrifuged (3,000 g, 20 min) to remove detritus. 1 ml of 0.5% BPL in saline bicarbonate was added to 9 ml viral suspension and was gently agitated at 4°C for 10 minutes. The solution was then incubated at 37°C for 120 min with agitation, then statically at +4°C overnight. The concentration of the inactivated viral stock was measured using the haemagglutinin assay<sup>¶</sup> and diluted to 7,500 HAU / ml in KO DMEM. This stock was then aliquoted into 1 ml aliquots and stored at -70°C. The BPL treated stock was subsequently tested for infectivity by inoculating hen's eggs with 1:4-1:20 dilution of the stock in KO DMEM. No hemagglutination activity was detected, verifying that the virus was no longer capable of infecting cells.

Attempts to induce human ES cell fusion using BPL-inactivated Sendai virus were carried out as follows: cells from several confluent T150 flasks were disaggregated separately using TEG. Flasks were physically agitated until the cells dislodged from the flask. 10 ml 1xHBS was added to the flask for every 1 ml of TEG used and the cell suspension was transferred to 50 ml Falcon tubes and pelleted.

Cells were resuspended in 1xHBS and counted. Cells were stained as outlined in **Section [2.2.5]**. Fusions were then exposed to 5 ml Sendai viral suspension and left for 30 minutes at 37°C while leakage controls were not exposed to the viral suspension

---

<sup>¶</sup> This assay is based on the fact Sendai virus particles bind erythrocytes. Normally, erythrocytes will form a sharp dot when added to a cell culture well full of medium. When virions are present however, the erythrocytes are bound by virus and the sharp dot does not form. By serially diluting the viral suspension and looking at the distribution of added erythrocytes, one can assay the virion concentration. Such a concentration is cited as haemagglutinin activity units (HAU).



[7,500 haemagglutinin activity units (HAU) / ml]. Cells were then washed three times in 1xHBS and plated on matrigel treated 10 cm plates ( $2 \times 10^7$  cells were typically plated across five 10 cm plates).

### [2.2.4] Selecting for cell hybrids

Murine heterokaryons were selected using HAT and/or G418 selection [Fig 2.1].

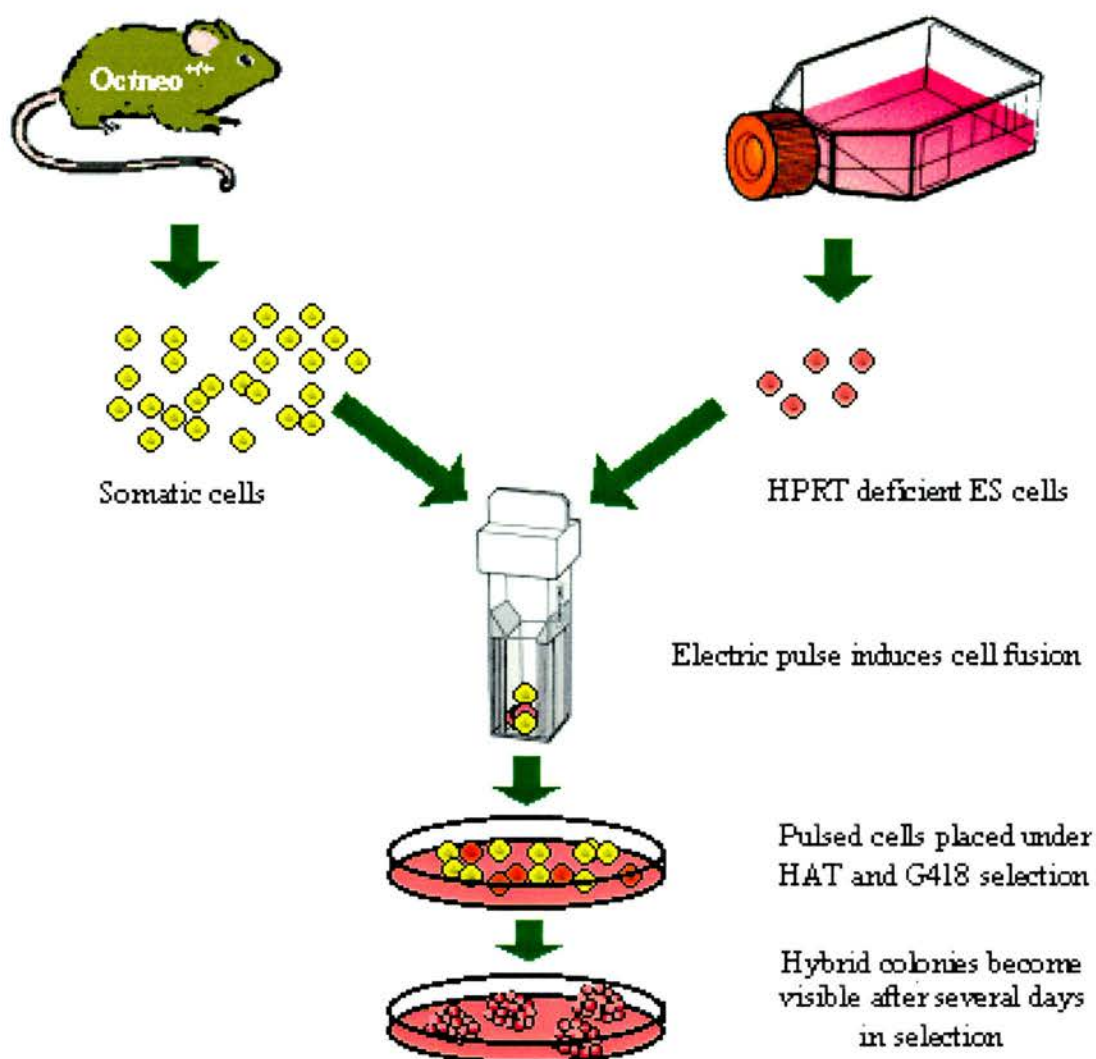


**Fig 2.1 Schematic showing electrofusion and selection for ES x somatic cell hybrids**

In a typical experiment  $1 \times 10^7$  HM-1 cells are mixed with  $5 \times 10^7$  CBA<sup>*Octneo/Octneo*</sup> thymocytes and electrofused in fresh D-mannitol electrofusion buffer [See Section [12.1] for details of buffer composition]. The cells are plated out on five 10cm plates ( $\sim 1.2 \times 10^7$  cells/plate), placed under selection after 24 hours and cultured for 12-14 days when hybrid colonies become visible. Note: Octneo is a knock-in of the endogenous *Oct4*-locus.

### **Inherent selection conditions of cell culture**

While culturable in serum supplemented GI medium [Sawa *et al.* 1997], murine thymocytes die under murine ES cell culture conditions. Thus these conditions alone select against unfused thymocytes, thymocyte homokaryons and cell hybrids displaying a thymocytic phenotype. In contrast, fibroblasts proliferate under mES culture conditions and in fusion experiments with fibroblasts an additional selection was required.

### **HAT selection**

HAT selection utilises growth medium containing Hypoxanthine, the folate reductase antagonist Aminopterin, and Thymine. Aminopterin is an inhibitor of *de novo* purine synthesis. Cells lacking the capacity to generate nucleotides via the salvage pathway will die in the presence of aminopterin as they will be unable to synthesise purines. Hypoxanthine guanine phosphoribosyl transferase (HPRT) is the enzyme catalysing the first step of the salvage pathway. Cells lacking this enzyme (e.g. HM-1 cells) will be unable to generate purines in the presence of aminopterin and will die. HAT selection is commonly used to select for hybrid cells (eg. somatic cell hybrids in monoclonal antibody production) where one of the parental cell types is HPRT deficient [Hope & Graves 1978]. Under this selection cells are forced to use exogenous bases, via the salvage pathways, as their sole source of purines and pyrimidines. Parental cells lacking HPRT cannot replicate their DNA under these circumstances. HM-1 cells were used in cell hybridisation experiments, so HAT selection could be used to select against unfused HM-1 cells or HM-1 x HM-1 fusion products.

### **6-thioguanine selection**

6-thioguanine (6-TG) is a purine analogue which is converted to a toxic nucleotide through a reaction that requires a functional *HPRT*-encoded enzyme. Thus, medium that contains 6-thioguanine kills normal cells but does not affect the growth of

mutant cell clones harboring inactivating mutations within the *HPRT* gene. It is used in this thesis to generate *HPRT* deficient lines which when unfused can be then selected against with HAT medium [Hope & Graves 1978].

### **G418 Selection**

G418 is an aminoglycosidic antibiotic that inhibits prokaryotic and eukaryotic protein synthesis. It is commonly used for the selection and maintenance of eukaryotic cells transfected with the *neo / kan* gene [Mohler & Blau 1994]. This gene allows production of aminoglycoside 3'-phosphotransferase, which inactivates G418, neomycin and kanamycin by phosphorylation.

G418 was used in hybridisation experiments to select against heterokaryons where the *Oct-4* locus had not been reprogrammed. In somatic <sup>*Octneo/Octneo*</sup> cells, the *Oct-4* promoter was shown to be off (See **Subsection [4.3.2]**) and so would not drive *neo* expression that would enable a cell to remain viable in appropriate concentrations of G418.

### **Puromycin**

Like G418, puromycin also inhibits protein synthesis in prokaryotes and eukaryotes. Specifically, it inhibits peptidyl transfer on ribosomes. It is commonly used for the selection and maintenance of mammalian cells transfected by the bacterial *pac* gene [de la Luna *et al.* 1988]. The *pac* gene encodes a puromycin N-acetyl transferase.

### **Blasticidin**

Again, blasticidin inhibits protein synthesis in prokaryotes and eukaryotes. Blasticidin specifically inhibits protein bond formation in ribosomal machinery. Resistance to blasticidin is conferred by the BSD gene which codes for the enzyme blasticidin deaminase [Kimura *et al.* 1994].

A table summarising all selection conditions used to isolate cell hybrids from different cell types is shown overleaf.

Cells fused	Selection applied
HM-1 cells & murine thymocytes	1xHAT or 1xHAT & 150µg/ml G418
HM-1 cells & murine splenocytes	1xHAT
HM-1 <sup>puro</sup> cells & murine thymocytes	1xHAT & 2.5µg/ml puromycin
NTERA2 <sup>puro</sup> & NTERA2 <sup>neo</sup>	4µg/ml puromycin & 300µg/ml G418
H9 & TG11.nR	1xHAT & 300µg/ml G418
H9 & Socs2	1xHAT & 300µg/ml G418

**Table 2.1 Summary of selection regimes used to isolate hybrid colonies**

The column on the left shows the cell types fused in hybridisation experiments and the right hand column shows what selection was used to isolate hybrids derived from heterokaryons.

### [2.2.5] Measuring heterokaryon formation

Cell fusion was assayed using a FACScan flow cytometer (Becton Dickson). The two cell aliquots were each stained with a different dye and then induced to fuse to form heterokaryons. Heterokaryons were identified as doubly-stained cells and these were measured using 2-dye FACS (Fluorescence Activated Cell Sorting) analysis.

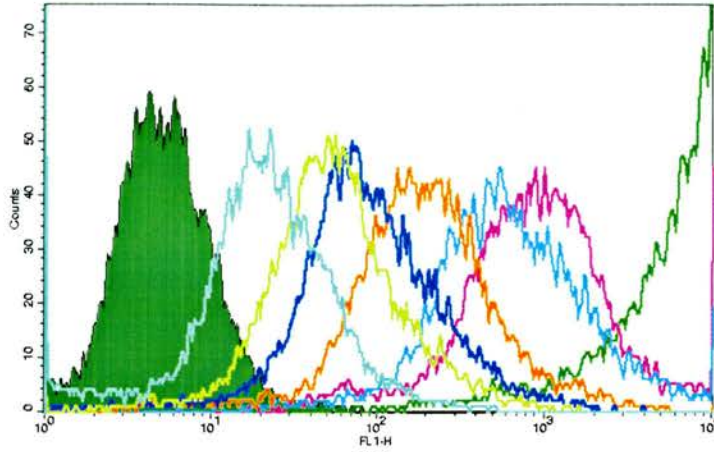
#### Cytoplasmic dye staining

Cytoplasmic dye staining was used to assess cell fusion using a similar method to that described by Scott-Taylor *et al.* (2000). CellTracker probe dyes 5-chloromethylfluorescein diacetate (CMFDA) and (5-(and-6)-(((4-chloromethyl)benzoyl)amino) tetramethylrhodamine) (CMTMR) (Cambridge Biosciences) were used to stain ES and somatic cells respectively. Where fusions were between different subclones, each subclone was exposed separately to one or other of these dyes. The dyes are membrane permeable and contain thiol-reactive chloromethyl groups, which interact with cytoplasmic glutathione transferases, forming fluorescent thioester adducts. Such adducts are membrane impermeable and so cannot diffuse back out of the cell [Jaroszki *et al.* 1994].

Use of these dyes therefore minimises problems associated with dye leakage and dye transfer between cells not fused. The dyes were stored at  $-80^{\circ}\text{C}$  as 10 mM stock solutions in DMSO. Scott-Taylor *et al.* (2000) found that the fluorescent intensity of human cells is altered if cells are stained within three hours of electropulsing. Based on this observation, it was decided that after electropulsing stained cell mixtures, the cells would be incubated in full medium for a minimum of 4 hours before harvesting and FACS analysis as described later in this section. Fluorescence spectra of HM-1 cells [Fig 2.2 overleaf], murine thymocytes [Fig 2.3], murine primary embryonic fibroblasts [Fig 2.4], and H9 cells [Fig 2.5] stained with different concentrations of dye were generated to identify appropriate concentrations of dye to use in 2-dye FACS experiments.



A



B

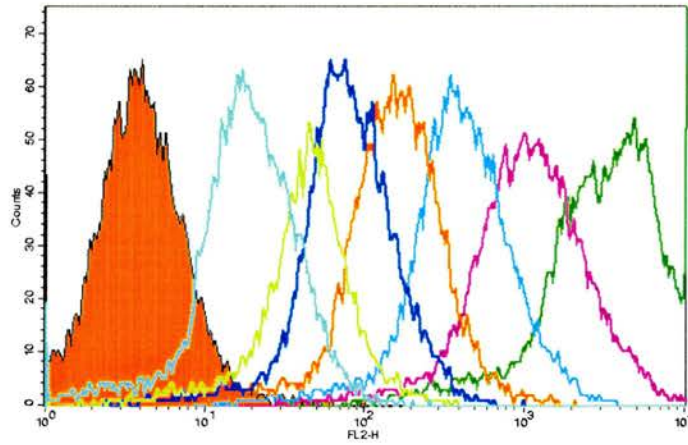
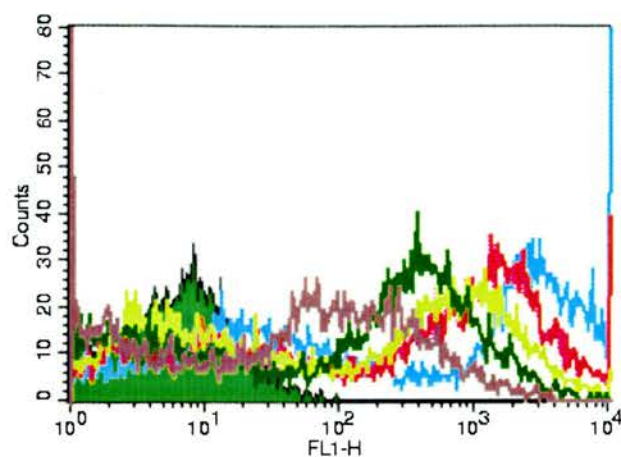


**Fig 2.2 Fluorescence of HM-1 cells exposed to seven concentrations of either CMFDA or CMTMR**

HM-1 cells were exposed to various concentrations of either CMFDA (green cytotracker dye) or CMTMR (orange cytotracker dye) at a cell density of  $10^7$  cells/ml dye solution for 30min. Fluorescence of single cells was then measured using a FACS sorter within 24hr of exposure to dye. **Panel A** shows HM-1 cells stained with various concentrations of CMFDA. The peaks from left to right in this panel correspond to the following concentrations of dye: 0 (■), 0.1 (□), 0.25 (△), 0.5 (▽), 1 (◇), 2.5 (○), 5.0 (●) and 10  $\mu$ M (○) [The axis label FL1-H indicates green fluorescence as measured using the FACS filter FL1.]. **Panel B** shows HM-1 cells stained with various concentrations with CMTMR. The peaks from left to right here correspond to the following concentration of dye: 0 (■), 0.1 (□), 0.25 (△), 0.5 (▽), 1 (◇), 2.5 (○), 5.0 (●) and 10  $\mu$ M (○). [The axis label FL2-H indicates that red fluorescence was measured using the FACS filter FL2]. 0.5 $\mu$ M CMFDA or 0.5 $\mu$ M CMTMR were judged to be appropriate dye concentration for staining these cells.



A



B

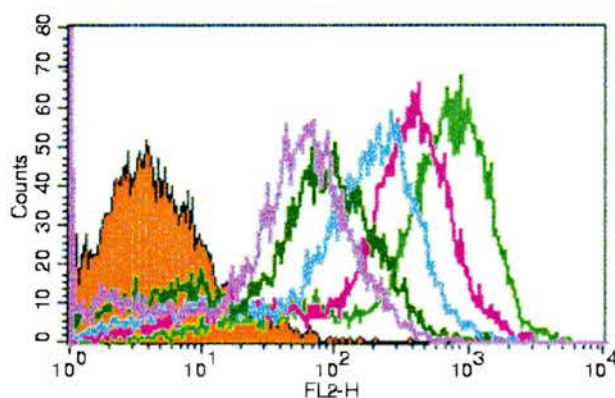
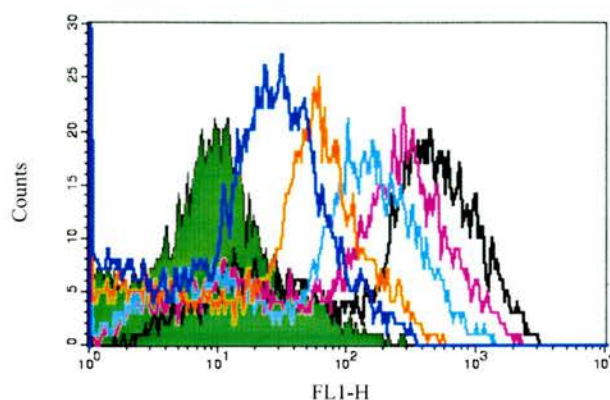


**Fig 2.3 Fluorescence of murine thymocytes exposed to five concentrations of either CMFDA or CMTMR**

Thymocytes derived from 6-7 week old CBA female mice were exposed to various concentrations of either CMFDA (green cytotracker dye) or CMTMR (orange cytotracker dye) at a cell density of  $10^7$  cells/ml dye solution for 30 min. Fluorescence of the cells was then measured using a FACS sorter. **Panel A** shows thymocytes stained with various concentrations of CMFDA. The peaks from left to right in this panel correspond to the following concentrations of dye: 0 (■), 1.25 (—), 2.5 (—), 5.0 (—), 10 (—) and 20  $\mu$ M (—) [Axis label FL1-H indicates green fluorescence is being measured]. **Panel B** shows thymocytes stained with various concentrations of with CMTMR. The peaks from left to right in this panel correspond to the following concentrations of dye: 0 (■), 1.25 (—), 2.5 (—), 5.0 (—), 10 (—) and 20  $\mu$ M (—) [Axis label FL2-H indicates red fluorescence is being measured]. 2.5 $\mu$ M CMFDA or 5.0 $\mu$ M CMTMR were judged to be appropriate dye concentrations for staining these cells.

A



B

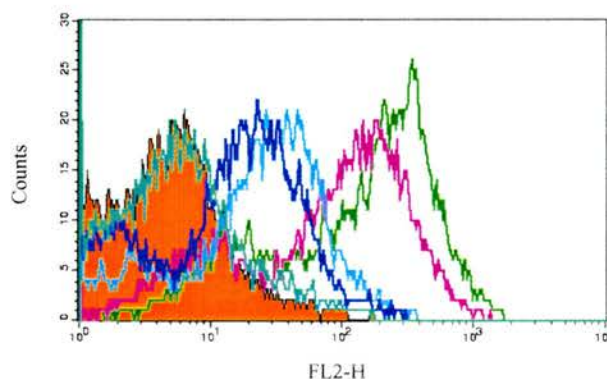
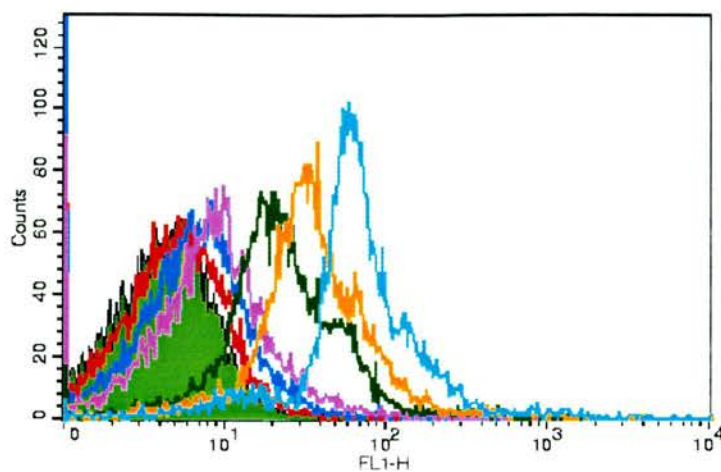


**Fig 2.4 Fluorescence of H9 cells exposed to five concentrations of either CMFDA or CMTMR**

Human ES (H9) cells were exposed to various concentrations of either CMFDA (green cytotracker dye) or CMTMR (orange cytotracker dye) at a cell density of  $10^7$  cells/ml dye solution for 30 min. Fluorescence of the cells was then measured using a FACS sorter. **Panel A** shows H9 cells stained with various concentrations of CMFDA. The peaks from left to right in this panel correspond to the following concentrations of dye: 0 (■), 1.25 (■), 2.5 (■), 5.0 (■), 10 (■) and 20  $\mu$ M (■) [Axis label FL1-H indicates green fluorescence is being measured]. **Panel B** shows H9 cells stained with various concentrations of CMTMR. The peaks from left to right in this panel correspond to the following concentrations of dye: 0 (■), 1.25 (■), 2.5 (■), 5.0 (■), 10 (■) and 20  $\mu$ M (■) [Axis label FL2-H indicates red fluorescence is being measured]. 20 $\mu$ M CMFDA or 20 $\mu$ M CMTMR were judged to be appropriate dye concentrations for staining these cells.

A



B

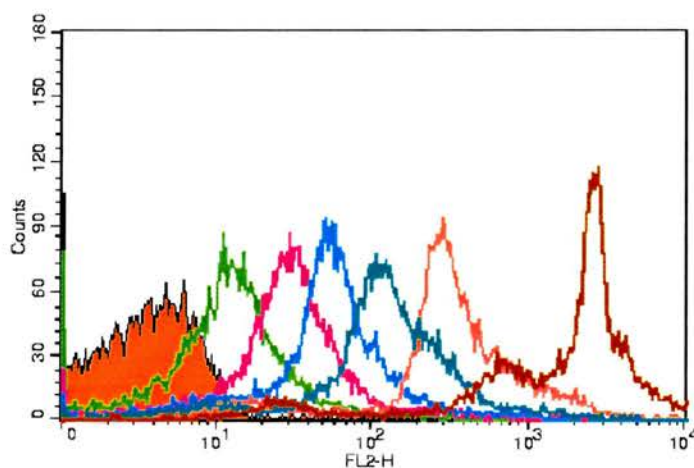


**Fig 2.5 Fluorescence of murine primary embryonic fibroblasts exposed to five concentrations of either CMFDA or CMTMR**

Primary embryonic fibroblasts were exposed to various concentrations of either CMFDA (green cytotracker dye) or CMTMR (orange cytotracker dye) at a cell density of  $10^7$  cells/ml dye solution for 30 min. Fluorescence of the cells was then measured using a FACS sorter. **Panel A** shows primary embryonic fibroblasts stained with various concentrations of CMFDA. The peaks from left to right in this panel correspond to the following concentrations of dye: 0 (■), 1.25 (■), 2.5 (■), 5 (■), 10 (■), 20 (■) and 50  $\mu$ M (■). [Axis label FL1-H indicates green fluorescence is being measured]. **Panel B** shows primary embryonic fibroblasts stained with various concentrations of CMTMR. The peaks from left to right in this panel correspond to the following concentrations of dye: 0 (■), 1.25 (■), 2.5 (■), 5.0 (■), 10 (■), 20 (■) and 50  $\mu$ M (■). [Axis label FL2-H indicates red fluorescence is being measured]. 20 $\mu$ M CMFDA or 5 $\mu$ M CMTMR were judged to be appropriate dye concentrations for staining these cells.

### **Data acquisition and analysis**

A FACScan FACS sorter and “Cellquest” software (Becton Dickson) was used to acquire and analyse FACS data. Once the cytometer had been calibrated, the cell samples (containing  $>10^6$  cells) were run, acquiring cells until 10,000 events had been registered by the machine. In the analysis of stained samples, control fluorescence was established using the negative (unstained) controls. The FACS analyser was equipped with two filters: FL1 measures green fluorescence and FL2 measures red fluorescence.

In the double staining experiments used to assess heterokaryon formation, the data were compensated manually as described in **Subsection [12.2]** to prevent false positive events being registered (this problem arises as there is overlap between wavelengths measured using the filters FL1 and FL2).

### **Two-dye FACS analysis for assessment of heterokaryon formation**

The FACS analyser was first calibrated using unstained cells. Histograms with Counts-FL1 axes or Counts-FL2 axes were drawn and the voltages for the two filters were modified until autofluorescent peaks were positioned at the least fluorescent end of each axis (See **Section [12.2]** Optimising Instrument Electronics for FACS analysis). After the peaks were properly positioned, a FL1-FL2 histogram showed the unstained cells as discrete compact bodies located near the origin. Calibration continued using populations of singly stained cells (either ‘green’ CMFDA or ‘orange’ CMTMR stained). The stained fluorescence peaks appeared further up the axes as the stained cells had a greater fluorescence than unstained cells. As the green fluorescence spectrum measured using the FL1 filter overlaps slightly with that measured using the FL2 filter, the data was be manually compensated. Using a FL1-FL2 plot, mixtures of green and orange cells were compensated by altering the FL1-%FL2 setting until that CMFDA - stained cells were distinct from CMTMR-stained cells (See **Section [12.2]**). The histogram was then divided into four quadrants so that the CMFDA stained cells appeared in the upper left quadrant and the CMTMR-stained cells appeared in the lower right quadrant, and unstained cells appeared in the lower left quadrant. Samples were then measured by the machine, and doubly stained cells appeared in the upper right



quadrant. The number of doubly stained cells was expressed as the percentage of the total cells gated.

To ensure dye leakage does not cause over estimation of heterokaryon formation, leakage controls were undertaken in all 2-dye FACS experiments. These used the same number and types of cells as actual fusions but the cells are exposed to the fusagen separately instead of together. The individually exposed cells were then mixed and plated as the cells from the fusion experiments. The percentage of double staining in leakage control is subtracted from that for the fusions in order to calculate actual percentage heterokaryon formation.

### **[2.2.6] Calculation of hybridisation frequency**

Hybrid colony yield on its own is not a good measure of reprogramming in the hybrid system. This yield (number of colonies generated / number of cells induced to fuse) is directly affected by the proportion of cells that are viable and the proportion of cells fusing to form heterokaryons. Hybridisation frequency (hybrid / heterokaryon) is calculated so that differences due to cell viability or cell fusion are taken into account when analysing data thus giving a clearer measure of the frequency of nuclear reprogramming.

Viable cells were identified using Forward Scatter/Side Scatter (FCS/SSC) plots generated by FACS analysis. Dead cells are represented as a smaller less granular population located near the origin of the plot [**Subsection 12.2**]. Gates were drawn to exclude this population and subsequently calculate cell viability (as a percentage of all cells used). This gating procedure removed dead cells allowing heterokaryon formation (as a percentage of viable cells) to be calculated. The two measurements cell viability and heterokaryon formation were used to control for changes in either cell viability or cell fusion that occurred between individual experiments. The measure of the incidence of nuclear reprogramming is used throughout this thesis termed “hybridisation

frequency". Assuming two cell types are being fused to generate hybrid cells, this is calculated as follows:

$$\begin{aligned}
 \text{Hybridisation frequency} &= \frac{\# \text{ hybrid colonies}}{\# \text{ viable heterokaryons}} \\
 &= \frac{\# \text{ hybrid colonies}}{(\# \text{ viable cells}) \times (\text{fraction of viable cells fusing})} \\
 &= \frac{\# \text{ hybrid colonies}}{\left( \text{total \# of cells in selection} \right) \left( \text{fraction of total cells that remain viable} \right) \times \left( \text{fraction of viable cells that fuse becoming doubly stained} \right)}
 \end{aligned}$$

So for example  $1 \times 10^7$  CMFDA stained HM-1 cells are electropulsed with  $5 \times 10^7$  CMTMR stained thymocytes. Electropulsed cells were split equally across five 10 cm plates. 4 plates ( $4.8 \times 10^7$  cells) were placed in selection for hybrid colonies and the other plate ( $1.2 \times 10^7$  cells) was used to assess cell viability and heterokaryon formation. FACS analysis showed that 9.2% of pulsed cells were viable. Two-dye FACS analysis showed 8.8% of viable cells in the fusion were doubly stained, whereas 0.9% of viable cells were in the leakage control. Subtracting the leakage control percentage from that of the fusion, it is calculated that 7.9% of all viable cells fused to form heterokaryons. 12 days later, 100 colonies were counted on the remaining 4 selection plates.

$$\text{Hybridisation Frequency} = \frac{100}{(4.8 \times 10^7) (0.092) (0.079)} = \frac{100}{3.488 \times 10^5} = 2.866 \times 10^{-4} \text{ hybrid/heterokaryon}$$

## **[2.3] Cytogenetic Analysis**

### **[2.3.1] Giemsa staining**

Giemsa stain is used to make transparent cells and their colonies more visible under the microscope so that morphologies may be more easily assessed or colonies more easily counted after they are fixed.

Colonies to be counted were gently washed with 1xPBS, fixed for 10 minutes in 70% methanol and stained for 10-15 minutes in a 10% Giemsa R-66 solution. After staining, plates were washed with water and air-dried.

### **[2.3.2] Mitotic spreads**

Mitotic spreads were prepared to assess the chromosome content of cells. Cells were incubated in medium containing 1 mM colcemid (Sigma) for 45 minutes. 50% confluent cultures were trypsinised and gently resuspended first in 1 ml of hypotonic solution (0.56% w/v KCl) and then up to 5 ml. Tubes were incubated at room temperature for 10 minutes, and then centrifuged at 1,500 g for 5 minutes. Supernatant was discarded and tubes flicked to ensure cell resuspension. 1 ml of ice-cold fixative (18 ml methanol, 6 ml glacial acetic acid) was added dropwise to the cells while flicking the tube. More fixative was added until the suspension was made up to 6 ml. After 5 minutes at room temperature, tubes were centrifuged at 1,000 g for 5 minutes. Supernatant was removed and cells were washed with fixative twice more as above. Pellets were then resuspended in 1 ml of fixative. Using a Pasteur pipette, single drops of this suspension were released from approximately 30 cm above 70% ethanol-treated slides. After evaporation of the fixative, slides were stained in 3% Giemsa R-66 for 10-15 minutes for chromosome counting.



### [2.3.3] G-banding and karyotyping

Mitotic spreads were left at room temperature for 72 hr. The slides were then incubated in 2x SSC. The slides were incubated at 60°C for 1hr and then dipped in 0.25% trypsin in PBS for 5 sec and then 2% Giemsa stain in Gurr's buffer pH6.8. The slides were left in the stain for 20 min and then washed with deionised water. The slides were then dried on top of a drying oven for 30 min and then left at room temperature overnight. Chromosomes were digitised and partially karyotyped using a MRC HGU Fip-2 (KMR programme) computer assisted chromosome analysis system [Piper & Granum 1989].

### [2.3.4] Fluorescence *In Situ* Hybridisation

Metaphase slides were generated as described in **Subsection [2.3.2]**. These were fixed with 3:1 methanol:acetic acid prior to being probed using FISH. The FISH protocol was carried out over two days: on the first day, the DNA of the chromosomes and of the X-chromosome paint were denatured and added together to hybridise and on the second day, unbound paint was washed away and the cells were then counterstained and mounted.

#### **Denaturation and Hybridisation**

The chromosome paint (human X-chromosome specific probe from Cambio kit 1153-Cy3-01, Cambridge Biosciences, [www.cambio.co.uk](http://www.cambio.co.uk)) was warmed to 37°C for 5 minutes and then denatured at 65°C for 10 minutes before being left at 37°C until it was used. Slides were serially dehydrated washing for 2 minutes each in 70% (v/v) EtOH, 70%, 90%, 90% and 5 minutes in 100% EtOH. The slides were air dried and left to age for 90 minutes at 65°C. The slides were then denatured by incubation in prewarmed denaturation solution at 65°C for 2 minutes. The slides were quenched in ice-cold 70% (v/v) EtOH for 4 minutes and dehydrated by repeating the serial EtOH washings. 15 µl of probe was applied to each slide and coverslip were applied and sealed with rubber

cement. The slides were then placed in an air tight humidified box and incubated overnight in the dark at 37°C.

### **Washing and Mounting**

Stringency Wash solution, 2x SSC solution and detergent wash solution were preheated to 45°C. Slides were removed from the incubator and incubated in 2x SSC solution at 45°C for 5 minutes. The rubber cement and coverslips were removed from slides and they were washed as follows: two 5 minute washes in Stringency Wash Solution (45°C), two 5 minute washes in 1x SSC solution (45°C) and one 4 minute wash in Detergent Wash solution (45°C). The slides were drained well and mounted with 50 µl of Working Reagent A. Glass overslips were then applied to the slides and these were sealed with nail varnish. Slides were viewed using standard epifluorescence filters for Cy3 and for counterstain DAPI.

### **[2.3.5] Propidium Iodide staining and associated FACS analysis**

Cells were disaggregated using EG, washed once with cold PBS, and processed for cell cycle analysis as follows:

Centrifuged cells were resuspended in one volume of cold "saline GM" and fixed by adding three volumes of 95% ethanol (-20°C). After overnight fixation at 4°C, cells were pelleted, washed once with PBS/EDTA (5 mM), and stained for 2 hours at room temperature with 50 µg / ml of propidium iodide and 100 µg / ml of RNase A in 1xPBS containing 0.1% sodium azide and 0.1% BSA. Samples were analysed using a FACScan cytometer (Becton Dickinson) equipped with an argon laser (excitation wavelength, 488 nM) and a 610-nM long-pass filter. For each sample, 10<sup>4</sup> events were stored for analysis. The doublet discrimination module was applied to exclude doublets or higher-order aggregates from DNA analysis. The percentage of cells existing in the various stages of the cell cycle were calculated using the CELLQuest program (Becton Dickinson) to visualize a histogram plot of red fluorescence (DNA) and by gating the cell populations with 2n(G0/G1 phase), 2n/4n (S phase), and 4n (G2/M phase) content of DNA.

### [2.3.5] PCNA staining

A marker commonly used to assess cell proliferation, Proliferating Cell Nuclear Antigen (PCNA) is expressed in two forms: an insoluble form, which is expressed at low levels in quiescent and senescent cells and highly expressed in cycling cells, and an insoluble nucleoplasmic form which is constitutively expressed during the cell cycle.

When staining for nuclear antigens, such as PCNA, fixation is the most critical step. The use of organic solvents (eg. ethanol, methanol, acetone) instead of cross-linking reagents (eg. paraformaldehyde) is recommended for three reasons: (i) they only fix insoluble PCNA, the marker for cell proliferation whereas cross-linking reagents denature it, (ii) they are better at preserving antigenicity and (iii) paraformaldehyde followed by acid treatment has been shown to generate artefacts [Campbell 1998]. An optimised method for staining mouse fibroblasts was developed based on Kill *et al.* 1991 and information from Alpha Laboratory's technical services department:

Cells were grown on glass slides. Cells were fixed in 50% acetone:50% methanol for 4 minutes at -20°C, washed twice with cold 1xPBS and stored in PBS at 4°C until ready to be stained. When staining the fixed slides, the slides were removed from the PBS and excess liquid was shaken off the slides. 25µl 1:10 αPCNA cyclin (Alpha labs Cat # 2037) in blocking solution (PBS with 1% FCS) was added to each slide and covered with parafilm cut to fit the surface area of each slide. The slides were incubated overnight at 4°C. Desiccation of the slides was avoided by placing them in a sealed box containing wet paper towels. After 24 hours the slides were washed five times with blocking solution before being incubated with the secondary antibody. 25 µl of secondary antibody (1:100 Texas red conjugated goat anti-human IgG3 in blocking solution) was added to each slide and covered with parafilm. Slides were placed in a sealed box with wet paper towels and left in darkness at room temperature for 1 hour. The slides were then washed three times in 1xPBS only. Excess liquid was removed and 1 drop of Vectashield mounting medium with DAPI (Vector Laboratories,

www.vectorlabs.com) was added to each slide. Coverslips were added and sealed with PANG solution (Pangus, www.pangus.com). After the slides had dried, they were examined with a 100x Fluor oil objective (Nikon, www.nikon.com), on a Nikon Microphot-SA microscope equipped for epifluorescence, and supplied with a mercury lamp (100W, Nikon HB 10101AF) and TXR (Nikon G-1A; excitation 546-556 nm) and DAPI (Nikon B-2A; excitation 450-490 nm) selective filter sets. Photographs were taken using a photomicrographic attachment (Nikon FX-35DX camera and Microflex UFX-DX).

## **[2.4] Analysis of phenotype**

### **[2.4.1] Alkaline phosphatase staining**

The alkaline phosphatase (EC 3.1.3.1) group of enzymes hydrolyse orthophosphoric monoesters at alkaline pH. The tissue-non-specific isozyme of this family (TNAP), is not expressed in adult murine tissues other than in the testis, while being highly expressed by undifferentiated cells (such as ES cells). Thus it can be used as a biochemical marker for ES and EC cells. The Vector BCIP/NBT Alkaline Phosphatase Substrate Kit IV (Vector Laboratories, www.vectorlabs.com) was used to assay for alkaline phosphatase activity. The active enzyme cleaves BCIP/NBT producing a dark blue/violet reaction product. The kit was used in accordance with the protocol outlined by the manufacturer. Typically, samples were left to stain for 10-15 minutes in darkness before being fixed and mounted.

## **[2.4.2] *In vitro* differentiation of murine hybrid clones**

### **Embryoid body formation**

Cells were disaggregated with TEG, resuspended in murine embryoid body medium and transferred to bacteriological plates. Cells were maintained in this medium until complex embryoid bodies formed, typically 8 days for HM-1s and 10 days for HM-1 derived hybrids.

### **Cardiomyogenic, neurogenic and myogenic differentiation**

3-8 complex embryoid bodies were seeded in TC chamber slides and grown in the relevant murine differentiation medium (Protocols for making cardiogenic, neurogenic and myogenic differentiation media are listed in **Section [12.1]**). After 11-14 days, cells were immunostained.

## **[2.4.3] Immunostaining**

### **Immunostaining cells on slides**

Cells to be stained were washed with PBS twice and fixed by incubating in freshly made 4% paraformaldehyde for 10 min. The cells were then washed twice with 1xPBS, then incubated in **Tris Buffered Saline (TBS)** containing 1% **Bovine Serum Albumin (BSA)** for 5 minutes. Non-specific binding was blocked using TBS-T (2% Triton in TBS) containing 1% BSA. The cells were incubated with primary antibody diluted in TBS-T containing 1% BSA for 1 hour at room temperature. Cells were washed again TBS and TBS-T containing 1% BSA as before. Cells were then incubated in secondary antibody anti-mouse IgG (biotinylated) for 1 hour at room temperature. The washing steps, using TBS and TBS-T containing 1% BSA, were then repeated a third time. Cells were then incubated in 1:200 dilution of Texas Red stain (Vector Laboratories) for 20 minutes. Cells were washed once again with TBS and then mounted using Vectashield with DAPI (Vector Laboratories, [www.vectorlabs.com](http://www.vectorlabs.com)).

### **Immunostaining cells for FACS analysis**

Cells to be immunostained were harvested using TEG and resuspended in 9 ml Glutamine-Free Glasgow's Modified Eagle's Medium (GMEM). 1 ml aliquots were dispensed into 9 prelabelled tubes (label specified cell line and antibodies to be used). The tubes were spun at 3,000 g for 5 minutes. The supernatant was decanted and the cells were resuspended in 50 µl of blocking buffer. Non-specific binding was blocked by leaving the cells in blocking buffer for 15 minutes on ice. The primary antibody or staining buffer was added to the appropriate tube. The samples were incubated on ice for 30 min. 3.0 ml staining buffer was added to each tube and the samples were spun at 3,000 g for 5 minutes. The supernatants were removed and 100 µl of appropriately diluted secondary antibody or preconjugated antibody in staining buffer was added to each sample. The samples were incubated for 30 minutes on ice in the dark. 3.0 ml 1xPBS was added to each sample to wash away excess antibody. The cells were spun for 3000 g for 5 minutes and resuspended in 1 ml 0.01% ParaFormAldehyde (PFA) in 1xPBS. The samples were stored at 4°C in darkness until they were FACS analysed. Samples were FACS analysed within a week of preparation.

### **[2.4.4] *In vivo* differentiation**

The potency of hybrid cell lines *in vivo* was assessed by injecting adult severe combined immunodeficient (SCID) mice strain C.B-17/Icr (Harlan UK Ltd, [www.harlan.com](http://www.harlan.com)) with cells and analysing the resultant tumours histologically.

### **SCID mice injections**

Single 200 µl aliquots containing  $2 \times 10^7$  cells in PBS were injected into the calf muscle of anaesthetised C.B-17/Icr mice. When tumours became evident, the injected mice were culled and their tumours were promptly removed and fixed in 4x PFA. Due to

their large size, the tumours were cut into segments to ensure complete perfusion with the fixative. Fixed tumour segments were stored in 4x PFA at 4°C.

The tumour segments were immersed in fresh 4x PFA the day prior to paraffin embedding and left on a roller overnight at room temperature. Each segment was then paraffin embedded using a Shandon Hypercentre XP processor (Shandon Scientific UK Ltd, [www.shandon.com](http://www.shandon.com)) that treated the tissue as detailed in **Table 2.2**.

Step	Solution	Concentration (%)	Time (min)	Temp (°C)
1	EtOH	70	90	RT
2	EtOH	96	90	RT
3	EtOH	96	90	RT
4	EtOH	100	90	RT
5	EtOH	100	90	RT
6	EtOH/PCA	50/50	90	RT
7	EtOH/PCA	50/50	60	RT
8	PCA	100	60	RT
9	PCA	100	60	RT
10	PCA	100	60	RT
11	PCA	100	60	RT
12	Paraffin Wax	100	60	60
13	Paraffin Wax	100	60	60

**Table 2.2 Protocol used to automatically embed tumour segments in paraffin**

A Shandon Hypercentre XP processor (Shandon Scientific UK Ltd, [www.shandon.com](http://www.shandon.com)) was programmed to treat the tumour segments as detailed. The tissue was first dehydrated using ethanol and cleared prior to embedding using Paraffin Clearing Agent (Sakura Finetek USA, INC., [www.sakuraus.com](http://www.sakuraus.com)). ‘PCA’ and ‘RT’ are abbreviations of ‘Paraffin Clearing Agent’ and ‘Room Temperature’ respectively.



Embedded tissue was cut into 6  $\mu\text{m}$  thick sections using a Microm HM325 rotary microtome (MICROM International GmbH, [www.microm.de](http://www.microm.de)). The sections were transferred to polylysine coated microscope slides. These slides were dried overnight at 37°C before staining.

### **Haematoxylin and Eosin (H&E) staining**

The dried slides were deparaffinised in xylene for 1 hour and rehydrated in successively more dilute solutions of ethanol (2 minute incubations in 100%, 90%, 80%, 70% EtOH, and H<sub>2</sub>O). These were then incubated in haematoxylin for 5 min and developed under running water for 5 minutes. The sections were then stained for 2-5 minutes with eosin (Sigma, [www.sigma.com](http://www.sigma.com)) and transferred to H<sub>2</sub>O for 2 minutes before being dehydrated in EtOH (15 second incubations in 70%, 80%, 90% and 100% EtOH). The slides were then incubated in xylene for 1 hour to remove the alcohol. Xylene was then allowed to evaporate from the slides by placing them in a fume cupboard for 1 hr. Finally the sections were mounted in DPX (a synthetic resin made from distyrene, tricresyl phosphate and xylene) and left to dry at 37°C overnight.

### **Histological analysis of H&E stained sections**

In addition to the student's own efforts, the sections were independently assessed by Dr. Bob Fleming (Roslin Institute) and Dr. Edward Duvall (Pathology Department, University of Edinburgh Medical School). Analysis was carried out using light microscopy (10-200 x magnification).

### **Paraffin removal and immunostaining of embedded sections**

Paraffin was removed by incubating sections in xylene (BDH) for five minutes (three times). Slides were rehydrated by incubation in absolute ethanol for five minutes (twice) followed by incubation in 95% ethanol for five minutes (twice). Slides were washed in dH<sub>2</sub>O for five minutes (twice) and then in PBS for five minutes. To unmask antigens, slides were incubated in 10 mM trisodium citrate (pH 6.0) for 10 minutes at 100°C. Slides were then washed in dH<sub>2</sub>O for five minutes (three times) and 1xPBS for five minutes. Stripped sections were immunostained with anti-ezrin to confirm the

presence of endoderm. This was done as follows: Slides were incubated in blocking solution for 1 hour and then incubated in ezrin antibody overnight at 4°C (1:100). Slides were washed for 20 minutes in PBST (three times) and incubated with AP-conjugated secondary antibody for 1 hour (1:200). Slides were washed for 20 minutes three times using 0.01% Tritin-T in 1xPBS (PBS-T) and incubated in AP staining solution. Slides were mounted in aquamount (BDH).

### **[2.4.5] *LacZ* staining**

Cells were washed in 1xPBS and fixed for 10 minutes at room temperature in fixing solution. The cells were subsequently washed 3 times with washing solution. The cells were covered in *LacZ* staining solution at 37°C until staining of appropriate intensity was achieved (3-6 hours typically). Cells were then washed three times in 1xPBS and examined under the microscope. *LacZ* expressing cells will stain blue, as the gene product of *LacZ* ( $\beta$ -galactosidase) catalyses the hydrolysis of X-gal.

## **[2.5] Manipulation and analysis of DNA**

### **[2.5.1] Extraction of mammalian genomic DNA**

The following procedure for mammalian DNA isolation has been adapted from Laird *et al.* (1991). Cell cultures were rinsed once with 1xPBS before addition of lysis buffer (3 ml for 25 cm<sup>2</sup> flasks, 10 ml for 75 cm<sup>2</sup> flasks). Following overnight incubation at 37°C with gentle shaking, one volume of isopropanol was added to the lysate. Samples were shaken for several hours until a white DNA precipitate was visible. Using a Pasteur pipette, the DNA was lifted and placed in an Eppendorf tube. Excess liquid was eliminated and the DNA was dissolved in 500  $\mu$ l of Tris HCl buffer pH 8.5. Vials were incubated at 70°C for 3 hours.

## **[2.5.2] Extraction of plasmid DNA from bacteria**

### **Minipreps**

For routine plasmid DNA extraction from bacteria, individually picked colonies were incubated overnight at 37°C in Falcon 15 ml tubes containing 5-7 ml of **Luria-Bertani** (LB) bacterial medium supplemented with 100 µg/ml of ampicillin. Following centrifugation of 1.5 ml cultures (10,000 g for 5 minutes) supernatants were discarded and pellets resuspended in 250µl of solution 1 (50 mM Tris-HCl pH 8.0, 10 nM EDTA, 100 µg / ml RNase A). Lysis buffer (250 µl of 200 mM NaOH, 1% SDS) was subsequently added to this solution, which was gently mixed and incubated for 5 minutes at room temperature. The lysis reaction was stopped by adding 350 µl of neutralising solution (3.0M potassium acetate pH 5.5). Immediately after centrifugation (13,000 g for 10 min) supernatant was recovered and taken to a fresh tube, where it was mixed with an equal volume of isopropanol and centrifuged again (13,000 g for 10 minutes). Pellets were air-dried for 5 minutes and then resuspended in a 50 µl of Tris-HCl buffer pH 8.5.

For those applications requiring high purity DNA (such as subcloning), the Qiagen miniprep kit was used as directed by the manufacturer.

### **Maxipreps**

Purification of large amounts of plasmid DNA for electroporation was done using the Qiagen Maxiprep kits. These procedures yielded an average of 500-1000 µg of DNA from 500 ml cultures.

### [2.5.3] DNA purification

Phenol/chloroform is used to extract and purify nucleic acids from a variety of sources [Sambrook *et al.* 1989]. An equal volume of 1:1 phenol:chloroform (Life Technologies) added to an aqueous DNA solution causes the denaturation and dissociation of proteins from DNA. After inverting several times the tube containing the mixture, centrifugation (13,000 *g* for 20 minutes) yields two distinct phases: a lower organic phenol:chloroform phase containing the protein (mostly in the white, flocculent interface) and the lighter aqueous phase with the DNA.

DNA was recovered from the aqueous solution by adding 1/10 volume of 3 M sodium acetate pH 5.5 and 2 volumes of 100% ethanol (alternatively, 1 volume of isopropanol can be used). The tube was mixed and then chilled for at least 30 minutes at  $-80^{\circ}\text{C}$  or 2 hours at  $-20^{\circ}\text{C}$ . This ensures a 75 % recovery for volumes  $<1$  ml containing at least 10  $\mu\text{g}$  of DNA. For very low DNA concentrations, 2  $\mu\text{l}$  of seeDNA (Amersham, [www.amersham.com](http://www.amersham.com)) were added to each tube, regardless of the volume. This pink-coloured reagent co-precipitates with the DNA and makes identification of the pellet easier. The tube was subsequently centrifuged for 30 minutes (13,000 *g*,  $4^{\circ}\text{C}$ ), supernatant removed, and the pellet rinsed once with 500  $\mu\text{l}$  70 % ethanol. This step is essential for removing the excess salt, and for very sensitive applications (such as blunt-end ligation) it was done twice. The tube was centrifuged as before for 5 minutes, and the pellet allowed to air-dry for 5 minutes after removal of excess ethanol. DNA was resuspended in an appropriate volume of distilled water or TE buffer pH 8.5.

## [2.5.4] DNA quantitation

Quantitation of diluted DNA (typically 1:100 in distilled water) was performed in an UNICAM 5625 UV/VIS spectrophotometer at a  $\lambda = 260$  nm. Since an optical density (O.D.) of 1 corresponds approximately to 50  $\mu\text{g/ml}$  of double-stranded DNA, DNA concentration can be calculated in the following manner:

$$\text{concentration of DNA} = \text{OD}_{260} \times 50 \mu\text{g/ml} \times \text{dilution ratio (e.g. 100 or 400)}$$

When there was not sufficient DNA for spectrophotometric assay, fluorescent yields of 1  $\mu\text{l}$  aliquots were compared to a series of standards of the same size in ethidium bromide-supplemented agarose gels.

## [2.5.5] DNA Analysis and Manipulation

### [2.5.5.1] Restriction analysis of DNA

Genomic and plasmid DNA were digested using restriction enzymes and buffers (Roche, [www.roche.com](http://www.roche.com)) according to the manufacturer's instructions. For DNA analysis, a 10-fold excess of enzyme was normally used. The following examples describe the typical proportions of reagents in a standard linearisation of plasmid DNA for electroporation (1) and restriction analysis (2), respectively.

- (1) 200  $\mu\text{l}$  (1  $\mu\text{g}/\mu\text{l}$ ) plasmid DNA, 50  $\mu\text{l}$  Buffer H, 30  $\mu\text{l}$  *EcoRI* (10 units/ $\mu\text{l}$ ), (1 unit restriction enzyme cuts 1  $\mu\text{g}$  DNA per hour), 220  $\mu\text{l}$  distilled  $\text{H}_2\text{O}$ . Total volume: 500  $\mu\text{l}$ . The reaction mixture was incubated for 2-4 hours at 37°C.
- (2) 1  $\mu\text{l}$  (1  $\mu\text{g}/\mu\text{l}$ ) plasmid DNA, 2  $\mu\text{l}$  Buffer H, 1  $\mu\text{l}$  *EcoRI* (10 units/ $\mu\text{l}$ ), 220  $\mu\text{l}$  distilled  $\text{H}_2\text{O}$ . Total volume: 500  $\mu\text{l}$ . The reaction mixture was incubated for 2-4 hours at 37°C.

After digestion, and following the addition of 6x loading buffer, samples were loaded in agarose gels (The gels were made with 0.1% (v/v) ethidium bromide and 0.6-3% (w/v) agarose in TAE depending on band size of interest). Agarose gels were run in TAE buffer either for 2hr (50-90 V) or overnight (25-40 V). A UV transilluminator was used to visualise bands on gels.

### **[2.5.5.1] Extraction of DNA bands from agarose gels**

DNA bands were extracted from agarose gels using the QIAquick Gel Extraction kit (Qiagen) according to the manufacturer's instructions. Dissolved gels are poured into minicolumns and centrifuged. DNA is retained in the minicolumns as it binds to positively charged silica gel within. The DNA is then eluted using a high salt elution buffer.

### **[2.5.5.3] DNA Ligation**

Ligation of DNA fragments was performed using the rapid DNA ligation kit (Roche, [www.roche.com](http://www.roche.com)) according to the manufacturer's instruction. This system enables sticky-end or blunt-end ligations in 5-10 minutes at room temperature. Ligation reactions contained no more than 200 ng of total DNA (insert and vector) in a total volume of 21  $\mu$ l. The molar ratio used was always 1:4. Prior to ligation, vectors were incubated (1 hr, 37°C) with shrimp alkaline phosphatase (SAP) (Amersham, [www.amersham.com](http://www.amersham.com)) in order to de-phosphorylate the ends and prevent self-ligation. SAP was heat inactivated by incubating the sample at 65°C for 15 min.

Where required, blunt ends were generated by adding 1-5 units of the Klenow enzyme and 1 $\mu$ l of 10mM each dNTP to the restriction digest mixture (30 minutes at room temperature). The Klenow fragment consists of the C-terminal domain of *E.coli* DNA polymerase I, which lacks the 5'-3' exonuclease activity while retaining the DNA polymerase and 3'-5' exonuclease activities [Joyce & Grindley 1983].

The following example described a typical ligation reaction with a 1:4 vector to insert ratio: 100 ng vector DNA (10 kb) and 40ng insert DNA were dissolved with 2 $\mu$ l of 5x DNA Rapid Ligation buffer (Roche) in a total volume of 10 $\mu$ l (distilled water added as required). After thorough mixing, 10  $\mu$ l of 2x DNA Rapid Ligation buffer (Roche) were pipetted into the vial. The solution was mixed again before the final addition of 5 units (1  $\mu$ l) of T4 DNA ligase (Roche, [www.roche.com](http://www.roche.com)). The ligation mixture was incubated for 5-10 minutes at room temperature.

#### **[2.5.5.4] Transformation of bacterial cells with DNA**

For routine circular plasmid transformation, Subcloning Efficiency DH5 $\alpha$  competent cells (Life Technologies, [www.lifetechnologies.com](http://www.lifetechnologies.com)) were used. 50  $\mu$ l aliquots of these cells were thawed on ice and incubated with 50-500 ng of plasmid DNA for 30 minutes. After a 20 second heat shock at 37°C, vials were placed on ice for two minutes. Following 1 hour of incubation in 900  $\mu$ l of the LB medium (37°C, on a cell shaker at 200 rpm), cultures were diluted as necessary, seeded on antibiotic supplemented agar plates (2  $\mu$ g/ml ampicillin was generally used, though when plasmids only containing a zeocin resistance cassette were used to transform cells, 5  $\mu$ g/ml zeocin was used). The agar plates were incubated overnight at 37°C



## [2.5.6] Plasmids

### **pPUR**

pPUR (Clontech) is a selection vector that confers puromycin resistance to eukaryotic cells [De la Luna *et al.* 1992]. The puromycin resistance gene of pPUR can be used as a dominant selectable marker to select for stably transformed mammalian cell lines. This resistance gene, the *Streptomyces alboniger* puromycin-N-acetyl-transferase (*pac*) gene, is cloned between the SV40 early promoter and polyadenylation signals to create a cassette that will be expressed in mammalian cells. Cells expressing *pac* are resistant to the antibiotic puromycin [See **Subsection [2.2.4]** for more on puromycin selection].

### **pSV40neo**

pSV40neo is a selection vector that confers G418 resistance to eukaryotic cells [Schmidhauser *et al.* 1992]. The neomycin resistance of pSV40neo can be used as a dominant selectable marker for stably transforming mammalian lines. The resistance gene, *neo*, is cloned in between the SV40 early promoter and polyadenylation polyadenylation signals to create a cassette that will be expressed in mammalian cells [See **Subsection [2.2.4]** for more on G418 selection].

### **pBI-G**

pBI-G Vector (Clontech) is a response plasmid that can be used to express a gene of interest and b-galactosidase from a bidirectional tet-responsive promoter Pbi which is responsive to the rtTA regulatory proteins in the Tet-On systems [Baron 1995][Gossen *et al.* 1995]. Pbi contains the Tet-responsive element (TRE), which consists of seven copies of the 42-bp tet operator sequence (tetO). The TRE element is between two minimal CMV promoters (PminCMV), which lack the enhancer that is part of the complete CMV promoter. Consequently, Pbi is silent in the absence of binding of TetR or rTetR to the

tetO sequences. PminCMV-1 controls the expression of the gene of interest; and PminCMV-2 controls the expression of beta-galactosidase. This plasmid was used in this work as the expression of a gene of interest could be monitored indirectly via the beta-galactosidase reporter function (See **Subsection [2.4.5]** for details on *LacZ* staining).

### **pB-RCME2722**

pB-RCME2722 contains a multiple cloning site (MCS) flanked by incompatible loxP sites (wild type loxP and lox2722). It was used in Chapter 8 to introduce incompatible loxP sites on either side of the nucleoplasmin cassette so that other transgenes could be inserted into pTetNPM (See **Fig 12.5**). This plasmid was a gift from Dr. Andreas Kolb. **pB-RCMEBSD** is a plasmid derived from this one. A 1.5kb blasticidin cassette was inserted into the *EcoRI* site in the multiple cloning site.

### **pUCNPM**

pUCNPM contains the nucleoplasmin coding sequence which may be excised as a 0.8kb *EcoRI* fragment [Dingwall *et al.* 1987]. This plasmid was a gift from Prof. Ron Laskey.

## **[2.6] Manipulation and analysis of RNA**

### **[2.6.1] RNA extraction and quantitation**

RNA was extracted from mammalian cell cultures using the TRIzol reagent (Life Technologies, [www.lifetechnologies.com](http://www.lifetechnologies.com)), according to manufacturer's instructions. This product is a mono-phasic solution of phenol and guanidine isothiocyanate that maintains the integrity of total RNA while lysing and dissolving cell components. Addition of chloroform and centrifugation separates the solution into an organic phase (bottom) and an aqueous phase (top), from which RNA can be isolated by isopropanol

precipitation. Quantitation was performed as described for DNA. 1 OD at 260 nm corresponds to ~40 µg / ml of single-stranded RNA.

## **[2.6.2] RNA analysis**

### **RNA Quantitation**

RNA has to be maintained at denaturing conditions at all times in order to avoid the formation of secondary structures by intramolecular base pairing. This was achieved by treating agarose gels with formaldehyde. In order to prevent degradation of the samples, RNase free solutions and glassware were used. Autoclaved water was treated with 0.1% diethyl pyrocarbonate (DEPC) and working surfaces were thoroughly cleaned with RNaseZAP. The following protocol has been adapted from that of Sambrook *et al.* (1989): The pH of 10x Running Buffer (RB) was adjusted to 7.0 with 5M NaOH. Formaldehyde agarose gels (0.8-1.2%) were prepared by melting the appropriate amount of agarose in 10 ml 10x RB, 72.1 ml DEPC-water and 17.9 ml of 38% formaldehyde. Gels were poured and set inside a fume hood. RNA samples (max 40µg) were dissolved in a total volume of 20µl of sample buffer (200µl of 10x RB, 1ml of deionised formamide and 356 µl of 38% formaldehyde) and then heated to 65°C for 5 minutes. 8 µl of dye solution (7.5% Ficoll 400 and bromophenol blue) were added to each sample before loading. After overnight running in 1xRB (20mA), gels were stained in 1x RB containing 5-10 mg of ethidium bromide and photographed under UV transillumination. The absence of RNA degradation was verified by running an aliquot of the RNA of a formaldehyde gel. The production of distinct clear bands and the absence of smearing indicated good RNA quality.

### **Reverse transcriptase polymerase chain reaction (RT-PCR)**

RT-PCR was performed using the First Strand preamplification kit (Amersham, [www.amersham.com](http://www.amersham.com)) as outlined by the manufacturer. This system is designed to

synthesise first strand complementary DNA (cDNA) from purified total RNA, making use of oligo (dT) primers for hybridisation with the 3' poly-A tails found in eukaryotic mRNAs. The first strand cDNA synthesis reaction is catalysed by the enzyme M-MLV RNase H<sup>-</sup> reverse transcriptase (RT). This enzyme degrades any DNA present while leaving the RNA intact. PCR was then used to amplify single stranded-cDNAs obtained by mRNA retrotranscription. PCR reactions using RT-untreated RNA extracts were made up as controls to rule out genomic contamination of the RNA samples.

## **[2.7] Polymerase Chain Reaction**

All PCRs were performed on the Omnigene Hybaid thermal cycler in 50 ml reaction mixtures with 16 mM (NH<sub>4</sub>)<sub>2</sub>SO<sub>4</sub>, 67 mM Tris-HCl pH 8.8, 0.01% Tween-20, 1.5 mM MgCl<sub>2</sub>, 2.5 units Taq polymerase, 200 μM dNTPs. Template genomic DNA or cDNA of 0.2 –1 μg was used with primers at a final concentration of 0.2 μM.

*$\alpha$ -FETOPROTEIN:*

Primers **AFPRT FWD** (5'-AGTTTTCTGAGGGATGAAACC-3') and **AFPRT REV** (5'-TCCAAAAGGCCCGAGAAATC-3') with 2 min at 94°C, 30 cycles of 30 secs at 94°C, 30 sec at 63°C and 1 min at 72°C and a final cycle of 5 min at 72°C. Expected fragment size: 200 bp.

 *$\beta$ -ACTIN:*

Primers **B-Act F1** (5'-AGAGGGAAATCGTGCGTGAC-3') and **B-Act R1** (5'-ATGGTGCTACCAGCCAGAGC-3') with 4 minutes at 94°C, followed by 35 cycles 30 seconds at at 94°C, 20 seconds at 58°C, 30 seconds at 72°C and a final cycle of 5 minutes at 72°C. Expected fragment size: 340 bp.

*NEO:*

Primers **NeoF1** (5'-CGGCCGCTTGGGTGGAGAGGC-3') and **NeoR1** (TCGGGCATGCGCGCCTTGAGC) with 3 minutes at 94°C, followed by 30 cycles of 30 seconds at 94°C, 30 seconds at 68°C and one minute at 72°C and a final cycle of 10 minutes at 72°C. Expected fragment size: 510 bp.

*TCR $\gamma$  (DNA rearrangement):*

Primers **GammaF1** (5'-CTCGGATCCTACTTCTAGCTTTCT-3') and **GammaR1** (5'-AAATACCTTGTGAAAACCTG-3') with 3 minutes at 94°C, followed by 30 cycles of 30 seconds at 94°C, 140 seconds at 49°C and one minute at 72°C and a final cycle of 10 minutes at 72°C. Expected fragment size: 2,100 bp.

## **[2.8] Protein analysis**

### **[2.8.1] Generation of whole cell lysates**

Whole thymuses were extracted from eight 6-7 week old CBA wild type female mice and placed in 2 ml 1xPBS supplemented with protease inhibitor cocktail as per the manufacturer's instructions (Roche, [www.roche.com](http://www.roche.com)). The thymuses were made into a single cell suspension by passing the cells through an 18G syringe after cutting up the glands in 1xPBS using fine dissecting scissors. This suspension was divided into two equal aliquots. One aliquot was heat shocked (42°C for 10 min) and the other was left at room temperature. The aliquots were then incubated for 2 hours at 37°C. The suspensions were homogenised using a sonicator. An equal volume of 2x **Sodium Dodecyl Sulphate (SDS)** loading buffer was added to the homogenate and the samples were boiled for 10 minutes to lyse the cells. Lysates were kept on ice when in use and stored at -70°C to prevent protein renaturation.

### **[2.8.2] Protein quantitation**

The protein concentration of each lysate was determined using a BCA Protein Assay Kit (Pierce, [www.piercenet.com](http://www.piercenet.com)). The assay is based on the formation of a purple complex formed when substances containing two or more peptide bonds react with copper salts in the reagent causing the reduction of  $\text{Cu}^{2+}$  to  $\text{Cu}^{1+}$ . Cuprous ions are then sequestered by the bicinchonic acid (BCA) in the reagent forming a purple complex that may be assayed by measuring absorbance at 562 nm. There is a linear relationship between absorbance of the purple  $\text{Cu}^{2+}$  BCA complex and protein concentration below 1000  $\mu\text{g} / \text{ml}$ . For each quantitation, diluted serum albumin (BSA) standards are prepared (0-500  $\mu\text{g} / \text{ml}$ ) using the kit as indicated by the manufacturer's protocol. These were used to generate a standard curve using the kit as indicated by the manufacturer's protocol. Various dilutions of samples were incubated in parallel with

the standards and 520 nm OD values were compared against the standard curve. The protein concentrations of the diluted samples were calculated from the standard curve.

### **[2.8.3] Western Blotting**

Western blotting was used to detect specific proteins in a complex mixture such as a cell lysate. The method consists of three steps:

- (a) fractionating the protein mixture by denaturing SDS-polyacrylamide gel electrophoresis;
- (b) transferring and immobilizing the mixture onto a solid membrane and
- (c) incubation of the membrane with an antibody raised to the protein of interest and assaying for specific antibody binding.

#### **Polyacrylamide Gel Electrophoresis**

This was carried out using an X-cell Surelock Mini-cell apparatus (Invitrogen, [www.invitrogen.com](http://www.invitrogen.com)). 10-12% gels were run in 1xTris-Glycine running buffer. Samples containing 150µg protein were boiled for 5 mins before being placed on ice to cool prior to loading. Gels were run according to manufacturer's instructions.

#### **Staining the blot for total protein**

Using wet gloved hands the portion of the gel to be stained was cut out and carefully transferred to a tank with 50 ml staining/fixative (50 ml 100% methanol, 75 ml acetic acid, 20 g TCA, 0.4 g coomassie blue g250, and 450 ml dH<sub>2</sub>O). This was then placed in an air-tight container to avoid evaporation and shaken on a cell shaker for two hours. The gel was then destained by gently shaking the gel in 50 ml destaining solution (230 ml methanol, 70 ml acetic acid, 700 ml dH<sub>2</sub>O) for 30 minutes. The destaining solution was then decanted before adding another 50 ml fresh destaining solution and shaking for another 30 minutes. The plate was then removed photographed and wrapped in Saran wrap and stored at 4°C.



### **Semi-Dry Electroblothing**

Semi-dry electroblotting was used in preference to traditional wet methods as it was quicker and required less buffer. Semi-dry electroblotting was carried out as follows: the gel to be transferred was equilibrated in transfer buffer for 30 minutes to remove salt and detergents which would hinder transfer of protein to the membrane. The membrane (Millipore Immobilon-P Transfer PVDF membrane, pore size 0.45  $\mu\text{m}$ ) was cut to the dimensions of the gel. The membrane was carefully placed in transfer buffer and left for 30 minutes. The membrane was kept wet at all times to insure proper binding. Gloves were worn when handling the membrane.

Filter paper was cut into the dimensions of the gel. Two pieces of thick filter paper per gel are needed for each gel/membrane sandwich. The filter paper was completely saturated by soaking in transfer buffer. The pre-wetted blotting media was placed on top of the filter paper and all the air bubbles were removed. The equilibrated gel was carefully placed on top of the gel on the centre of the membrane. It was made sure that the gel did not hang over the blotting media. All air bubbles were removed. Another sheet of pre-soaked filter paper was placed on top of the gel, and again air bubbles were carefully removed from between the gel and filter paper.

The cathode was carefully placed onto the stack. The latches were engaged without disturbing the filter paper stack. The safety cover was placed on the unit and then plugged into a power supply. Normal transfer polarity is cathode to anode. Transfer was performed at 200-300 mA (<22 V) for 1 hour.

### **Immunoblotting**

If the hybrid membrane was allowed to dry, it was rehydrated by placing it in methanol for 10 seconds, and then washing it in water before being transferred to blocking solution.

The membrane was pre-blocked in blocking solution for 2-4 hr at 37°C. A second membrane similar to the first was always prepared and blotted with the secondary antibody only as a control for non-specific secondary antibody binding.

The primary antibody was mixed in fresh blocking solution (1:1000) and the membrane was incubated in this overnight at 4°C. The membrane then washed six times at room temperature (each wash lasted 10 minutes and used >10ml wash solution). The membrane was then washed twice for 5 minutes in 1xPBS. The secondary antibody was diluted 1:100 in blocking solution and the membrane was incubated in this for 2 hours at room temperature. Subsequently the membrane was washed in wash solution and then 1xPBS in a similar manner to that carried out after incubation with the primary antibody.

Secondary antibodies used for Western Blotting were conjugated to horseradish peroxidase (HRP), which catalyses the oxidation of luminol in the ECL<sup>®</sup> chemiluminescence reaction mix (Amersham, [www.amersham.com](http://www.amersham.com)). This resulted in the emission of light and detection after quick exposures of X-ray films. The membrane was developed using ECL western reagents (as directed by the manufacturer). The membrane was covered in Saran wrap and X-ray film was exposed to it using a film exposure cassette. The exposed X-ray film was then developed using a Konica SRX 101A developer.

## **[3] Generation of cell hybrids from murine ES cells**

### **[3.1] Introduction**

The process underpinning lineage commitment and differentiation of the mammalian somatic cell is poorly understood and has, until recently, been assumed to be unidirectional. However, several observations now show that the differentiated state of the cell can be experimentally manipulated [See **Section [1.4]** for details].

Cell fusion is a versatile technique, which has been utilised in characterising, and mapping genes involved in tumour suppression [as reviewed by Stanbridge 1998], cell senescence [as reviewed by Ning & Pereira-Smith 1991] and aspects of differentiation [as reviewed by Blau 1999]. This technique has potential to contribute to the understanding of somatic cell reprogramming and the molecular events leading to differentiation.

Nuclear reprogramming has been defined as the process by which a differentiated somatic nucleus reacquires developmental potential [Singh 2000]. ES phenotypic cell hybrids have been generated from fusions between murine ES cells and murine somatic cells [Pells *et al.* 2002][Tada *et al.* 2001]. These observations indicate that somatic cells can be reprogrammed via fusion with Embryonic Stem cells.

This chapter details the generation of cell hybrids by fusing murine ES cells with murine somatic cells. It describes attempts to optimise the protocol so large numbers of cell hybrids are reproducibly generated. Subsequently **Chapter [4]** deals with the characterisation of the cell hybrids generated. **Chapters [5-9]** then uses this hybrid system to study the affect of various factors known or thought to perturb patterns of gene expression on the nuclear reprogramming of somatic cells.

## [3.2] Objectives

- 1) To generate cell hybrids from fusions of murine ES cells and somatic cells.
- 2) To optimise the generation of such hybrids.

## [3.3] Results and discussion

### [3.3.1] Development of selection regimes to isolate murine hybrid cells

When two cell types are mixed and induced to fuse [See **Fig 2.2**], some cells do not fuse, others fuse to cells of the same cell type (homokaryon formation) and yet others fuse to cells of the other cell type (heterokaryon formation). Without an appropriate selection regime hybrid cells are quickly overgrown by unfused cell types. In order to isolate cell hybrids derived from fusions of murine ES cells and somatic cells, it was necessary to develop selection regimes where unfused cells and hybrids derived from homokaryons are removed.

As outlined in **Subsection [2.2.4]**, various forms of selection were used to isolate cell hybrids derived from fusions of murine ES cells and somatic cells. In nearly all murine experiments, unfused ES cells were removed using HAT selection. The murine ES cell line used was HM-1, a hypoxanthine phosphoribosyltransferase deficient line developed by Selfridge *et al.* (1992). Aminopterin prevents both unfused HM-1 cells and HM-1 homokaryons from synthesizing nucleotides *de novo* (See **Subsection [2.2.4]**) and consequently such cells die in HAT selection.

Unfused somatic cells and somatic homokaryons can also be removed by selection. In fact, inherent conditions of culture can, on their own, act as a form of selection. Murine thymocytes [Sawa *et al.* 1997] and splenocytes [Matveeva *et al.* 1998] require considerably different culture conditions from murine ES cells and die when cultured in murine ES cell medium. They also grow in suspension rather than on the flask surface like

ES cells and other adherent cell-types do. Thus when fusing mES cells to these cell types, additional levels of selection are not required to isolate hybrid colonies. Other cell types however can grow under the murine ES cell culture conditions (e.g. fibroblasts). In such cases, additional levels of selection against unfused somatic cells and somatic homokaryons are required.

In order to isolate cell hybrids from fusions of PEFs and HM-1 cells, puromycin was used to select against unfused PEFs and PEF homokaryons. A puromycin kill curve for PEFs was generated (**Fig 3.1**) showed that  $2.5\mu\text{g} / \text{ml}$  puromycin is the minimum concentration required to completely kill all PEFs.

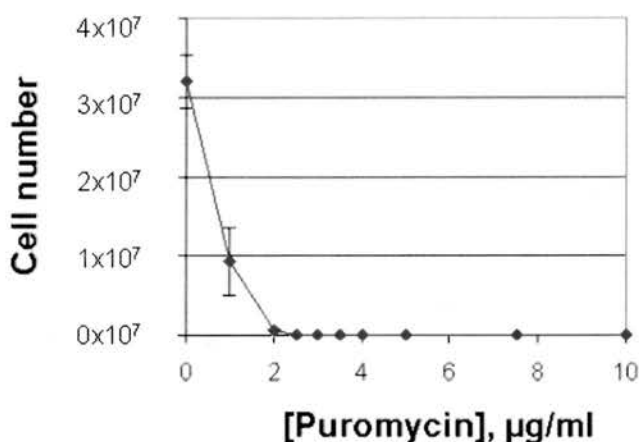


**Fig 3.1 Puromycin kill curve for primary embryonic fibroblasts**

15 gelatinised 10cm plates were each seeded with  $1 \times 10^5$  primary embryonic fibroblasts (passage number 1) and were incubated in murine ES medium. After 24hr, plates were divided into groups of three and each group was fed murine ES media supplemented with a different concentration of puromycin antibiotic [0-5  $\mu\text{g} / \text{ml}$ ]. Cells were cultured for an additional 12 days while maintaining the concentration of puromycin. Cells incubated in 0  $\mu\text{g} / \text{ml}$  puromycin reached confluence during this time and these cells were trypsinised and transferred to larger gelatinised dishes. After 9 days in puromycin, PEFs were trypsinised and the number of cells in each well as counted. The graph shows the mean cell count calculated from each group of triplicate plates incubated with a different concentration of puromycin. Error bars represent standard error of the mean cell number.

As wild-type HM-1 cells also die at this concentration of puromycin and so a puromycin resistant HM-1 clone, HM-1<sup>puro</sup>, had to be generated. This was done by lipofecting HM-1 cells (passage 13) with pPUR (See **Subsection [2.1.2.1]** for details of how cells were transfected and **Subsection [2.3.5]** for a description of pPUR). pPUR contains a cassette where the SV40 promoter constitutively drives expression of the puromycin resistance gene, *pac*. After transfection with pPUR, stably transfected clones were selected using murine ES medium supplemented with 2.5 µg / ml puromycin. After 12 days in selection, *pac* expressing, puromycin resistant colonies was picked and expanded. One of these transfected subclones, HM-1<sup>puro</sup>, was used in all hybridisation experiments where hybrid cells were to be derived from murine ES cell x PEF fusions. Puromycin was chosen as it quickly kills unfused PEFs or PEF derived homokaryons before they overgrew hybrid colonies derived from heterokaryons.

Previous forms of selection isolated hybrids generated from heterokaryons. An additional level of selection was developed to isolate hybrids in which reprogramming of a somatically derived *Oct-4* transgene was required (See **Subsection [2.2.4]**). It was assumed and later confirmed that in somatic cells derived from CBA<sup>Octneo/Octneo</sup> mice, the transgenic *Oct-4* promoter is inactive and did not drive *neo* expression (**Fig [4.3]**). By placing cells in the appropriate concentration of G418, only cells expressing *neo* would survive (due to the reprogramming of the somatically derived *Oct4* transgene). The appropriate concentration of G418 to use was identified by generating a G418 kill curve for HM-1 cells [**Fig 3.2**]. All HM-1 cells are killed with G418 concentrations of 150µg / ml or greater. In subsequent fusion experiments, double selection of 1xHAT and 150µg / ml G418 was applied to isolate reprogrammed hybrids.

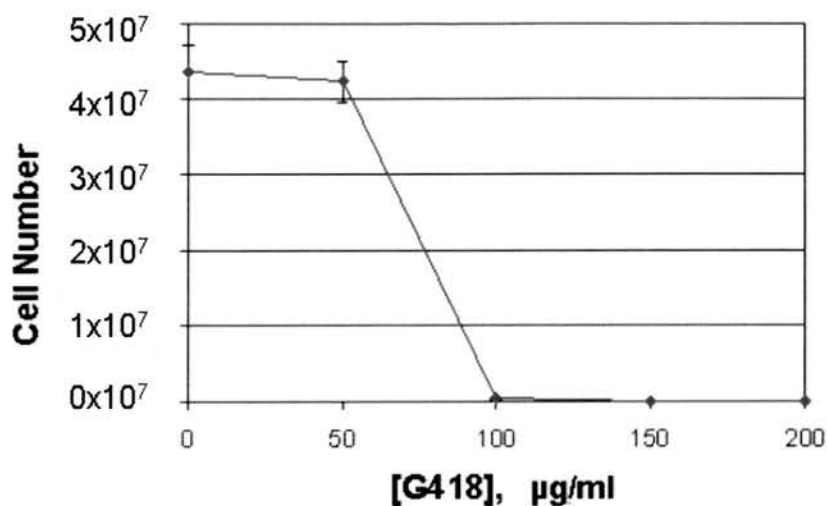


**Fig 3.2 G418 kill curve for HM-1 cells**

Fifteen gelatinised 10cm plates were each seeded with  $2 \times 10^5$  HM-1 cells and incubated in murine ES medium. After 24 hours, plates were divided into groups of three and each group was fed murine ES media supplemented with a different concentration of G418 [0, 50, 100, 150 and 200 µg / ml]. Cells were cultured for an additional 9 days while maintaining the concentration of G418. Cells incubated in both 0 and 50 µg / ml G418 reached confluence during this time and these cells were trypsinised and transferred to larger gelatinised dishes. After 9 days in G418, cells were trypsinised and the number of cells in each well as counted. The graph shows the mean cell count calculated from each group triplicate plates incubated with a different concentration of G418. Error bars represent standard error of the mean cell number.

Before attempting to generate cell hybrids, cell fusion was assayed under the physical conditions that were to be used to generate cell hybrids. As large numbers of cells would be required for hybridisation experiments, it was important to ensure cell fusion was occurring at a sufficient frequency. Obviously if heterokaryon formation was not occurring, no cell hybrids could be produced.



### [3.3.2] HM-1 cells can be fused to other HM-1 cells or to thymocytes

The prevailing dogma in the literature states that cells of the same cell type more readily fuse to each other than to cells of another cell type or species. Thus HM-1 cells were first electropulsed with other HM-1 cells in order to perfect the method of staining and fusing cells. As described in **Subsection [2.2.5]**, the two cell aliquots were previously stained, each with a different cytoplasmic dye. The cells are then mixed and electropulsed. Two-dye FACS analysis (**Subsection [12.1]**) was then used to measure the proportion of cells that are stained with both dyes. Controlling for dye leakage, an assessment of the proportion of viable cells fusing can be made [**Fig 3.3**]. It was calculated that 12.4% of HM-1 cells were fused to form homokaryons.

Next, HM-1 cells were electropulsed with a different cell type (thymocytes) to generate heterokaryons. **Fig 3.4** shows data from which the proportion of viable cells forming viable heterokaryons was calculated to 7.2%. Unfused thymocytes died within a few hours of being placed in murine ES cell medium, so the leakage control and fusion histograms do not show a cluster of CMTMR stained cells in the upper left quadrant as previously seen in **Fig 3.3**. Unfused thymocytes, along with other dead cells, had been gated out using the Forward Scatter / Side Scatter histogram as discussed in **Section [2.2.5]**.

It should be noted that the percentages in **Fig 3.3** and **Fig 3.4** are not directly comparable because in the first experiment the HM-1 cells are viable in the culture conditions used, whereas in the second experiment > 16% of the cells (thymocytes and hybrids displaying a thymocyte phenotype) are not.

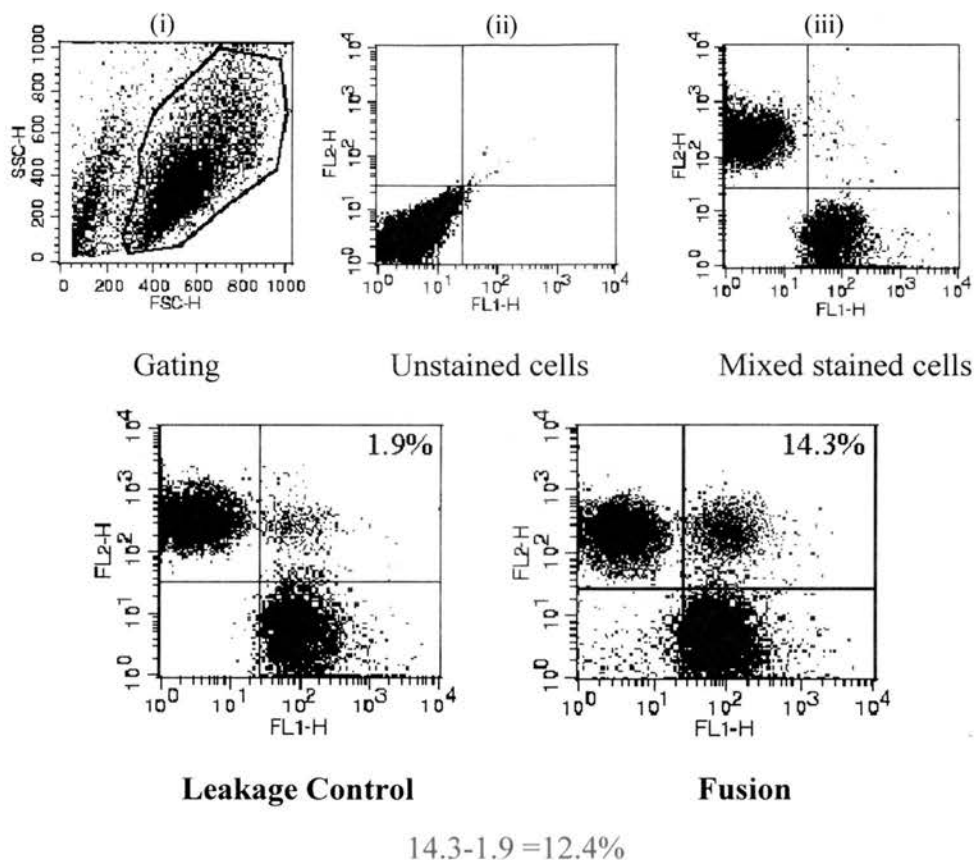


### Fig 3.3 Electrofusion of HM-1 cells generates viable homokaryons

Two aliquots of HM-1 were stained with either CMTMR or CMFDA cytoplasmic dye as described in **Subsection [2.2.5]**. The dye leakage control consisted of  $10^7$  CMTMR stained cells electropulsed and then mixed with previously electropulsed  $10^7$  CMFDA stained HM-1 cells. The fusion sample consisted of  $10^7$  CMTMR stained cells mixed with  $10^7$  CMFDA stained HM-1 cells and then electropulsed together. **Panel A** Gating and compensation data. (i) Dead cells were gated out using Forward Scatter / Side Scatter FACS analysis (See **Subsection [12.2]**). A typical gate is illustrated. (ii) Quadrant axes were defined so that unstained cells appeared in the lower left quadrant while CMTMR stained HM-1 cells (upper left quadrant) were distinct from CMFDA stained HM-1 cells (lower right quadrant) in the upper left quadrant. (iii) Unstained cells appear in the lower left quadrant. The same gate and quadrants were used throughout individual experiments. **Panel B** Histograms showing percentage of total gated events were double stained in the dye leakage control and fusion. Using these data, the percentage of cells forming viable homokaryons is 12.4%

**Abbreviations on axes:** **SSC** Side scatter (which is proportional to cell complexity), **FCS** Forward Scatter (which is proportional to cell size), **FL1-H** (Green fluorescence as measured using the green FACS filter FL1) and **FL2-H** (Red fluorescence as measured using the red FACS filter FL2).

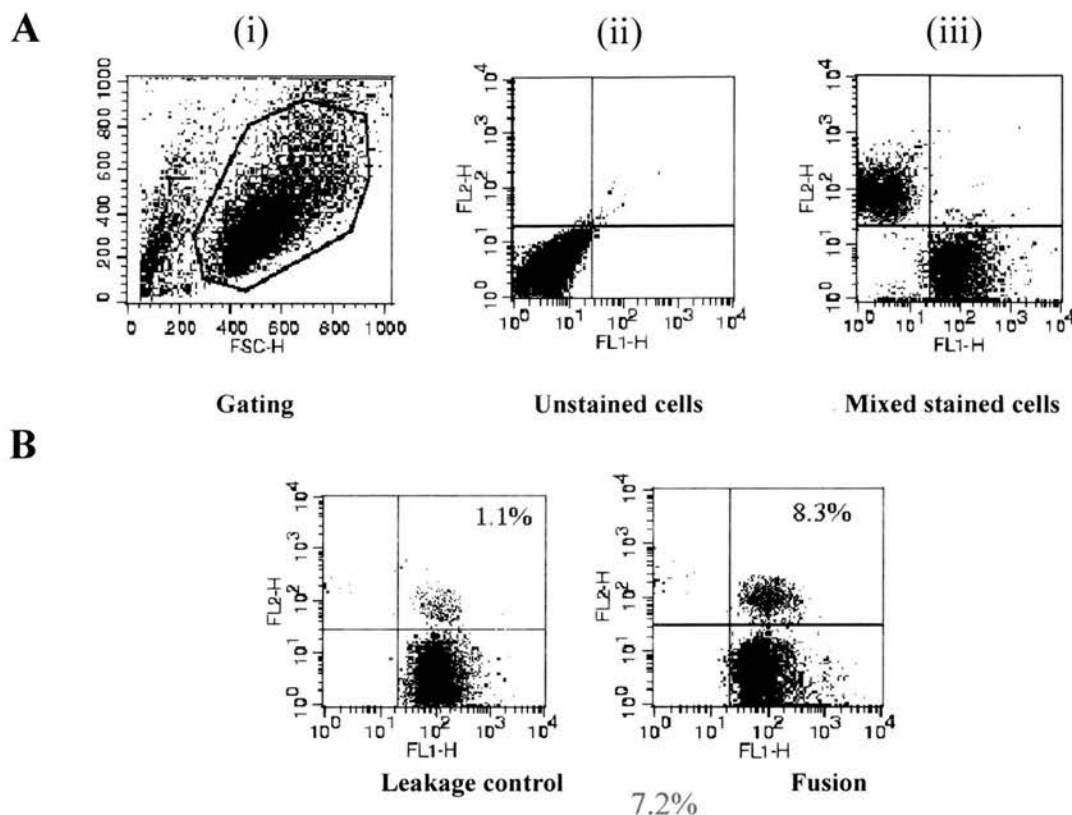


**Fig 3.4 Electrofusion of HM-1 cells and CBA<sup>Octneo/Octneo</sup> thymocytes generates viable heterokaryons**

Aliquots of CBA<sup>Octneo/Octneo</sup> thymocytes and HM-1 cells were stained with either CMTMR or CMFDA cytoplasmic dyes respectively as described in **Subsection [2.2.5]**. The dye leakage control consisted of  $5 \times 10^7$  CMTMR thymocytes electropulsed and then mixed with previously electropulsed  $10^7$  CMFDA stained HM-1 cells. The fusion sample consisted of  $5 \times 10^7$  CMTMR thymocytes mixed with  $10^7$  CMFDA stained HM-1 cells and then electropulsed together. **Panel A** Gating and compensation data. (i) Dead cells were gated out using Forward Scatter / Side Scatter FACS analysis. See **Subsection [12.2]** for further details of how this was done. A typical gate is illustrated. (ii) Quadrant axes were defined so that unstained cells appeared in the lower left quadrant while CMTMR stained thymocytes (upper left quadrant) were distinct from CMFDA stained HM-1 cells (lower right quadrant) in the upper left quadrant. (iii) Unstained cells appear in the lower left quadrant. The same gate and quadrants were used throughout individual experiments. **Panel B** Histograms showing percentages of total gated events that were double stained in the dye leakage control and fusion. Using these data, the % of cells forming viable heterokaryons was calculated as 7.2% (8.3-1.1%).

**Abbreviations on axes:** **SSC** Side scatter (which is proportional to cell complexity), **FCS** Forward Scatter (which is proportional to cell size), **FL-1** (Green fluorescence as measured using the green FACS filter FL-1) **and FL-2** (Red fluorescence as measured using the red FACS filter FL-2).

### [3.3.3] Colonies were generated by electropulsing mixtures of HM-1 cells and thymocytes and then selecting for cell hybrids generated from heterokaryons

HM-1 cells and thymocytes could be electrofused to produce viable heterokaryons. Whether hybrid cells could be derived from such fusions of HM-1 cells and thymocytes was now investigated. Two fusion experiments were carried out, the results of which are summarised in **Table 3.1** and **Fig 3.5**. Control and electropulsed mixtures of HM-1 cells and thymocytes, which were not placed in selection, quickly reached confluence within two days. This confirmed that electropulsing the cells, in itself, did not significantly affect cell viability.

Cells	Selection	Colony number (all pulsed cells placed in selection)
1x10 <sup>7</sup> HM1 cells & 5x10 <sup>7</sup> Thymocytes, Unelectropulsed	None	Grew to confluency
1x10 <sup>7</sup> HM-1 cells & 5x10 <sup>7</sup> Thymocytes, Electropulsed	None	Grew to confluency
1x10 <sup>7</sup> HM-1 cells & 1x10 <sup>7</sup> HM-1 cells, Electropulsed	1xHAT	0
5x10 <sup>7</sup> Thymocytes & 5x10 <sup>7</sup> Thymocytes, Electropulsed	1xHAT	0
1x10 <sup>7</sup> HM-1 cells & 5x10 <sup>7</sup> Thymocytes, Electropulsed	1xHAT	109

**Table 3.1 Colonies are generated by electropulsing HM-1 cells and thymocytes and selecting for hybrids generated from heterokaryons**

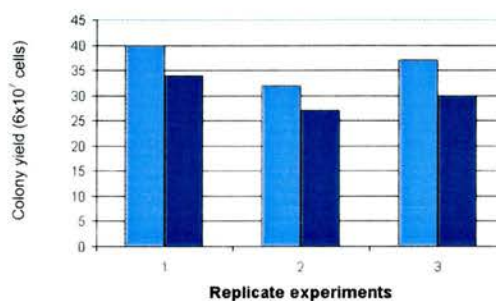
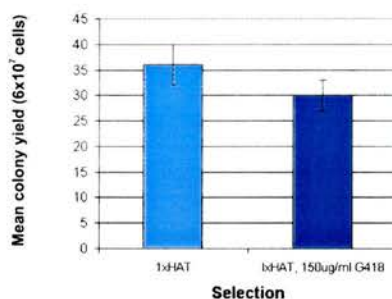
As outlined in the table above, aliquots of thymocytes freshly extracted from 6-7 week old CBA<sup>Octneo/Octneo</sup> mice and HM-1 cells were mixed and either electroelectropulsed and seeded onto gelatinized plates as described in **Subsection [2.2.5]** or else seeded unelectropulsed. Seeded plates were fed murine ES medium for 48 hours prior to selection being applied. Plates were maintained in 1xHAT selection for 12 days by which time colonies had stopped appearing on the plates.

**A**

■ 1xHAT ■ 1xHAT, 150µg/ml G418

**B**

Selection	Colony yield ( $2 \times 10^7$ cells)		
	Experiment 1	Experiment 2	Experiment 3
No selection	Grew to confluency	Grew to confluency	Grew to confluency
1xHAT	40	32	37
1xHAT, 150µg/ml G418	34	27	30

**C****D**

**Fig 3.5 Colonies are reproducibly generated under single and double selection for hybrids generated from heterokaryons**

$1 \times 10^7$  HM-1 cells and  $5 \times 10^7$  CBA<sup>Octneo/Octneo</sup> thymocytes were electropulsed as described in **Subsection [2.2.5]**. The electropulsed cells were divided equally between three 15cm gelatinised plates and cultured in mES medium for 24hr. After 24hr, mES medium was applied to the first plate, mES medium supplemented with 1xHAT to the second, and mES medium supplemented with both 1xHAT and 150µg / ml G418 to the third. Plates were maintained under these conditions for 12 days by which time colonies had stopped appearing on the plates. **Panel A** The colour code used to highlight whether single or double selection had been applied to plates to select hybrid colonies. **Panel B** Table summarizing colony yields from three replicate experiments. **Panel C** Graph showing colony yields under single and double selection for three replicate experiments. **Panel D** Graph showing mean hybrid yield for single and double selection plates from three replicate experiments (n=3).

Electropulsed mixtures of cells where only one cell type (HM-1 cells or thymocytes) was present did not generate colonies [Table 3.1]. This shows that as expected homokaryons and unfused cells are not viable in 1xHAT selection as expected. An electropulsed mixture of  $1 \times 10^7$  HM-1 cells and  $5 \times 10^7$  thymocytes yielded 109 colonies under 1xHAT selection verifying hybrids could be generated as others has previously done [Tada *et al.* 2001][Gallagher & McWhir Unpublished]. Electrofusions of HM-1 cells and thymocytes yielded colonies at low frequencies ( $\sim 1$  colony per  $6 \times 10^5$  cells electropulsed) similar to those generated by Gallagher & McWhir (Unpublished). Previous studies electrofusing EG cells with thymocytes also reported similar hybridisation frequencies using HAT selection [Surani *et al.* 1997]. Chemically induced fusion, using polyethylene glycol reported similar hybridisation frequencies both using HM-1 cells and splenocytes [Matveeva *et al.* (1983)] or EC cells and thymocytes [Tagaki *et al.* (1983)].

All colonies generated here displayed a classic murine ES cell morphology [Fig 3.6]. However, only cell hybrids expressing an ES cell phenotype were being selected for and it is unknown whether hybrids of a somatic phenotype could have also arisen.

Fewer colonies were generated in double selection plates than single selection plates (99 versus 109). The lower colony number in double selection plates could be due to the necessary retention within the hybrid nucleus of two chromosomes, one containing the active *hprt* gene and the other containing the integrated *neo* gene, instead of just one chromosome, that containing the *hprt* gene, which would be required for viability in single selection plates. It could also be due cells not being completely resistant to the concentration of G418 used in double selection.

Colonies were picked and expanded. These lines maintained an ES cell morphology. Such cells are hereafter referred to as TESH cells (abbreviated from 'putative Thymocyte ES cell Hybrid').



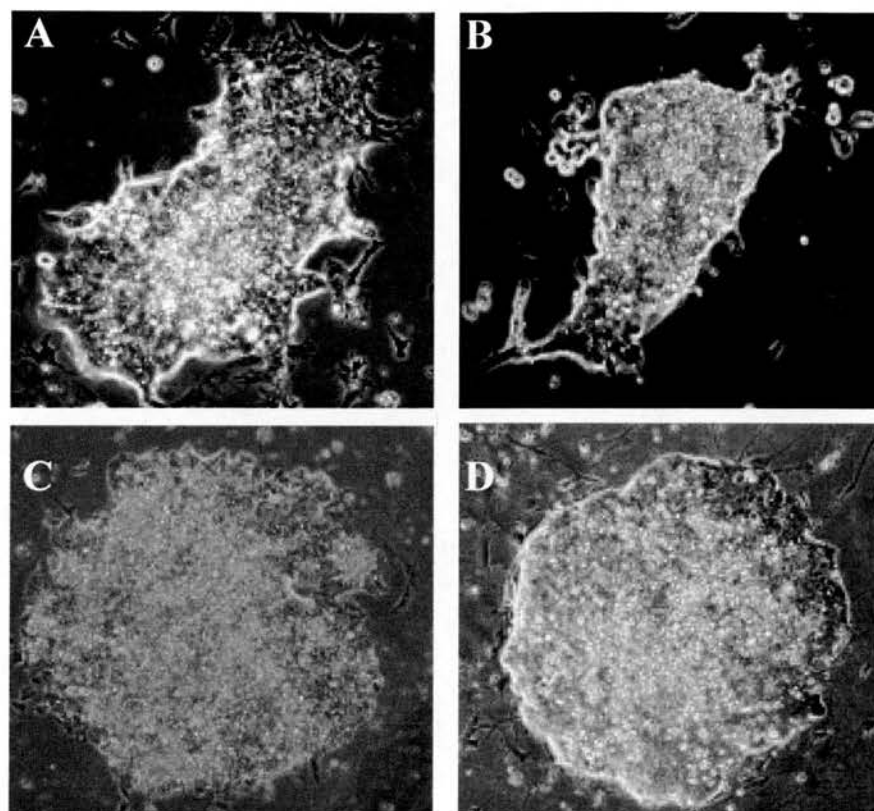


**Fig 3.6 All colonies derived from selection plates displayed a murine ES cell morphology**

Representative images of colonies are shown. All colonies, derived either from HM-1 fusions with either thymocytes or fibroblasts, displayed morphology indistinct from HM-1 cells. Images A, B and C are typical hybrid colonies derived from thymocyte fusions. Image D is a typical colony from a primary embryonic fibroblast fusion (See Section [3.3.4]).

**[3.3.4] Colonies were generated by pulsing HM-1<sup>puro</sup> cells and primary embryonic fibroblasts and selecting for cell hybrids generated from heterokaryons**

In order to investigate whether cell hybrids could be generated from other somatic cell types, HM-1 electrofusions with primary embryonic fibroblasts (PEF<sup>Octneo/Octneo</sup>) were performed. Cells were fused, resuspended in mES medium and



plated on 10 cm gelatinised plates. Twenty four hours after plating the cells were placed under 1xHAT and 2 $\mu$ g/ml puromycin selection. Fibroblasts grew to confluency before dying in HAT selection, so the cells were disaggregated with TEG and plated in larger 40 cm gelatinised dishes. Selection was maintained for 12 days. Colonies were generated (**Table 3.2**).

Cells	Selection	Colony yield ( $2 \times 10^7$ cells)
$1 \times 10^7$ HM1 <sup>puro</sup> cells & $1 \times 10^7$ PEFs, Unelectropulsed	None	Grew to confluency
$1 \times 10^7$ HM1 <sup>puro</sup> cells & $1 \times 10^7$ PEFs, Electropulsed	None	Grew to confluency
$1 \times 10^7$ HM-1 cells & $1 \times 10^7$ HM-1 cells, Electropulsed	1xHAT & 2.5 $\mu$ g/ml puromycin	0
$1 \times 10^7$ PEF & $1 \times 10^7$ PEFs, Electropulsed	1xHAT & 2.5 $\mu$ g/ml puromycin	0
$1 \times 10^7$ HM-1 cells & $1 \times 10^7$ PEFs, Electropulsed	1xHAT & 2.5 $\mu$ g/ml puromycin	10

**Table 3.2 Cell hybrids can be generated from electrofusions of HM-1 cells and CBA<sup>Octneo/Octneo</sup> primary embryonic fibroblasts**

$1 \times 10^7$  HM-1 cells and  $5 \times 10^7$  CBA<sup>Octneo/Octneo</sup> PEFs were resuspended in 400 $\mu$ l mannitol and fused at 300 V in a 0.2 cm cuvette. Cells were placed in selection (1xHAT and 2.5  $\mu$ g / ml puromycin) 24 hours after fusion and left for 3 days before being disaggregated with TEG and transferred to gelatinised 40 cm dishes due to fibroblast confluency. Selection was continued for 12 days by which time colonies had stopped appearing on the plates.

### **[3.3.5] Colonies were generated by PEG induced fusions of HM-1 cells with thymocytes but not splenocytes**

Colonies had been derived from fusions using thymocytes and PEFs. In order to show a broader range of cell types could be reprogrammed, attempts were made to generate ES cell hybrids from splenocytes. Initial experiments, each electrofusing  $10^7$

cells HM-1 cells with  $5 \times 10^7$  CBA splenocytes in a manner similar to the previous thymocyte experiments, failed to generate colonies under single (1xHAT) selection.

Matveeva *et al.* (1998) has successfully generated hybrids from HM-1 cells and murine splenocytes using polyethylene glycol (PEG). This PEG protocol (described in **Subsection [2.2.2]**) was used to attempt cell hybrid generation using either thymocytes or splenocytes as somatic fusion partners with HM-1 cells. As **Table 3.3** shows hybrids were derived from both electrofusion and PEG experiments where thymocytes were used as somatic fusion partners. Electrofusion proved more efficient than PEG exposure under the conditions used at generating colonies from HM-1 cells and thymocytes: colony yield is, on average, over 4 greater with electrofusion than with PEG ( $108 \pm 3$  versus  $26 \pm 1$ ).

Cells	Method of fusion	Colony yield ( $6 \times 10^7$ cells), 1xHAT selection	
		Experiment 1	Experiment 2
$1 \times 10^7$ HM-1 & $5 \times 10^7$ CBA <sup>Octneo/Octneo</sup> Thymocytes	Electrofusion	111	105
$1 \times 10^7$ HM-1 & $5 \times 10^7$ CBA <sup>Octneo/Octneo</sup> Thymocytes	PEG exposure	25	27
$1 \times 10^7$ HM-1 & $5 \times 10^7$ CBA <sup>Octneo/Octneo</sup> Splenocytes	Electrofusion	0	0
$1 \times 10^7$ HM-1 & $5 \times 10^7$ CBA <sup>Octneo/Octneo</sup> Splenocytes	PEG exposure	0	0

**Table 3.3 Colonies could be generated from thymocytes but not from splenocytes using either electropulsing or PEG exposure to induce fusion**

Electropulsing (**Subsection [2.2.1]**) or PEG exposure (**Subsection [2.2.2]**) were used to fuse HM-1 cells to either thymocytes or splenocytes taken from 6-7 week old CBA<sup>Octneo/Octneo</sup> mice. After being induced to fuse, cell mixtures were left in full medium for 24 hours before being placed under single (1xHAT) selection for 12 days. The table above shows colony yields for two replicate experiments.

Experiments optimising the generation of cell hybrids from HM-1 cells and thymocytes (**Subsection [3.3.5]**) were prioritised over those attempting to generate hybrids from splenocytes and the reason for failure to generate cell hybrids from splenocytes was not further investigated. One possible explanation is that splenocytes did not fuse to HM-1 cells under the conditions used. This could be tested using the 2-dye FACS analysis similar to that applied in experiments fusing HM-1 cells and

thymocytes (**Fig 3.4**). Why the splenocytes would not fuse to HM-1 cells when the protocol used had previously generated hybrids [Matveeva *et al.* 1998] is unknown. Another possible explanation is that the splenocytes were dead when fused to HM-1 cells but again why this would be so is unclear given that Matveeva's protocol was followed. It is suspected that some small technical difference between the protocol followed here and that carried out by Matveeva *et al.* is the reason for failure to isolate colonies from splenocytes fusions.

### [3.3.6] Optimisation of hybridisation

Optimisation of the protocols for generating cell hybrids from HM-1 cells and thymocytes was sought as the colony yield was thought to be low (1 colony per  $10^6$ - $10^7$  cells), even though similar figures were reported by both electrofusion [Tada *et al.* (1997)] and PEG mediated fusion [Matveeva *et al.* (1998)]. If more cell hybrids could be generated for a given number of cells, fewer cells would be required to carry out fusion experiments. If less somatic cells were required for hybridisation experiments, less mice could be sacrificed, but it was principally the need for large numbers of HM-1 cells that was the main limitation to the number of hybridisation experiments carried out.

300 V was found to be the optimal voltage of a range of four for generating hybrid colonies in either single or double selection plates (**Table 3.4**).

Voltage (V)	No selection control	Colony yield ( $6 \times 10^7$ cells)	
		Selection	
		1xHAT	1xHAT & 150 $\mu$ g/ml G418
150	Confluent after 2 days	6	5
300	Confluent after 2 days	118	101
400	Confluent after 2 days	60	53
600	Cells dead	0	0

**Table 3.4 Voltage affects hybrid colony yield from electropulsed cells**

HM1 x thymocyte fusions were carried out in 0.2cm cuvettes with various voltages. In each fusion experiment,  $1 \times 10^7$  HM-1 cells and  $5 \times 10^7$  CBA<sup>Octneo/Octneo</sup> thymocytes were resuspended in 400 $\mu$ l mannitol and placed in the appropriate cuvette. Cells were placed in selection 24hr after fusion and left for 12 days before colonies were counted.

Chamber conductivity is known to affect cell fusion and hybridisation frequencies [Jaroszeski *et al.* 1994]. The effect of cell conductivity on hybridisation frequency was investigated. Three conditions known to alter cell conductivity were altered in three separate experiments. The conditions varied were (i) the gap distance i.e. the distance between the electrodes of the cuvette (**Table 3.5**), (ii) the chamber volume (**Table 3.6**) and (iii) polarisation of the electrofusion chamber (**Fig 3.7**).

Gap distance (cm)	Voltage (V)	No selection control	Colony yield ( $6 \times 10^7$ cells), 1xHAT
0.1	150	Confluent after 2 days	72
0.2	300	Confluent after 2 days	108
0.4	600	Cells dead	0

**Table 3.5 Hybrid colony yield is affected by gap distance**

HM1 x thymocyte fusions were carried out in cuvettes with various distances between their electrodes (gap distances). In each fusion experiment,  $1 \times 10^7$  HM-1 cells and  $5 \times 10^7$  CBA<sup>Octneo/Octneo</sup> thymocytes were resuspended in 400 $\mu$ l D-mannitol buffer and placed in the appropriate cuvette. The V/cm ratio was kept constant i.e. single pulses of 150V, 300V, 600V were applied to cuvettes with gap distances of 0.1, 0.2, 0.4cm respectively. Cells were placed in selection 24hr after fusion and left for 12 days before colonies were counted.

**Table 3.5** showed that hybridisation frequency is affected by gap distance. The voltage was increased in proportion to the distance between electrodes so that 1500 V / cm was applied in each case. Fusions using 0.1 cm and 0.2 cm cuvettes produced hybrid colonies. It was hypothesised that the 0.1 cm cuvette fusion failed to yield as many colonies as the 0.2 cm cuvette because approximately one third of the cellular suspension lay above the electrodes in the smaller cuvette. Most of the cells in 0.4 cm cuvettes lysed after application of 600 V. No colonies were isolated from cells fused in this cuvette size. The highest colony yield was observed in 0.2 cm cuvettes electropulsed with 300V.

The effect of chamber volume on hybridisation frequency was then investigated (**Table 3.6**). The voltage applied was increased in proportion to the chamber volume.

Gap distance (cm)	Voltage (V)	Chamber Volume ( $\mu$ l)	No selection control	Colony number ( $6 \times 10^7$ cells fused) 1xHAT
0.1	150	200	Confluent after 2 days	61
0.2	300	400	Confluent after 2 days	117
0.4	750	1000	Cells dead	0

**Table 3.6 Hybrid colony yield is affected by chamber volume**

HM1 x thymocyte fusions were carried out in cuvettes with various chamber volumes. Cellular suspension was added to each cuvette until the meniscus of the cellular suspension reached the top of the cuvette electrodes. The V / cm ratio was kept constant for each cuvette. Cells were placed in selection 48hr after fusion and left for 12 days before colonies were counted.

Colonies were derived from cells in 0.1 cm and 0.2 cm cuvettes. No colonies were derived from the 0.4 cm cuvette, despite no cell lysis being evident. The highest colony yield was observed using the 0.2 cm cuvette electropulsed with 300V.

The next experiment investigated the effect of polarising the electrofusion chamber (**Table 3.9**). Application of an insulating wax to one electrode of the cuvette affects the functional area of one electrode and polarises the electrofusion chamber. This polarisation changes the chamber conductivity, increasing the pulse duration. Elongation of the pulse has been observed to enhance both survival of electropulsed cells and hybridisation frequency [Scott-Taylor *et al.* 2000]. Despite this observation, waxing failed to increase hybridisation frequency (See **Table 3.7**). The lack of colonies generated under HAT selection from the waxed cuvette was not caused by the wax being toxic to the cells as the waxed control without selection showed no sign of toxicity and reached confluency at the same time as the unwaxed unselected control.

<b>Electrode waxed?</b>	<b>No selection control</b>	<b>Colony yield</b> ( $6 \times 10^7$ cells fused) 1xHAT
Yes	Confluent after 2 days	0
No	Confluent after 2 days	108

**Table 3.7 Polarisation of the electrofusion chamber did not increase colony yield**

HM1 x thymocyte fusions were carried out in waxed and unwaxed cuvettes to assess whether polarisation of the electrofusion chamber increased colony yield.  $1 \times 10^7$  HM-1 cells and  $5 \times 10^7$  CBA<sup>Octneo/Octneo</sup> thymocytes were fused in waxed and unwaxed 0.2 cm cuvettes (300V). Cells were placed in selection 48hr after fusion and left for 12 days before colonies were counted.

In summary, experiments indicated that of all the conditions tested, pulsing HM-1 cells and thymocytes resuspended in 400 $\mu$ l, in an unwaxed 0.2cm cuvette, with a voltage of 300V gives the highest hybridisation frequency.

### [3.4] Conclusions

Appropriate levels of selection, for isolating cell hybrids generating from fusion of HM-1 cells and somatic cells, were identified. A puromycin resistant HM-1 clone, HM-1<sup>puro</sup>, was generated so puromycin selection could be used to select against unfused PEFs in hybridisation experiments.

Electropulsing induced the fusion of HM-1 cells both to themselves (to form homokaryons) and to thymocytes (to form heterokaryons). Colonies were generated by pulsing mixtures of HM-1 cells and either thymocytes or primary embryonic fibroblasts and selecting for hybrids generated from heterokaryons. All colonies generated in selection displayed a murine ES cell morphology even when cells displaying the somatic phenotype are viable in the culture conditions (i.e. HM-1 x PEF fusions). This shows that the ES cell morphology is dominant over the somatic cell morphology in ES x somatic hybrids.

In addition to pulsing, colonies were also generated by exposing mixed pellets of HM-1 cells and thymocytes to polyethylene glycol (PEG). Experiments using mixtures of HM-1 cells and splenocytes failed to generate colonies using either pulsing and PEG to induce fusion.

Attempts were made to optimise colony generation from fusions of HM-1 cells and thymocytes. Colony yield was affected by gap distance (the distance between the cuvette electrodes) and not found to be directionally proportional to chamber volume of the cuvette. Polarisation of the chamber by applying a thin layer of wax to one electrode did not increase colony yield. Of all the conditions tested, application of a single pulse (300 V, 25  $\mu$ F) to cells resuspended in 400  $\mu$ l D-mannitol buffer in a 0.2 cm cuvette gave the highest colony yields.



## [4] Characterisation of murine hybrid cells

### [4.1] Introduction

In **Chapter [3]** colonies of cells were recovered from mixtures of ES cells and somatic cells that had been fused and placed under culture conditions that selected for reprogramming of somatic cells to an ES phenotype. Colonies were picked and expanded and this chapter describes the characterisation of three lines: TESH1 (generated from HM-1 cells and CBA<sup>Octneo/Octneo</sup> thymocytes via electrofusion); TESH2 (also generated from HM-1 cells and CBA<sup>Octneo/Octneo</sup> thymocytes but via exposure to PEG); and FESH1 (generated from HM-1 and CBA<sup>Octneo/Octneo</sup> primary embryonic fibroblasts via electrofusion).

These lines were studied to see whether reprogramming of the somatic nucleus had taken place. If reprogramming of the somatic nucleus had truly occurred, one would expect the patterns of gene expression to change so that cell type specific genes active in the thymocyte would be silenced and genes associated with ES cell phenotype would be activated. Additionally, reprogrammed nuclei would behave functionally as ES cells (i.e. they could direct the formation of embryoid bodies and display pluripotency both *in vivo* and *in vitro*). Thymocytes and fibroblasts are differentiated cells and if cell hybrids derived from these cells displayed pluripotency this would show that nuclear reprogramming had taken place.

### [4.2] Objective

To investigate whether clones (TESH-1, TESH-2 and FESH-1) were phenotypic ES cell hybrids and whether reprogramming of the somatic nuclei had taken place.

### [4.3] Results and discussion

#### [4.3.1] Clonal lines are cell hybrids displaying sub-tetraploid chromosome number

Mitotic spreads were made from TESH-1, TESH-2, and FESH-1 clones at passage number 7. Fifty representative spreads were counted for each cell line. All spreads displayed tetraploid or near tetraploid chromosomal numbers verifying that TESH-1, TESH-2, and FESH-1 were all cell hybrid lines. Representative mitotic spreads of TESH-1 (showing complete tetraploidy at passage 7) and HM-1 cells (showing a diploid chromosome number) are shown in **Fig 4.1 Panel A**. The modal chromosomal number for both TESH-1 and FESH-1 was 80 at passage 7, whereas it was 76 for TESH-2. TESH-2 was generated using PEG, and unlike the electrofusion derived lines, it displayed a constant and noticeable degree of cell death during culture.

The effect of passage number on cell hybrid genotype was investigated. Two of the cell hybrid lines, TESH-1 and TESH-2, were cultured beyond passage number 7 and mitotic spreads were made from them at passage numbers 12 and 17. **Fig 4.1 Panel B** shows that the two lines tested lost chromosomes during culture. It was observed that the modal chromosomal number of TESH-2 cells decreased more rapidly than that of TESH-1 cells at the same passage number ( $P < 0.05$  as calculated using Student's unpaired t-test [Caria 2000]). A possible explanation for this is that TESH-2 cells needed to undergo more cell divisions than TESH-1 cells before approaching confluence as they display a low level of spontaneous cell death. Cells were only passaged when approaching confluence, thus viable TESH-2 cells will have divided more times than TESH-1 cells of equivalent passage number.

The literature describing fusion of ES cells and somatic cells also suggests that PEG-fused cell hybrids lose chromosomes more quickly with respect to passage number when cultured in HAT selective medium. Tada *et al.* 2001 electrofused murine ES cells with murine thymocytes and reported a full tetraploid complement in all 10 mitotic spreads (passage 7). Matveeva *et al.* (1998) however reported hybrid clones derived from PEG fusion of HM-1 with splenocytes as having as few as 41-43 chromosomes at passage 12. It would be interesting, but beyond the remit of this

work, to investigate whether genomic stability of cell hybrids is affected by the fusagen used. No explanation could be given for how PEG might affect genomic stability of cells.

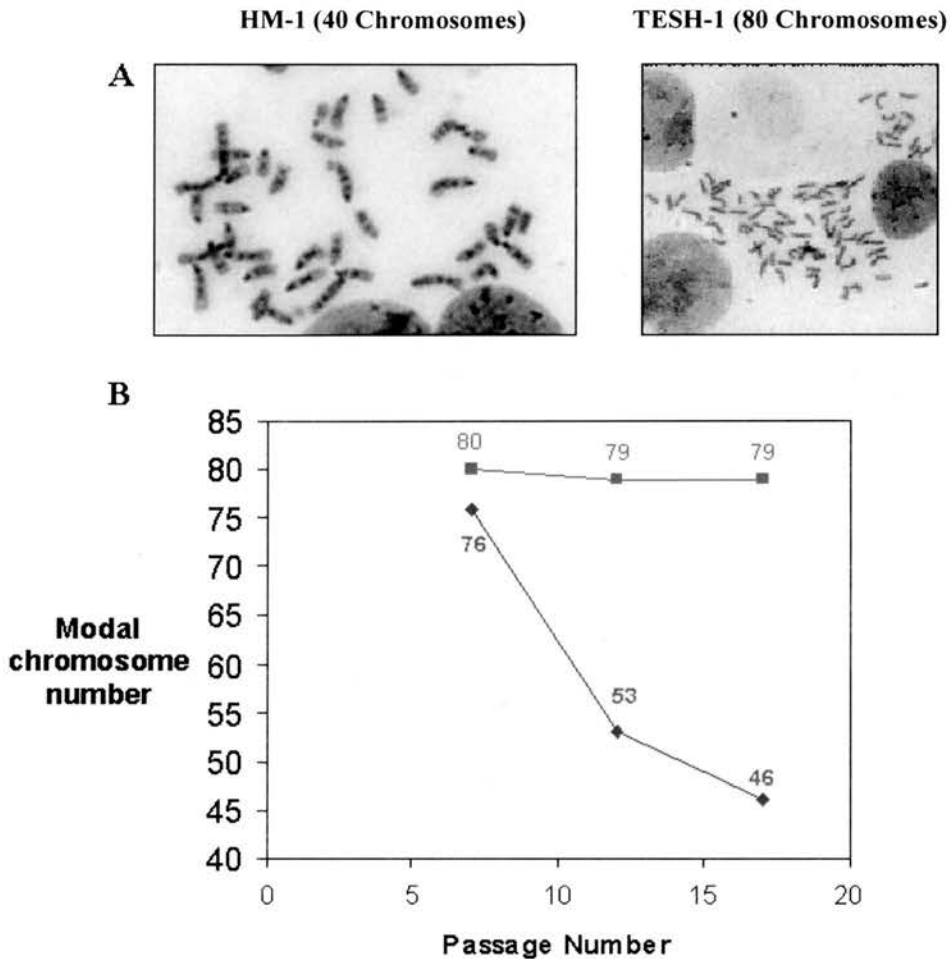


**Fig 4.1 Clones are hybrid cells**

Mitotic spreads were made from HM-1 cells and cell hybrid lines as described in **Subsection [2.3.2]**. **Panel A** Mitotic spreads showing a diploid complement in a HM-1 cell and a tetraploid complement of chromosomes in hybrid TESH-1 at passage number 7. At passage number 7, the modal chromosome number for TESH-1 and FESH-1 was 80, whereas for TESH-2, it was 76. **Panel B** As TESH-1 (■) and TESH-2 (◆) cells are passaged, the modal chromosome number of the spreads, decreases. Mitotic spreads of hybrid clones TESH-1 and TESH-2 were generated at higher passage numbers (12 and 17). Cells were continuously grown in 1xHAT selective medium. The modal chromosome number was calculated from 50 good spreads for each passage.



A PCR experiment was performed using primer sets specific to the V-J region of *Tcr $\gamma$*  [Fig 4.2]. Rearrangement of the V-J region of *Tcr $\gamma$*  was found in TESH-1 cells. Thus, this line was derived from HM-1 cells fusing with adult thymocytes and not with an endogenous stem cell. Tada *et al.* (2001) had previously investigated T-cell receptor gene rearrangement in ES phenotypic cell hybrid lines generated from ES cells. Out of 31 hybrids clones analysed, 17 carried at least one rearrangement of the following genes: *Tcr $\gamma$* , *Tcr $\beta$* , *IgH*, and *Tcr $\delta$* . Rearrangement in the *Tcr $\alpha$*  gene was not assessed.

#### [4.3.2] A somatically derived transgenic *Oct-4* promoter is silent in thymocytes but is reactivated after fusion with HM-1 cells

Whether reprogramming of the somatic chromatin had taken place within the hybrid cells was now investigated. As discussed in detail in Section [1.6], *Oct-4* is a transcription factor expressed in all pluripotent cell types of the mouse. When the activity of the *Oct-4* promoter decreases within a pluripotent cell, the cell differentiates. The activity of the somatically derived *Oct-4* promoter was assayed in thymocytes and TESH-1 cells to see if there is epigenetic reprogramming at this locus.

TESH-1, TESH-2 and FESH-1 lines were all derived from fusions of HM-1 cells with somatic cells derived from CBA<sup>Octneo/Octneo</sup> mice. Total RNA was isolated intact from 4 cell types: CBA<sup>Octneo/Octneo</sup> ES cells, HM-1 cells, CBA<sup>Octneo/Octneo</sup> thymocytes and TESH-1 cells (Fig 4.3 Panel A). cDNA was made from these RNA samples and their integrity was verified by RT-PCR with  *$\beta$ -actin* primers (Fig 4.3 Panel B). A series of RT-PCR reactions using *neo* specific markers was then performed using the same cDNA. No *neo* expression was seen in controls lacking reverse transcriptase showing that genomic DNA contamination of the cDNA had not taken place. *neo* expression was detected in the positive control (ES<sup>Octneo/Octneo</sup> cells) where the *Oct-4* promoter was actively driving *neo* expression. *neo* was not expressed in unfused thymocytes showing that the *Oct-4* promoter is inactive in this terminally differentiated cell type. No *neo* expression was observed in HM-1 cells either (here the *Oct-4* promoter is active but the *neo* coding sequence is absent).



Finally *neo* was expressed in TESH-1 hybrid cells. Together these data show that the somatic derived *Oct-4* promoter was inactive in unfused thymocytes but reactivated following hybridisation with HM-1 cells. This confirms that epigenetic reprogramming of the somatic *Oct-4* locus has occurred as a result of cell fusion.

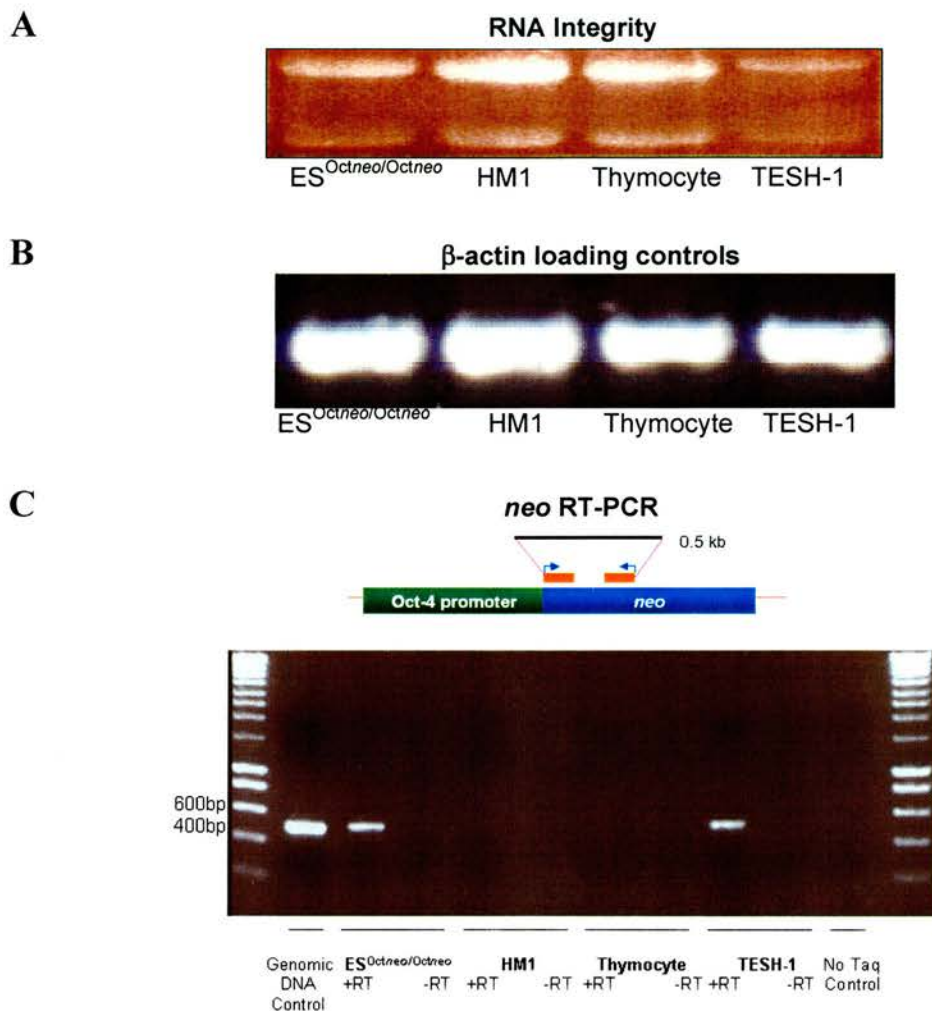


**Fig 4.3 A somatically derived transgenic *Oct-4* promoter is reactivated in hybrid cells**

Primers were designed to amplify a 0.5kb sequence of the transcript produced from the integrated neomycin cassette in order to investigate whether it was expressed in unfused somatic cells taken from CBA<sup>Octneo/Octneo</sup> mice [Section 2.7]. **Panel A** Total RNAs were isolated from CBA<sup>Octneo/Octneo</sup> ES cells, HM-1 ES cells, CBA<sup>Octneo/Octneo</sup> thymocytes and TESH-1 hybrid cells. The two major bands, corresponding to 28S and 18S ribosomal RNA, are distinct, indicating that the RNA for each sample has not been degraded. **Panel B** β-actin loading controls. **Panel C** A schematic showing *neo* primers amplifying a 0.5kb fragment and *neo* RT-PCR showing that while the somatic *Oct-4* promoter is inactive in thymocytes, it is reactivated in the cell hybrid, as shown by the amplification of the *neo* fragment. Reactivation of the *Oct-4* promoter occurred in TESH-1 which had been selected using G418 but also in other hybrid clones where G418 had not been used (data not shown).

### [4.3.3] Cell hybrid lines display high alkaline phosphatase activity

Tissue non-specific alkaline phosphatase activity is high in the ICM of preimplantation embryos [Johnson *et al.* (1977)] and in murine primordial germ cells [Matsui *et al.* 1992]. Consequently, it is a commonly used biochemical marker for undifferentiated pluripotent cells like ES and EC cells. Activity of this enzyme was assessed in hybrid cells to better define the ES cell-like phenotype of the hybrid clones. **Figure 4.4** shows that cell hybrid lines TESH-1, TESH-2 and FESH-1, as well as the HM-1 control, all displayed high endogenous alkaline phosphatase activity. Unfused thymocytes showed no alkaline phosphatase activity and unfused PEFs showed a small portion of cells that displayed comparatively weak alkaline phosphate activity. The PEFs are isolated by a crude method of mashing up embryos (**Subsection [2.1.1.2]**) and consequently there is a mixture of cell types present. The morphology and relatively weak level of alkaline phosphatase activity of these PEF-associated cells suggest that they are somatic cells and not undifferentiated cells. Similar to the data described here, Matveeva *et al.* (1998) showed high alkaline phosphatase activity in cell hybrids generated from HM-1 cells and murine splenocytes.



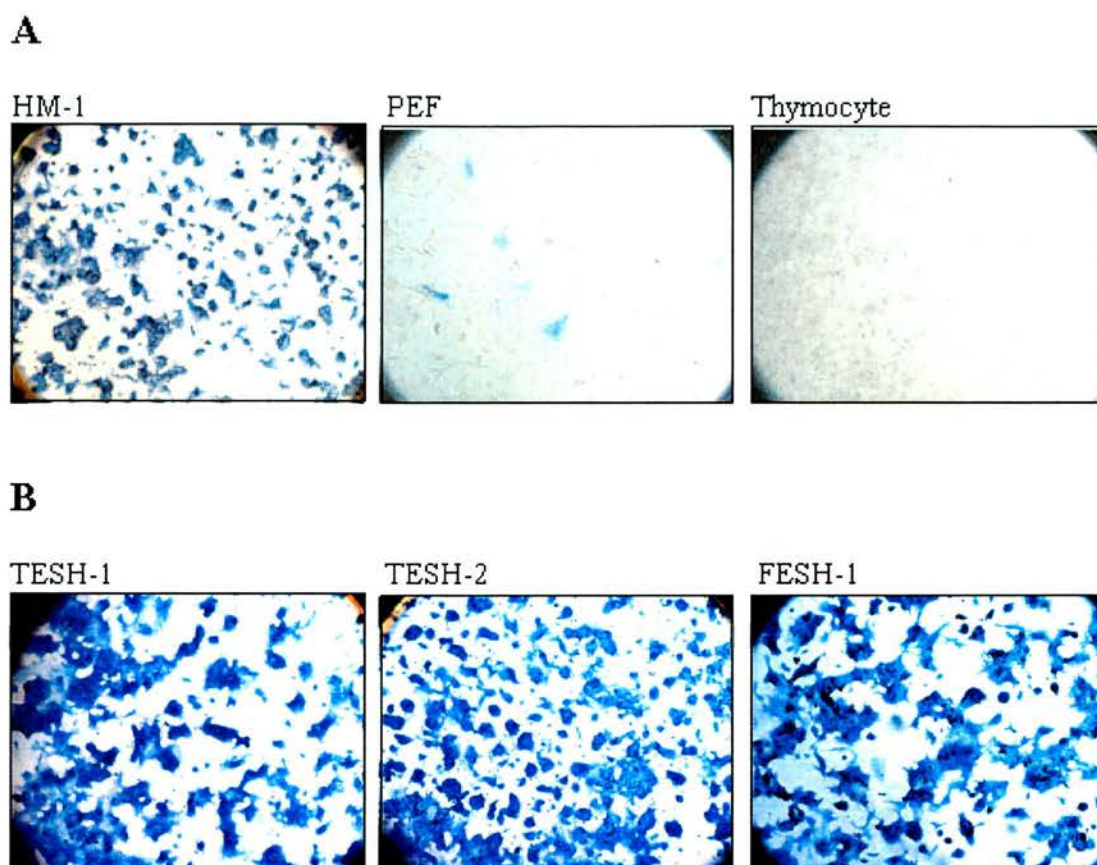


**Fig 4.4 Cell hybrid lines displayed alkaline phosphatase activity**

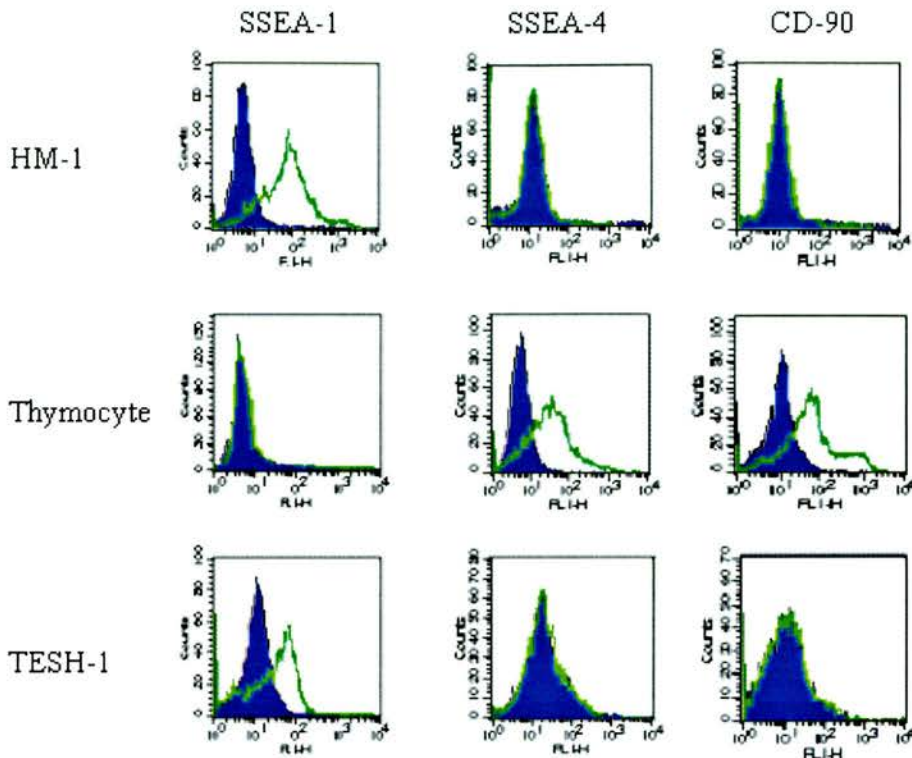
Subconfluent cultures of cells were stained for alkaline phosphatase activity as described in **Subsection [2.4.1]**. Undifferentiated pluripotent stem cells are characterised by high levels of alkaline phosphatase expression which is down-regulated following stem cell differentiation. **Panel A** Alkaline phosphatase staining for HM-1 cells, PEFs and thymocytes. **Panel B** Three cell hybrid lines generated from fusions of these cell types. All cells in the HM-1 control, TESH-1, TESH-2 and FESH-1 wells stained positive for alkaline phosphatase activity. A small proportion of cells in the PEF well displayed comparatively weak staining.

#### [4.3.4] Cell hybrid lines display cell surface marker expression profiles similar to HM-1 cells

Next, the expression of cell surface markers by the cell hybrids was investigated. Cells were immunostained for SSEA-1 (a cell surface marker for undifferentiated murine cell types), SSEA-4 (a cell surface marker for primitive endoderm) and CD90 (a thymocyte-specific cell surface marker, this is also called Thy-1). **Fig 4.5** shows histograms compiled after the cells were FACS analysed for expression of these three markers. The HM-1 control was SSEA-1 positive and did not express either SSEA-4 or CD90. In contrast, the thymocyte control expressed both SSEA-4 and CD90 but not SSEA-1. Hybrid clones TESH-1, TESH-2 and FESH-1 all displayed a marker expression profile similar to that of the HM-1 cells.

Again similar to these data, Matveeva *et al.* 1998 reported hybrid cell expression of the undifferentiated cell marker ECMA-7 and suppression of the differentiated cell marker TROMA-1 in their hybrid lines. Andrews & Goodfellow (1980) generated cell hybrids from murine EC (PCC4azaR) cells and thymocytes and also found the expression of SSEA-1 and the extinction of CD90. They also reported continued expression of another embryonic antigen (3C4-10) and the suppression of expression of another thymocyte antigen (Ly-2) in the hybrid cells. Not all EC markers were expressed and thymocyte specific markers suppressed in these hybrid cells however (*i.e.* the PCC4azaR specific marker, H-2Db, was not expressed in the while the thymocyte specific marker, H-2Kk, still was).

A



B

Cell line	Marker		
	SSEA-1	SSEA-4	CD90
HM-1	+	-	-
Thymocyte	-	+	+
TESH-1	+	-	-
TESH-2	+	-	-
FESH-1	+	-	-

**Fig 4.5 TESH-1 cells express the undifferentiated cell marker SSEA-1 but not SSEA-4 or the thymocyte specific marker CD90**

Cells were disaggregated and immunostained for SSEA-1, SSEA-4 and CD90 as described in **Subsection [2.4.3]**. **Panel A** Histograms generated by FACS analysis of stained cells. In each histogram, (■) indicates the control fluorescence spectrum using a mock primary antibody (IgM for SSEA-1 and CD90, IgG3 for SSEA-4) while (—) indicates the fluorescent spectrum using specific antibodies to SSEA-1, SSEA-4 and CD-90 as labelled. Representative spectra for HM-1 cells, thymocytes and TESH-1 cells are shown. If cells are not expressing a marker, the two fluorescent spectra will overlap. If cells are expressing the marker, then the spectrum for the specific primary antibody will display bandshift to the right. **Panel B** Table summarising marker expression profiles of each cell line. '+' indicates that cells expressed a specific marker, '-' indicates that they did not.

#### **[4.3.5] Hybrid cells generate tumours in SCID mice that contain cells representing all three embryonic germ layers**

As highlighted in **Section [1.6]**, one of the hallmarks of ES cells is that they generate tumours which comprise all three embryonic germ layers (endoderm, mesoderm and ectoderm) when injected into immunodeficient mice. To investigate tumourigenicity and developmental competence,  $2 \times 10^7$  HM-1 cells or hybrid cells respectively were injected into adult severe combined immunodeficient (SCID) mice (strain C.B-17/Icr) as described in **Subsection [2.4.4]**. The two HM-1 controls and the three hybrid lines all generated tumours within 3 weeks of cell injection. The hybrid lines took longer to produce tumours than the HM-1 controls (19 days as opposed to 14). This may be due to the longer doubling time of hybrid cells *in vivo* which was also observed in culture. TESH-2 produced the smallest tumour. It is suspected that this is due to a low level of spontaneous cell death *in vivo* that had previously observed *in vitro*.

All five tumours were then fixed, paraffin embedded, and sectioned as described in **Subsection [2.4.4]**. H&E staining of both control and cell hybrid derived sections was carried out (see **Subsection [2.4.4]**) and this provided histological evidence that tumours contained cells representing the ectoderm and mesoderm (**Fig 4.7 Panels B,C,D & E**). Visual examination of tumour sections failed to provide unequivocal histological evidence for endoderm. Consequently unstained sections were dewaxed, rehydrated (See **Subsection [2.4.4]** for details) and immunostained for ezrin as described in **Subsection [2.4.3]**. Ezrin is a marker of endodermal cells [Abelev 1971][Bretscher 1986]. Immunostained sections of all the HM-1 and hybrid line derived tumours showed ezrin-positive epithelium (**Fig 4.7 Panel A**), providing evidence that tumours also contained cells representing the endoderm. Thus hybrid cells are capable of generating cells of all three embryonic germ layers *in vivo* and display an equivalent developmental potential to HM-1 cells.



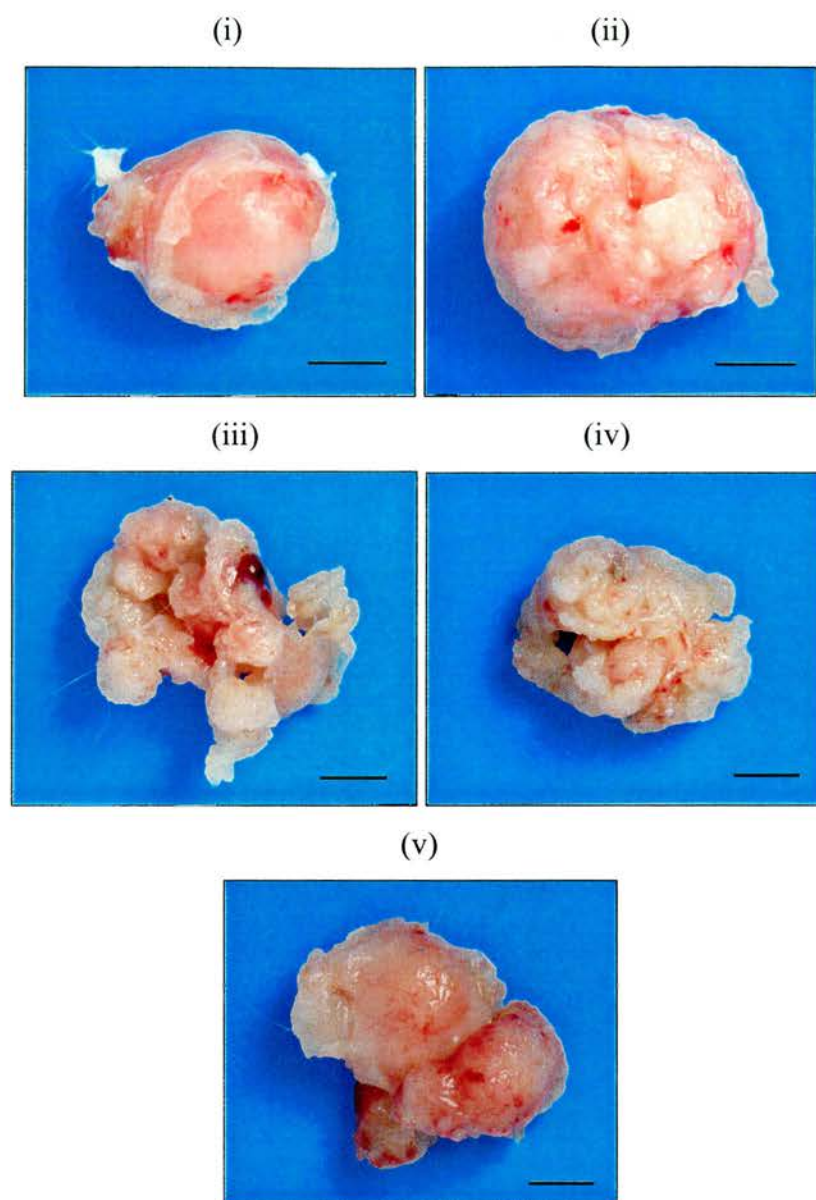


**Fig 4.6 Hybrid cells and HM-1 cells generate benign tumours when injected into SCID mice**

$2 \times 10^7$  cell aliquots of HM-1 cells (Passage #21) and the three cell hybrid lines (Passage #6) were injected into adult SCID mice strain C.B-17/Icr as described in **Subsection [2.4.4]**. Two SCID mice each injected with  $2 \times 10^7$  HM-1 cells generated detectable tumours after 14 days: the excised tumours (i) and (ii) weighed 0.97g and 1.12g. Three SCID mice injected with cell hybrid lines all generated tumours 19 days post injection. Tumours (iii), (iv) and (v) were derived from mice each injected with  $2 \times 10^7$  TESH-1, TESH-2, and FESH-1 cells respectively. Excised tumours weighed 0.92g, 0.87g, and 1.21g in that order. Scale bar in each figure represents 5mm.

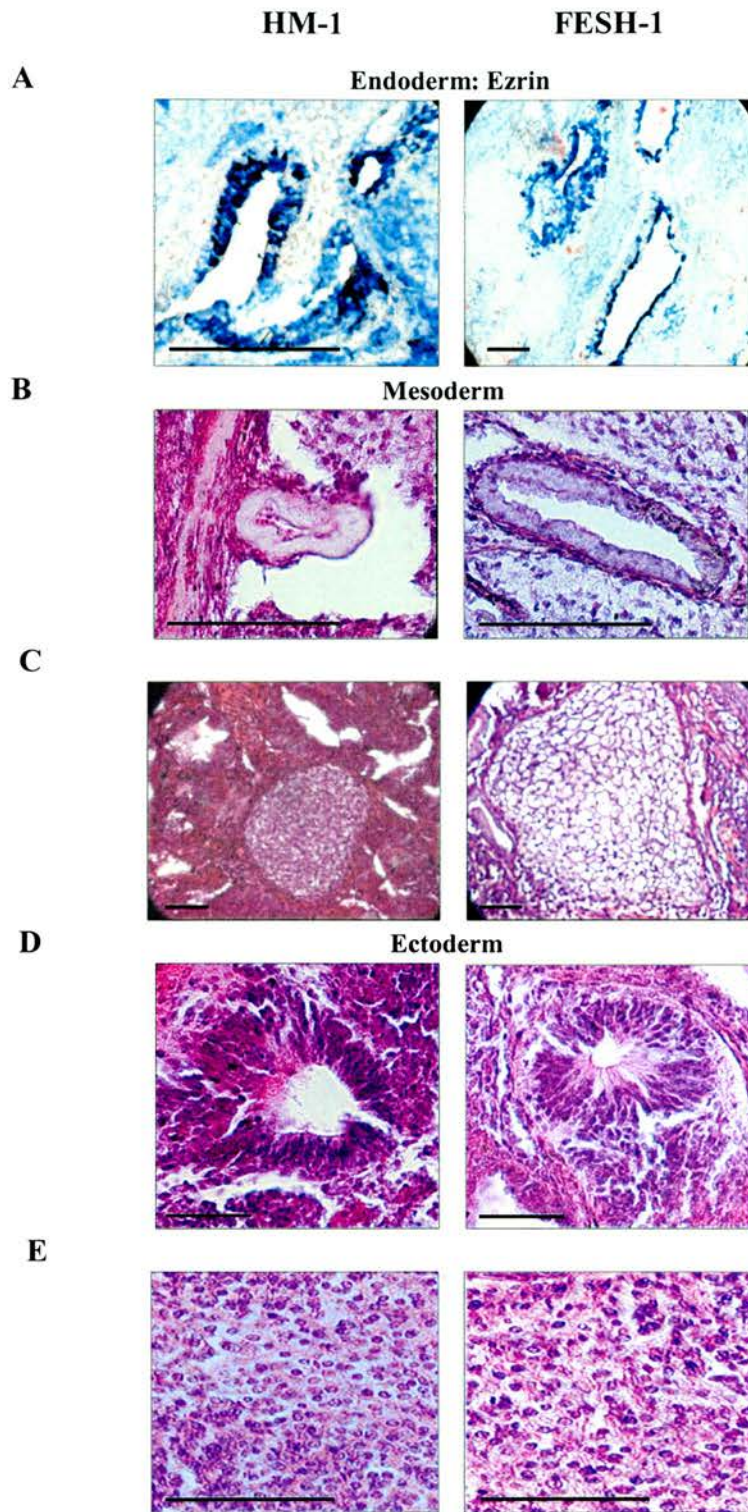


**Fig 4.7 *In vivo* differentiation in SCID mice shows that hybrid cells have similar potential to HM-1 cells**

The teratomas generated from HM-1 cells and ES cell derived hybrids were extremely dense and all showed differentiation into all three embryonic germ layers: (a) ezrin staining epithelium (endoderm), (b) columnar epithelium (mesoderm), (c) early cartilage formation (mesoderm) (d) rosettes of neural epithelium (ectoderm) and (e) early neuronal tissue (ectoderm). Scale bar in each figure represents 200 $\mu$ m.

#### **[4.3.6] Hybrid cells can be differentiated *in vitro* into cells representing all three embryonic germ layers**

Finally, the ability of hybrid lines to differentiate *in vitro* was investigated [Fig 4.8]. HM-1 cells and cells from all three cell hybrid lines generated embryoid bodies after being grown in suspension in LIF free ‘murine embryoid body’ medium for one week. Fig 4.8 Panel A shows representative images of one-week-old HM-1 and FESH-1 derived embryoid bodies. Approximately thirty one-week-old embryoid bodies were disaggregated with TEG and total RNA was isolated from these cells as described in Section [2.6.1]. cDNA from HM-1 cells and all three hybrid lines was generated. This was used in a series of RT-PCR reactions to detect whether the endodermal marker  $\alpha$ -fetoprotein was expressed (See Subsection [2.6.3] for PCR conditions). Fig 4.8 Panel B Lane 1 showed the ‘no reverse transcriptase’ control that confirmed that cDNA has not been contaminated with genomic DNA. Lane 2 showed that  $\alpha$ -fetoprotein was not expressed in undifferentiated HM-1 cells but lanes 3-6 showed that it was in 1 week old embryoid bodies derived from HM-1 cells and the three hybrid cell lines. These data verify that both HM-1 cells and the hybrid lines can be differentiated into endodermal cells *in vitro*.

One-week-old embryoid bodies derived from all four lines (HM-1, TESH-1, TESH-2, and FESH-1) were also grown in either murine cardiomyogenesis or neurogenesis differentiation media as described in Subsection [2.4.2]. In cardiomyogenic medium, beating clumps of cells were found in HM-1 cell cultures after 9 days and in all three hybrid cell derived cultures after 10 days. After 14 days in cardiomyogenesis differentiation medium, the cultures were immunostained for troponin T (cardiac isoform) and all cultures displayed positive staining. Fig 4.8 Panel C shows representative images of Troponin T staining of HM-1 and FESH-1 derived cultures. These data verify that all four lines can be differentiated into cardiomyocytes, a mesodermal cell type.

In a similar fashion, cultures fed neurogenesis differentiation medium for 14 days were immunostained for  $\beta$ -tubulin III, a neuronal cell marker. Cultures of all four lines displayed the marker and positively staining cells displayed long cylindrical outgrowths consistent with the morphology of neuronal tissue. Fig 4.8



**Panel D** shows representative images showing  $\beta$ -tubulin III expression in cultures derived from HM-1 cells and FESH-1 cells. This verifies that the cell hybrid lines and ES cells can be differentiated down the neurogenic pathway and give rise to ectodermal cells. In summary, the data described in this section shows that cell hybrid lines can be differentiated *in vitro* into cells comprising all three embryonic lineages and these lines possess a similar potential to HM-1 cell controls.

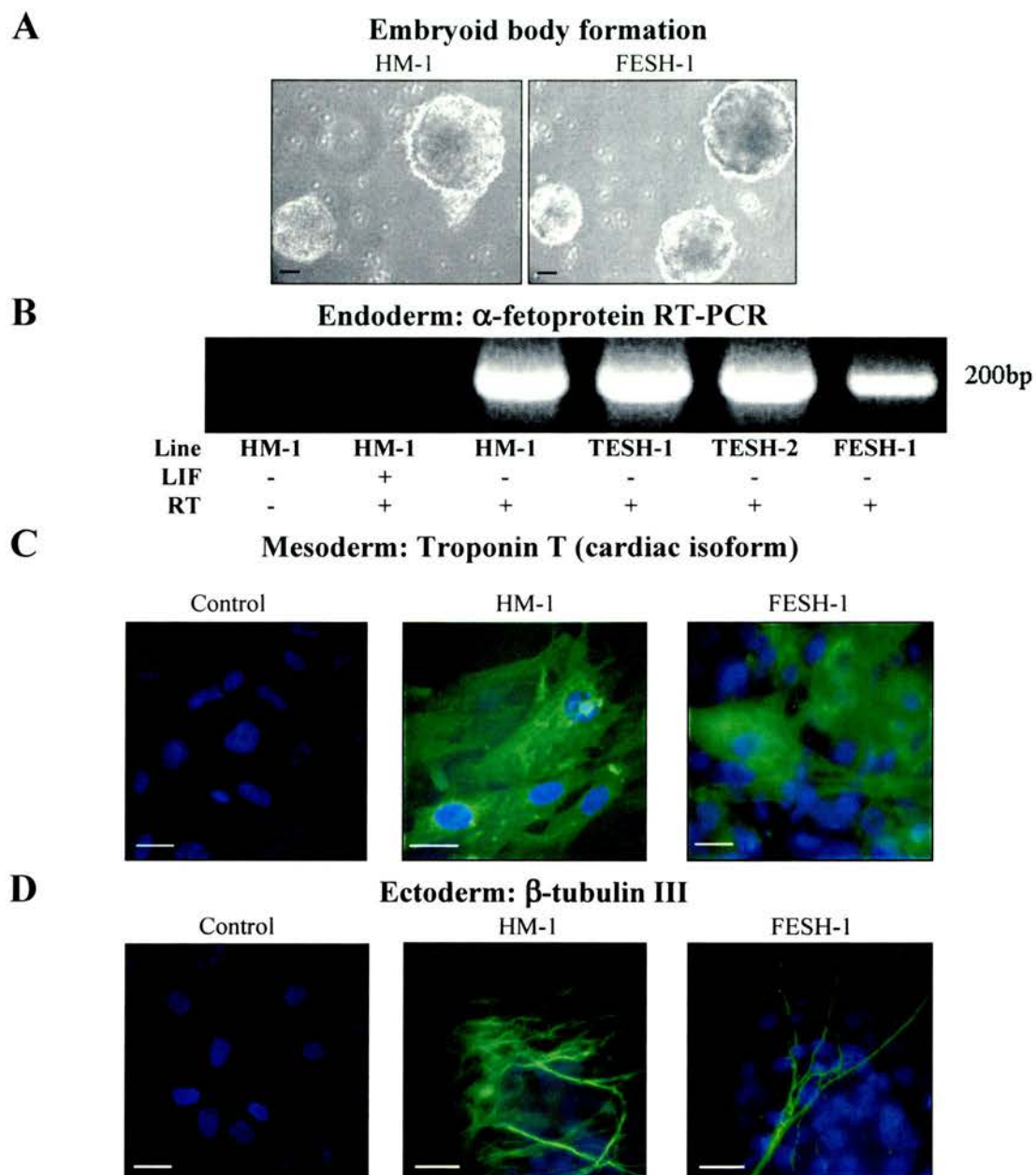


**Fig 4.8 *In vitro* differentiation shows that hybrid cells have similar potential to HM-1 cells**

HM-1 cells and hybrid cells were differentiated *in vitro* as described in **Subsection [2.4.2]**. **Panel A** HM-1 cells and hybrid cells formed complex embryoid bodies were cultured in suspension in the absence of LIF. Photographs were taken 1 week after LIF removal. **Panel B**  $\alpha$ -fetoprotein expression is detected by RT-PCR in 1 week-old embryoid bodies derived from HM-1 cells and hybrid cells. **Panel C** Cultures of differentiated HM-1 cells and hybrid cells stained positive for mesoderm marker Troponin T. **Panel D** Cultures of differentiated HM-1 cells and hybrid cells stained positive for ectoderm marker  $\beta$  tubulin III. Scale bar in each figure represents 100  $\mu$ m. Controls for Panels C & D were stained with secondary antibody only.

## [4.4] Conclusions

The three clonal lines (TESH-1, TESH-2, and FESH-1) displayed sub-tetraploid complements of chromosomes confirming that they were cell hybrids. Cell hybrid lines TESH-1 and FESH-1 were found to be genomically stable whereas TESH-2 (generated using PEG) lost more chromosomes the longer they were cultured. TESH-1 displayed DNA rearrangement of Tcr $\gamma$  verifying that this cell hybrid line was the result of a fusion between an ES cell and an adult thymocyte and not an endogenous stem cell.

All three hybrid lines displayed an ES phenotype. In TESH-1 cells the somatically derived *Oct-4* promoter is reactivated, showing epigenetic reprogramming had occurred at this locus. All three cell hybrid clones displayed strong alkaline phosphatase activity. They also expressed the undifferentiated cell surface marker SSEA-1 but not either the differentiated cell surface marker SSEA-4 or the thymocyte specific marker CD90.

When injected into SCID mice, all three cell hybrid lines formed tumours that contained cells from all three embryonic germ layers. In addition, *in vitro* differentiation of the three cell hybrid lines produced embryoid bodies from which cells representing the three embryonic germ layers could be derived. These two observations show that ES cell derived genome can retain pluripotency even when it is in contact with the differentiated cell genome.

In summary, data in this chapter show that hybrid and HM-1 cells display similar phenotypic characteristics. These data indicate that ES cell phenotype is dominant over somatic cell phenotype in hybrid cells. This is consistent with the findings of others [Tada *et al.* 2001][Matveeva *et al.* 1998].

## **[5] The effect of heat shock on the murine cell hybrid system**

### **[5.1] Introduction**

Cells transiently placed in an environment several degrees above physiological optimum display a heat shock response [See **Section [1.9]** for a detailed review of the heat shock response]. Heat shocked cells can show profound changes in gene expression [Csermely *et al.* 1994] and chromatin structural changes [Iliakis & Pantelias 1989].

It was hypothesised that inducing such a response in murine thymocytes would alter somatic chromatin structure affecting the amenability of somatic nuclei to being reprogrammed when fused with an ES cell. This hypothesis would be tested by investigating the effect of heat shocking thymocytes in the murine cell hybrid system.

### **[5.2] Objective**

To investigate the effect of heat shock on nuclear reprogramming in the murine cell hybrid system.

## [5.3] Results and discussion

### [5.3.1] Thymocytes are heat shocked when incubated at 42°C for 10 minutes

In order to investigate the effect of heat shock on nuclear reprogramming, conditions in which the heat shock response could be reliably induced in murine thymocytes were sought. Wells (1983) had shown that optimal heat shock conditions for deriving ES cell lines from mouse blastocysts was 42°C for 10 minutes prior to ICM extraction. As reprogramming the somatic nucleus to an ES cell-like state is the goal of hybridisation experiments, it was thought that these conditions would be suitable for heat shocking murine thymocytes. In order to verify that incubation of cells at 42°C for 10 minutes induced a heat shock response in murine thymocytes, whole cell lysates of thymocytes were generated and probed for inducible heat shock protein hsp72. “Treated” lysate had been derived from thymocytes that had been incubated at 42°C for 10 minutes, whereas “control” lysate was generated from thymocytes that had not been exposed to such hyperthermic conditions. Hsp72 was assayed as it is a good marker for the heat shock response: it is not expressed in normal unstressed mammalian cells but is quickly induced to high levels following stresses such as heat shock [Welch & Suhan (1986)]. **Fig 5.1** (overleaf) shows a Western blot that verifies that murine thymocytes are heat shocked under the conditions used. Control lysate contained only a low level of hsp72 induction whereas in treated lysate a significantly higher level of Hsp72 was observed (at least a three fold induction over the control level).

During lysate generation, thymocytes were disaggregated mechanically and then with TEG, before either being exposed to hyperthermia (treated lysate) or left at room temperature (control lysate). Subsequently the cells were incubated in 1xPBS at 37°C for 2 hours prior to lysis, denaturation and fixation [See **Subsection [2.8.1]** for details]. It is thought that the low level of Hsp72 observed in the control lane was due to the stress that disaggregation and incubation in a serum-free environment caused the cells.

Mosser *et al.* 1993 had previously shown the induction of a heat shock response in adult mouse thymocytes by incubating the cells at 42°C for 20 minutes. It was reported that hsp68 levels rose rapidly after such hyperthermic exposure but decreased after 1 hour. The heat shock response was induced in mouse thymocytes in subsequent experiments by incubating the cells at 42°C for 10 min.

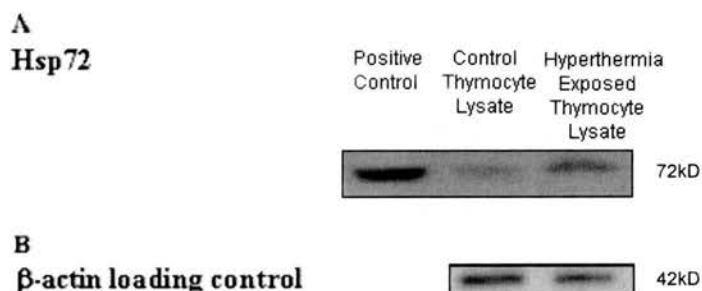


**Fig 5.1 Increased expression of heat shock protein Hsp72 in murine thymocytes exposed to hyperthermia**

Whole cell lysates were generated from two populations of thymocytes derived from the same mice, one that had been exposed to 42°C for 10 minutes and the control was kept at room temperature (see **Subsection [2.7.1]** for details). **Panel A** Western blot probed with anti-Hsp72. Manufacturer's antibody control, a heat shocked Hela cell lysate (lane 1). Control T-cell lysate, 150  $\mu$ g protein (lane 2). Hyperthermia exposed T-cell lysate, 150  $\mu$ g protein (lane 3). **Panel B** The same blot stripped and reprobbed with anti- $\beta$ -actin.

### [5.3.2] Heat shocking thymocytes increases the hybrid colony yield

In order to test the hypothesis that heat shocking thymocytes prior to fusion with ES cells would make them more amenable to being reprogrammed, control and heat shocked thymocytes were used in parallel hybridisation experiments. HM-1 cells were electropulsed in the presence of either control or heat shocked thymocytes in a ratio of 1:5 under standard electrofusion conditions. One fifth of the electropulsed cells were used to assess heterokaryon formation and cell viability [See **Figs 5.4 & 5.5**]; the remainder was placed under selection for cell hybrids (1xHAT).

**Table 5.1** shows the hybrid colony number from experiments using both control and heat shocked thymocytes. In each case, more hybrid colonies were counted on plates where heat shocked thymocytes has been used. **Fig 5.2** shows that, on average,  $84.6 \pm 16.9\%$  more hybrid colonies were derived using heat shocked rather than control thymocytes. When statistically analysed, using the Student's paired t-test [Caria 2002], heat shocking thymocytes is found to significantly affect hybrid colony yield ( $P < 0.0026$  for the corrected data).

	Hybrid colony number ( <i>cell number electropulsed</i> )				
	Experiment 1	Experiment 2	Experiment 3	Experiment 4	Experiment 5
<b>HM-1 x control thymocytes</b>	292 ( <i>1.2x10<sup>8</sup></i> )	152 ( <i>6x10<sup>7</sup></i> )	81 ( <i>4.8x10<sup>7</sup></i> )	128 ( <i>6x10<sup>7</sup></i> )	85 ( <i>4.8x10<sup>7</sup></i> )
<b>HM-1 x Heat shocked thymocytes</b>	539 ( <i>1.2x10<sup>8</sup></i> )	315 ( <i>6x10<sup>7</sup></i> )	137 ( <i>4.8x10<sup>7</sup></i> )	234 ( <i>6x10<sup>7</sup></i> )	152 ( <i>4.8x10<sup>7</sup></i> )

**Table 5.1 Heat shocking thymocytes prior to fusion with ES cells increases hybrid colony yield**

Thymocytes were removed from 6-7 week old female CBA mice and either incubated at room temperature (control) or at 42°C for 10 min (heat shocked). Control or heat shocked thymocytes and HM-1 cells (5:1) were then electropulsed using standard fusion conditions and placed under HAT selection. This table shows number of hybrid colonies generated in five replicate experiments. The figures in italics indicate the number of cells electropulsed in each fusion experiment.



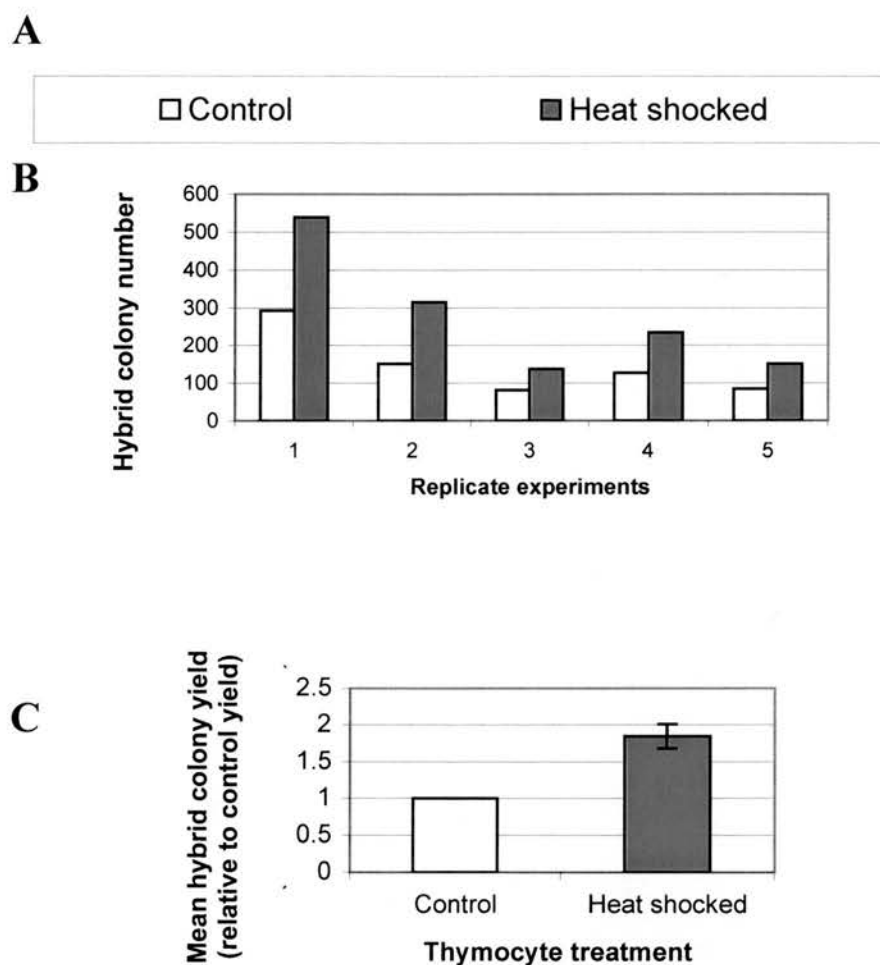


**Fig 5.2 Heat shocking thymocytes increases hybrid colony yield**

Thymocytes were removed from 6-7 week old female CBA mice and either incubated at room temperature (control) or at 42°C for 10 min (heat shocked). Control or heat shocked thymocytes and HM-1 cells (1:5) were then electropulsed using standard fusion conditions and placed under HAT selection. **Panel A** Legend for control and heat shocked fusions. **Panel B** Hybrid colony numbers for control and heat shocked fusions for all five replicate experiments. **Panel C** Mean hybrid yield for fusions using control and heat shocked thymocytes. Fusions with heat shocked thymocytes generated on average  $84.6 \pm 16.9\%$  more hybrid colonies than control fusions.

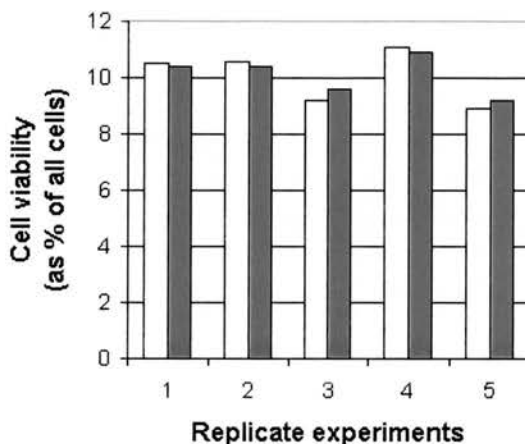
### **[5.3.3] Heat shocking thymocytes does not affect cell viability of electropulsed mixtures of cells but does increase heterokaryon formation**

Hybrid colony yield on its own is not a good measure of nuclear reprogramming. Such a yield may be affected by other factors (i.e. cell fusion, or more precisely heterokaryon formation, and also cell viability). In order to investigate the effect of heat shock on nuclear reprogramming, both of these parameters were measured. **Fig 5.3** shows that the heat shock of thymocytes did not affect the viability of electropulsed cells as measured between 6 and 13 hours after seeding ( $P>0.05$  as calculated using a Student's paired t-test (1 tailed) [Caria 2000]). In control and heat shocked samples respectively, only  $10.6\pm 1.2\%$  and  $10.1\pm 1\%$  of electropulsed cells remained viable. This was consistent with the observation that most of the cells in electropulsed ES cell/thymocyte mixtures died: The low levels of cell viability were expected as thymocytes are not viable under murine ES cell culture conditions.

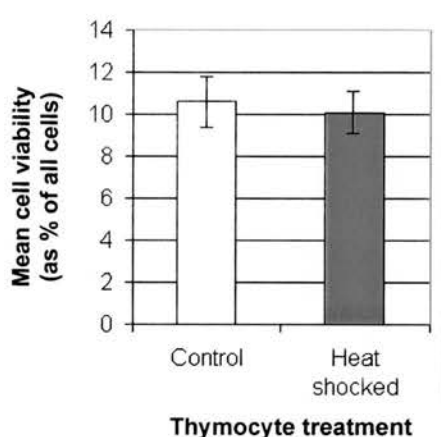
**Fig 5.4** shows 2-dye FACS analysis data from which the percentage of cells forming heterokaryons was calculated [See **Subsection [2.2.5]** for details]. **Fig 5.5** shows heterokaryon formation (as percentage of viable cells) for control or heat shocked fusions. In all replicates, heat shocked fusions showed an increase in heterokaryon formation over control levels. Statistical analysis showed heat shocking thymocytes prior to fusion to have a significant effect on heterokaryon formation ( $P<0.05$  as calculated by the Student's paired t-test (2 tailed) [Caria 2000]). On average, fusions with heat shocked thymocytes displayed  $39\pm 5\%$  more heterokaryon formation than that measured in control fusions. This increase in heterokaryon formation was unexpected. Despite an extensive review of the literature, no reports of exposing cells to a hyperthermic state prior to fusion induction were found. It was speculated that heat shocking thymocytes destabilised cell membranes making them more fusogenic. There is data showing that increased fusion of liposomes to cultured cells when the liposomes had previously been exposed to hyperthermia ( $41.5^{\circ}\text{C}$ , 2hr) [Arancia *et al.* 1994]. The outer bilayer of multilamellar liposomes fused more readily to cell membrane under these hyperthermic conditions and induced changes in the fluidity and molecular organisation of the plasma membrane. In a similar

way, heat shocked thymocytes might experience membrane disruption that affects their ability to fuse. It was noted that even in the leakage controls, a higher percentage of cells were double stained, indicating that thymocytes remained in this fusogenic state for some time after heat shock.

**A**

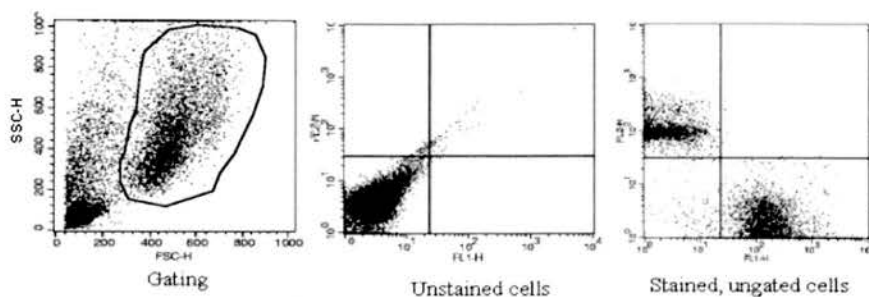
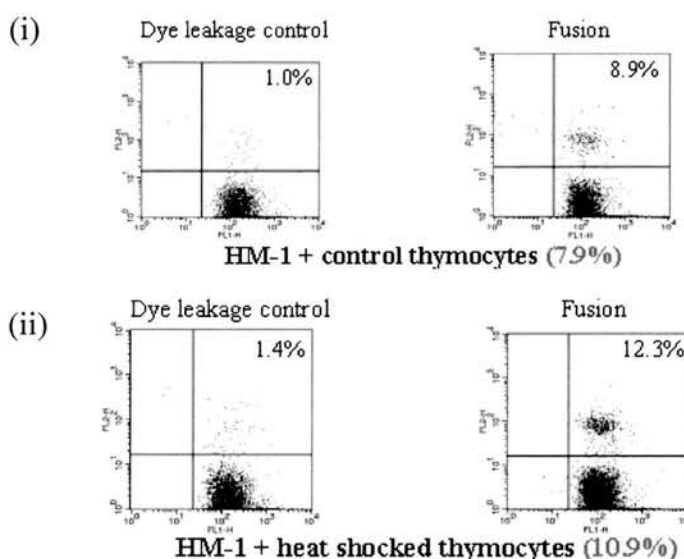


**B**



**Fig 5.3 Heat shocking thymocytes does not affect electropulsed cell viability**

Cell viability for fused mixtures of cells was measured using FACS analysis (Forward Scatter / Side Scatter plotting) as described in **Subsection [12.2]**. Between 6 and 13 hours after pulsing and seeding the cell mixtures, 1 of 5 representative plates from each fusion was trypsinised. Cells from the used media and all post-trypsinisation washings were combined and pelleted before being washed and resuspended in 1xPBS. Cell viability (as % of total cells) was measured using FCS/SSC plots. Results were verified using trypan blue staining. Columns are colour coded to denote the pre-fusion treatment of thymocytes: □ control and ■ heat shocked. **Panel A** Cell viability (as % of all cells) measured by FSC/SSC FACS analysis for three replicate experiments. **Panel B** The mean cell viability (as % of all cells) for both treatments ± S.E.M. There was no significant difference in cell viability between control and heat shock fusions ( $P > 0.05$  as calculated using a Student's paired t-test (1 tailed) [Caria 2000]).

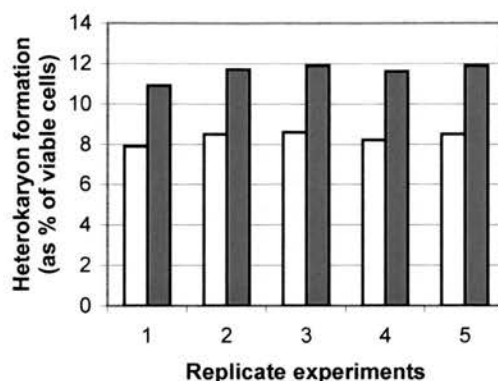
**A****B****C**

	Heterokaryon formation (as % of viable cells)				
	Experiment 1	Experiment 2	Experiment 3	Experiment 4	Experiment 5
HM-1 x control thymocytes	7.9	8.5	8.6	8.2	8.5
HM-1 cells x heat shocked thymocytes	10.9	11.7	11.9	11.6	11.9

**Fig 5.4 The effect of heat shock on heterokaryon formation was assessed using 2-dye FACS analysis**

**Panel A** Gating and compensation data. The same gate and quadrants were used throughout individual experiments. Quadrant axes were defined so that CMTMR stained thymocytes (upper left quadrant) were distinct from CMFDA stained HM-1 cells (upper right quadrant). **Panel B** Histograms showing fluorescence of cells in dye leakage control and fusions using HM-1 cells and either control (i) or (ii) heat shocked thymocytes. Data displayed in Panels A and B are taken from one representative experiment. Percentage cell fusion was calculated by subtracting the percentages for leakage controls from that for the fusion (these figures are highlighted in red). **Panel C** Summary of data from replicate experiments (n=5). Heat shocking thymocytes has a significant effect on heterokaryon formation ( $P < 0.001$  as calculated by the Student's paired t-test (2 tailed) [Caria 2000]).

A



B

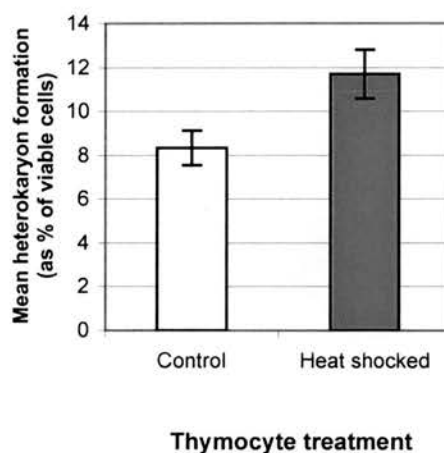


### Fig 5.5 Heat shocking thymocytes increases heterokaryon formation

Between 6 and 13 hours after pulsing and seeding the cell mixtures, 1 of 5 representative plates from each fusion was trypsinised. Cells from the used media and all post-trypsinisation washings were combined and pelleted before being washed and resuspended in 1xPBS. Heterokaryon formation (as % of viable cells) was measured using 2-dye FACS analysis (See **Section [2.2.5]**). Columns are colour coded to denote the pre-fusion treatment of thymocytes: □ control and ■ heat shocked. **Panel A** Heterokaryon formation (as % of viable cells) for both control and heat shocked fusions in 5 replicate experiments. **Panel B** The mean heterokaryon formation (as % of viable cells) ± S.E.M. for control and heat shocked fusions from five replicate experiments. Heat shocking thymocytes has a significant effect on heterokaryon formation ( $P < 0.05$  as calculated by the Student's paired t-test (2 tailed) [Caria 2000]).

### [5.3.4] Heat shocking thymocytes prior to fusion does not affect hybridisation frequencies

When hybridisation frequencies were calculated, the mean frequency was higher in heat shocked fusions than that found in controls, however this difference was not found to be significant [Fig 5.6] ( $P > 0.05$ , as calculated by the Student's paired t-test (2 tailed) [Caria 2000]. It is possible that reprogramming to an ES cell state was facilitated by heat shocking but such an increase could not be detected with only five replicate experiments. Consultation with a statistician revealed that  $>100$  replicate experiments would be required to identify whether enhanced nuclear reprogramming, in addition to increased heterokaryon formation, caused the observed increase in hybrid colony yield.

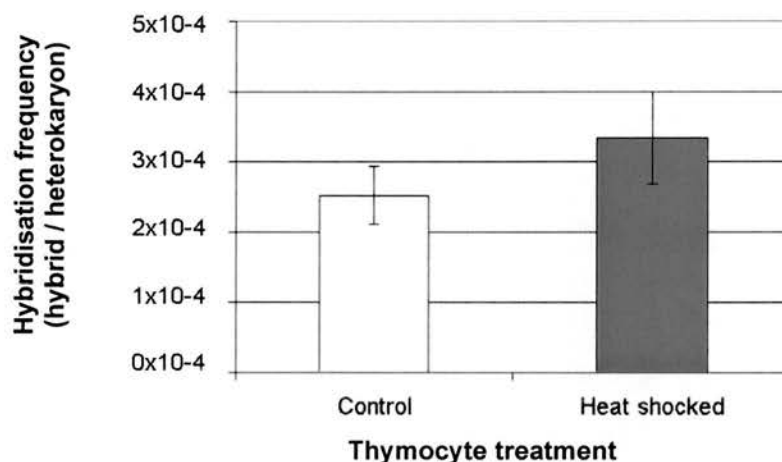


**Fig 5.6 Heat shocking thymocytes did not significantly affect hybridisation frequency**

Mean hybridisation frequency were calculated for all five replicate experiments as described in **Subsection [2.2.6]**. The mean and standard error of the mean of these yields is shown. There was no significant difference between control and heat shocked experiments ( $P > 0.05$  as calculated using the Student's paired t-test (2 tailed) [Caria 2000])

### [5.3.5] Heat shocking cells after fusion did not increase hybridisation frequency

It was decided to investigate the effect of heat shocking cell mixtures after they were electropulsed to induce fusion. It was reasoned that such treatment might still facilitate nuclear reprogramming of the somatic nucleus. This approach would also avoid the problem of discriminating between increased heterokaryon formation and nuclear reprogramming as the cause of increased hybrid yield. However this approach would mean that the ES cell derived part of hybrids would also be exposed to hyperthermic conditions. **Fig 5.7** shows that heat shocking cells after electrofusion did not increase hybridisation frequencies. Only two experiments were carried out and thus too little data were generated to apply statistical analysis. However in both experiments, there was no indication that heat shocking after electrofusion facilitated nuclear reprogramming.

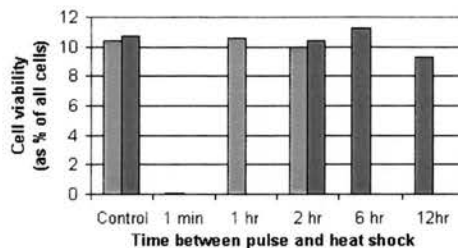
On the contrary, heat shocking thymocytes after electrofusion only caused a decrease in hybrid colony yield. One explanation for this is that unlike previous experiments, the ES cell derived moiety of heterokaryons / hybrids is being heat shocked in addition to the thymocyte derived moiety. Perhaps the reprogramming factors in the HM-1 cell are sensitive to heat shock. Applying this hypothesis one would expect that longer the duration between electrofusion and heat shock, the longer the reprogramming factors will be active before being exposed to heat shock and the more hybrids will have been reprogrammed. Thus as the duration between electropulsing and heat shock gets longer, the greater the hybrid colony yield. This is consistent with the data in **Fig 5.7** and could be tested by heat shocking HM-1 cells prior to electrofusion to somatic cells and investigating whether there is a change in hybrid colony yield. If reprogramming factors are sensitive to heat shock, one would expect a decrease in hybrid colony yield when heat shocked HM-1 cells are used. Another explanation for the data is that heat shock just interrupts the reprogramming process, without affecting the reprogramming factors *per se*. If this is the case one might expect the hybrid yield of heat shocked HM-1 cells to be similar to control HM-1 cells when both are electropulsed with the same numbers of thymocytes.



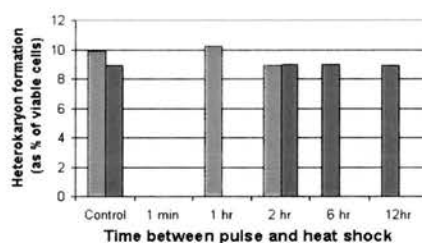
A

Heat shock time points (relative to pulse)	Cell hybrid colony yield ( $4.8 \times 10^7$ cells)	
	Experiment 1	Experiment 2
Control	82	78
1 min	0	-
1 hour	25	-
2 hour	43	42
6 hour	-	47
12 hour	-	66

B



C



D

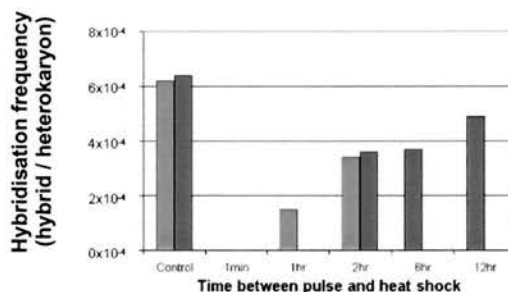


**Fig 5.7 Heat shocking, at various time points after electrofusion, does not increase hybridisation frequency**

Aliquots, each consisting of  $1 \times 10^7$  HM-1 cells electrofused with  $5 \times 10^7$  CBA thymocytes under standard conditions, were heat shocked ( $42^\circ\text{C}$ , 10 min) at various time points after pulsing (1 min, 1 hr, 2 hr, 6 hr and 12 hr). Cell viability and heterokaryon formation were measured 14 hr after fusion). Aliquots were seeded on gelatinised plates with mES medium where the interval between electrofusion and heat shock was  $>1$ min. Two separate experiments were carried out with different durations between electrofusion and heat shock. Samples from the first experiment are highlighted with colour  whereas samples from the second experiment are represented using colour . **Panel A** Hybrid colony yields for aliquots heat shocked at various time points after electrofusion. **Panel B** Cell viability data for these samples. **Panel C** Heterokaryon formation data for these samples. **Panel D** Hybridisation frequencies for these samples.

## [5.4] Conclusion

Heat shock can be induced in thymocytes by incubating them at 42°C for 10 minutes. Heat shocked thymocytes showed at least a stronger induction of hsp72 that seen in control thymocytes. Heat shocking thymocytes prior to pulsing increased both hybrid colony yield ( $P<0.05$ ) and heterokaryon formation ( $P<0.05$ ). With five replicate experiments, the increase in heterokaryon formation made it impossible to determine whether the frequency of nuclear reprogramming had changed. With the data acquired, there was no significance difference between the hybridisation frequencies of control and heat shocked samples ( $P>0.05$ ).

Heat shocking cells at various time points after pulsing decreased the hybrid colony yield. In the experiments where heat shock was applied between 1 min and 12 hours after electrofusion, the longer the duration between electropulsing and heat shock, the higher the hybrid colony yield. This could be due to ES cell derived nuclear reprogramming factors being sensitive to heat shock or perhaps a non-specific effect that does not directly affect nuclear reprogramming activity within the cell. These hypotheses could be tested by heat shocking HM-1 cells prior to electropulsing and investigating whether there is an effect on hybrid colony yield.

## **[6] The effects of ES cell confluence and passage number on the murine cell hybrid system**

### **[6.1] Introduction**

Gao *et al.* (2003) observed that confluence of HM-1 cells affected their ability to be completely reprogrammed to totipotency in nuclear transfer experiments. When nuclei from HM-1 cells at 80-90% confluence were transferred into ooplasts and reprogrammed by oocyte cytoplasm, 49.0% of the reconstructed embryos developed to morula/blastocyst stage and 9.1% of these went on to develop into adult animals. When nuclei from HM-1 cells at 60-70% confluence were used however, only 22.2% of the embryos developed to the morula / blastocyst stage of which 2.3% went on to adulthood. The first aim of work discussed in this chapter was to investigate if reprogramming of somatic cells *by* ES cells was affected by ES cell confluence. At the time this work was carried out, cell hybrids could not be repeatedly produced from fusions of ES cells and PEFs, so investigating the effect of somatic cell confluence on their ability to be reprogrammed could not be investigated.

The term “confluence” describes the relationship between adherent cells and the surface area of the substratum to which they are attached. “percentage confluence” refers to the percentage of surface area of the flask that is covered by cells *e.g.* a 50% confluent culture is one in which half the surface area of the flask is covered with cells. The term “superconfluent” will be used throughout this chapter to describe cultures kept growing 24 hours after the entire flask surface has been covered with cells.

The biological consequences of confluence are cell-type dependent [McAteer & Douglas 1979]. As cells grow to confluence in culture for example, most somatic cell types enter into a quiescent state where they cease proliferating. In contrast, ES cells

continue to proliferate and begin to differentiate. There is no evidence that ES cells ever become quiescent.

If ES cell confluence was found to affect nuclear reprogramming, the optimal degree of confluence for nuclear reprogramming would then be sought and used in subsequent experiments. Additionally, differences between ES cells at different ranges of confluence would also be sought with the aim of elucidating further what aspect of confluence affects nuclear reprogramming.

The second aim of work done in this chapter was to investigate the effect of ES cell passage number on nuclear reprogramming in the hybrid system. In nuclear transfer experiments reported by Gao *et al.* (2003) the developmental potential of reconstituted embryos was affected by passage number of the donor ES cells. When R1 ES cells of passage 19 were used as nuclear donors, 47.2% of the reconstructed embryos reached morula/blastocyst stage and of these 1.69% went on to generate live offspring. With R1 ES cells of passage 22-25 were used, however only 27% of the embryos reached blastocyst/morula stage and no live offspring were produced. It was hypothesised that ES cell passage number would also affect the ES cells' capacity to reprogram somatic nuclei in the cell hybrid system.

## **[6.2] Objectives**

To investigate the effect of murine ES cell confluence on the murine cell hybrid system.

To investigate the effect of passage number of murine ES cells on the murine cell hybrid system.

## **[6.3] Results and discussion**

### **[6.3.1] HM-1 cell seeding densities, that yield cultures at different ranges of confluence, were identified empirically**

Seeding densities, to generate HM-1 cell cultures at various ranges of confluence, were identified empirically. The densities shown in **Fig 6.1 Panel A** are those which reproducibly yielded ES cell cultures at 50-60%, 70-80%, 90-100% and >100% confluence 48 hours after seeding. Images of representative ES cell cultures at each range of confluence are shown in **Fig 6.1 Panel B**. In order to test the hypothesis that confluence of ES cells affected their capacity to reprogram somatic nuclei, experiments fusing ES cells, grown to four different ranges of confluence, to murine thymocytes were undertaken. Standard cell numbers and electrofusion conditions for HM-1/thymocyte fusions were used (See **Subsection [2.2.1]**) and reprogrammed hybrids were selected in the usual manner (murine ES medium supplemented with 1xHAT).

### **[6.3.2] HM-1 cell confluence affects hybrid colony yield**

HM-1 cells at different levels of confluence were fused to CBA thymocytes using standard electrofusion cell numbers and conditions. **Fig 6.1 Panel C** and **Fig 6.2** show that hybrid colony yields were affected by HM-1 cell confluence ( $P < 0.05$  as calculated using 2-way Analysis of Variance [Caria 2000]). In all five replicate experiments the same trend is seen: the hybrid colony yield increased as ES cell confluence is increased until the cells reach 100% confluence.  $411 \pm 51\%$  more hybrid colonies were generated using HM-1 cells at 90-100% confluence than were generated in equivalent fusions using HM-1 cells at 50-60% confluence. After the HM-1 cells have reached 100% confluence however, the colony yield quickly declined to below that observed with 50-60% confluent HM-1 cells. The probable explanation for this decrease

in hybrid colony yield is that in fusions using >100% confluent HM-1 cells, a significant portion of ES cells have already started to differentiate and were no longer able to reprogram the somatic *Oct4* locus. Indeed, as shown in **Fig 6.1 Panel C**, differentiation of some HM-1 cells was routinely observed in >100% confluent cultures (i.e. small clusters of cells had lost ES cell morphology and had begun differentiating).

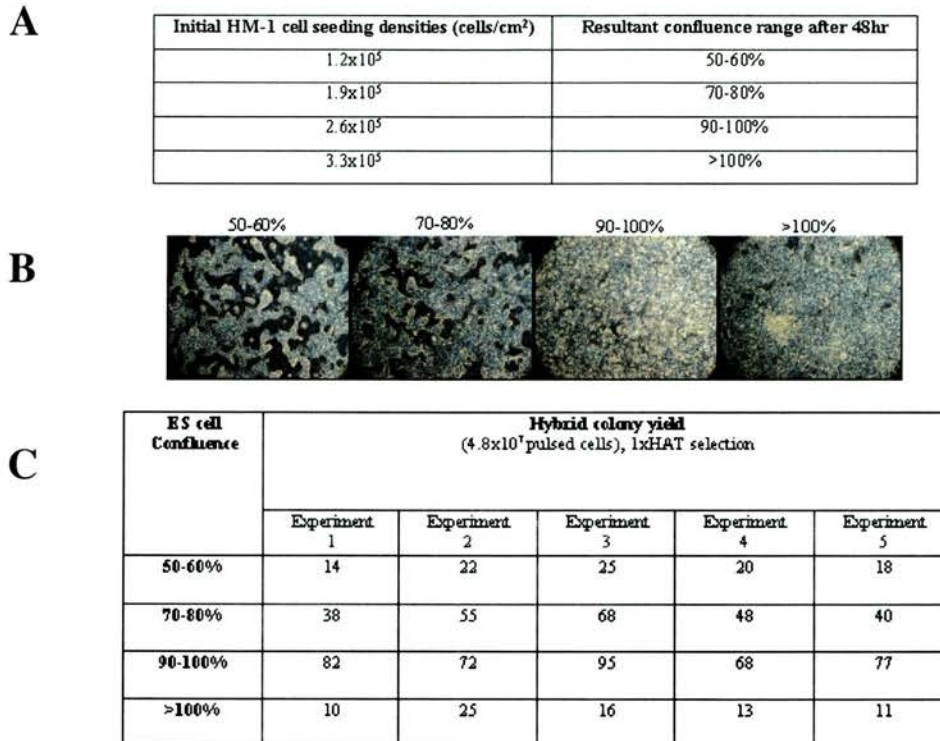


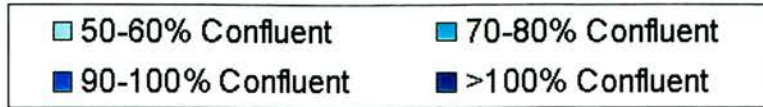
### Fig 6.1 ES cell confluence affects hybrid colony yield

Seeding densities generating HM-1 cultures displaying four ranges of confluence identified empirically. HM-1 cells from each confluence range were electrofused with thymocytes from 6-7 week old CBA<sup>+/+</sup> mice as described in **Subsection [2.2.1]**.

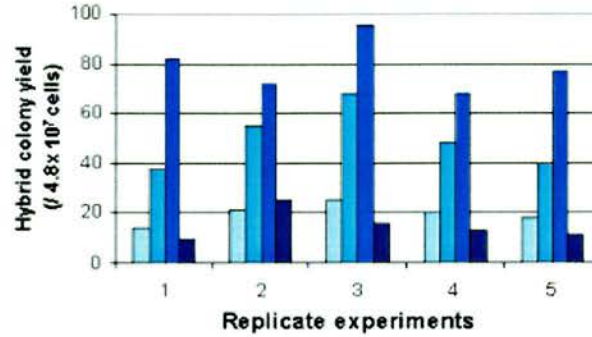
**Panel A** HM-1 cell seeding densities and resultant confluence ranges 48 hours after seeding. **Panel B** Representative fields of view of HM-1 cell cultures at each range of confluence. **Panel C** Summary of hybrid colony yields from five replicate experiments.



A



B



C

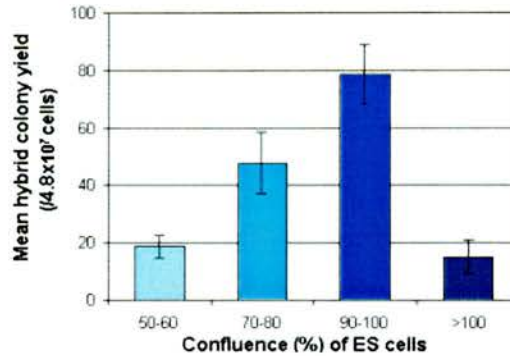


**Figure 6.2 Confluence of HM-1 cells affects hybrid colony yield**

HM-1 cells at different ranges of confluence were electrofused with murine thymocytes as described in **Subsection [2.2.1]**. *Panel A* The same colour code was used throughout this chapter to represent ranges of ES cell confluence. *Panel B* Graph showing individual hybrid colony yields for each ES cell confluence range in five replicate experiments. *Panel C* Graph showing mean hybrid colony yields for each ES cell confluence range as calculated from the data derived from five replicate experiments. Error bars represent the standard error of the mean hybrid colony yield as calculated for each confluence range.



### [6.3.3] HM-1 cell confluence does not affect viable heterokaryon formation or cell viability

In order to investigate the effect of HM-1 cell confluence on nuclear reprogramming, viable heterokaryon formation and cell viability had to be measured for each experiment in addition to calculating the hybrid colony yields. These measurements were made using FACS analysis as described in **Subsection [2.2.6]** and **Section [13.3]**.

**Fig 6.3** shows data from 2-dye FACS analysis experiments from which percentages of cells forming viable heterokaryons was calculated. **Fig 6.3 Panel C** shows a table where calculated percentage of cells forming viable heterokaryons in five representative experiments are summarised. **Fig 6.4 Panel A** shows a graph of these data for individual experiments while **Panel B** shows the mean percentage values. These data show that HM-1 cell confluence did not affect viable heterokaryon formation as a percentage of all cells ( $P>0.05$  as calculated using 2-way Analysis of Variance [Caria 2000]).

**Fig 6.5 Panel A** shows cell viability data from five replicate experiments and **Panel C** shows mean cell viability (as percentage of all cells) for each HM-1 cell confluence range. HM-1 confluence does not affect cell viability of pulsed mixtures of HM-1 cells and thymocytes ( $P>0.05$  as calculated using 2-way Analysis of Variance [Caria 2000]).

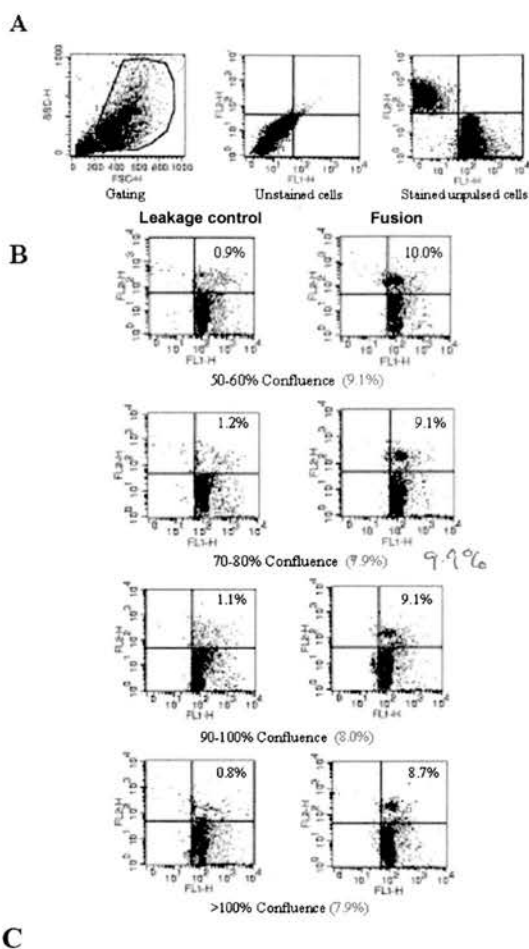
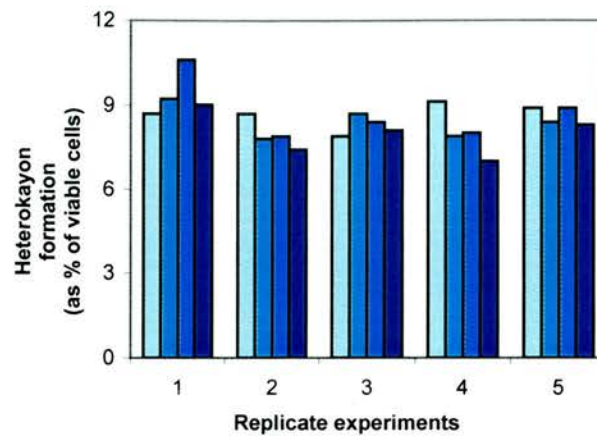


**Fig 6.3 The effect of ES cell confluence on heterokaryon formation was assessed using 2-dye FACS analysis**

**Panel A** Gating and compensation data (See **Subsection [12.2]**). Quadrant axes were defined so that unstained appeared in the lower left quadrant and CMTMR stained thymocytes (upper left quadrant) were distinct from CMFDA stained HM-1 cells (lower right quadrant). The same gate and quadrants were used throughout individual experiments. **Panel B** Histograms showing heterokaryon formation using HM-1 cells at different levels of confluence with CBA thymocytes. The percentage of gated events that were double stained is highlighted in the upper right hand corner of each histogram. Dye leakage controls appear on the left, fusions on the right. The absolute percentage of cells forming heterokaryons (% fusion - % dye leakage control) is highlighted in red for each confluence range. **Panel C** Table summarizing heterokaryon formation data from all five replicate experiments.

A



B

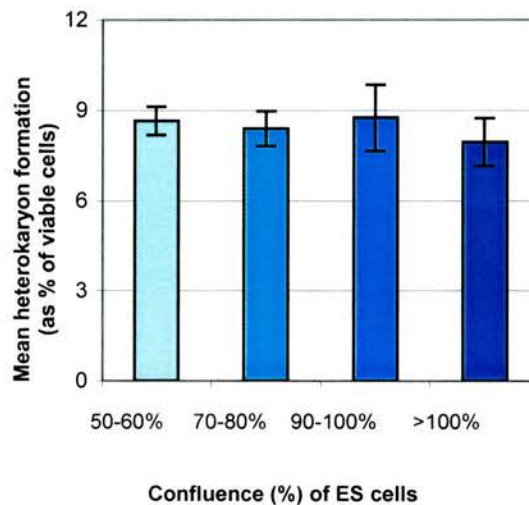
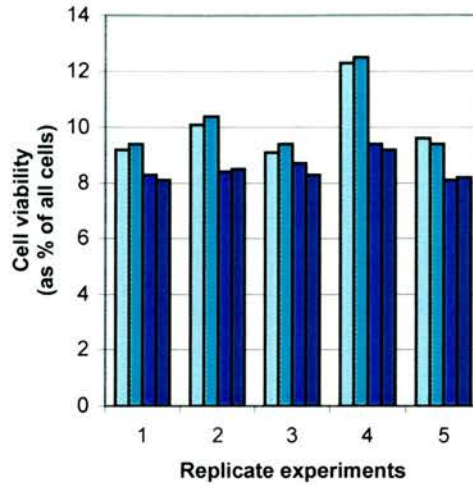


**Fig 6.4 HM-1 cell confluence does not affect heterokaryon formation**

HM-1 cells were grown to four degrees of confluence. Aliquots of  $10^7$  CMFDA stained HM-1 cells were fused to aliquots of  $5 \times 10^7$  CMFDA thymocytes using murine electrofusion conditions. 6-13 hours after electropulsing and seeding the cell mixtures, 1 plate containing  $1.2 \times 10^7$  cells was disaggregated with TEG and used to measure cell viability and heterokaryon formation. Two-dye FACS analysis was used to assess heterokaryon formation (See **Fig 6.3**). Columns are colour coded to denote what confluence range the HM-1 cells were grown to prior for each fusion: □ 50-60% ■ 70-80% ■ 90-100% ■ >100%.

**Panel A** Heterokaryon formation (as a percentage of viable cells) for all replicate experiments. **Panel B** The mean heterokaryon formation for each range of ES cell confluence  $\pm$  S.E.M.

A



B

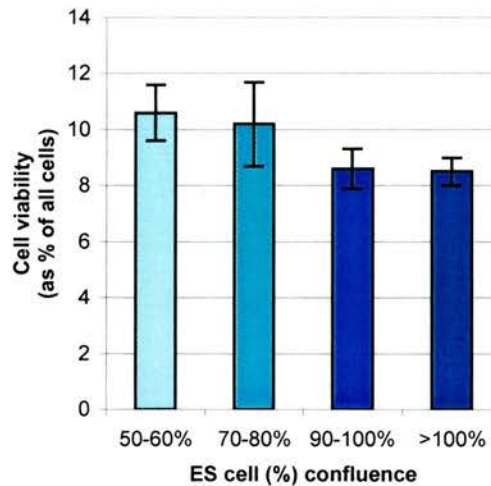


**Fig 6.5 HM-1 cell confluence does not affect viability of electropulsed cell mixtures** HM-1 cells were grown to four degrees of confluence. Aliquots of  $10^7$  CMFDA stained HM-1 cells were fused to aliquots of  $5 \times 10^7$  CMFDA thymocytes using murine electrofusion conditions. 6-13 hours after electropulsing and seeding the cell mixtures, 1 plate containing  $1.2 \times 10^7$  cells was disaggregated with TEG and used to measure cell viability and heterokaryon formation. Cell viability for fused mixtures of cells was measured using Forward Scatter/ Side Scatter FACS analysis (as described in **Section [12.2]**). Columns are colour coded to denote what percentage confluence the HM-1 cells were grown to prior to each fusion: ■ 50-60% ■ 70-80% ■ 90-100% ■ >100%. **Panel A** shows cell viability (as a percentage of all cells) measured by FSC/SSC FACS analysis for all replicate experiments. **Panel B** shows the mean cell viability (as a percentage of all cells) for each range of HM-1 cell confluence  $\pm$  S.E.M.

### [6.3.4] HM-1 cell confluence affects nuclear reprogramming of thymocytes

Using hybrid colony yields, heterokaryon formation and cell viability data detailed in **Subsections [6.3.2]** and **[6.3.3]**, hybridisation frequencies were calculated as described in **Subsection [2.7.5]**. **Fig. 6.6** shows mean hybridisation frequencies for each HM-1 cell confluence range from five replicate experiments. These yields are affected by HM-1 cell confluence ( $P=0.014$  when  $P$  is calculated using 2-way Analysis of Variance [Caria 2000]) highlighting that confluence of ES cells affects the reprogramming of thymocyte nuclei in the hybrid system.

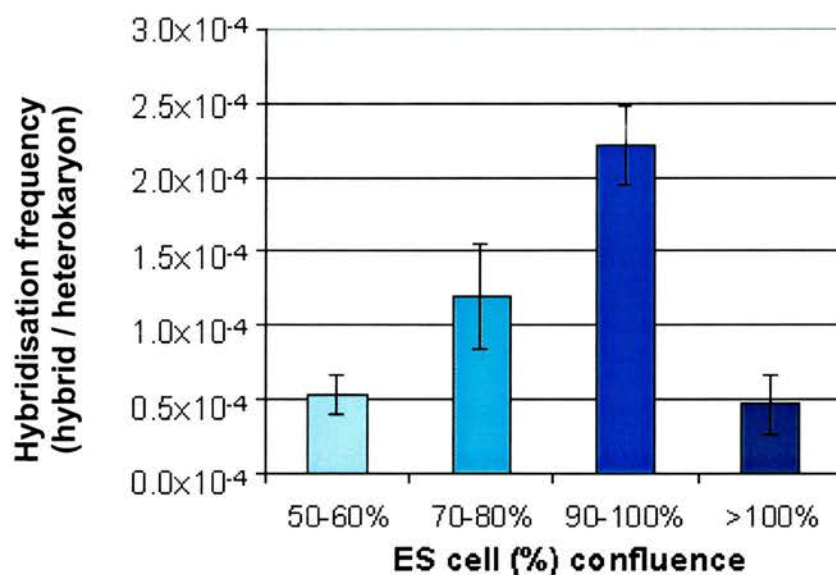


**Fig 6.6 HM-1 cell confluence affects hybridisation frequency**

Five replicate experiments electrofused HM-1 cells at four different stages of confluence to murine thymocytes and the pulsed cell mixture was seeded and selected for reprogrammed hybrids. Experiments generated data on hybrid colony yield, viable heterokaryon formation and cell viability for each range of HM-1 cell confluence. These data were used to calculate hybridization frequencies (hybrid / heterokaryon) as described in **Section [2.7.5]**. The mean and standard error of the mean of these frequencies is shown in the graph above.



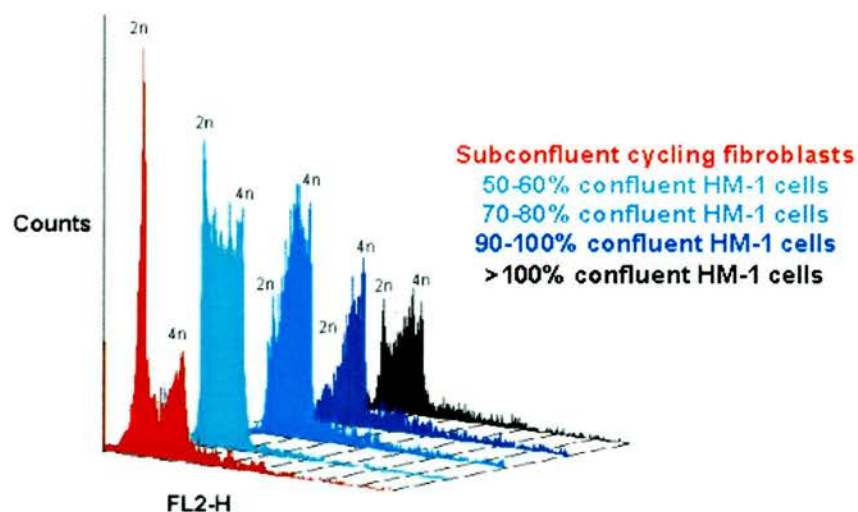
### **[6.3.5] 90-100% confluent ES cells display the greatest capacity to reprogram thymocytes**

Fusions using 90-100% confluent HM-1 cells showed the highest hybridisation frequencies (hybrid per heterokaryon) highlighting that this ES cell confluence has the greatest capacity to reprogram thymocyte nuclei. Fortunately, due to the large number of cells needed for each fusion, HM-1 cells had been consistently grown to this confluence in all experiments previously described in this thesis.

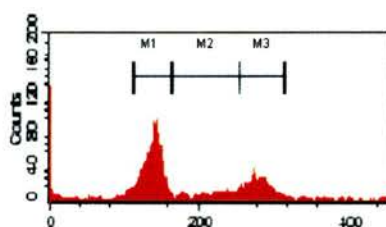
### **[6.3.6] Confluence of HM-1 cells affect their cell cycle characteristics**

Campbell *et al.* 1996 stated that cell cycle stages of both recipient cytoplasm and donor nucleus affected complete reprogramming in nuclear transfer experiments [More in **Subsection [1.8.1]**]. The cell cycle profiles of the HM-1 cell populations were assessed to see if there was any correlation between cell cycle stage and the increase in nuclear reprogramming in cell hybrids. HM-1 cell populations at different ranges of confluence were stained with propidium iodide [Krisan 1975] and FACS analysed [See **Section [1.3]** for details]. The resultant spectra are shown overlaid in **Fig 6.7 Panel A**. ES cells proliferate quickly and have short G1 and G2 phases [Savatier *et al.* 2000]. To ensure accurate differentiation between the various cell cycle stages, a subconfluent cycling population of PEFs was used as a control for positioning the stage gates [**Fig 6.7 Panel B**]. **Fig 6.7 Panel C** highlights the relationship between the gates M1, M2 and M3 and the phases of the cell cycle.

A



B



C

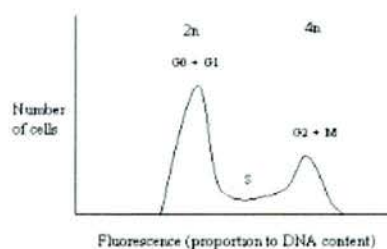


**Fig 6.7** Confluence affects the cell cycle characteristics of HM-1 cells

HM-1 cells were grown to four different ranges of confluence and their nuclei were fixed and stained with propidium iodide as described in **Subsection [2.3.5]**. **Panel A** PI fluorescence spectra for cycling PEFs and HM-1 cells at each confluence range. **Panel B** Cycling PEFs were also stained with PI and analysed and their spectrum was used for the positioning of gates M1, M2, M3. **Panel C** This schematic highlights the gates M1, M2 and M3 correspond to G1, S, and G2/M phases of the cell cycle respectively.



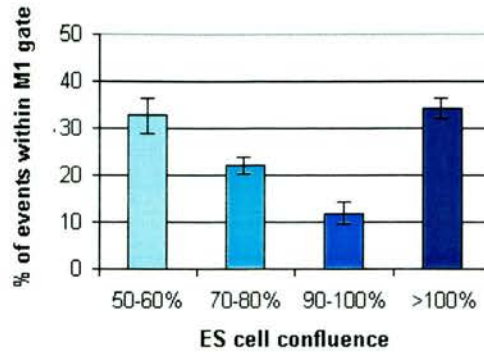
	% G1 gated			% S gated			% G2/M gated		
	Rep 1	Rep 2	Rep 3	Rep 1	Rep 2	Rep 3	Rep 1	Rep 2	Rep 3
	Mean±SEM			Mean±SEM			Mean±SEM		
<b>PEFs</b>	49.4	47.8	54.5	28.6	30.3	24.2	22.0	21.9	21.3
	<b>50.6±2.9</b>			<b>27.7±2.5</b>			<b>21.7±0.3</b>		
<b>50-60% Confluent ES cells</b>	33.2	37.3	27.9	47.1	44.8	54.5	19.8	17.8	17.5
	32.8±3.8			48.8±4.1			18.4±1.0		
<b>70-80% Confluent ES cells</b>	23.8	19.6	23.2	36.9	47.3	37.3	39.3	33.1	39.5
	22.2±1.9			40.5±4.8			37.3±3.0		
<b>90-100% Confluent ES cells</b>	11.8	11.8	12.3	48.2	47.0	45.8	40.0	41.2	42.0
	11.9±0.2			47.0±1			41.1±0.8		
<b>&gt;100% Confluent ES cells</b>	31.7	36.7	34.5	44.4	44.0	42.0	23.9	19.2	23.5
	34.3±2.1			43.5± 1.1			22.2±2.1		

**Table 6.1 HM-1 cell confluence affects the percentage of HM-1 cells lying within the G1, S, and G2/M gates**

Raw data showing the percentage of cells lying within each gate for HM-1 cell populations at different ranges of confluence. Mean percentages (±S.E.M.) were calculated from data taken from three replicate experiments.

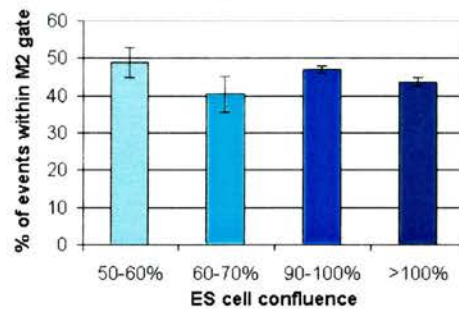
A

G1



B

S



C

G2/M

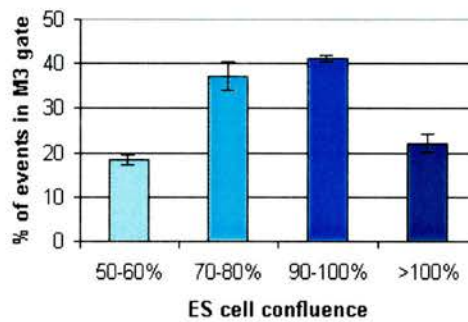


**Fig 6.8 HM-1 cell confluence affects the mean percentage of HM-1 cells lying within each gate**

PI fluorescence spectra shown in **Fig 6.7** were divided into gates corresponding to G1, S, and G2/M phases of the cell cycle. The percentage of events within each gate showed the cell cycle characteristics of the HM-1 cell populations. **Panel A** Mean percentage of HM-1 cells in G1 phase at four different ranges of confluence ( $\pm$ S.E.M). **Panel B** Mean percentage of HM-1 cells in S phase at four different ranges of confluence ( $\pm$ S.E.M). **Panel C** Mean percentage of HM-1 cells in G2/M phases at four different ranges of confluence ( $\pm$ S.E.M).

The cell cycle profiles of HM-1 cell populations were affected by confluence [Fig 6.7]. As Table 6.1 shows the proportion of cells in each gate changed with HM-1 cell confluence range in each of three replicate experiments. Fig 6.8 shows the mean percentages lying within each gate as calculated from the five replicates. Percentage of HM-1 cells at each stage of the cell cycle was affected by confluence ( $P < 0.05$  in each case as calculated using 2-way Analysis of Variance [Caria 2000]). The percentage of events in G2/M increased from 18.4 to 41.1% as cells approached 100% confluence while the percentage of cells in G1 decreased from 32.8% to 11.9%. The proportion of cells in S phase did not change significantly ( $P > 0.05$ ) as 100% confluence was approached. Zhou *et al.* 2001 had previously carried out similar analysis on a subconfluent murine ES (R1) cell population. They reported that 18% of the cells were in G1 phase, 64% were in S phase and 18% were in G2/M phase. While the proportion of cells in G2/M phase was similar to the 50-60% confluent HM-1 population observed here (18% versus  $17.2 \pm 0.7\%$ ), more cells were in G1 phase (18% as opposed to  $32.8 \pm 3.8\%$ ) and less in S phase (64% compared to  $48.8 \pm 4.1\%$ ). Fewer cells in S phase may suggest the HM-1 cells are growing more slowly than R1 cells however R1 and HM-1 cells do not have a significantly different doubling time (11.4 hr versus 11-13 hr) when grown in similar culture conditions [Udy *et al.* 1997]. This suggests inherent differences between the cell lines might not be the reason for differences in the proportion of cells in S phase. A possible explanation for the differences in cell cycle profile is the different culture regimes used to grow the cells (R1 cells were grown on inactivated feeders whereas HM-1 cells were grown on gelatin with serum supplemented medium). Gao *et al.* 2003 shows 60-70% subconfluent HM-1 populations as having a different cell cycle profile (33.8% in G1, 37.3% in S and 28.9% in G2/M) to 50-60% HM-1 populations analysed here (32.8% in G1, 48.8% in S, and 18.4% in G2/M). Gao's cells were grown in serum depleted medium (5% serum) for 24 hours prior to analysis and this appears to change cell characteristics. Comparing Gao's data with data detailed

in **Table 6.1** there is a decrease in the percentage of HM-1 cells in S phase, suggesting a slowing of the cell cycle. This would be expected in serum depleted conditions.

The observed increase of 2c cells in the superconfluent population compared to HM-1 cells at other confluence ranges may be due to differentiation of the ES cells. In general, differentiated cells cycle more slowly than embryonic cells [Savatier *et al.* 2000][Murray & Hunt 1993], and have more checkpoints that need to be overcome prior to the cells initiating DNA synthesis [Murray & Hunt 1993]. Thus, the probability of differentiated cells being 2c at any given time will be higher than that of an ES cell.

It is interesting that the 90-100% confluent population gave the highest phenotypic ES hybridisation frequencies and also contained the highest proportion of ES cells in G<sub>2</sub>/M. These cells, poised to undergo mitosis, not only contain a tetraploid complement of DNA but also contain twice the volume of cytoplasm. One might speculate that by fusing these G<sub>2</sub>/M ES cells to a somatic cell, one has a better chance of reprogramming the nucleus given this greater abundance of ES derived regulatory factors. If this was the case, one might expect where tetraploid hybrids, generated by ES cell x ES cell fusions, were themselves fused to somatic cells there may be an even greater incidence of thymocyte nuclear reprogramming.

As discussed in **Section [1.3]**, cells in M phase induce mitosis in the fusion partner regardless of its previous cell cycle stage. If a G<sub>2</sub> cell fuses to another cell that is in interphase, G<sub>2</sub> nucleus remains arrested at the G<sub>2</sub>/M checkpoint until the second nucleus has also progressed to G<sub>2</sub> and then both nuclei initiate mitosis simultaneously. As others have shown the proportion of cycling ES cells in G<sub>2</sub> to be relatively small [Savatier *et al.* 2000], one might speculate that the number of ES cells in M phase increases as 100% confluence is approached. Cells, at the G<sub>2</sub>/M transition or in the M phase, display high MPF activities [Jung *et al.* 1993]. MPF activity promotes the breakdown of the nuclear membrane, and as many suspect that exposure of chromatin to cytoplasm is a necessary trigger for reprogramming, then one might expect cells with high MPF activity to promote greater reprogramming. The decrease in the proportion of ES cells in G<sub>1</sub> (G<sub>1</sub> cells have low MPF levels) and the increase in the proportion of ES

cells in G2/M (G2/M cells have high levels) means that the ES cell population will contain more cells with a high level of MPF [See **Fig 1.5**]. Perhaps this causes more frequent somatic and ES nuclear membrane breakdown and thus nuclear reprogramming is more common. To test this hypothesis, one could disrupt MPF activation (eg. partial suppression of *cdc2* kinase) in the confluent ES cell populations prior to fusion or express MPF in subconfluent ES cells and observe whether these treatments affects reprogramming.

### **[6.3.7] HM-1 cell confluence affects the induction of heat shock protein Hsp72**

Growing cells to confluence is a classic trigger for inducing a stress response in many cell types [Garrido *et al.* 1997]. Another potential explanation for the data is as ES cells approach confluence they express progressively higher levels of stress shock proteins that facilitate somatic nuclear reprogramming after fusion. Chaperone activity of induced stress response proteins repairs misfolded protein and RNA components of the cell's machinery necessary for many function including altering the somatic chromatin. Some Hsps have even been shown to play a role in chromatin structural changes directly [Nover 1994]. **Fig 6.9** shows the induction of Hsp72 expression in ES cells as they approach confluence.

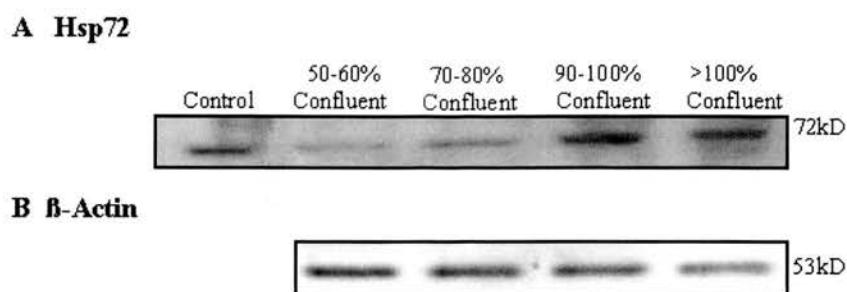


**Fig 6.9 HM-1 cell confluence affects the induction of Hsp72**

Whole cell lysates were generated from ES cell populations displaying four different ranges of confluence. 150 $\mu$ g protein of HM-1 cell lysate representing each confluence range was loaded onto a polyacrylamide gel, run, transferred and probed with anti-Hsp72 as described in **Subsection [2.7.3]**. **Panel A** Western blot probed with anti-Hsp72. The control was the antibody manufacturer control lysate, a heat shocked HeLa cell lysate. As the confluence of HM-1 cells increased, more Hsp72 was detected in the lysates. **Panel B** The same plot was reprobed with anti- $\beta$ -actin to confirm the same amount of protein lysate had been added to each lane.

Hsp72 induction increased as HM-1 cells became more confluent. However it remains unclear if this or other stress induced factors are important for nuclear reprogramming. This could explain why both reprogramming of and by ES cells is increased when more confluent ES cells are used.

The hypothesis that stress induced proteins (Hsps) are important to nuclear reprogramming could be tested if their induction in HM-1 cells could be temporarily disrupted in some way [eg. addition of protein synthesis inhibitor cycloheximide prior to fusion]. If such HM-1 cells failed to show elevated hybridisation frequencies (hybrid / heterokaryon) after cell confluence this might suggest stress induced proteins may be involved in reprogramming.



### [6.3.8] Confluence does not affect HM-1 cell size

The only difference Gao *et al.* observed between their ES populations of different degrees of confluence was that “more small sized cells” were observed at the 80-90% confluent population than the 60-70% confluent one. This was based on visual analysis looking at the cells under the microscope. No discernable difference was seen in cell size when similar assessments were repeated here. However HM-1 cell morphology was difficult to assess as individual cell boundaries become less distinct at higher densities [See **Fig 6.1 Panel B**]. In order to make a more objective assessment, Forward Scatter (FCS) FACS analysis was used to measure cell sizes of different populations [See **Fig 6.10**]. The forward scatter spectra of the four cell populations representing each confluence range overlaid perfectly indicating there was no significant change in cell size as populations became more confluent. Only the >100% confluent (blue) spectrum showed any difference: a small proportion of larger cells that also exhibited a greater degree of granularity when FACS analysed for side scatter. Such cells are almost certainly newly differentiated cells.



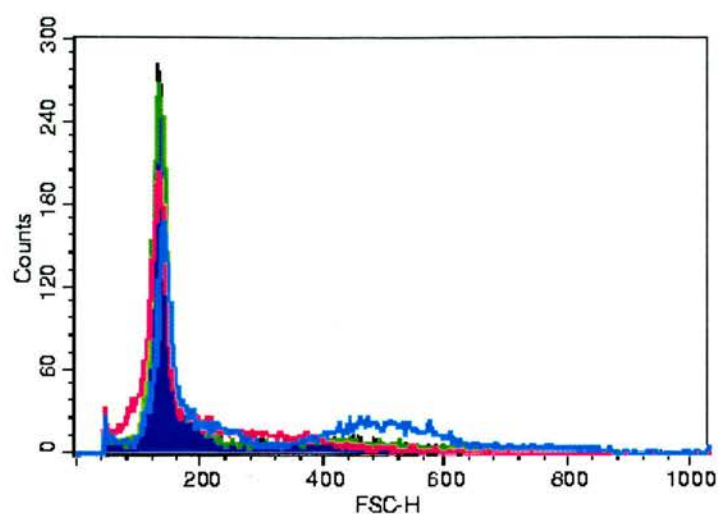


**Fig 6.10 HM-1 cell size does not change at different levels of confluence**

ES cells were grown to various ranges of confluence and FACS analysed to measure mean viable cell size. Forward Scatter (FSC) spectra for the four ranges of ES confluence are overlaid using identical settings and axes. 50-60% confluent ES cells are represented by the purple spectrum, 70-80% confluent by the green, 90-100% by the pink and >100% by the blue. The spectra overlaid perfectly showing that ES cell confluence does not affect cell size.

### **[6.3.9] HM-1 cell passage number affects their capacity to reprogram PEF nuclei in cell hybrids**

Finally, the effect of ES cell passage number on the cell's capacity to reprogramme somatic nuclei was investigated. Although many reports linked a decline of germline transmission in ES chimeras with increasing passage number [Longo *et al.* 1997][Zhou *et al.* 2001], its effect on successful nuclear reprogramming in nuclear transfer experiments is less clear. A correlation between cloning problems and increasing cell passage was made in sheep studies [Wilmut *et al.* 1997][McCreath *et al.* 2000][Schnieke *et al.* 2000]. Additionally Gao *et al.* 2003 had also reported that passage number of R1 ES cells affected developmental potential of reconstructed embryos. In contrast though, many reports have failed to show that passage number affects nuclear transfer efficiencies. Wakayama *et al.* (1999), using R1 cells at passage 34, failed to

observe such a passage number related effect. Zhou *et al.* (2001) reported that using high R1 cell passage (28) resulted in no change in the proportion of reconstructed embryos developing to morula / blastocyst stage. There was a decrease in the rate of embryo implantation compared to control embryos derived from lower passage ES nuclei. Bovine studies have also shown a lack of evidence that cell passage affects nuclear transfer efficiencies [Hill *et al.* 2000][Kubota *et al.* 2000].

Several standard electrofusion experiments using CBA PEFs (Passage 3) and HM-1<sup>puro</sup> of various passage numbers (ranging from 17 to 53) were carried out. As **Fig 6.11** shows the hybrid colony yield was affected by passage number. Experiments where HM-1<sup>puro</sup> cells at passage number  $\geq 36$  were used failed to produce hybrid colonies ( $n = 4$ ); whereas experiments using cells of lower passage number produced hybrid colonies ( $n = 4$ ).

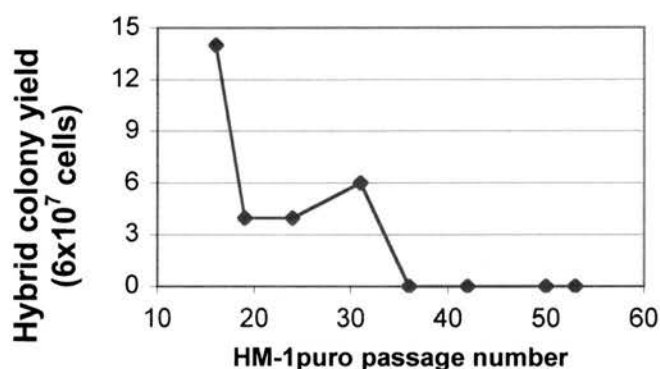


**Fig 6.11 HM-1<sup>puro</sup> passage number affects hybrid colony yield**

Fusions between CBA PEFs (Passage 3) and HM-1<sup>puro</sup> cells of various passage number were carried out under standard electrofusion conditions. The resultant hybrid colony number is plotted against passage number of the ES cells used in each fusion.

In research generating chimeras from ES cells, a decrease in germline transmission has long been observed with ES cells of high passage. This, in some cases, has been found to be related to progressive loss of euploidy [Longo *et al.* 1997] while in others this was not found to be so [Zhou *et al.* 2001]. The ploidy of HM-1<sup>puro</sup> cells was assessed to investigate whether cells became aneuploid as they were grown to higher passage. Mitotic spreads of HM-1<sup>puro</sup> cells at passage 31 and 36 were generated using the cells

from the same frozen stocks used to carry out the previous fusions. Cells at these passages were chosen as this was where the cells lost their capacity to generate phenotypic ES hybrids. Interestingly, cells at passage 31 were euploid, while passage 36 cells were not: of the 50 spreads counted, 5 had an extra chromosome and 5 had two extra chromosomes. The loss of nuclear reprogramming activity in the ES cell line correlated with the appearance of aneuploidy. Karyotypic analysis showed random chromosome duplication rather than the copying of any particular chromosome was enough to disrupt nuclear reprogramming. Representative karyotypes of HM1<sup>puro</sup> cells at passage 31 and 36 are shown in **Fig 6.12**. 40 of 50 spreads still have a euploid number so this alone would only account for a 20% reduction in the number of hybrids, so there must be other factors in addition to misregulation of chromosome number that are involved. Perhaps the mechanisms that regulates genotypic stability are necessary for nuclear reprogramming.

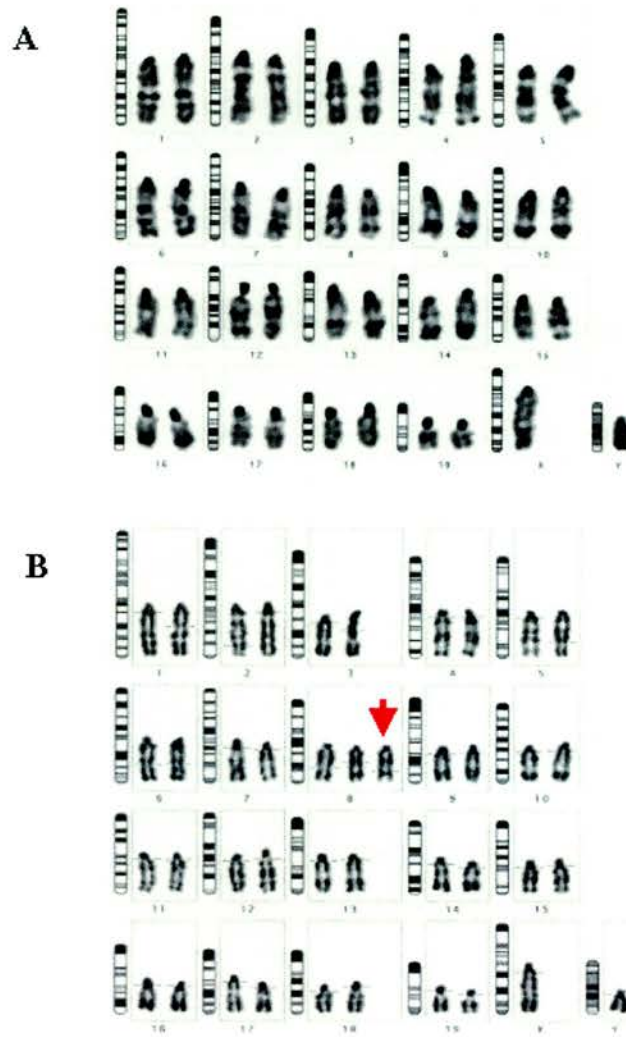


**Fig 6.12 Loss of reprogramming activity correlates with loss of euploidy in HM1<sup>puro</sup> cells**

Mitotic spreads of HM1<sup>puro</sup> cells at passage 31 and 36 were generated. At passage 31, all 50 spreads counted displayed a diploid complement (40 chromosomes). At passage 36 however, only 40 of the spreads were diploid, 5 contained 41 chromosomes and 5 contained 42. Karyotypic analysis revealed that in no chromosome was triplicated more than once suggesting random chromosome duplication. In the representative karyotype shown, there are three copies of chromosome 8 (the red arrow highlights the third inappropriate copy).

## [6.4] Conclusions

Confluence of HM-1 cells affected their capacity to reprogram thymocyte nuclei in cell hybrids ( $P=0.014$ ). Hybrid colony yield increased as HM-1 confluence increased until HM-1 cells reached 100% confluence and began to differentiate. The optimum ES cell confluence range for nuclear reprogramming was found to be 90-100%, which had previously been used in all hybridisation experiments because of the high cell numbers required for each experiment. It would be interesting to investigate whether somatic cell confluence also affects hybridization frequencies. Gao *et al.* 2003 showed that the more confluent an ES cell population, the more readily nuclei from those ES cells could be completely reprogrammed when transferred into oocytes.

In an effort to understand why HM-1 cell confluence affected nuclear reprogramming the cell cycle characteristics of HM-1 cells were analysed. As the cells approach 100% confluence, the proportion of cells in G1 decreases, the proportion in G2/M phases increased while the proportion in S remains unchanged. As MPF triggers nuclear membrane breakdown and G1 cells have a low level of MPF activity while G2/M cells have a high level, it was hypothesised that perhaps the overall increase in MPF levels of HM-1 cell populations as they approach confluence may account for the increase in reprogramming. This could be tested by altering the MPF activity of HM-1 cells (either by expressing the genes coding for the factor, or by decreasing MPF activity by partially suppressing *cdc2* kinase expression with RNA interference) and investigating whether there is any change in their nuclear reprogramming capacity.

In addition to affecting cell cycle characteristics, ES cell confluence was associated with induction of stress response factor Hsp72. As HM-1 cells approached confluence, higher levels of Hsp72 were observed. This indicates that confluence is a trigger for the stress response in HM-1 cells. It was hypothesised that some aspect of the stress response may facilitate reprogramming.

The passage number of HM-1 cells affected their capacity to reprogram PEFs. Fusion experiments using HM-1<sup>puro</sup> cells of passage number  $\geq 36$  yielded no hybrids whereas those of passage  $\leq 31$  did. This correlated with the cells becoming aneuploid. It was hypothesised that mechanisms required for genotypic stability also have a role in nuclear reprogramming.



## **[7] The effect of serum starvation and quiescence on the murine cell hybrid system**

### **[7.1] Introduction**

In the absence of factors that stimulate proliferation, some mitotic cell types stop dividing and enter a reversible state termed quiescence or G0. A quiescent cell can reinitiate proliferation if growth factors are re-introduced. This distinguishes quiescence from senescence (another viable though non-proliferative cellular state) where cells can no longer re-enter the cell cycle (**Subsection [1.3]** reviews the cycle cell and quiescence in more detail).

It has been suggested that quiescent nuclei are more amenable to being reprogrammed than cycling nuclei [Campbell 1996, Campbell *et al.* 1999]. The successful production of Dolly used a nucleus from a cultured adult differentiated somatic cell taken from a population of cells that had been serum starved into quiescence [Wilmut *et al.* 1997]. Quiescence affects the histone composition of chromatin and also the sub-nuclear distribution of chromatin structural proteins [Khochbin & Wolffe 1994][Dimitrov & Wolffe 1996]. It is thought that some aspect of these changes may make the nuclei of quiescent cells more amenable to being reprogrammed [Pallante 2002].

Interpretation of nuclear transfer data from various groups has failed to resolve whether quiescence affects nuclear reprogramming. The central problem lies in not being able to verify the quiescent state of a cell and use its nuclei for nuclear transfer at the same time, therefore no direct correlation between the quiescent state and nuclear reprogramming success can be drawn. Campbell's contention that a quiescent nucleus is more amenable to being reprogrammed than a nucleus at a random cell cycle stage has yet to be proven (see **Subsection [1.8.1]** for more detail). Two observations have raised doubt as to whether quiescence is beneficial for nuclear reprogramming: (a) quiescent cells such as terminally differentiated neurons



fail to support development to term of nuclear transfer embryos [Yamazaki *et al.* 2001], and (b) cattle have been successfully cloned using apparently non-quiescent foetal fibroblasts as nuclear donors [Cibelli *et al.* 1998].

The aim of this chapter was to investigate the effect of quiescence on nuclear reprogramming on the murine cell hybrid system. The successful generation of ES phenotypic cell hybrids from primary embryonic fibroblasts (**Section [3.3.4]**) provided the opportunity to do this. Fibroblasts could be rendered quiescent by serum starvation [Itahana *et al.* 2002][Kill *et al.* 1991].

## **[7.2] Objective**

To investigate the effect of serum starving fibroblasts into quiescence on the murine cell hybrid system.

## **[7.3] Results and discussion**

### **[7.3.1] Serum starvation of primary embryonic fibroblast renders them quiescent**

In order to investigate the effect of quiescence on nuclear reprogramming, one had first to verify that serum starvation of primary embryonic fibroblasts rendered them quiescent. **Figure 7.1** (overleaf) shows that fibroblasts, cultured in low serum conditions, ceased proliferating, whereas control PEFs continued until they became contact inhibited (day 4). At day 6 serum starved PEFs were re-introduced to normal serum conditions, and by day 7 they had resumed proliferating.

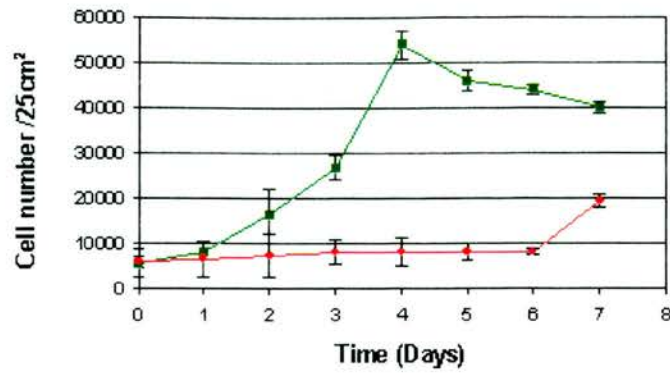


**Figure 7.1 Primary embryonic fibroblasts cease proliferation under low serum conditions but resume when normal serum conditions are restored**

Sixteen 25cm<sup>2</sup> tissue culture flasks were seeded at a density of 4,000 PEFs per cm<sup>2</sup> and left for 24hr in PEF medium. After 24 hours (Day 0), serum starvation medium was used to feed seven of the flasks, while the other seven were fed with PEF medium. The flasks were maintained in either PEF or serum starvation medium for up to six days. Normal serum levels are applied to both control and serum starved populations on day 6. Growth curves were generating by sacrificing and counting the number of viable PEFs in one control flask and one serum starved flask every 24hr. The graph shows overlaid growth curves for control (■) and serum starved PEFs (●). Error bars show associated S.E.M. from replicate samples from the same flask.

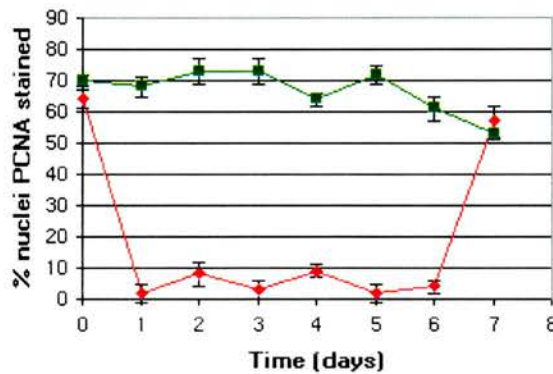


**Figure 7.2 The percentage of primary embryonic fibroblasts expressing proliferating cell nuclear antigen (PCNA) decreases under low serum conditions but returns to initial levels when normal serum conditions were restored**

Glass slides were seeded at a density of 4,000 PEF cells/cm<sup>2</sup> and fed with either PEF medium or serum starvation medium for up to 6 days. Normal serum levels are applied to both control and serum starved populations on day 6. Throughout the experiment, the slides were fixed and immunostained daily with anti-PCNA to identify proliferating cells. At day 6 serum starved cells were re-introduced to full serum conditions. PCNA staining of control and serum starved PEFs. The graph shows the percentage of nuclei staining positively for PCNA in control (■) and serum starved (●) PEF populations over 7 days. Error bars show associated S.E.M. from replicate samples from the same flask.

Fibroblast populations grown in low serum conditions contained fewer cells expressing PCNA than control populations (**Fig 7.2**). During the first six days of the experiment, less than 10% of nuclei stained positive for PCNA whereas in control populations over 60% of nuclei stained positive. Serum starved PEFs were reintroduced to normal serum conditions on day 6 and on day 7,  $57\pm 5\%$  of nuclei derived from these serum reactivated cells were PCNA positive.

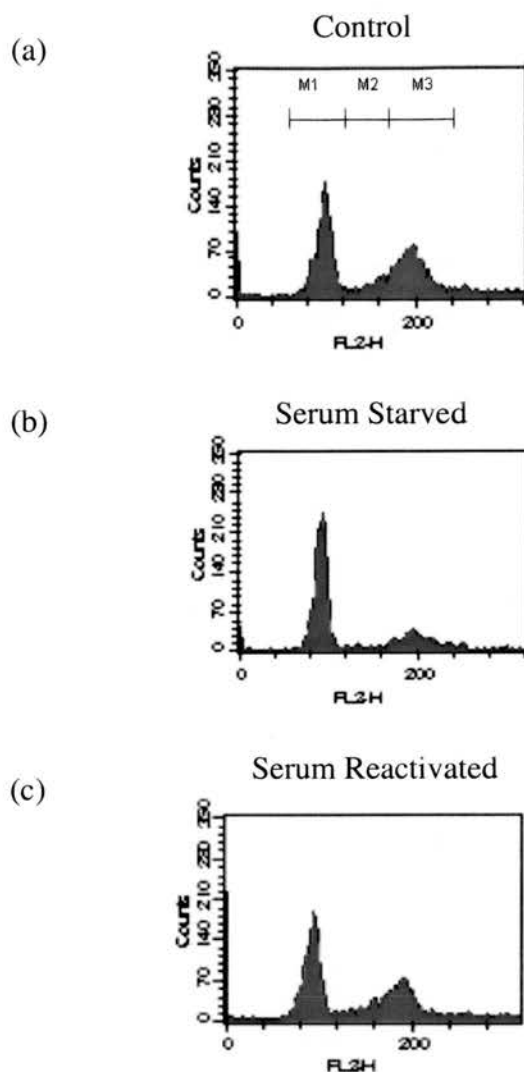
Furthermore, the cell cycle characteristics of fibroblasts were affected by serum levels (**Fig 7.3** overleaf). When fibroblasts were serum starved, the proportion of cells in G1/G0 rose (from 53.7 to 73.0%) while the relative amount in S and G2/M fell (from 8.6 to 2.7% and from 37.7 to 24.3% respectively). Reintroduction of serum starved fibroblasts to normal serum conditions resulted in the cell cycle characteristics changing until they became similar to control PEFs (52.5% in G1/G0, 8.7% in S, and 38.8% in G2/M).

Pallante (2002) had also shown an increase in the number of cells in G1/G0 when she serum starved murine PEFs (63.9 to 65.9%). She also noted that there was a decline in the proportion of cells in S phase (10.6% to 3.5%). However unlike data presented here, she reports an increase in the proportion of cells in G2/M (from 25.5% to 30.5%). This difference could not be accounted for.

It was also found that serum starvation altered the morphology of the cells (**Fig 7.4**). Fibroblasts, placed in low serum conditions, lost their long tapered morphology and flattened out. However when these cells were reintroduced to normal serum levels, they quickly reacquired their original fusiform morphology. Pillante 2002 had previously reported that murine PEFs changed morphology when they were rendered quiescent. Her observations were consistent with those described here.

In summary, serum starvation stopped cell proliferation, down-regulated PCNA expression, increased the number of cells in G1/G0 of the cell cycle, and caused loss of the fibroblast fusiform morphology. Reintroduction of serum reversed all these effects. Taken together these data confirm that the serum starvation conditions used here renders fibroblasts quiescent.

A



B

	% in G1/G0 (M1 gate)	% in S (M2 gate)	% in G2/M (M3 gate)
<b>Control PEFs</b>	53.7	8.6	37.7
<b>Serum Starved PEFs</b>	73.0	2.7	24.3
<b>Serum Reactivated PEFs</b>	52.5	8.7	38.8

**Fig 7.3 Serum starvation of primary embryonic fibroblasts affects their cell cycle characteristics**

CBA<sup>+/+</sup> primary embryonic fibroblasts (Passage 3) were either grown in either full PEF medium (a) or serum starvation medium (b) for six days or were grown in serum starvation medium for six days and then reintroduced into full medium for 24hr (c). Cells were then trypsinised and staining with propidium iodide as described in **Subsection [2.3.5]**. The stained cells for each treatment were then FACS analysed. The spectrum of fluorescence indicates the ploidy of cells in a population when fixed and stained.

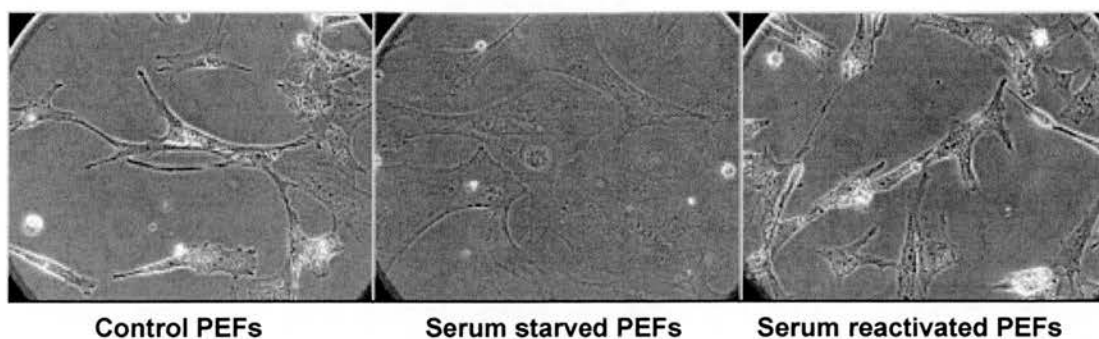


**Fig 7.4 Morphological changes in serum starved and serum reactivated primary embryonic fibroblasts**

Representative views of cells cultured on full PEF medium, serum starved for 6 days and then restimulated for 24 hr with 20% FCS. Cells spread out during serum starvation but reacquired a fusiform, fibroblast-like shape after serum reactivation.

### **[7.3.2] Serum starvation of primary embryonic fibroblasts increases hybrid colony yield**

Large numbers of quiescent PEFs were required for the subsequent fusion/hybridisation experiments, and to minimise the amount of time and materials needed to generate these cells, a greater plating density was required than used in previous experiments. The maximum initial seeding density (IPD) which did not result in significant amount of cell death under conditions used (*i.e.* 24hr culture in murine ES medium followed by serum starvation) was empirically found to be 15,000 cells / cm<sup>2</sup> [Fig 7.5]. This plating density was used for all subsequent fibroblast fusion experiments.

Serum starvation of the fibroblasts into quiescence increased hybrid colony yield (Fig 7.6) ( $P < 0.05$  as calculated using the Student's paired t-test [Caria 2000]). Hybridisation experiments using quiescent fibroblasts yielded on average  $38.6 \pm 11.6$  fold more colonies than control experiments.



A



B

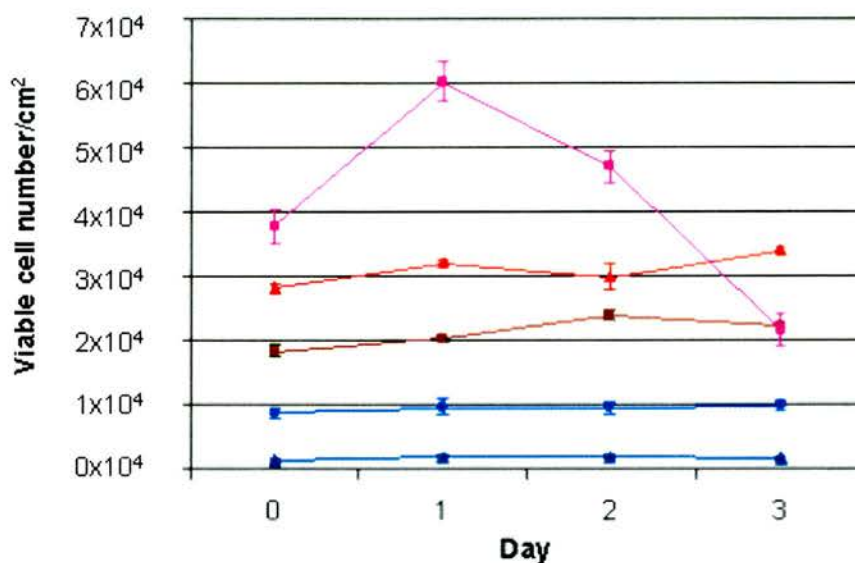


**Fig 7.5 Identification of an appropriate PEF plating density for subsequent fusion experiments**

PEFs, seeded at various densities ranging from 1,000 to 20,000 cells/cm<sup>2</sup>, were incubated in full mES medium for 24hr. Subsequently (at day 0), wells were washed three times in 1xPBS and incubated in serum starvation medium. Cell viability was assayed by Forward Scatter / Side Scatter FACS analysis at 24 hour intervals. **Panel A** Populations of cells derived from various plating densities were highlighted by various symbol.

**Panel B** Graph showing viable cell number counts at 24 hours intervals. Each point represents the mean  $\pm$  S.E.M. of two separate cell counts of the same sample from one experiment. Absence of error bars indicates that the symbol is larger than the error.

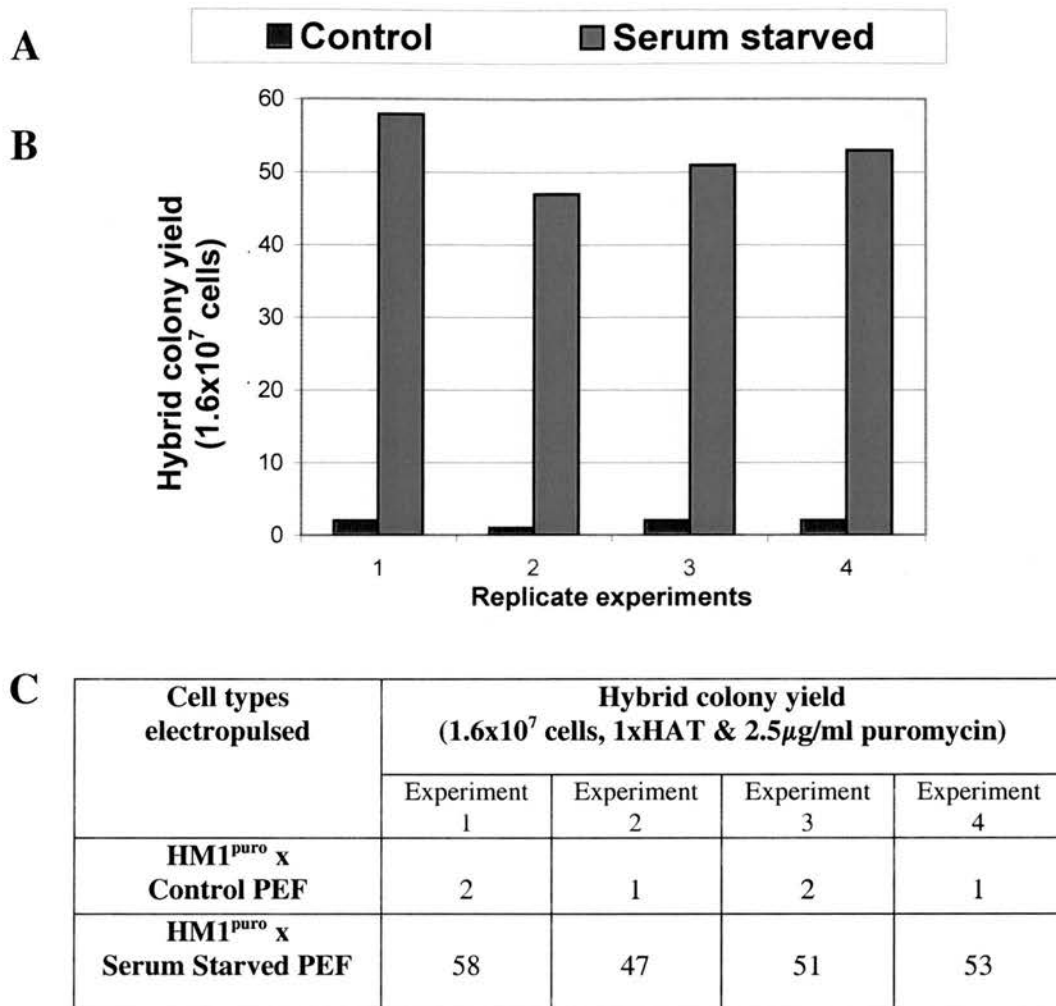


**Fig 7.6 Serum starvation of PEFs increases hybrid colony yield**

$10^7$  HM-1<sup>puro</sup> cells (passage number 20-25) were electropulsed with  $10^7$  PEFs (passage 3) using standard electrofusion conditions. PEFs were maintained in either full PEF medium (Control PEFs) or Serum Starvation medium (Serum starved PEFs) for 6 days prior to electropulsing. Electropulsed cell mixtures were plated equally in 5 12 cm plates. One plate was used for FACS analysis to measure cell viability and heterokaryon formation. Twenty four hours after electropulsing, double selection mES medium (1xHAT and 2.5  $\mu$ g/ml puromycin) was applied to the cells in the remaining plates. **Panel A** The colour code used throughout this chapter to represent fusions using either control or serum starved PEFs. **Panel B** Graph showing hybrid colony yields for all three replicate experiments. **Panel C** Table summarising the data from all replicate experiments (n = 4).



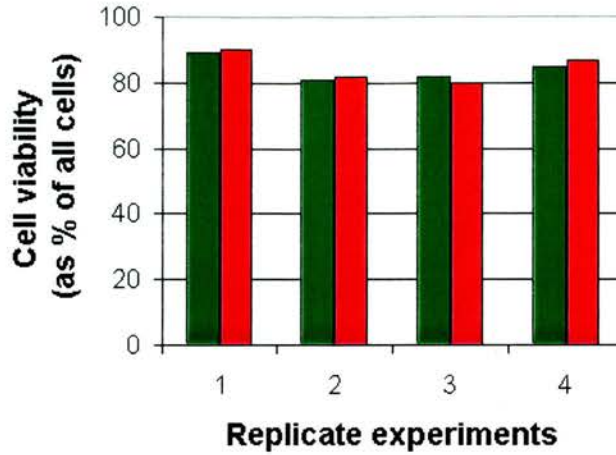
### **[7.3.3] Serum starvation of fibroblasts does not affect cell viability of electropulsed cells but does decrease heterokaryon formation**

In order to see if quiescence affected nuclear reprogramming of fibroblasts, viability of cells after electropulsing and the proportion of viable cells forming heterokaryons was measured for each replicate experiment.

**Fig 7.7** shows that serum starving the PEFs did not affect viability of electropulsed cell mixtures ( $P > 0.05$  as calculated using a Student's paired t-test (one tailed) [Caria 2000]). When 2-dye FACS analysis was performed on the cells, it was found that serum starving the cells decreased heterokaryon formation [**Figs 7.8 & 7.9**] ( $P < 0.05$  as calculated using the Student's paired t-test (2 tailed) [Ciara 2000]).

It was speculated that perhaps proliferating cells are more likely to fuse than quiescent cells, although no reports were found in the literature investigating whether this is true.

A



B

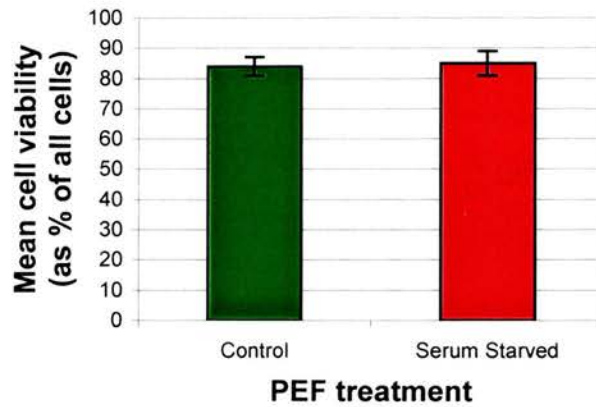
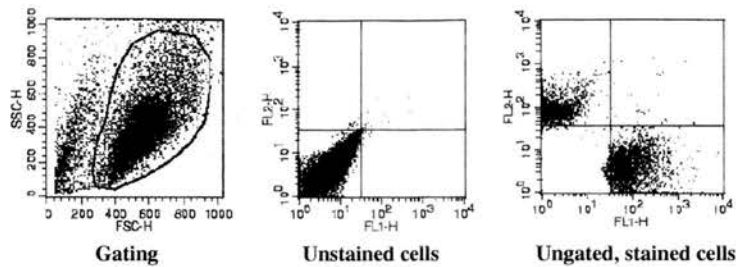


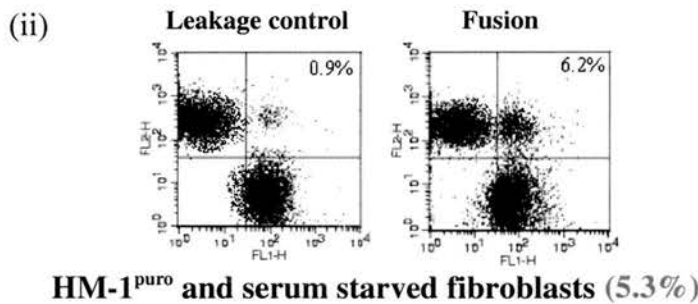
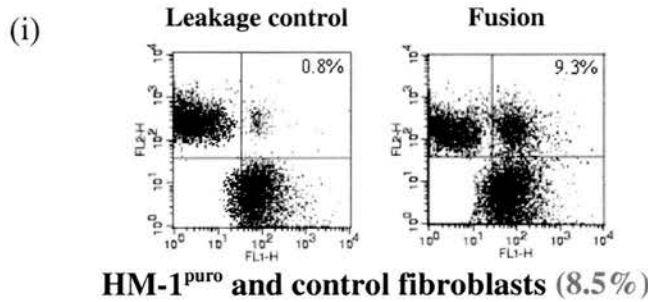
**Fig 7.7 Serum starvation of primary embryonic fibroblasts does not affect viability of electropulsed cell mixtures**

Cell viability for fused mixtures of cells was measured using Forward Scatter / Side Scatter FACS analysis (As described in **Subsection [12.2]**). Between 6 and 13 hours after electropulsing and seeding the cell mixtures, 1 of 5 representative plates from each fusion was trypsinised. Cells from the used media and all post-trypsinisation washings were combined and pelleted before being washed and resuspended in 1xPBS. Cell viability (as percentage of total cells) was measured using FCS/SSC plots. Results were verified using trypan blue staining. Columns are colour coded to denote whether control or serum starved PEFs had been used. **Panel A** Cell viability (as percentage of all cells) measured by FCS/SSC FACS analysis for all replicate experiments. **Panel B** Mean cell viabilities as calculated from four replicate experiments.

A



B



C

	Heterokaryon formation (as % of viable cells)			
	Experiment 1	Experiment 2	Experiment 3	Experiment 4
HM-1 <sup> puro</sup> x control PEFs	8.5	8.3	9.5	8.3
HM-1 <sup> puro</sup> cells & serum starved PEFs	5.3	5.4	5.8	5.1

**Fig 7.8 The effect of serum starving fibroblasts on heterokaryon formation was assessed using 2-dye FACS analysis**

**Panel A** Gating and compensation data (See **Subsection [12.2]**). Quadrant axes were defined so that CMTMR stained primary embryonic fibroblasts (upper left quadrant) were distinct from CMFDA stained HM-1 cells (upper right quadrant). The same gate and quadrants were used throughout individual experiments. **Panel B** Histograms showing fluorescence of cells in dye leakage control and fusions using HM-1 cells and either (i) control or (ii) serum starved PEFs. Data displayed in panels A and B are taken from one representative experiment. Percentage heterokaryon formation was calculated by subtracting the percentages for leakage controls from that for the fusion (these figures are highlighted in red). **Panel C** Summary of data from replicate experiments (n=4). Serum starving fibroblasts decreased heterokaryon formation ( $P < 0.05$  as calculated by a Student's paired t-test (one tailed) [Caria 2000]).

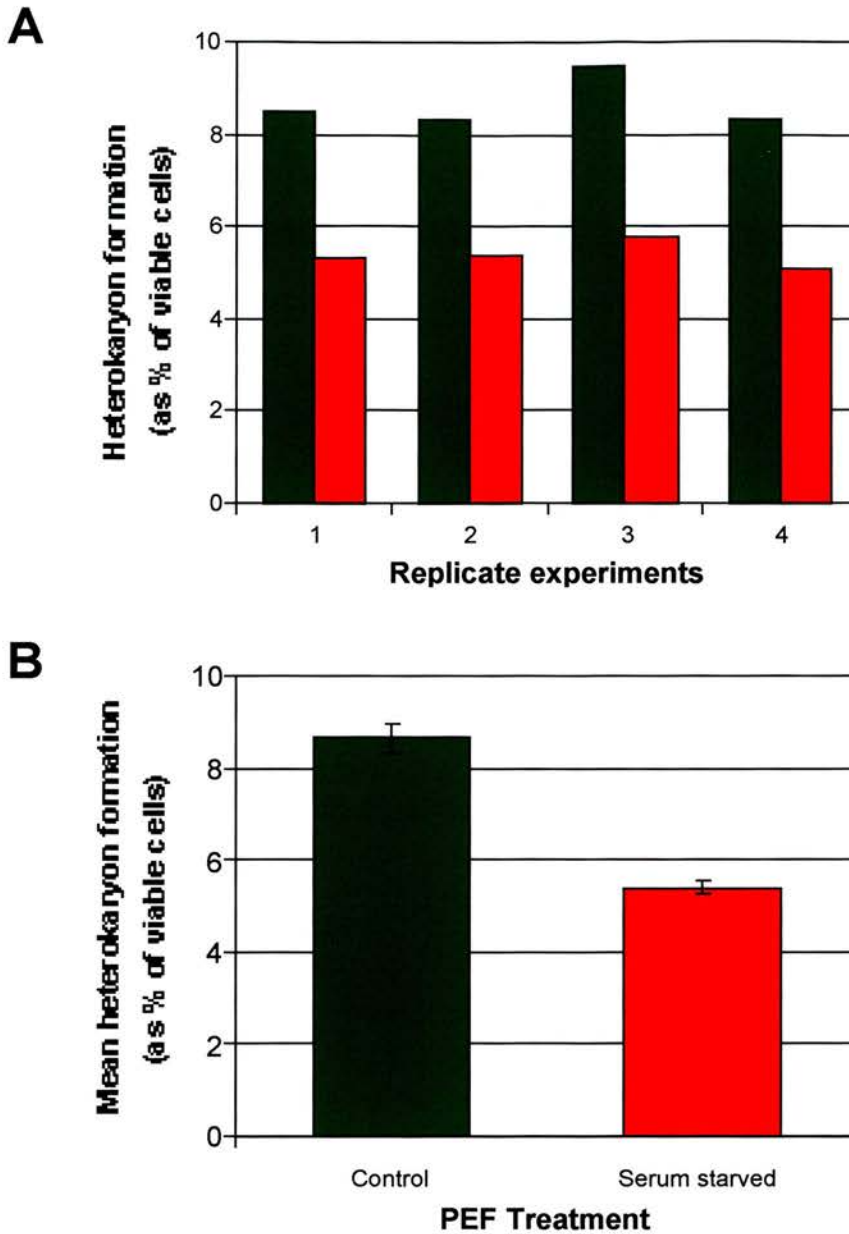


**Fig 7.9 Serum starving fibroblasts decreases heterokaryon formation**

$10^7$  HM-1<sup>puro</sup> cells were mixed with the same number of either control or serum starved fibroblasts and electropulsed using standard murine electrofusion conditions. Columns are colour coded to denote whether control (■) or serum starved (■) fibroblasts had been used in each fusion. **Panel A** Heterokaryon formation (as percentage of viable cells) measured by 2-dye FACS analysis (Section [12.2] for four replicate experiments. **Panel B** Mean heterokaryon formation ( $\pm$  S.E.M) for control and serum starved fusions as calculated from four replicate experiments.

### [7.3.4] Serum starvation of fibroblasts increases nuclear reprogramming

Fusions with serum starved fibroblasts had higher phenotypic ES hybridization frequencies than controls ( $P < 0.05$  as calculated by the Student's paired t-test (2 tailed) [Caria 2002]). On average, the hybridisation frequencies (hybrid / heterokaryon) were  $53 \pm 11$  fold higher than controls [Fig 7.10].

This result is consistent with observations that quiescence render nuclei more amenable to being reprogrammed [Campbell 1999]. Campbell assumed that the characteristic of serum starved cells that made their nuclei easier to reprogram was related to the cells being quiescent. However serum starvation has a much broader affect on cells that just affecting their cell cycle.

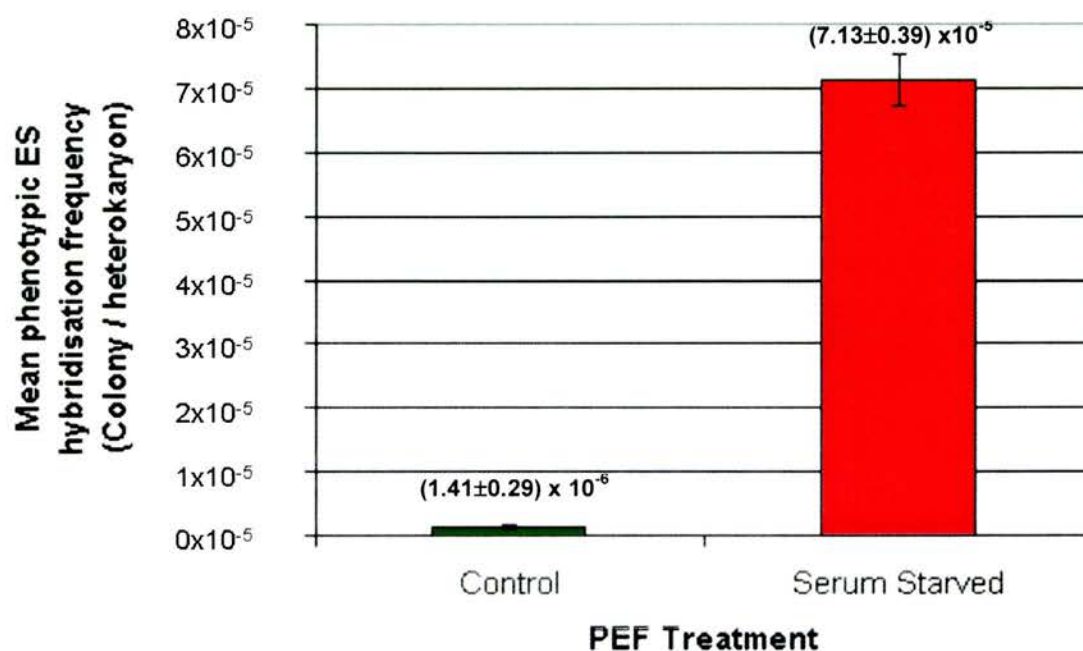


**Fig 7.10 Serum starvation increases reprogramming of fibroblast nuclei in cell hybrids**

Four replicate experiments electrofused HM-1<sup>Puro</sup> cells to either control or serum starved fibroblasts. Experiments generated data on hybrid yield, viable heterokaryon formation and cell viability. These data were used to calculate ES phenotypic hybridisation frequencies as described in Section [2.2.6]. The graph shows mean phenotypic ES hybridisation frequencies and associated error for both treatments as calculated from four replicate experiments.



### [7.3.5] Serum starvation of fibroblasts strongly induces expression of Hsp72

**Fig 7.11** shows the serum starved PEFs show high levels of Hsp72, indicating the cells are undergoing a stress response. This result illustrates that there are serum starvation does a lot more to the cell than just render it quiescent. It was decided to investigate whether quiescence was the characteristic of cells that made their nuclei easier to reprogram. An experiment was designed where serum starved fibroblasts were reintroduced to normal serum levels. If Campbell's hypothesis is correct, then one would expect that the nuclei of reactivated PEFs would be more difficult to reprogram as they will have re-entered the cell cycle. This experiment is discussed in the next subsection.

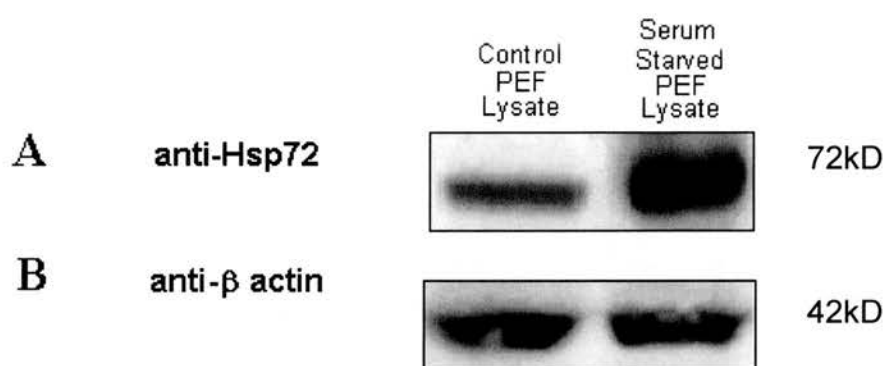


**Fig 7.11 Serum starvation induces expression of Hsp72**

Whole cell lysates were generated from ES cell populations displaying four different ranges of confluence. 150  $\mu$ g protein of lysate generated from control or serum starved PEFs was loaded onto a polyacrylamide gel, run, transferred and probed with anti-Hsp72 as described in **Subsection [2.7.3]**. *Panel A* Western blot probed with anti-Hsp72. The control was the antibody manufacturer control lysate, a heat shocked Hela cell lysate. More Hsp72 expression was found in the serum starved lysate. *Panel B* The same plot was reprobed with anti- $\beta$ -actin to confirm the same amount of protein lysate had been added to each lane.

It is also interesting that here and in Chapter 6 where there are significant increases in nuclear reprogramming, that there are also corresponding inductions of hsp72. Perhaps some aspect of the stress response is facilitating reprogramming. In Chapter 5, the effect of stressing the cells was investigated. Heat shocking thymocytes at 42°C for 10 minutes induced a moderate rise of Hsp72 expression over control levels [**Fig 5.1**] but as it is unknown whether the incidence of nuclear reprogramming was increased (due to increased cell fusion and insufficient

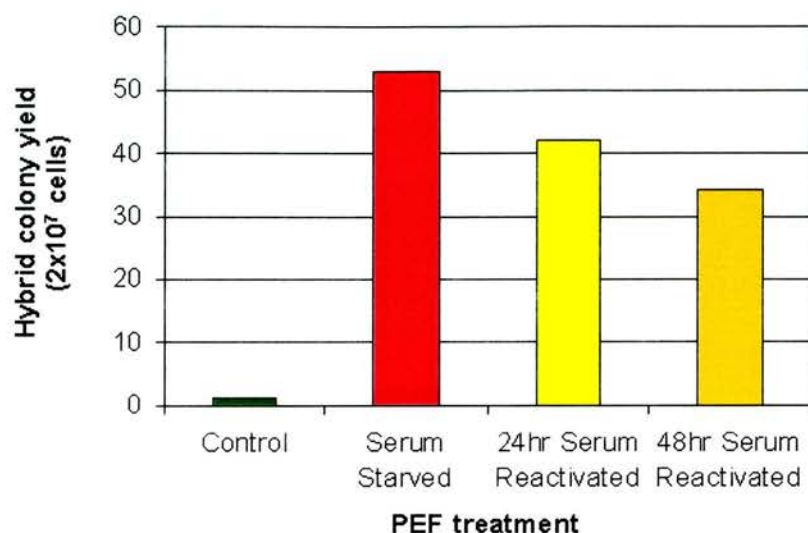


replication of the experiment) these heat shock data cannot be used to either support or refute this stress response hypothesis.

#### **[7.4.6] Hybrid colony yields remain elevated after serum reactivation**

Within 24 hours after normal serum were reintroduced, previously starved fibroblast populations began to proliferate (**Fig 7.1**). Soluble PCNA expression level rapidly increased to that consistent with the control fibroblasts (**Fig 7.2**). If quiescence is the characteristic making serum starved PEFs more amenable to being reprogrammed, one would expect the hybrid colony yield to decrease when serum reactivated PEFs are used for fusions. Surprisingly however this was not the case in the pilot experiment ( $n = 1$ ) (**Fig 7.12**).

**Fig 7.12** shows that hybrid colony yield does not decrease to control levels when serum reactivated PEFs are used in fusions. **Figs 7.1-7.4** highlight that these cells are no longer quiescent. Reactivated PEFs were observed to reinitiate proliferation when looked at down the microscope. If time had permitted, the Hsp72 level in serum reactivated PEFs would have been measured to see if there was a correlation between elevated hybridisation frequency (hybrid / heterokaryon) and Hsp72 levels. Previous work in rodent fibroblasts has show that Hsp70 levels remain high for 36 hours and more [Li & Werb 1982].

**A****B**

Cells electropulsed	Hybrid colony yield (1.6x10 <sup>7</sup> cells), 1xHAT & 2.5μg/ml puromycin
HM1 <sup>puro</sup> cells & control PEFs	1
HM1 <sup>puro</sup> cells & serum starved PEFs	53
HM1 <sup>puro</sup> cells & 24hr serum reactivated PEFs	42
HM1 <sup>puro</sup> cells & 48hr serum reactivated PEFs	34

**Fig 7.12 Hybrid colony yield remains elevated after serum reactivation**

In addition to a standard control and serum starvation fusions,  $1 \times 10^7$  HM-1<sup>puro</sup> cells (Passage 22) were also fused with serum starved  $1 \times 10^7$  PEFs (Passage 3) that had been reintroduced to normal serum conditions for either 24 or 48hr prior to being fused. PEFs to be serum reactivated were seeded at lower plating densities than normal (10,000 cells/cm<sup>2</sup> for 24hr reactivation and 7,500 cells/cm<sup>2</sup> for 48hr reactivation) so that any affect of serum reactivation could not be attributed to differences in PEF confluence. These plating efficiencies resulted in serum reactivated PEF populations with comparable levels of confluence to the control and serum starved PEF populations prior to disaggregation and electropulsing. **Panel A** shows a graph of hybrid colony yield versus PEF treatment. **Panel B** shows the same data in tabular form. This experiment was unable to be replicated (n=1) due to time restrictions.

## [7.4] Conclusions

Serum starvation of primary embryonic fibroblasts resulted in several changes: a cessation in proliferation; a decrease in PCNA expression, a loss of fusiform morphology; and a change in the proportion of cells at different stages of the cell cycle. Reintroduction of normal serum levels to such cells reversed these changes. These results show that serum starvation renders PEFs quiescent.

Fusions using serum starved fibroblasts yielded on average 35 fold more hybrid colonies than similar fusions using control fibroblasts ( $52.3 \pm 4.0$  versus  $1.5 \pm 0.5$ ). Serum starvation caused decreases in both the viability of electropulsed cells and viable heterokaryon formation. Experiments using serum starved fibroblasts displayed hybridisation frequencies (hybrid / heterokaryon) on average  $53 \pm 11$  fold higher than in controls. This indicates that serum starvation of primary embryonic fibroblasts affects nuclear reprogramming in the murine hybrid system.

Serum starvation induced a stress response in primary embryonic fibroblasts as shown by the strong induction of inducible heat shock protein, Hsp72.

A single experiment using serum reactivated fibroblasts showed that the hybrid colony yield remained elevated even after the cells had re-entered the cell cycle. If reproducible, this experiment would suggest that a characteristic of serum starved fibroblasts other than quiescence, is facilitating nuclear reprogramming.

## [8] The effect of *Xenopus* nucleoplasmin expression on the murine cell hybrid system

### [8.1] Introduction

The aims of this chapter are two fold: (a) to investigate the effect of expressing the *Xenopus* molecular chaperone, nucleoplasmin, on nuclear reprogramming in the murine hybrid system and (b) to generate a lab resource pTetNPM, an expression plasmid into which different transgenes could be easily introduced and controllably expressed. This introduction deals first with the evidence suggesting nucleoplasmin might affect nuclear reprogramming. Then in order to clarify how pTetNPM may be used to transiently induce the expression of *Xenopus* nucleoplasmin and other 'exchanged' transgenes, the Tet-On expression system, and Cre mediated cassette exchange are described.

#### [8.1.1] *Xenopus* nucleoplasmin and reprogramming

The factors involved in a nucleus's reacquisition of developmental potential are unknown. Development of the mouse cell hybrid system, as a model for nuclear reprogramming, provided the opportunity to attempt to identify such factors. Global changes in gene expression, which occur during nuclear reprogramming are associated with major structural changes of chromatin [as reviewed by Wolffe (1996)].

The *Xenopus* nuclear chaperone nucleoplasmin [**Subsection 1.10.1.1**] plays a part in altering chromosome structure [Laskey *et al.* 1978]. Dilworth *et al.* 1987 have shown that *Xenopus* nucleoplasmin, which is expressed in extremely high levels in *Xenopus* oocytes (it comprises 9-10% of all cellular protein), induces changes in the chromosome structure in *Xenopus* erythrocyte nuclei. Dimitrov & Wolffe (1996) found that nucleoplasmin directs the specific removal of somatic linker histones from chromatin. Linker histone exchange from embryonic to somatic histone subtypes is a

common developmental feature (Linker histone exchange is discussed in **Subsection [1.10.3]**).

Although genes with sequences very similar to *Xenopus* nucleoplasmin have been cloned in mouse [Lange et al. 2003], rat [Szebeni et al 2003] and human [Chan et al. 1989][McArthur & Shackelford 1997], it has never been shown that such genes produce proteins which interact with chromatin. Hence *Xenopus* nucleoplasmin and not a related mammalian gene was chosen for these experiments.

Although it was assumed as this work was being done, it has since been shown that nuclei of mammalian somatic cells (specifically adult mouse thymocytes and adult human blood lymphocytes) are reprogrammed when injected into *Xenopus* oocytes. These mammalian nuclei ceased expressing differentiation markers and began to strongly express the pluripotent cell marker Oct-4 [Byrne et al. 2003] (*Oct-4* is discussed in **Section [1.6]**). This showed that factors in *Xenopus* ooplasm have the capacity to reprogram *Oct-4* promoter. The work carried out in this chapter sought to test the hypothesis that *Xenopus* nucleoplasmin was the one of the key factors involved in such reprogramming.

It was hypothesised that the removal of somatic linker histones from somatic chromatin would facilitate the reprogramming of the somatic nucleus when fused to an ES cell. The hypothesis is based on at least three assumptions:

- (1) *Xenopus* nucleoplasmin could perform somatic linker histone stripping in the murine cell hybrid system.
- (2) As a result of somatic histone removal, embryonic linker histones would have a greater access to chromatin.
- (3) Incorporation of embryonic linker histones into the chromatin would facilitate reprogramming.

### **[8.1.2] Tet-On system for inducible transgene expression**

The Tet-On system was developed to permit the conditional activation of a transgene [Gossen et al. 1995]. It is based on the tetracycline resistance operon 'tet' from *E. coli* transposon Tn10 [Gossen et al. 1992][Furth et al. 1994]. This system is a particularly good system for conditional transgene expression in animal cells. The

Tet-On system comprises a reverse transactivator protein (rtTA) which is a regulatory protein composed of a mutant tet repressor fused to the activating domain of viral protein VP16 of herpes simplex virus. Upon activation, transcription is driven from a minimal promoter fused to seven tet operator sequences from Tn10. Transcriptional activation from this promoter is activated by administration of tetracycline to the animal cell and inactivated upon withdrawal of the antibiotic. The activation is caused by the binding of the antibiotic to rtTA. This changes the conformation of this rtTA allowing it to interact with the tet operon. Although initially discovered using tetracycline, it has since been found that a similar antibiotic, doxycycline, activates transcription in this constellation in the same way. This antibiotic is now normally used in Tet-expression systems as it is cheaper and less persistent in cells.

The Tet-On system would be used to inducibly express nucleoplasmin in HM-1 cells. This requires the presence of both the regulatory plasmid pTNG (which constitutively expresses the gene coding for the reverse transactivator) and a response plasmid pTetNPM (which will express *Xenopus* nucleoplasmin in the presence of rtTA and doxycycline) in this cell type. Once this has been accomplished nucleoplasmin would be induced by addition of the antibiotic doxycycline to the system (See **Fig 8.1** overleaf).



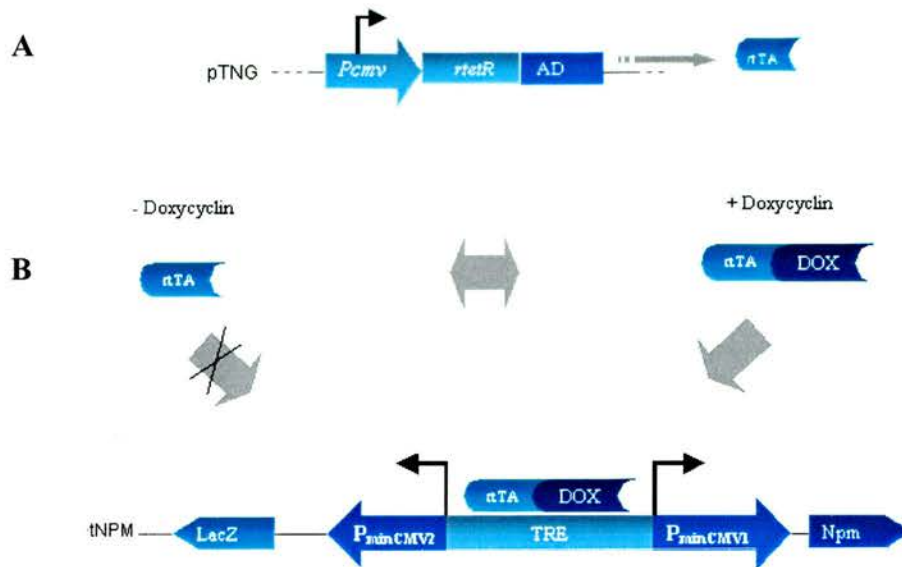


**Fig 8.1 Using the Tet-On system to transiently express *Xenopus* nucleoplasmin transgene and *LacZ* reporter**

**Panel A** Regulatory Plasmid, pTNG (See Fig 8.4 for description of pTNG), codes for reverse transactivator rtTA. The reverse transactivator (rtTA) is a regulatory protein which can only stimulate expression when bound to doxycycline (or indeed tetracycline). **Panel B** Response Plasmid, pTetNPM (See Fig 8.4 for description of pTetNPM). The doxycycline rtTA complex binds the tet response element (TRE) on the response plasmid activating transcription of the nucleoplasmin gene immediately downstream and also the *lacZ* gene immediately upstream.

While not directly used in work outlined in this chapter, RCME requires discussion to clarify how pTetNPM can be used and why introduction of ‘incompatible *loxP* sites’ were incorporated into its design (Fig 12.5).

### [8.1.3] Recombinase-mediated cassette exchange (RMCE)

The successful integration and expression of transgenes in mammalian cells is subject to several technical hurdles being surmounted e.g. the transgene must be incorporated into a site permissive for expression [Clark *et al.* 1994], or integration of multiple copies of a transgene may result in transgene expression being silenced [McBurney *et al.* 2002][Dorer (1997)]. Recombinase-mediated cassette exchange (RMCE) is a useful strategy which allows the introduction of a single copy transgene into a chromosomal locus previously shown to be permissive to transgene expression.

RMCE is dependent on the specific activity of Cre recombinase [Sauer 1993][Mack *et al.* 1992]. Cre recombinase is a bacteriophage P1 derived member of the integrase family of enzymes [Sternberg 1979][Sternberg *et al.* 1986], indeed Cre is an acronym for “causes recombination”. The enzyme mediates precise site-specific recombination between short DNA sequences called *loxP* sites. The structure and sequence of *loxP* sites is outlined in **Fig 8.2** (overleaf).

A *loxP* site consists of two 13bp inverted repeats and a central unique spacer region. The role of the spacer region has been investigated and it has been shown that Cre recombinase can only recombine efficiently *loxP* sites with identical spacer sequences [Lee & Saito 1998], *loxP* sites with different spacer sequences are said to be incompatible *loxP* sites (**Fig 8.2** overleaf).

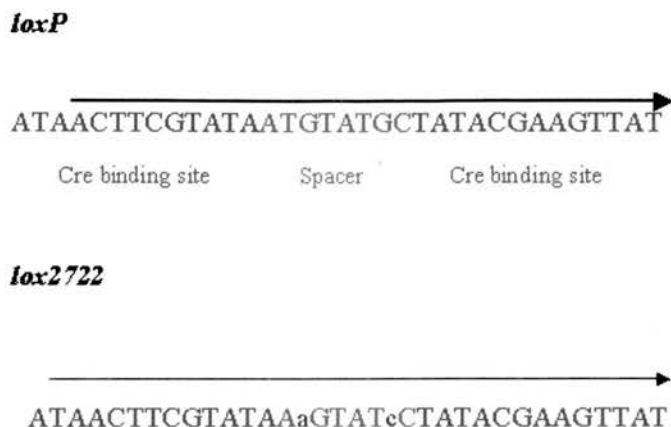


**Fig 8.2 Sequence and structure of incompatible *loxP* sites**

All *loxP* sites are 34-bp double stranded DNA fragments containing two Cre binding sites (blue) flanking a spacer sequence (red). The spacer region sequence of a *loxP* site affects its compatibility with other *loxP* sites i.e. *loxP* sites with different mutations within the spacer sequence cannot be recombined by Cre activity. In work done described in this chapter, wild type *loxP* sites and *lox2722* sites (so called incompatible *loxP* sites) were used to prevent Cre activity resulting in inversions of an integrated cassette or the integration of an exchanged cassette in the wrong orientation. The mutations to the *lox2722* spacer sequence are denoted by green lower case letters.

Cleavage and strand exchange of recombining compatible *loxP* sites occurs within the spacer region of the sites. *loxP* sites have a directionality due to the asymmetry of the spacer sequence [Hoess & Abremski 1984]. The directionality of *loxP* sites affects the result of Cre mediated recombination: recombination between two directly repeated compatible *loxP* sites results in excision of the intervening DNA sequence. Cre-mediated recombination between pairs of compatible *loxP* sites that have an opposite orientation results in inversion of the intervening DNA rather than excision.

The possibility of Cre-mediated recombination with an endogenous eukaryotic sequence is minute due to the length of the *loxP* sequence and specificity of the Cre recombinase [Kilbey *et al.* 1993]. However, recombinase recognition sites have been identified in mouse and human genomes and these “pseudo-*loxP* sites” complicate matters *in vitro* [Thyagarajan *et al.* 2000] and *in vivo* [Schmidt *et al.*

2000]. Only two reports of such “illegitimate Cre recombination” have been published however while many papers report successful application of the system. One way of minimising illegitimate recombination is by removing the recombinase from the system after the desired recombination event has occurred [Bunting *et al.* 1999].

The action of Cre recombinase at *loxP* sites represents a valuable tool for manipulating the mammalian genome. Several transgenic strategies such as integrated transgene excision and inversion have proved very efficient using this system [Metzger and Feil 1999]. Furthermore, Cre also has the advantage of not requiring any other cofactors to carry out recombination, unlike other members of the integrase family.

The RMCE system was to be used when pTetNPM has been stably transfected into mES cells and integrated at a site permissive for transgene expression. It would allow exchange of cassettes between an integrated site on the genome and episomal DNA. The nucleoplasmin cassette will be exchanged with other cassettes containing transgenes of interest. This strategy is outlined in **Fig 8.3** (overleaf).

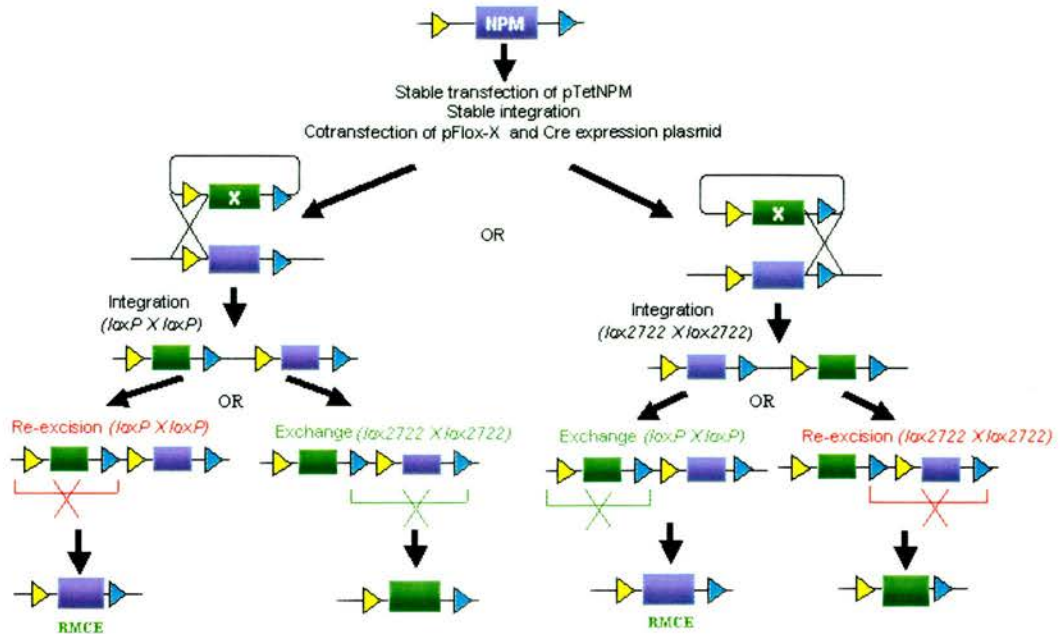


**Fig 8.3 Use of recombinase-mediated cassette exchange (RMCE) to insert other genes besides nucleoplasmin into a site permissible for Tet inducible transgene expression**

When pTetNPM is stably integrated into mES cells at a site permissible for transgene expression, RMCE would be used to exchange the nucleoplasmin cassette for other cassette. Using this strategy, the nucleoplasmin cassette (purple rectangle) located on the chromosome would be exchanged for any cassette X (green rectangle) present on a plasmid. Both genes are flanked by wild type and mutated *loxP* sites [*loxP* (yellow triangle) and *lox2722* (blue triangle) respectively]. Use of incompatible *loxP* site prevents chopping of the nucleoplasmin cassette out altogether when Cre is activated. Several possible products of Cre recombination can be generated. High concentrations of plasmid DNA should be added to the cells to alter the reaction equilibrium such that transgene exchange becomes a more probable outcome of the reaction. The exchange of the X cassette for the nucleoplasmin cassette may occur via two different series of reactions. Ideally, the X cassette would contain a selectable marker so that cells in which the RMCE has taken place can be isolated. This figure was modified from Bouhassira *et al.* (1997).

## [8.2] Objectives

- 1) To investigate the role of *Xenopus* nucleoplasmin on the murine cell hybrid system.
- 2) To build pTetNPM, an inducible expression vector into which transgenes could be easily inserted and controllably expressed.



## **[8.3] Results and discussion**

### **[8.3.1] Expression strategies for investigating the effect of nucleoplasmin on nuclear reprogramming**

Two expression vectors, pSV40NPM and pTetNPM, were built to study the effect of *Xenopus* nucleoplasmin on nuclear reprogramming. pSV40NPM was constructed, as shown in **Fig 12.4**, by cloning a nucleoplasmin cassette into constitutive expression vector pTracerSV40 (described in **Subsection [2.5.3]**). pTetNPM was constructed, as shown in **Fig 12.5**, by cloning a floxed nucleoplasmin cassette into the inducible expression vector pBI-G (described in **Subsection [2.5.3]**).

The two plasmids constructed, in addition to pTNG (the Tet-On response plasmid), are described in **Fig 8.4**. Using these three plasmids, two strategies for expressing nucleoplasmin in the hybrid system would be investigated. The first strategy would constitutively express nucleoplasmin using pSV40NPM. As *Xenopus* nucleoplasmin affects lower chromatin structure [Dimitrov & Wolffe 1996], it was suspected that cells would be sensitive to constitutive high levels of nucleoplasmin expression. A second more complicated strategy which allowed transient expression of nucleoplasmin at different levels was also developed as a backup in case constitutive expression was toxic to the cells. The principle steps in both the 'constitutive' and 'inducible' expression strategies are shown in **Fig 8.5**.



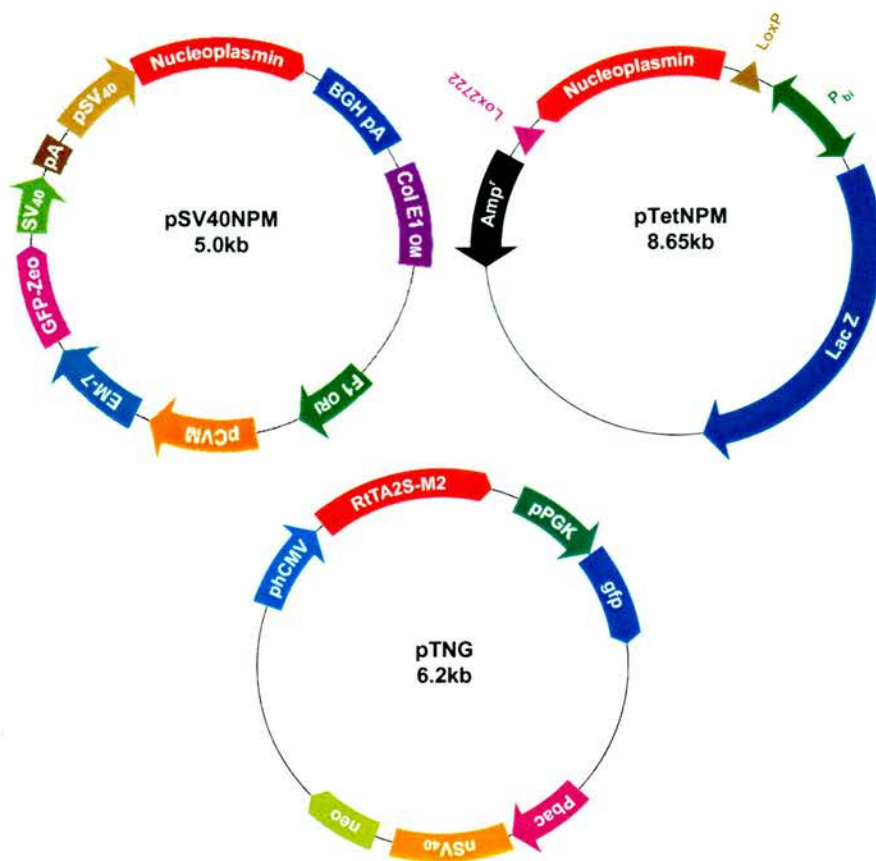


**Fig 8.4 Description of plasmids pSV40NPM, pTNG and pTetNPM**

**pSV40NPM** is an expression vector used to study the constitutive expression of nucleoplasmin. pSV40NPM contains the viral pSV40 promoter driving the constitutive expression of the nucleoplasmin gene. It also contains a constitutively expressed GFP/Zeocin fusion cassette that allows pSV40NPM cells to be identified by GFP fluorescence and selected for with antibiotic zeocin.

**pTetNPM** is a Tet-inducible response plasmid, with a bi-directional promoter (P<sub>bi</sub>) driving a reporter gene (*LacZ*) and a floxed nucleoplasmin cassette. This construct was primarily developed as a resource for inducible transgene expression within the research group: once the plasmid is stably transfected into cells, single copy transgenes could be integrated into sites permissive for transgene expression via recombinase-mediated cassette exchange and expression of these genes could be induced with doxycycline. With regards to work described in this thesis however, pTetNPM would be used to overexpress one particular transgene coding for the nuclear chaperone, nucleoplasmin, in order to investigate its effect on nuclear reprogramming.

**pTNG** is a regulatory plasmid used to produce the reverse transactivator, a necessary regulator protein required for tetracycline induced transgene expression (See **Fig 8.1**). The plasmid contains the reverse transactivator gene constitutively driven by a modified viral promoter (phCMV). pTNG also contains a constitutively expressing GFP cassette. TNG-8, a HM-1 subclone stably transfected with this plasmid and which strongly expressing the rtTA gene, was acquired from Dr. Edward Gallagher.

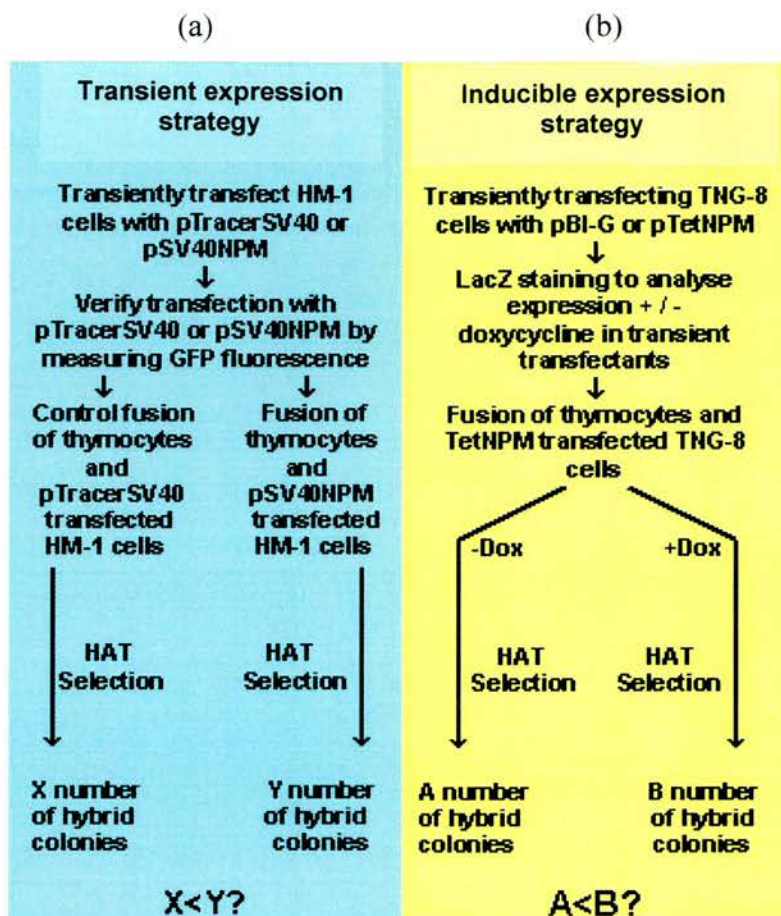


**Fig 8.5 Strategies for *Xenopus* nucleoplasmin expression in the mouse hybrid system**

In the first strategy, the effect of constitutive nucleoplasmin expression is investigated. **(a)** HM-1 cells were transiently transfected with either pTracerSV40 or pSV40NPM (pTracerSV40 with an integrated nucleoplasmin cassette). Transfection is verified by measuring GFP expression. The two transfected populations are placed in selection for reprogrammed hybrid cells after 24 hours. **(b)** In the second strategy, the effect of inducible NPM expression was investigated. TNG-8 cells (HM-1 cells constitutively expressing the reverse transactivator) are transfected with pTetNPM (pBI-G with an integrated floxed nucleoplasmin cassette). *LacZ* staining of a portion of these cells is carried out to confirm that the bi-directional promoter was activated in response to doxycycline addition. Populations of such cells exposed to different concentrations of doxycycline were then fused to thymocytes.

### [8.3.2] Constitutive expression of *Xenopus* nucleoplasmin affects HM-1 cell viability

HM-1 cells were lipofected with pTracerSV40 and pSV40NPM to assess the effects of transient nucleoplasmin expression on HM-1 cells. Both pTracerSV40 and pSV40NPM both contained the same independently expressing GFP cassette allowing the assessment of transfection efficiencies using the two plasmids. The proportion of cells expressing GFP one day after transfection was analysed by FACS (**Fig 8.6 Panel A**). This verified that transfection efficiencies for transfection using either plasmid were similar.

The cell viabilities of transfected and untransfected HM-1 wells were assessed every twenty four hours for four days after transfection. Cell viabilities of transfected wells were expressed as a percentage of those in untransfected control wells. **Fig 8.6 Panel B** shows after 48 hours, pSV40NPM transfected wells displayed significantly higher levels of cell death than in either pTracerSV40 transfected or untransfected wells. This indicates that transient nucleoplasmin expression is toxic to HM-1 cells. 96 hours after transfection, pTracerSV40 transfected wells contained  $80.4 \pm 6.2\%$  the number of viable cells present in untransfected wells whereas pSV40NPM wells contained only  $18.4 \pm 2.1\%$ . Furthermore, the number of viable GFP expressing cells decreased more rapidly in pSV40NPM wells than in the pTracerSV40 wells (**Fig 8.6 Panel C**). 48 hr after transfection for example,  $40.2 \pm 1.1\%$  of viable cells expressed GFP in pTracerSV40 transfected wells whereas only  $17.1 \pm 0.8\%$ . Taken together, these data indicate that the level of nucleoplasmin expression is toxic to HM-1 cells. **Fig 8.6 Panel D** shows an image of wells Giemsa stained 96 hours after transfection. Almost all the cells in the pSV40NPM wells have died in contrast to untransfected and pTracerSV40 transfected wells where cells had not.

These data are consistent with the hypothesis that *Xenopus* nucleoplasmin will interact with murine chromatin and mediate linker histone exchange but may also arise as a consequence of non-specific toxicity. It was probable that the system would be sensitive to strength and duration of nucleoplasmin expression. The inducible expression strategy was now pursued.



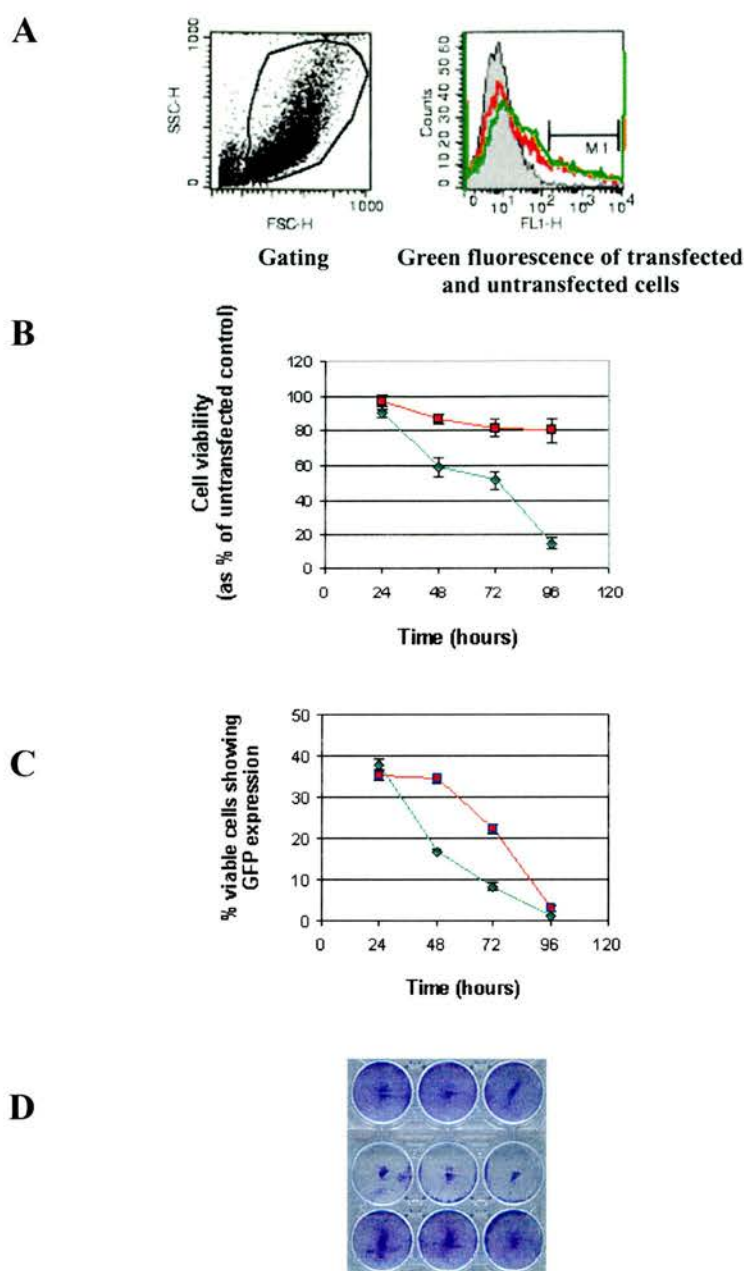


**Fig 8.6 Constitutive expression of *Xenopus* nucleoplasmin affects HM-1 viability within 48 hours after transfection**

**Panel A** (i) Histogram showing gating of viable cells (ii) Histogram showing overlaid green fluorescence spectra for untransfected (—), pTracerSV40 transfected (—) and pSV40NPM transfected HM-1 cells (—). Gating of viable cells expressing GFP is shown (M1). **Panel B** Graph showing cell viabilities (as percentage of viable cell number in untransfected controls) for both pSV40NPM (—◆—) and pTracerSV40 (—■—) transfected cells at different time points after transfection. **Panel C** Graph showing percentages of viable cells expressing GFP for both pSV40NPM (—◆—) and pTracerSV40 (—■—) transfected cells at different time points after transfection. (iii) **Panel D** 96 hours after transfection the wells were Giemsa stained. The top row are untransfected control wells, the middle row are pSV40NPM transfected wells and the bottom row are pTracerSV40 transfected wells. This data is from one representative experiment carried out in duplicate.

### [8.3.3] Transient nucleoplasmin expression affects the viability of TNG-8 cells and decreases a decrease in hybrid colony yield

Data described in this section come from an experiment where TNG-8 cells were transfected on Day 0, exposed to either 0, 10 or 100 nM doxycycline for 1 hour on day 1, and either assessed for cell viability or fused to thymocytes on day 2. TNG-8 cells used for lacZ staining [Fig 8.6], cell viability assessment [Fig 8.7] cells and fusions [Table 8.1] came from the same transfection experiment.

TNG-8 cells transfected with either pBI-G or pTetNPM and exposed to two concentrations of doxycycline (10 or 100nM) for one hour were stained for *LacZ* expression 24hours after doxycyclin exposure as described in Subsection [2.4.3].

As Fig 8.7 shows,

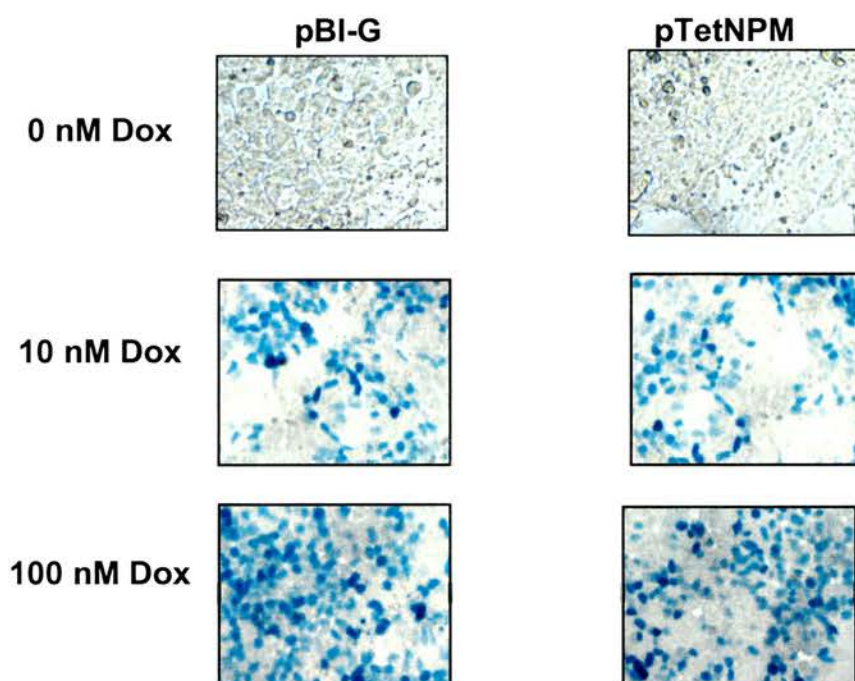


**Fig 8.7 Exposure of transfected TNG-8 cells to doxycycline induced expression of  $\beta$ -galactosidase**

TNG-8 cells were lipofected with either pBI-G or pTetNPM as described in Subsection [2.1.2.1]. Twenty four hours after transfection transfected and untransfected cells were incubated in the presence or absence of doxycycline for 1 hr. Twenty four hours after doxycycline exposure cells were fixed, permeabilised and *LacZ* stained as described in Subsection [2.4.5].

similar proportions of positively stained cells were found in pBI-G and pTetNPM transfected wells that had been exposed to similar concentrations of doxycycline indicating that pBI-G and pTetNPM transfections had similar transfection efficiencies indicating that there was no toxic effect of nucleoplasmin in the first 24 hour period. It also showed that doxycycline exposure activates transcription from the bidirectional promoters of pBI-G and pTetNPM. Cells exposed to 100nM doxycycline concentrations displayed stronger staining intensity than those exposed to 10nM concentrations. Control wells where TNG-8 cells transfected with either pBI-G or pTetNPM but had not been exposed to doxycycline showed no detectable *lacZ* staining [Fig 8.7]. This indicates a dose dependent relationship between doxycycline and transcription from the bi-directional promoter.

The effect of transfection and doxycycline exposure on cell viability was assessed for cells exposed to 10 nM concentrations of doxycycline. Fig 8.8 (overleaf) shows TNG-8 cells transiently transfected with either pBI-G or pTetNPM (hereafter called TNG-8<sup>pBI-G</sup> and TNG-8<sup>pTetNPM</sup> cells respectively) that were exposed for one hour to 10 $\mu$ M doxycycline 24 hours prior to staining. Cell viability was expressed as a percentage of untransfected TNG-8 cells exposed to 10 $\mu$ M doxycycline for 1 hour. The graph shows that TNG-8<sup>pTetNPM</sup> cell viability decreased more rapidly than the pBI-G transfected controls indicating that transient expression of nucleoplasmin at this level was toxic to TNG-8 cells.



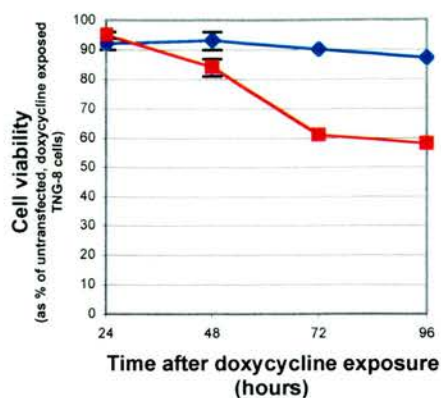


**Fig 8.8 TNG-8 cell viability is affected by nucleoplasmin expression induced by exposing the cells to 0.1 $\mu$ M doxycycline for 1 hour**

Wells containing TNG-8, TNG-8<sup>pBI-G</sup> and TNG-8<sup>pTetNPM</sup> cells were incubated with 10nM doxycycline for 1 hr. The proportions of viable cells in replicate wells were assessed at four time points after doxycycline exposure (24, 48, 72, 96 hr) using Forward Scatter / Side Scatter FACS analysis as described in **Section [12.3]**. Cell viabilities of pBI-G ( $\blacklozenge$ ) and pTetNPM ( $\blacksquare$ ) transfected wells were expressed as percentages of those measured in untransfected control wells. Error bars show associated standard error of the mean cell viability calculated for each well.

Before cell viabilities were assessed, TNG-8 cells from the same transfection experiment were fused to thymocytes under standard murine electrofusion conditions and placed in selection for hybrids. The hybrid colony yields for these fusions are shown in **Table 8.1**. TNG-8 cells not exposed to doxycycline generated the approximate number of colonies seen in standard HM-1 x thymocyte fusions. Exposure to 10 or 100nM doxycycline did not significantly decrease hybrid colony yield from fusions with these cells, nor fusions using TNG-8<sup>pBI-G</sup> cells.

In fusions using TNG-8<sup>pTetNPM</sup> cells, no decrease in hybrid yield was observed in the absence of doxycycline exposure. If however the cells were exposed to either 10nM or 100nM concentrations of doxycycline, there was a >40% decrease in hybrid colony yield. This result may be explained by fusion products dying due to too high a level of nucleoplasmin expression being induced. Due to time constraints, other similar experiments exposing cells to lower concentrations of doxycycline were not carried out.

Cells	[Doxycycline]	Hybrid colony yield ( $4.8 \times 10^7$ cells), 1xHAT
$1 \times 10^7$ TNG-8 cells & $5 \times 10^7$ thymocytes	0nM	98
$1 \times 10^7$ TNG-8 cells & $5 \times 10^7$ thymocytes	10nM	93
$1 \times 10^7$ TNG-8 cells & $5 \times 10^7$ thymocytes	100nM	96
$1 \times 10^7$ TNG-8 <sup>pBI-G</sup> cells & $5 \times 10^7$ thymocytes	0nM	102
$1 \times 10^7$ TNG-8 <sup>pBI-G</sup> cells & $5 \times 10^7$ thymocytes	10nM	94
$1 \times 10^7$ TNG-8 <sup>pBI-G</sup> cells & $5 \times 10^7$ thymocytes	100nM	96
$1 \times 10^7$ TNG-8 <sup>pTetNPM</sup> cells & $5 \times 10^7$ thymocytes	0nM	94
$1 \times 10^7$ TNG-8 <sup>pTetNPM</sup> cells & $5 \times 10^7$ thymocytes	10nM	41
$1 \times 10^7$ TNG-8 <sup>pTetNPM</sup> cells & $5 \times 10^7$ thymocytes	100nM	45

**Table 8.1 Transient nucleoplasmin expression in ES cells prior to fusion with murine thymocytes decreased hybrid colony yield**

TNG-8 cells (untransfected and transfected with either pBI-G or pTetNPM) were exposed to three different concentration of doxycycline (0, 10, 100nM). 24 hr after exposure,  $1 \times 10^7$  cell aliquots were fused with  $5 \times 10^7$  CBA thymocytes according to standard murine electrofusion conditions. Cells were placed in selection 48hr after fusion and left for 12 days before colonies were counted.

## [8.4] Conclusion

A lab resource, pTetNPM, was generated. This expression vector allowed controllable transgene expression using the Tet-On expression system and was used to transiently express *Xenopus* nucleoplasmin in the murine cell hybrid system. The nucleoplasmin coding sequence was flanked with incompatible *loxP* sites so, when stably integrated into cells at a site permissive for transgene expression, different cassettes can be inserted using RMCE.

Transient transfection of HM-1 cells with pSV40NPM, which constitutively expressed nucleoplasmin in the cells, caused significant cell death after 48 hours, and after 96 hours, nearly all the transfected cells were dead.

TNG-8 cells were transiently transfected with either pBI-G or pTetNPM and after 24 hours were exposed to either 0, 10 or 100 nanomolar concentrations of doxycyclin. *LacZ* staining showed a dose dependent relationship between transcription from the bi-directional promoters of pBI-G and pTetNPM.

In the wells containing TNG-8<sup>pTetNPM</sup> cells that had been exposed to 10 nM doxycycline, decreased cell viability was observed. This did not occur on pBI-G transfected or untransfected control wells. This indicates nucleoplasmin was toxic to the TNG cells at the induced levels of expression.

Fusions using TNG-8<sup>pTetNPM</sup> cells exposed to doxycycline showed decreased hybrid colony yields compared to doxycycline exposed TNG-8<sup>pBI-G</sup> or non-doxycycline exposed TNG-8<sup>pTetNPM</sup> controls. The most probable explanation is that levels of nucleoplasmin induced in TNG-8 cells exposed to either 10nM or 100nM concentrations of doxycycline are killing hybrid cells. Future experiments should use lower doxycycline concentrations or shorter doxycycline exposure times to stimulate nucleoplasmin expression.

## [9] Attempts to generate cell hybrids from human ES and EC cells

### [9.1] Introduction

The ultimate goal of scientists studying nuclear reprogramming is to restore a human ES cell phenotype to a human adult differentiated cell. Such a reprogrammed cell could be multiplied and differentiated into human cells required for biological and therapeutic purposes, see **Fig 1.1**.

The aim of this chapter is to develop a system in which the nuclear reprogramming activities of human ES and EC cells could be assessed and factors affecting successful reprogramming could be identified. This would be done in a manner similar to the murine work discussed earlier in this thesis *i.e.* via whole cell hybridisation between selectable cell lines.

Work described in this chapter initially used human EC cells, but when human ES cells became available, these were then subsequently used for two reasons:

- (i) it was assumed that ES cells would be a better model for studying reprogramming as they should be untransformed and karyotypically normal.
- (ii) Unlike hEC cells [Duran *et al.* 2001][Tageki *et al.* 1983], no work had been published investigating whether human ES cells can reprogram somatic cells like their murine counterparts.

## [9.2] Objectives

- 1) To generate cell hybrids from human ES or EC cell fusions
- 2) To optimise conditions for the generation of cell hybrids from human ES cells

## [9.3] Results and discussion

### [9.3.1] Development of selection regimes to isolate human cell hybrids

In order to carry out hybridisation experiments, selection for cell hybrids derived from heterokaryons had to be developed for human cells as had previously been done for murine cells (**Subsection [3.3.1]**). Several selectable cell lines were generated:

#### **HPRT deficient hEC subclones**

6-thioguanine (6-TG) selection was used to attempt generation of HAT sensitive (*HPRT* deficient) hEC clones (**Subsection [2.2.4]** discusses 6-TG & HAT selection and the *HPRT* gene). Three experiments where progressively greater numbers of NTERA-2 cells ( $1 \times 10^8$ ,  $5 \times 10^8$  and  $1 \times 10^9$ ) were placed in 6-TG selection ( $5 \mu\text{g} / \text{ml}$  for 2 weeks) failed to generate resistant colonies. This was surprising as the cells are male and spontaneous mutation rates at the *HPRT* locus were expected to be higher than those seen in mouse ES cells (typically  $1:10^6$ - $10^7$  as in Abuin *et al.* 2000). A similar experiment using  $1 \times 10^9$  NCCIT cells also failed to generate *HPRT* deficient colonies.

It was hypothesised that abnormal duplication of the *HPRT* locus in the hEC cells might be the reason for this failure to isolate *HPRT* deficient clones. Should multiple copies of the *HPRT* gene exist in these cells then the numbers of cells placed in selection would be insufficient to isolate a *HPRT* deficient clone by



spontaneous mutation in in 6-TG selection. FISH analysis with an X-chromosome specific paint was used to probe NTERA-2 mitotic spreads to investigate whether there was abnormal duplication of X-chromosome segments (**Fig 9.1**). In 74% of all spreads probed, abnormal duplication of segments of X-chromosome existed. Consequently, it seems probable that attempts to generate HAT sensitive clones failed due to these isochromosomal replications of *HPRT* containing region of the chromosome. This was also assumed to be the reason for failure of similar experiments using NCCIT cells.

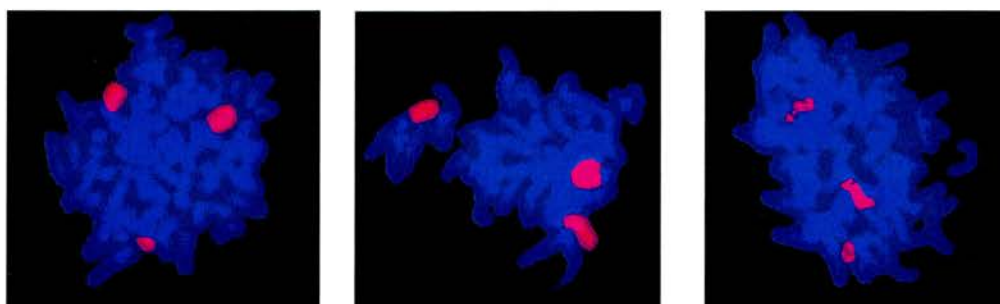


**Fig 9.1 Aneuploid NTERA-2 nuclei frequently have abnormally replicated segments of the X-chromosome**

Fluorescent *in situ* hybridisation (FISH) with a DNA probe for X chromosome (pink) was performed on NTERA-2 metaphase slides as described in **Subsection [2.3.4]**. Slides were counterstained with DAPI (blue). Images show three representative metaphases, where abnormal duplications of segments of the X-chromosome are evident. Of the 50 spreads probed, 37 exhibited such abnormal duplication.

#### **Antibiotic resistant hEC subclones**

Kill curves generated for NTERA-2 cells showed that either 300 $\mu$ g / ml G418 or 3  $\mu$ g / ml puromycin was sufficient to kill all wild type cells (**Fig 9.2 & Fig 9.3** respectively – shown overleaf). Two selectable clones (NTERA-2<sup>neo</sup> and NTERA-2<sup>puro</sup>) were generated by lipofecting cells with either pSV40neo and pPUR (**Subsection [2.1.2.1]** contains details of how of hEC cells were lipofected while **Subsection [2.5.5]** describes these plasmids). Stably transfected clones were selecting in either 300 $\mu$ g / ml G418 (for SV40neo) or 3 $\mu$ g / ml puromycin (for pPur).



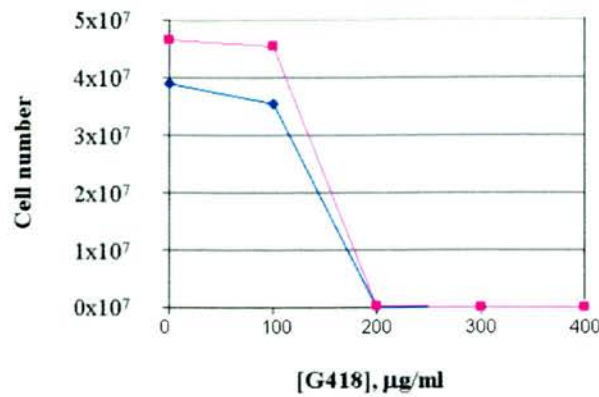


**Fig 9.2 G418 kill curves for NTERA-2 and NCCIT cells**

Gelatinised 10cm plates were seeded with either  $2 \times 10^5$  NTERA-2 or NCCIT cells. Plates were incubated overnight in murine ES medium. After 24 hours, plates were fed murine ES media supplemented with a different concentration of G418 [0, 100, 200, 300 and 400  $\mu\text{g/ml}$ ]. Cells were cultured for an additional 9 days while maintaining the concentration of G418. Cells incubated in both 0 and 100  $\mu\text{g/ml}$  G418 reached confluence during this time and these cells were disaggregated and transferred to larger gelatinised dishes. After 9 days in G418, cells were trypsinised and the number of cells in each plate was counted. Numbers of NTERA-2 cells and NCCIT cells are represented by (■) and (◆) respectively.

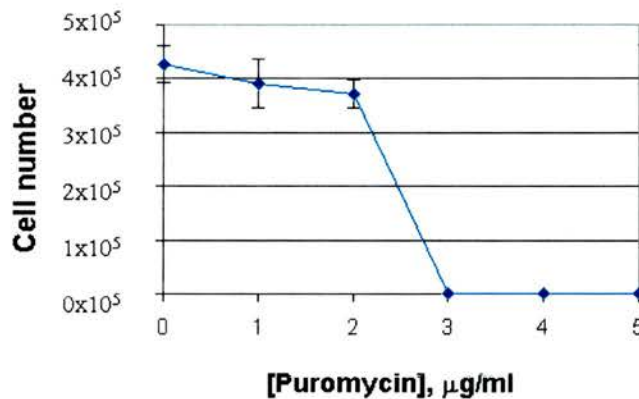


**Fig 9.3 Puromycin kill curve for NTERA-2 cells**

Gelatinised 10cm plates were each seeded with  $2 \times 10^5$  NTERA-2 cells and were incubated in murine ES medium. After 24 hours, plates were divided into groups of three and each group was fed murine ES media supplemented with a different concentration of puromycin antibiotic [0–5  $\mu\text{g/ml}$ ]. Cells were cultured for an additional 9 days while maintaining the concentration of puromycin. Cells incubated in 0  $\mu\text{g/ml}$  puromycin reached confluence during this time and these cells were disaggregated and transferred to larger gelatinised dishes. After 9 days in puromycin, PEFs were trypsinised and the number of cells in each well as counted. The graph shows the mean cell count calculated from each group triplicate plates incubated with a different concentration of puromycin. Error bars represent standard error of the mean cell number.

### **Antibiotic resistant hES lines**

In collaboration with Dr. Alison Thomson a blasticidin selectable hES clone, H1<sup>blast</sup>, was generated by transfecting male hES (H1) cells with pLoxBSD2a, a plasmid with a blasticidin gene driven by a constitutively active promoter [described in **Section 2.1.2.2**]. Several targeted clones were received from Dr. Thomson and these were expanded and placed in 2 µg / ml blasticidin. Dr. Thompson has previously generated a blasticidin kill curve which showed all wild type H1 cells die with this level of selection. Three expanded clones were resistant to blasticidin selection. Controls wells transfected with pLoxBSD2b (a plasmid similar to pLoxBSD2a except for the BSD coding sequence had been inserted in the wrong orientation) died in the blasticidin selection. This confirmed that the expression of the blasticidin transgene had made the cells resistant to the antibiotic.

### **HPRT deficient hES lines**

Again in collaboration with Dr. Alison Thomson, HPRT deficient human ES (H1) cells were generated. Dr. Thomson targeted the *HPRT* locus of H1 cells with an adeno-associated viral vector AAV-Hpe3PN [Hirata *et al.* 2002] and selected for targeted clones. The student expanded three clones (H-1-6-1, H1-6-2 and H1-6-3) and tested to see whether they were HAT sensitive. Untargetted H1 cells grew to confluence and showed no significant levels of cell death when placed in 1xHAT selection whereas H1-6-1, H1-6-2 and H1-6-3 cells all died within four days under the same conditions. The *HPRT* gene had been successfully targeted in all three clones rendering them HAT sensitive.

### **[9.3.2] Attempts to generate cell hybrids from human ES and from human EC cells failed**

Before human ES cells became available, attempts to generate cell hybrids from hEC lines was attempted. Using standard electrofusion conditions that had successfully fused murine cells, two attempts were made to derive cell hybrids from fusions of  $1 \times 10^7$  NTERA-2<sup>nco</sup> and  $1 \times 10^7$  NTERA-2<sup>puro</sup> cells. After electropulsing and

culture in mES medium for 24 hours, cells were placed in selection (i.e. mES medium supplemented with 4 $\mu$ g / ml puromycin and 300  $\mu$ g / ml G418). These were the minimum antibiotic concentrations shown to kill all NTERA-2 cells when applied separately [See **Fig 9.2 and Fig 9.3** (overleaf)]. No colonies were generated and it was realised that perhaps inappropriate selection levels had been applied. Both G418 and puromycin inhibit protein synthesis and would probably be more potent at killing cells when applied together rather than singly. A control experiment was planned where NTERA-2<sup>neo</sup> would be stably transfected with pPUR generating a doubly resistant subclone NTERA-2<sup>neo/puro</sup>. Double selection kill curves of this subclone would then reveal appropriate selection levels to use when fusing singly resistant NTERA-2 subclones. At this time, human ES cells became available and this experiment was deprioritised in favour of experiments seeking to generate hybrids from human ES cells. A *hprt* deficient, neomycin resistant NTERA-2 subclone, called TG11.nR, had been received from Prof. Peter Andrews (University of Sheffield). TG11.nR was especially useful as one could fuse such a clone with wild type hES cells and apply double selection to isolate cell hybrids. It was felt that attempts to fuse this line with human ES lines might prove more productive than continuing with the hES experiments.

Prior to the using PEG in fusion experiments, the effect of duration of PEG exposure on the viability of cells used for the fusions was investigated [**Fig 9.4** overleaf]. Exposing TG11.nR or H9 cells to PEG for up to 4 minutes did not affect cell viability and this duration was used in subsequent fusion experiments. TG11.nR cells (and Soc2 cells) were cultured in conditioned hES medium supplemented with LIF for 3 passages prior to fusion experiments. This was done to prevent H9 cells being exposed to serum from the murine ES medium which would cause the differentiation of H9 cells. Twenty four hours after fusion, selection for cell hybrids was applied (selection medium consisted of conditioned human ES medium supplemented with 1,000U / ml LIF, 1% non essential amino acids, 1xHAT and 300  $\mu$ g / ml G418). Despite three attempts however, where 5x10<sup>7</sup> TG11.nR cells were added to a confluent T175 flask of H9 cells and induced to fuse by exposing the cells to PEG for 4 minutes (an exposure time which was not toxic to the H9 cells [**Fig 9.4** (overleaf)]), no hybrid colonies were generated.

Two attempts were made to generate cell hybrids by fusing H9 cells and Socs2 cells. Socs2 cells were similar to TG11.nR in that they are HAT sensitive and neomycin resistant but they were murine ES cells.  $5 \times 10^7$  Socs2 cells were applied to T175 flasks confluent with H9 cells and selected in a similar manner to the previous experiments. Again no hybrid colonies were generated. The cells were exposed to PEG for 4 minutes, a duration that did not significantly reduce viability of Socs2 cells (**Fig 9.4**).

As these experiments were being completed, Ray Ansell and Jim McWhir successfully generated viable single cell suspensions of H9 cells using a TEG disaggregation protocol. One could now use electrofusion to attempt to generate cell hybrids from ES cells and so the PEG experiments were deprioritised. Had they not been, a longer PEG exposure time would have been used (8 min) to induce fusion.

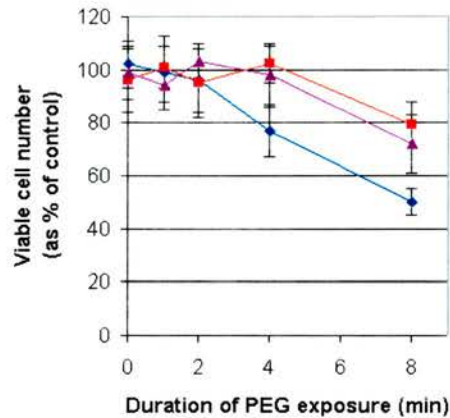


**Figure 9.4 Duration of PEG exposure affects viability of H9, Socs2 and TG11.nR cells**

Cells were exposed to PEG for a range of durations (0, 2, 4, and 8 min) and their viability was assessed. Cells from the used media and all post-trypsinisation washings were combined and pelleted before being washed and resuspended in 1xPBS. Cell viability (as % of total cells) was measured for H9 (◆), Socs2 (■) and TG11.nR (▲) cells using Forward Scatter/Side Scatter FACS analysis as outlined in **Section [12.2]**. The graph shows mean cell viability (as percentage of all cells) for each cell line at each time interval  $\pm$  S.E.M.

Using standard electrofusion conditions, two attempts at generating fusion from H9 and TG11.nR, and then from Socs2 cells again failed to generate hybrids. It was decided to use 2-dye FACS analysis to investigate where lack of fusion was the reason for the failure to generate cell hybrids from H9 cells.



### **[9.3.3] Under a range of conditions human ES cells are less fusable than their murine counterparts**

After the failure of several experiments to generate hybrid colonies from human ES or EC cells (outlined in **Subsection [9.3.2]**), a series of 2-dye FACS analysis experiments was performed to assess fusion of H9 cells under the conditions used. The human ES line was found to be less fusable than its murine counterpart. **Fig 9.5** shows only  $2.01 \pm 0.10\%$  of all viable H9 cells generated homokaryons when induced to fuse using standard murine electrofusion conditions ( $n=2$ ). This is a smaller percentage than that seen in similar experiment using HM-1 cells **Fig 3.3** shows that 12.4% of viable HM-1 cells formed homokaryons (**Fig 3.3**).

Subsequently a range of different electrofusion conditions was tested to identify optimal conditions for fusing H9 cells [**Fig 9.6**]. Single or double pulses with voltages ranging from 200-800V were applied to 0.2cm cuvettes, each containing  $10^7$  CMTMR stained H9 cells and  $10^7$  CMFDA stained H9 cells suspended in 0.3M mannitol buffer (280mOs). The optimal fusion conditions were found to be those used in previous experiments (i.e. 300V, single pulse).

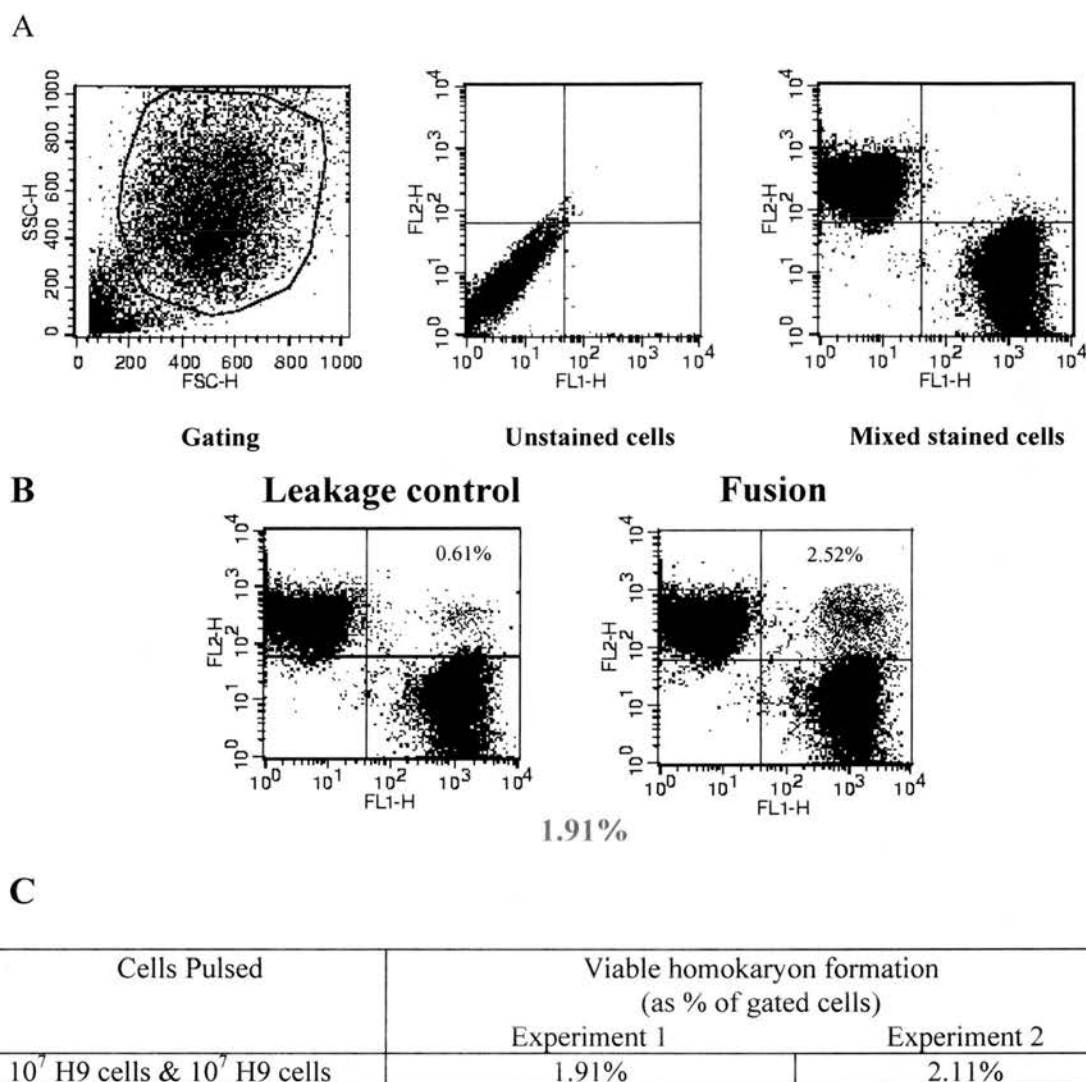
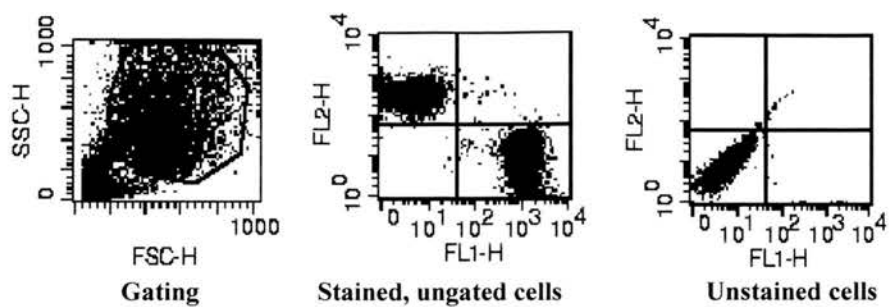


**Fig 9.5 H9 homokaryon formation was assessed using 2-dye FACS analysis**

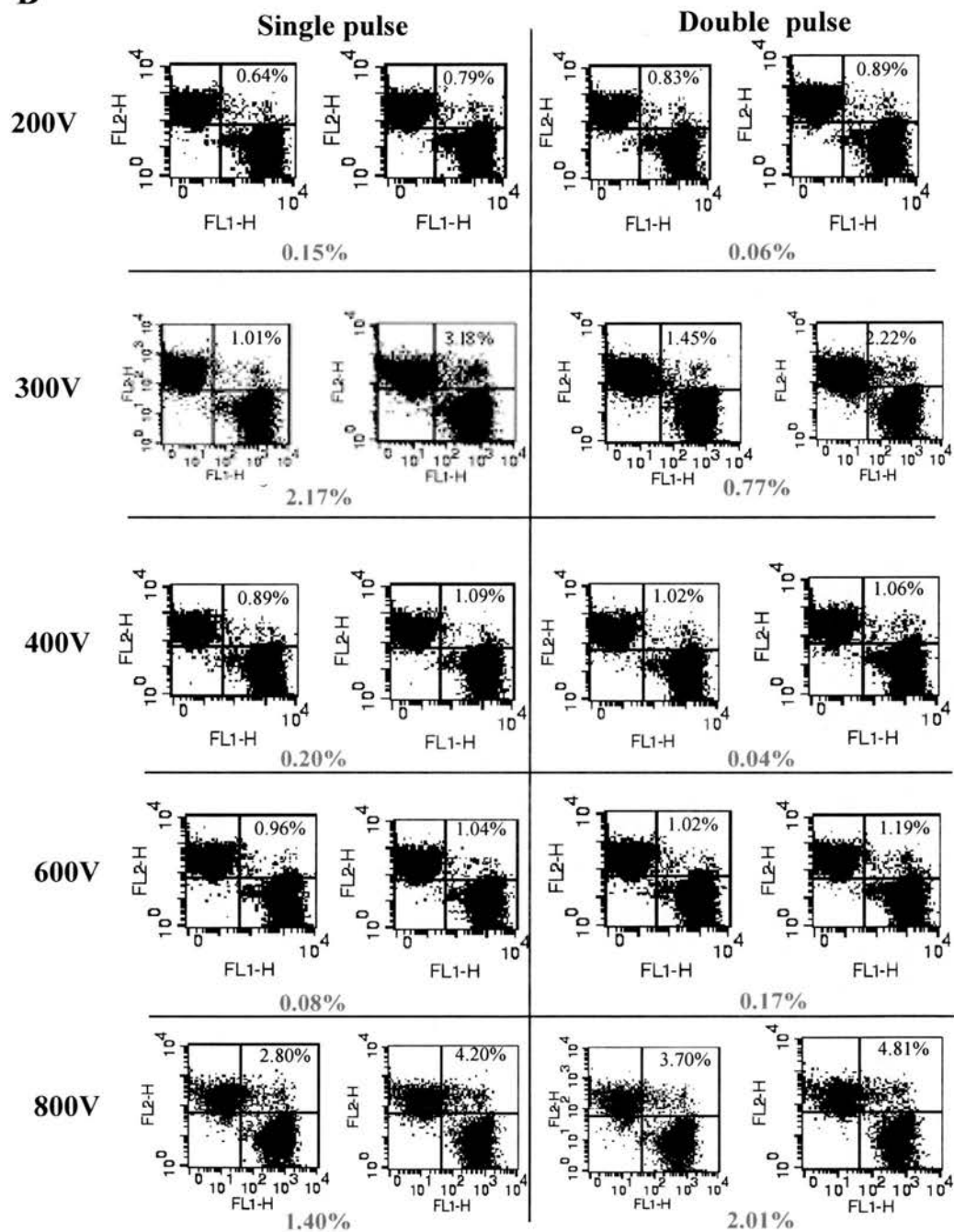
**Panel A** Gating and compensation data. Quadrant axes were defined using ungated data so that CMTMR stained H9 cells (upper left quadrant) were distinct from CMFDA stained H9 cells (lower right quadrant) in the upper left quadrant. Unstained cells appear in the lower left quadrant. The same gate and quadrants were used throughout individual experiments. **Panel B** Histograms showing fluorescence of cells in dye leakage control and fusion using H9 cells. The percentage of gated events that were double stained is highlighted in the upper right hand corner of each histogram. Data displayed in panels A & B are taken from one representative experiment replicated twice. Percentage cell fusion was calculated by subtracting the percentages for leakage controls from that for the fusion (this figure are highlighted in red). **Panel C** Summation of data from two replicate FACS experiments.



A



B



(Legend for this figure appears overleaf)

**Fig 9.6 Optimisation of electrofusion conditions for H9 homokaryon formation using 2-dye FACS analysis**

**Panel A** Gating and compensation data. Quadrant axes were positioned so that CMTMR stained H9 cells (upper left quadrant) were distinct from CMFDA stained H9 cells (lower right quadrant) in the upper left quadrant. (iii) Unstained cells appear in the lower left quadrant. The same gate and quadrants were used throughout individual experiments. **Panel B** Histograms showing fluorescence of cells in dye leakage controls and electrofusions of H9 cells using increasing voltages and number of pulses are shown. For each condition, the leakage control appears on the left and the actual fusion appears to the right. The percentage of gated events that were double stained is highlighted in the upper right hand corner of each histogram. The percentage of gated cells fusing for each condition (shown in red underneath the histograms) was calculated by subtracting the percentage of gated cells doubled stained in the leakage control from that of the electrofusion treatment. The data is taken from one of three replicate experiments.

As PEG and electrofusion had failed to induce fusion at a frequency needed to produce hybrid colonies, it was decided to try a different fusagen, the Sendai virus. This virus contains two proteins on its coat (haemagglutinin neuraminidase (HN) protein and F glycoprotein) that induce membrane fusion [Bousse *et al.* 1994] This viral had been used to fuse both human and mouse somatic cells for many years [Harris *et al.* 1965] (See **Section [2.2.3]** for more details). Experiments in which either stained HM-1 cells or stained H9 cells were exposed to Sendai virus suspension (7,500 HAU / ml) for 30 minutes were carried out. After viral exposure, cells were seeded on matrigel-treated plates and incubated for 10 hours in conditioned human ES medium prior to measuring homokaryon formation using 2-dye FACS analysis. Only 0.01% of the H9 cells formed homokaryons when exposed to the viral fusagen but 4.42% of HM-1 cells did in the control [**Fig 9.7** overleaf]. Again it seemed human ES cells were less fusable than murine ES cells.

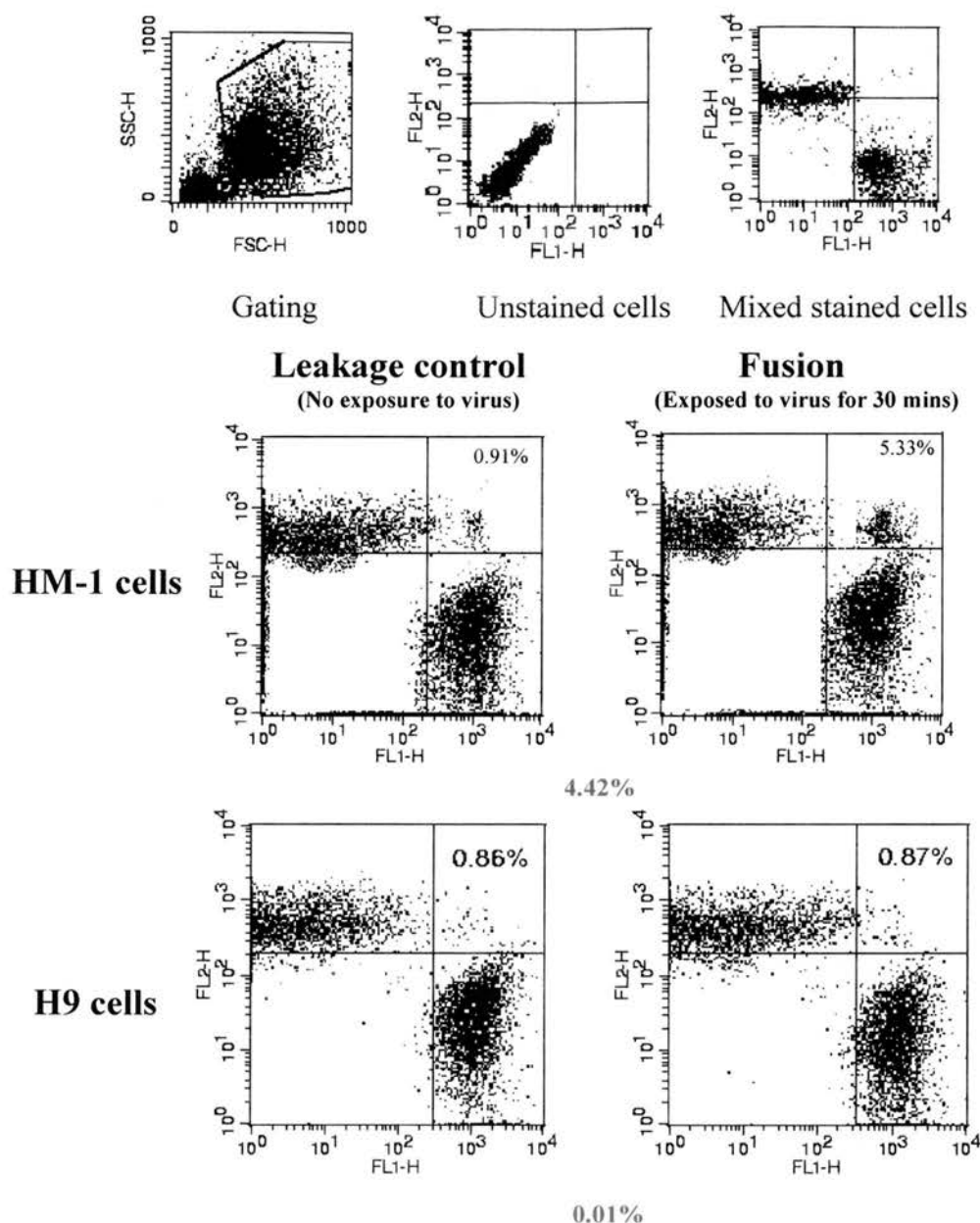


**Fig 9.7 Two-dye FACS analysis shows that H9 cells fuse at a lower frequency than HM-1 cells when Sendai virus is used as a fusagen**

Stained mixtures of HM-1 and H9 cells were exposed to a Sendai viral suspension for 30 min at 37°C as described in **Subsection [2.2.3]**. Leakage controls were equivalent cell mixtures that were not exposed to the viral suspension. 2-dye FACS analysis was used to measure HM-1 and H9 homokaryon formation. **Panel A** Gating and compensation data. (i) Dead cells were gated out manually. A typical gate is illustrated. (ii) Quadrant axes were defined using ungated data so that CMTMR stained cells (upper left quadrant) were distinct from CMFDA stained H9 cells (lower right quadrant) in the upper left quadrant. The same gate and quadrants were used throughout individual experiments. **Panel B** Histograms showing fluorescence of cells in dye the leakage control and fusion using HM-1 cells. **Panel C** Equivalent histograms using H9 cells. Percentage cell fusion (shown in red) was calculated by subtracting the percentages for leakage controls from those for fusions.

### [9.3.4] Growing cells on matrigel does not decrease their ability to fuse

Chemically, electrically and virally induced fusion of H9 cells were considerably lower than that seen with HM-1 cells. It was hypothesised that the reason for this may be the matrix on which human ES cells was being grown, i.e. Matrigel. Whether matrigel inhibits fusion was tested using HM-1 cells grown either gelatin or matrigel.

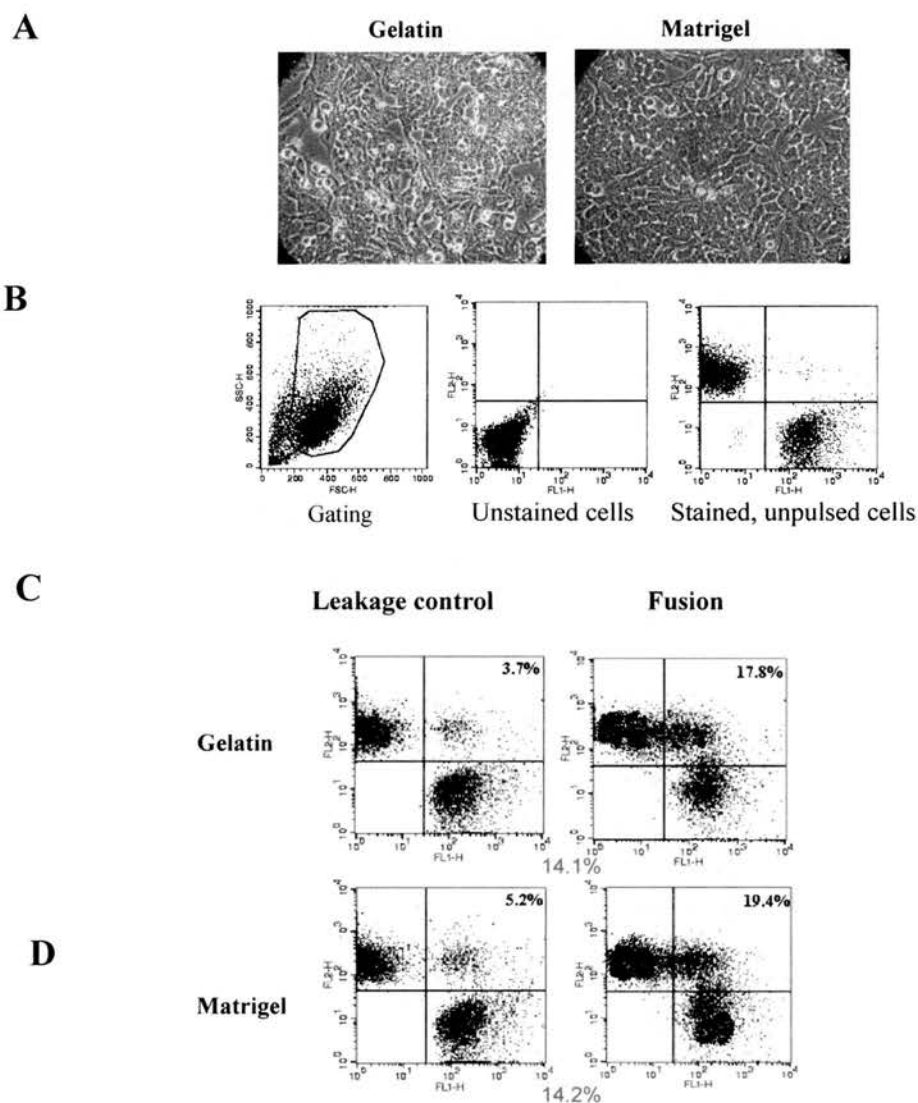


**Fig 9.8 The effect of matrigel on HM-1 homokaryon formation is assessed using 2-dye FACS analysis**

HM-1 cells were grown in either matrigel or gelatin coated flasks for 3 days. Cells were then disaggregated and stained. HM-1 cells grown on either matrigel or gelatin were assessed for homokaryon formation using 2-dye FACS analysis.

**Panel A** Images showing morphology of HM-1 cells grown on matrigel and gelatin.

**Panel B** Gating and compensation data. Quadrant axes were defined using so that

CMTMR stained thymocytes (upper left quadrant) were distinct from CMFDA stained HM-1 cells (lower right quadrant) in the upper left quadrant. Unstained cells appear in the lower left quadrant. The same gate and quadrants were used throughout individual experiments. **Panel C** Histograms showing fluorescence of cells in dye leakage control and fusion for experiments using HM-1 cells grown on gelatin. **Panel D** Histograms showing fluorescence of cells in dye leakage control and fusion for experiments using HM-1 cells grown on matrigel. The percentage of gated events that were double stained is highlighted in the upper right hand corner of each histogram.

**Fig 9.8** shows that matrigel did not inhibit fusion of HM-1 cells. Percentages of cell fusion for both HM-1 cells grown on gelatin or matrigel were not significantly different (14.1% versus 14.2%). Thus this was probably not the problem with H9 cells either.

### **[9.3.5] H9 cell fusion increases five fold after hyaluronidase treatment**

No evidence was found which indicated that growing the cells on matrigel inhibited fusion of H9 cells. Now the hypothesis that the cells own natural extracellular matrix was inhibiting fusion was tested. Many embryonic tissues have an extracellular matrix of which hyaluronic acid is a major component [Caplan 2003]. It was decided to investigate whether enzymatic cleavage of this component using hyaluronidase would breakdown the cells own extracellular matrix and facilitate fusion [See **Subsection 1.8.3**]. Ohno-Shosaku and Okada (1984) refers to experiments where pronase had successfully been used to increase mouse cell hybrid yield. Pronase cleaved cell surface glycoproteins, increasing membrane-membrane interaction which was thought to cause the resultant increase in yield of hybrid colonies.

First an experiment was carried out to investigate whether hyaluronidase broke down the ECM of H9 cells. As hyaluronan is itself non-immunogenic, control and hyaluronidase treated H9 cells were stained for hyaluronidase binding protein. **Fig 9.9** (overleaf) shows data suggesting that hyaluronidase treatment removes the hyaluronan based extracellular matrix from H9 cells. Treatment with hyaluronidase



reduces the binding of this protein to H9 cells, indicating that hyaluronan-based ECM has been broken down.

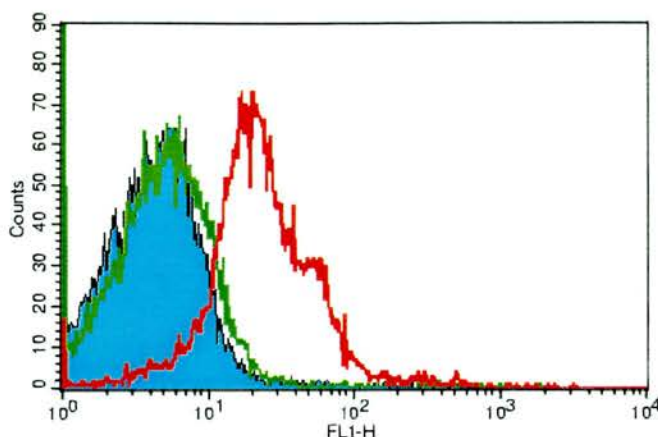


**Fig 9.9 Hyaluronidase breaks down the natural hyaluronan-based extracellular matrix of H9 cells.**

Control and hyaluronidase treated H9 cells were immunostained with a FITC labelled antibody raised to hyaluronan (as described in **Section [2.4.3]**). Green fluorescence spectra of unstained H9 cells (—), control immunostained H9 cells (—) and hyaluronidase immunostained H9 cells (—) were overlaid. After the cells are treated with hyaluronidase, there is bandshift to the left, showing that much less hyaluronan binding protein is binding to the cells. This strongly suggests that the hyaluronan-based extra cellular matrix of the cells has been broken down by hyaluronidase.

Experiments were carried out where control and hyaluronidase treated H9 cells were electrofused under standard conditions. Again 2-dye FACS analysis was used to assess homokaryon formation. **Fig 9.10** (overleaf) shows that hyaluronidase treatment also repeatedly increased electrofusion of H9 cells. On average the hyaluronidase increased fusion five fold over control levels ( $5.37 \pm 0.38\%$  versus  $1.05 \pm 0.06\%$ ,  $n=3$ ). It seems probable that the hyaluronan-based extra cellular matrix produced by H9 cells was inhibiting higher levels of fusion in previous experiments.



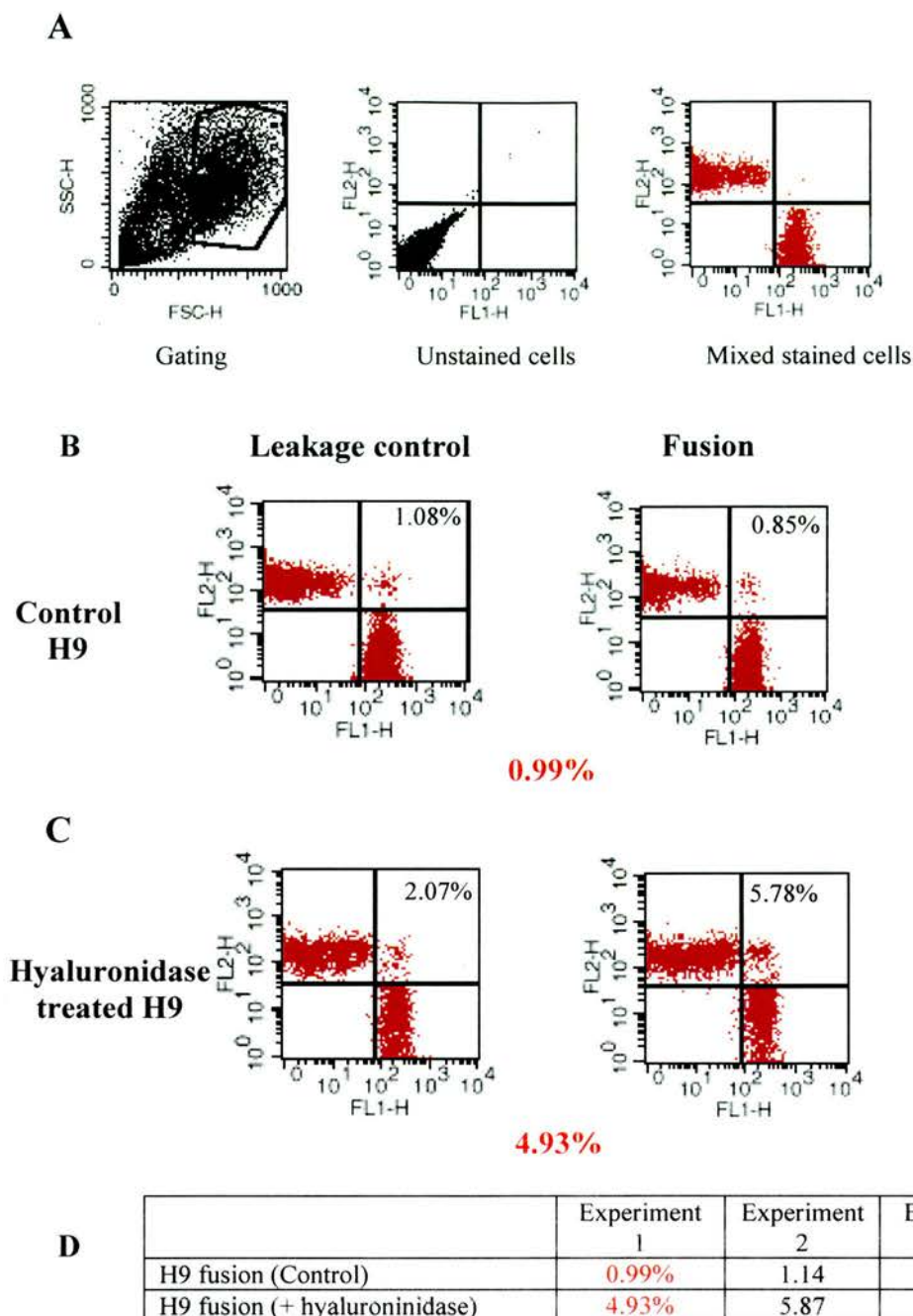


**Fig 9.10 Hyaluroninidase treatment increases H9 homokaryon formation.**

**Panel A** Gating and compensation data. Quadrant axes were defined using ungated data so that orange stained H9 cells (upper left quadrant) were distinct from green stained H9 cells (lower right quadrant) in the upper left quadrant. Unstained cells appear in the lower left quadrant. The same gate and quadrants were used throughout individual experiments. **Panel B** Histograms showing fluorescence of cells in dye leakage controls using untreated H9 cells. **Panel C** Equivalent histograms for hyaluronidase treated H9 cells. Data displayed in panels A, B & C are taken from one representative experiment. % cell fusion was calculated by subtracting the percentages for leakage controls from that for the fusion (these figures are highlighted in red). **Panel D** Summation of data from individual FACS experiments (n=3).

## [9.4] Conclusion

Selectable lines were generated to allow the isolation of human cell hybrids derived from heterokaryons was generated. Attempts to generate *hprt* deficient hEC subclones using 6-TG selection failed. FISH analysis of NTERA-2 mitotic spreads revealed abnormal duplication of segments of the X-chromosome which could account for the failure to generate colonies.

Attempts to generate cell hybrids from somatic fusions with either hEC and hES cells failed. Early hES experiments used PEG as a fusagen because H9 cells were not viable in single cell suspension when disaggregated with collagenase. It was later discovered that TEG disaggregation of H9 cells could generate a viable single cell suspension, and electrofusion experiments were attempted. These also failed to generate hybrid colonies.

Two-dye FACS analysis revealed that human ES and EC cells were less fusable than their murine counterparts under the conditions used. Attempts to optimise conditions for H9 cell fusion showed that the artificial matrix matrigel on which the cells were cultured did not inhibit cell fusion. The most probable reason for failure to generate cell hybrids was that the degree of fusion was insufficient to generate hybrids from the cell numbers used. Breakdown of the native ECM of H9 cells with hyaluronidase increased the level of fusion five fold. Such treatment should be used in future attempts to generate cell hybrids from H9 cells.

## [10] General discussion and conclusions

### Use of the cell hybrid system for studying nuclear reprogramming

Murine somatic nuclei can be epigenetically reprogrammed by factors present in murine Embryonic Stem cells [Tada *et al.* 2002][Matveeva *et al.* 1998]. Hybridising murine ES cells with somatic cells alters somatic chromatin structure causing major changes both in patterns of global DNA methylation [Tada *et al.* 2002] and in gene expression [Tada *et al.* 2002][Matveeva *et al.* 1998]. Functionally, the hybrid cells are pluripotent highlighting extensive reprogramming of the somatic chromatin has taken place [Tada *et al.* 2002][Matveeva *et al.* 1998]. The work described in this thesis sought to identify factors that affect such reprogramming. To do this, a system for consistently generating large numbers of hybrid colonies from fusions of murine ES cells and somatic cells was developed and optimised. ES cell hybrids were successfully generated from two somatic cell types: thymocytes and fibroblasts. To the best knowledge of the student, work described in **Chapter 3**, where murine ES cells and primary embryonic fibroblasts were hybridised, is the first report of generating such hybrids from a somatic cell type that can be grown in culture. It is also the first example of ES cell hybrid generation where ES cell hybrids can display either murine ES cell or also in theory somatic cell phenotypes and remain viable in hybrid selection conditions. Although similar experiments fusing with EC cells could generate hybrids with either phenotype (as reviewed in **Subsection [1.8.3.2]**), work described in this thesis shows that murine ES x PEF hybrid cells only ever displayed a murine ES cell morphology, even when <sup>Octneo/Octneo</sup> somatic cells and selection for reprogramming with G418 were not used. This suggests that the ES cell phenotype is dominant over the somatic cell phenotype.

Hybrid cells generated by fusing HM-1 cells with somatic cells (either thymocytes or fibroblasts) were morphologically indistinguishable from HM-1 cells and phenotypic characteristics assessed in the hybrids cells were similar to those observed in HM-1 cells but not in their somatic fusion partners. Both *in vitro* and *in vivo* studies showed that such hybrid cells were pluripotent. These data, outlined in **Chapter 4**, are similar to those previously described in the literature where

thymocytes [Tada *et al.* 2002] and splenocytes [Matveeva *et al.* 1998] were used as somatic fusion partners to generate ES cell hybrids.

Whether ES phenotypic dominance within these hybrid cells is complete is still unknown. Andrews and Goodfellow (1980) fused murine EC (PCC4azaR) cells with thymocytes and resultant hybrid cells still expressed differentiated cell marker H-2K<sup>k</sup>. This shows that reprogramming to an EC phenotype was not complete (even though these hybrid cells were still pluripotent as assessed by tumour generation in SCID mice). Incomplete change in gene expression profiles in these hybrid cells may be just a consequence of EC cell genomic instability but the extent to which murine ES cell-specific genes are expressed and somatic cell-specific genes are repressed requires further analysis in order to understand the extent of reprogramming that has taken place. Microarray technology, for example, could be used to assess the transcripton levels of many ES cell specific and somatic cell specific genes in hybrid cells.

The cell hybrid system was used to investigate the effect of different treatments on nuclear reprogramming. This system was chosen because ES cells contain little cytoplasm, making nuclear transfer or cytoplasm incubations technically very difficult to carry out. Use of this system has both benefits and limitations for the study of nuclear reprogramming. In addition to being technically simpler than either nuclear transfer [Campbell 1999] or cytoplasmic incubation [Hakelien *et al.* 2002], it quickly generates large amounts of reproducible data. The system not only allows the effects of broad treatments (such as heat shock, confluence and serum starvation) on nuclear reprogramming, but also allows the effect of transient expression of specific transgenes to be studied. This approach was exemplified in **Chapter 8**, where the Tet-On inducible gene expression system was used to transiently express nuclear chaperone *Xenopus* nucleoplasmin in the hybrid system.

Unlike nuclear transfer and cytoplasmic incubations however, the nucleus of the reprogramming cell are still present. Only cytoplasmic factors are required to direct complete reprogramming of mammalian nuclei as shown by nuclear transfer [Wilmut *et al.* 1997] and one could argue that the presence of ES cell chromatin and

associated nuclear components might directly influence reprogramming of somatic chromatin.

A novel approach was developed and used in this thesis to assess the nuclear reprogramming activities of ES cell population. Two-dye FACS analysis was used to measure the fraction of viable cells forming heterokaryons. Hybridisation frequencies, calculated by dividing the number of hybrid colonies by the number of viable heterokaryons, were used as a measure of the frequency of nuclear reprogramming. Ideally however, the total number of viable hybrid cells could have been measured at the onset of selection for reprogramming. The proportion of successfully reprogrammed hybrid cells could then be directly calculated providing a direct measure of nuclear reprogramming. This was not possible as non-toxic nucleus-specific probes were not available. If they had been, nuclei of ES cells and somatic cells would have been labeled with different probes and analysed to determine the number of hybrid cells, rather than the number of heterokaryons. It is probable however that one would not be able to discriminate accurately between viable hybrid cells and heterokaryons because of the cytoplasm surrounding the nuclei. One would also be unable to control for probe leakage meaning an overestimation of the number of hybrid cells would be made.

As heterokaryons are not viable in culture for longer than a few hours [Blau and Blakely 1999], this cell hybrid system requires nuclear fusion of the ES and somatic nuclei. For hybridisation frequencies (hybrid / heterokaryon) to be an accurate measure of the incidence of nuclear reprogramming, the rate of nuclear fusion in heterokaryons will be relatively constant between different treatments in experiments.

Nuclear fusion does seem to be relatively constant in hybrid generating experiments where cells are treated similarly (e.g. under standard conditions experiments electrofusing HM-1 cells and thymocytes consistently produced one viable cell hybrid for every ~4,000 viable heterokaryons). This however does not argue that nuclear fusion is constant in heterokaryons derived from cells that have been treated differently. Very little is known about factors affecting nuclear fusion so it is not yet possible to assess how much nuclear fusion will vary with different cell treatments.



The serum starvation data presented in **Chapter 7** suggests that nuclear fusion is relatively constant and that hybridisation frequency (hybrid / heterokaryon) is actually a good measure of reprogramming (at least in this case). These data are similar to nuclear transfer data in that nuclei of serum starved primary embryonic cells underwent nuclear reprogramming more frequently [Campbell *et al.* 1996][Campbell 1999]. However more needs to be done to investigate whether nuclear fusion is relatively constant where cells have been differentially treated in other ways (e.g. growing cells to different levels of confluence).

### **Cellular stress and nuclear reprogramming**

In **Chapter 5**, the effect of heat shocking somatic cells prior to fusion with ES cells was tested. It was hypothesised that disruption of higher chromatin structure at hyperthermic temperatures would make the somatic cell more amenable to being reprogrammed by the ES cell. Heat shocking thymocytes to 42°C for 10 min prior to fusion increased not only hybrid colony yield (84.6±16.9% increase over control yields) but also heterokaryon formation (39±5% increase over control levels). The data from five replicate experiments were not enough to assess whether the increase in hybrid colony yield could be accounted for solely by increased heterokaryon formation or whether an increase in the frequency of nuclear reprogramming had also taken place. Thus nothing could be concluded about whether heat shocking thymocytes prior to fusion affected reprogramming of the thymocytes. Just after this work was completed, Loi *et al.* (2002) published data showing that heat shocking granulosa cells at either 55°C and 75°C prior to injecting their nuclei into enucleated metaphase II oocytes increased the number of reconstructed embryos developing to blastocyst stage and beyond. Their data also shows that exposing granulosa cells to such non-physiological temperature destabilised higher orders of chromatin structures. Thus, some evidence for the hypothesis being tested in **Chapter 5** now exists. Unfortunately application of Loi *et al.*'s heat shock conditions to thymocytes



before cell fusion only caused lysis and cell clumping so similar experiments using the cell hybrid system could not be carried out.

Experiments where HM-1 cells and thymocytes were heat shocked at 42°C for 10 min *after* being fused caused a decrease in hybridisation frequencies (hybrid / heterokaryon). In samples that were heat shocked between 1 and 12 hours after electropulsing, cell viability and heterokaryon formation were relatively constant between samples, while hybrid yield gradually increased. Thus, heat shocking cells *after* fusion only resulted in a decreased hybridisation frequencies. This suggests that such post-fusion treatment impairs rather than assists reprogramming of thymocyte nuclei. As ES cell components are also being heat shocked here, one possible explanation is that reprogramming factors present in the ES cell are sensitive to the heat shock treatment. The later the heat shock is after cell fusion, the more hybrids will have already been successfully reprogrammed. One might test this hypothesis by heat shocking the HM-1 cells prior to fusion with thymocytes and observing the resultant hybridisation frequencies (hybrid / heterokaryon). If ES cell derived reprogramming factors are sensitive to heat shocking, one would expect a decrease in hybridisation frequencies. However, analysis of data from such an experiment is likely to have the same problems associated with increased heterokaryon formation as pre-fusion heat shock experiments.

If one assumes that reprogramming factors are sensitive to stresses such as heat shock, one might expect that the more stressed an ES cell is, the less reprogramming capacity it is likely to have. Data shown in **Chapter 6** do not seem to support this view. As HM-1 cells approach confluence, and more stressed they become (as measured by Hsp72 induction) and yet the greater the nuclear reprogramming capacity they appear to have. One possibility is that if HM-1 cells are stressed and allowed to express significant levels of heat shock proteins, they are more likely to reprogram somatic nuclei successfully. In the case of heat shocking after HM-1 cells and thymocytes have fused, heat shock protein expression may not be induced to sufficient levels quickly enough to have an effect on reprogramming.

As HM-1 cells approach confluence, the more they express heat shock proteins (including Hsp72 as measured here in **Fig 6.8**). Many heat shock proteins act as chaperones repairing misfolded protein and RNA which are denatured as a

consequence of stress. The higher the expression of such proteins, the quicker denatured proteins and RNA will be refolded correctly, and the greater the probability of the cell withstanding further stress. Hsp72 levels [Fig 6.8] and hybridisation frequencies [Fig 6.6] both increase as HM-1 cells approach confluence. It is possible that nuclear reprogramming is assisted by the expression of such proteins (by correcting denaturation of chromatin remodeling complexes for example). If this is true, one would expect that moderately stressing either fusion partner in a fusion experiment and allowing heat shock proteins to be induced would result in increased nuclear reprogramming. In Chapter 7, where PEFs are serum starved to induce quiescence, these somatic cells are also stressed by this treatment and induce Hsp72 strongly [Fig 7.2]. The hybridisation frequencies (hybrid / heterokaryon) of experiments where serum starved controls were used were  $53 \pm 11$  fold higher than in control experiments.

Considering both the data described in Chapter 6 and data generated by Gao *et al.* 2003, it seems that reprogramming both *by* and *of* HM-1 cells is affected by HM-1 cell confluence. These observations are consistent with the heat shock protein hypothesis, where stress induction of such factors in either the cell doing the reprogramming or the cell being reprogrammed would increase nuclear reprogramming.

It is important to bear in mind however, that these observations only correlate induction of the stress response and increases in nuclear reprogramming and do not show a direct effect. More evidence will be needed before this hypothesis is taken seriously. There will be major difficulties in testing this hypothesis given the range of heat shock proteins.

### **Changes in the cell cycle and nuclear reprogramming**

In Chapters 6 and 7 respectively, the cell cycle characteristics of HM-1 cells approaching confluence and serum starved primary embryonic fibroblasts were investigated to see if there was any relationship between cell cycle and nuclear reprogramming. In the case of HM-1 cells grown to different levels of confluence,

the mean proportions of cells at different stages of the cell cycle changed as follows: the proportion in G1 dropped from 32.8% to 11.9%, the proportion in S remained unchanged and the proportion in G2/M rose 18.4% to 41.1%. Assuming that cell cycle characteristics are directly influencing nuclear reprogramming, HM-1 cells in G1 seem less efficient at reprogramming thymocytes or HM-1 cells in G2/M seem to be more efficient. This could be due to different levels of the putative reprogramming factor MPF, which is expressed at low levels in G1 cells and at high levels in G2/M cells [Murray & Hunt 1993]. This could be tested by expressing MPF in the somatic cell line prior to fusion. Recently published bovine nuclear transfer work however shows no correlation between MPF levels and nuclear reprogramming [Tani et al. 2003]. An alternative explanation could be that as HM-1 cells in G2/M phases have duplicated cytoplasmic components in preparation for cell division, and such cells consequently may contain more reprogramming factors. When fused to somatic cells, they may have a greater capacity to reprogram these cells. This hypothesis could be tested by fusing HM-1 cells to form HM-1xHM-1 hybrid cells and then fusing these cells to somatic cells so see if there is an increase in hybridisation frequency.

In chapter 7, the cell cycle characteristics of the cells to be reprogrammed were assessed. When primary embryonic fibroblasts were serum starved, the proportion of cells in G1/G0 phases increased (53.7% to 73.0%), that in S phase decreased (8.6% to 2.7%) and that in G2/M phases decreased from 37.7% to 24.3% [Fig 7.4]. Experiments using serum starved PEFs produced significantly higher hybridisation frequencies indicating that they were more amenable to being reprogrammed than control fibroblasts. Since these PEFs were shown to be in a quiescent state, such an increase in nuclear reprogramming is consistent with Campbell's hypothesis that quiescent nuclei are more amenable to being reprogrammed. However, in the final experiment of **Chapter 7**, fusions using serum reactivated PEFs displayed an elevated hybrid colony yield even though the cells were no longer quiescent. Obviously, no conclusion can be drawn from only one experiment but should these data be repeatable, it might suggest that some characteristic of serum starved PEFs other than their quiescent state make them more easily reprogrammed. It is surprising similar experiments have not been previously

done in the nuclear transfer system given the controversy surrounding the role of quiescence in nuclear reprogramming.

### **Role of specific genes in nuclear reprogramming**

The murine cell hybrid system developed here allowed the effect of expression of a specific transgene on nuclear reprogramming to be studied. In **Chapter 8**, the effects of constitutive and transient expression of *Xenopus* nucleoplasmin on reprogramming in the cell hybrid system were studied. Unfortunately the levels at which nucleoplasmin were expressed proved toxic to HM-1 cells, and had time permitted, the effect of lower expression levels would have been tested. As this work was being completed, Byrne *et al.* 2003 published data showing that transferring murine thymocyte nuclei in *Xenopus* oocytes reprogrammed the nuclei such that they began to express the pluripotent cell specific transcription factor Oct-4. As *Xenopus* oocytes express nucleoplasmin at very high levels (constituting 9-10% of all protein produced by the cell [Krohne & Franke 1980]), there is even more justification to continue this line of investigation in the hybrid system.

Had more time been available, *Xenopus* nucleoplasmin would have been expressed in the somatic fusion partner rather than ES cell prior to fusion. A suitable somatic cell line would have been chosen and stably transfected with both pTNG and pTetNPM. A clone appropriately expressing nucleoplasmin inducibly in response to doxycycline addition would have been used in experiments where various levels of nucleoplasmin expression induced in somatic cells prior to fusion with HM-1 cells. Inducing nucleoplasmin expression after cell fusion would also have been tested. Thus by transiently expressing nucleoplasmin at different levels and at different time points, the effect of nucleoplasmin expression on reprogramming of the somatic nucleus would be further investigated.

### **Difficulties overcome in attempts to develop a human ES cell hybridisation system**

Several steps were made toward developing a human ES cell hybrid system to study reprogramming. In collaboration with others, selectable human ES cell lines have now been produced and fusion with other cell types was measured. Human ES cells were less fusable with other cell types than their murine counterparts even when a range of conditions and fusagens (electropulsing, PEG and Sendai virus) were used. Establishing that breaking down the native extracellular matrix of human ES cells facilitates cell fusion is an important step toward generating hybrids from human ES cells. Whether hyaluronidase treatment of hES cells also increases lipofection efficiencies should also be investigated.

In future attempts to generate hybrids from human ES cells, it would be advisable to use low passage cells given that human ES cells may also lose their capacity to reprogram somatic cells when they reach high passage number, as murine ES cells have been shown to do (**Fig 6.9**). Had time permitted, a selectable human somatic cell line would have developed and experiments fusing hyaluronidase-treated human ES cells with these selectable human somatic cells would have been attempted. It would have been interesting to see whether human ES cells were phenotypically dominant over human somatic cells and whether or not resultant hybrid cells were pluripotent. Generation of such a human ES hybrid system will in the future provide the opportunity to identify factors necessary for reprogramming human somatic cells to a pluripotent state.

## [11] Bibliography

Alami R, Fan Y, Pack S, Sonbuchner TM, Besse A, Lin Q, Greally JM, Skoultchi AI, Bouhassira EE. Mammalian linker-histone subtypes differentially affect gene expression in vivo. *Proc Natl Acad Sci U S A*. 2003 May 13;100(10):5920-5.

Amit M, Carpenter MK, Inokuma MS, Chiu CP, Harris CP, Waknitz MA, Itskovitz-Eldor J, Thomson JA. Clonally derived human embryonic stem cell lines maintain pluripotency and proliferative potential for prolonged periods of culture. *Dev Biol*. 2000 Nov 15; 227(2): 271-8.

Amit M, Itskovitz-Eldor J. Derivation and spontaneous differentiation of human embryonic stem cells. *J Anat*. 2002 Mar;200(Pt 3):225-32.

Andrews PW. Human teratocarcinomas. *Biochim Biophys Acta*. 1988 Aug 3;948(1):17-36. Review.

Andrews PW, Damjanov I, Simon D, Banting GS, Carlin C, Dracopoli NC, Fogh J. Pluripotent embryonal carcinoma clones derived from the human teratocarcinoma cell line Tera-2. Differentiation in vivo and in vitro. *Lab Invest*. 1984 Feb;50(2):147-62.

Andrews PW, Goodfellow PN. Antigen expression by somatic cell hybrids of a murine embryonal carcinoma cell with thymocytes and L cells. *Somatic Cell Genet*. 1980 Mar;6(2):271-84.

Babinet C, Cohen-Tannoudji M. Genome engineering via homologous recombination in mouse embryonic stem (ES) cells: an amazingly versatile tool for the study of mammalian biology. *An Acad Bras Cienc*. 2001 Sep;73(3):365-83.

Baguisi A, Behboodi E, Melican DT, Pollock JS, Destrempe MM, Cammuso C, Williams JL, Nims SD, Porter CA, Midura P, Palacios MJ, Ayres SL, Denniston RS, Hayes ML, Ziomek CA, Meade HM, Godke RA, Gavin WG, Overstrom EW, Echelard Y. Production of goats by somatic cell nuclear transfer. *Nat Biotechnol*. 1999 17(5):456-61.

Balbi C, Abelmoschi ML, Gogioso L, Parodi S, Barboro P, Cavazza B, Patrone E. Structural domains and conformational changes in nuclear chromatin: a quantitative thermodynamic approach by differential scanning calorimetry. *Biochemistry*. 1989 Apr 18;28(8):3220-7.

Baqir, S. and Smith, L.C. Cell cycle arrest by means of serum starvation and confluency is associated with altered expression of imprinted genes in mouse embryonic stem cells. 2000 *Theriogenology* 53:402.

Bannister AJ, Zegerman P, Partridge JF, Miska EA, Thomas JO, Allshire RC, Kouzarides T. Selective recognition of methylated lysine 9 on histone H3 by the HP1 chromo domain. *Nature*. 2001 Mar 1;410(6824):120-4.



Barkai U, Gubler ML, Sherman MI. Retinoid-binding proteins and retinoid-induced differentiation of embryonal carcinoma cells. 1986 *Prog Clin Biol Res.* 226:205-13. Review.

Barlow DP. Methylation and imprinting: from host defense to gene regulation? 1993 *Science.* Apr 16;260(5106):309-10.

Barnea E, Bergman Y. Synergy of SF1 and RAR in activation of Oct-3/4 promoter. 2000 *J Biol Chem.* Mar 3;275(9):6608-19.

Baron MH. Reversibility of the differentiated state in somatic cells. 1996 *Curr Opin Cell Biol* 5:1050

Baron, U. (1995) Co-regulation of two gene activities by tetracycline via a bidirectional promoter. *Nucleic Acids Res.* 17:3605-3606.

Barr ML, Bertram D. A morphological distinction between neurons of a male and female, and the behaviour of the nucleolar satellite during accelerated nucleoprotein synthesis. 1949 *Nature* 163:676-7.

Barton SC, Arney KL, Shi W, Niveleau A, Fundele R, Surani MA, Haaf T. Genome-wide methylation patterns in normal and uniparental early mouse embryos. *Hum Mol Genet.* 2001 Dec 15;10(26):2983-7.

Bell AC, Felsenfeld G. Methylation of a CTCF-dependent boundary controls imprinted expression of the *Igf2* gene. *Nature.* 2000 May 25;405(6785):482-5.

Bensaude O, Babinet C, Morange M, Jacob F. Heat shock proteins, first major products of zygotic gene activity in mouse embryo. 1983 *Nature.* Sep 22-28;305(5932):331-3.

Ben-Shushan E, Pikarsky E, Klar A, Bergman Y. Extinction of Oct-3/4 gene expression in embryonal carcinoma x fibroblast somatic cell hybrids is accompanied by changes in the methylation status, chromatin structure, and transcriptional activity of the Oct-3/4 upstream region. *Mol Cell Biol.* 1993 Feb;13(2):891-901.

Ben-Shushan E, Thompson JR, Gudas LJ, Bergman Y. Rex-1, a gene encoding a transcription factor expressed in the early embryo, is regulated via Oct-3/4 and Oct-6 binding to an octamer site and a novel protein, Rox-1, binding to an adjacent site. 1998 *Mol Cell Biol.* Apr;18(4):1866-78.

Benz R, Zimmermann U. The resealing process of lipid bilayers after reversible electrical breakdown. 1981 *Biochim Biophys Acta.* 640(1):169-78.

Berry IJ, Burns JE, Parkinson EK. Assignment of two human epidermal squamous cell carcinomas cell lines to more than one complementation group for the immortal phenotype. 1994 *Mol Carcinog.* 9(3):134-42.

Betts D, Bordignon V, Hill J, Winger Q, Westhusin M, Smith L, King W. Reprogramming of telomerase activity and rebuilding of telomere length in cloned cattle. *Proc Natl Acad Sci U S A*. 2001 Jan 30;98(3):1077-82.

Betts DH, King WA. Telomerase activity and telomere detection during early bovine development. *Dev Genet*. 1999;25(4):397-403.

Bishop CP, Jackson CM. Genomic imprinting of chromatin in *Drosophila melanogaster*. 1996 *Genetica*. 97(1):33-7.

Biniszkievicz D, Gribnau J, Ramsahoye B, Gaudet F, Eggan K, Humpherys D, Mastrangelo MA, Jun Z, Walter J, Jaenisch R. Dnmt1 overexpression causes genomic hypermethylation, loss of imprinting, and embryonic lethality. *Mol Cell Biol*. 2002 Apr;22(7):2124-35.

Bjornson CR, Rietze RL, Reynolds BA, Magli MC, Vescovi AL. Turning brain into blood: a hematopoietic fate adopted by adult neural stem cells in vivo. 1999 *Science*. 283(5401):534-7.

Blau HM, Blakely BT. Plasticity of cell fate: insights from heterokaryons. *Semin Cell Dev Biol*. 1999 Jun;10(3):267-72.

Blow JJ, Laskey RA. A role for the nuclear envelope in controlling DNA replication within the cell cycle. *Nature*. 1988 Apr 7;332(6164):546-8.

Boggs BA, Cheung P, Heard E, Spector DL, Chinault AC, Allis CD. Differentially methylated forms of histone H3 show unique association patterns with inactive human X chromosomes. *Nat Genet*. 2002 Jan;30(1):73-6.

Boshart M, Nitsch D, Schutz G. Extinction of gene expression in somatic cell hybrids--a reflection of important regulatory mechanisms? 1993 *Trends Genet*. Jul;9(7):240-5. Review.

Bourc'his D, Viegas-Pequignot E. Direct analysis of chromosome methylation. *Methods Mol Biol*. 2001;181:229-42.

Bousse T, Takimoto T, Gorman WL, Takahashi T, Portner A. Regions on the hemagglutinin-neuraminidase proteins of human parainfluenza virus type-1 and Sendai virus important for membrane fusion. 1994 *Virology* 204(2):506-14.

Bradley A, Evans M, Kaufman MH, Robertson E. Formation of germ-line chimaeras from embryo-derived teratocarcinoma cell lines. 1984 *Nature*. May 17-23;309(5965):255-6.

Bradley A. *Teratocarcinomas and Embryonic Stem cells* (ed. E.J. Robertson) (1987) IRL press Ltd. Oxford.

Bravo R, Macdonald-Bravo H. Existence of two populations of cyclin/proliferating cell nuclear antigen during the cell cycle: association with DNA replication sites. 1987 *J Cell Biol* 105(4):1549-54.

Brehm A, Ovitt CE, Scholer HR. Oct-4: more than just a POUerful marker of the mammalian germline? 1998 *APMIS*. Jan;106(1):114-24; discussion 124-6. Review.

Briggs, R. & King, T. J. Transplantation of living nuclei from blastula cells into enucleated frogs eggs *Proc. Natl. Acad. Sci. USA* 1952 38, 455-463.

Brinster RL. The effect of cells transferred into the mouse blastocyst on subsequent development. *J Exp Med*. 1974 Oct 1;140(4):1049-56.

Broyles RH. Use of somatic cell fusion to reprogram globin genes. 1999 *Semin Cell Dev Biol*. Jun;10(3):259-65. Review.

Brüstle O, Jones KN, Learish RD, Karram K, Choudhary K, Wiestler OD, Duncan ID, McKay RD. Embryonic stem cell-derived glial precursors: a source of myelinating transplants. 1999 *Science*. Jul 30;285(5428):754-6.

Burglin TR, De Robertis EM. The nuclear migration signal of *Xenopus laevis* nucleoplasm. 1987 *EMBO J*. Sep;6(9):2617-25.

Byrne JA, Simonsson S, Western PS, Gurdon JB. Nuclei of adult mammalian somatic cells are directly reprogrammed to oct-4 stem cell gene expression by amphibian oocytes. *Curr Biol*. 2003 Jul 15;13(14):1206-13.

Campbell KH. Nuclear transfer in farm animal species. 1999 *Semin Cell Dev Biol*. Jun;10(3):245-52. Review.

Campbell KH, McWhir J, Ritchie WA, Wilmut I. Sheep cloned by nuclear transfer from a cultured cell line. 1996 *Nature*. Mar 7;380(6569):64-6.

Campbell KH, Loi P, Otaegui PJ, Wilmut I. Cell cycle co-ordination in embryo cloning by nuclear transfer. 1996 *Rev Reprod*. Jan;1(1):40-6. Review.

Caplan AI. Embryonic development and the principles of tissue engineering. *Novartis Found Symp*. 2003;249:17-25; discussion 25-33, 170-4, 239-41.

Caria M. *Measurement Analysis: An Introduction to the Statistical Analysis of Laboratory Data in Physics, Chemistry and the Life Sciences*. Imperial College Press, London, 2000. ISBN 1-86094-231-8.

Carpenter MK, Rosler E, Rao MS. Characterization and differentiation of human embryonic stem cells. *Cloning Stem Cells*. 2003;5(1):79-88.

Cattanach BM *Genome Analysis*. Editors: Davies Ke, Tilghman SM. 1991 Cold Spring Press. 2:41.

Chan WY, Liu QR, Borjigin J, Busch H, Rennert OM, Tease LA, Chan PK. Characterization of the cDNA encoding human nucleophosmin and studies of its role in normal and abnormal growth. *Biochemistry*. 1989 Feb 7;28(3):1033-9.

Chappell TG, Welch WJ, Schlossman DM, Palter KB, Schlesinger MJ, Rothman JE. Uncoating ATPase is a member of the 70 kilodalton family of stress proteins. *Cell*. 1986 Apr 11;45(1):3-13.

Chen RZ, Pettersson U, Beard C, Jackson-Grusby L, Jaenisch R. DNA hypomethylation leads to elevated mutation rates. *Nature*. 1998 Sep 3;395(6697):89-93.

Chesne P, Adenot PG, Viglietta C, Baratte M, Boulanger L, Renard JP. Cloned rabbits produced by nuclear transfer from adult somatic cells. (2002) *Nat Biotechnol*. 20(4):366-9.

Cibelli JB, Stice SL, Golueke PJ, Kane JJ, Jerry J, Blackwell C, Ponce de Leon FA, Robl JM. Cloned transgenic calves produced from nonquiescent fetal fibroblasts. 1998 *Science*. 280(5367):1256-8.

Clark AJ, Bissinger P, Bullock DW, Damak S, Wallace R, Whitelaw CB, Yull F. Chromosomal position effects and the modulation of transgene expression. 1994 *Reprod Fertil Dev*. 6(5):589-98. Review.

Clarke HJ, McLay DW, Mohamed OA. Linker histone transitions during mammalian oogenesis and embryogenesis. 1998 *Dev Genet*. 22(1):17-30. Review.

Craig EA. The heat shock response. 1986 *CRC Crit. Rev. Biochem*. 18:239-280.

Condorelli G, Borello U, De Angelis L, Latronico M, Sirabella D, Coletta M, Galli R, Balconi G, Follenzi A, Frati G, Cusella De Angelis MG, Gioglio L, Amuchastegui S, Adorini L, Naldini L, Vescovi A, Dejana E, Cossu G. Cardiomyocytes induce endothelial cells to trans-differentiate into cardiac muscle: implications for myocardium regeneration. 2001 *Proc Natl Acad Sci U S A* 98(19):10733-8.

Counter CM, Avilion AA, LeFeuvre CE, Stewart NG, Greider CW, Harley CB, Bacchetti S. Telomere shortening associated with chromosome instability is arrested in immortal cells which express telomerase activity. 1992 *EMBO J*. May;11(5):1921-9.

Cowell IG, Aucott R, Mahadevaiah SK, Burgoyne PS, Huskisson N, Bongiorno S, Prantera G, Fanti L, Pimpinelli S, Wu R, Gilbert DM, Shi W, Fundele R, Morrison H, Jeppesen P, Singh PB. Heterochromatin, HP1 and methylation at lysine 9 of histone H3 in animals. *Chromosoma*. 2002 Mar;111(1):22-36.

Csermely P, Kajtar J, Hollosi M, Oikarinen J, Somogyi J. The 90 kDa heat shock protein (hsp90) induces the condensation of the chromatin structure. *Biochem Biophys Res Commun.* 1994 202(3):1657.

Davidson EA. Purification and properties of an endo-alpha-N-acetyl-D-galactosaminidase from *Diplococcus pneumoniae*. *J Biol Chem.* 1977 Dec 10;252(23):8609-14

Davidson RL. Gene expression in somatic cell hybrids. *Annu Rev Genet.* 1974 8:195-218. Review.

Dean W, Bowden L, Aitchison A, Klose J, Moore T, Meneses JJ, Reik W, Feil R. Altered imprinted gene methylation and expression in completely ES cell-derived mouse fetuses: association with aberrant phenotypes. *Development.* 1998 Jun;125(12):2273-82.

Dean W, Ferguson-Smith A. Genomic imprinting: mother maintains methylation marks. *Curr Biol.* 2001 Jul 10;11(13):R527-30.

Dean W, Santos F, Stojkovic M, Zakhartchenko V, Walter J, Wolf E, Reik W. Conservation of methylation reprogramming in mammalian development: aberrant reprogramming in cloned embryos. *Proc Natl Acad Sci U S A.* 2001 Nov 20;98(24):13734-8.

de la Luna, S. & Ortin, J. pac gene as efficient dominant marker and reporter gene in mammalian cells. *Methods Enzymol.* 1992; 216:376-385.

de la Luna S, Soria I, Pulido D, Ortin J, Jimenez A. Efficient transformation of mammalian cells with constructs containing a puromycin-resistance marker. *Gene.* 1988;62(1):121-6.

Dilworth SM, Black SJ, Laskey RA. Two complexes that contain histones are required for nucleosome assembly in vitro: role of nucleoplasmin and N1 in *Xenopus* egg extracts. *Cell.* 1987 Dec 24;51(6):1009-18.

Dimitrov S, Wolffe AP. Remodeling somatic nuclei in *Xenopus laevis* egg extracts: molecular mechanisms for the selective release of histones H1 and H1(0) from chromatin and the acquisition of transcriptional competence. *EMBO J.* 1996 Nov 1;15(21):5897-906.

Dingwall C. Protein structure: plugging the nuclear pore. *Nature.* 1990 Aug 9;346(6284):512-4.

Dingwall C, Laskey RA. Nucleoplasmin: the archetypal molecular chaperone. *Semin Cell Biol.* 1990 Feb;1(1):11-7. Review.

Dingwall C, Dilworth SM, Black SJ, Kearsey SE, Cox LS, Laskey RA. Nucleoplasmin cDNA sequence reveals polyglutamic acid tracts and a cluster of

- sequences homologous to putative nuclear localization signals. *EMBO J.* 1987 Jan;6(1):69-74.
- Doerksen T, Trasler JM. Developmental exposure of male germ cells to 5-azacytidine results in abnormal preimplantation development in rats. *Biol Reprod.* 1996 Nov;55(5):1155-62.
- Doherty AS, Mann MR, Tremblay KD, Bartolomei MS, Schultz RM. Differential effects of culture on imprinted H19 expression in the preimplantation mouse embryo. *Biol Reprod.* 2000 Jun;62(6):1526-35.
- Dorer DR. Do transgene arrays form heterochromatin in vertebrates? *Transgenic Res.* 1997 Jan;6(1):3-10. Review.
- Draetta G, Beach D. (1988) Activation of cdc2 protein kinase during mitosis in human cells: cell cycle-dependent phosphorylation and subunit rearrangement. *Cell.* Jul 1;54(1):17-26.
- Draetta G, Luca F, Westendorf J, Brizuela L, Ruderman J, Beach D. (1989) Cdc2 protein kinase is complexed with both cyclin A and B: evidence for proteolytic inactivation of MPF. *Cell.* Mar 10;56(5):829-38.
- Duran C, Talley PJ, Walsh J, Pigott C, Morton IE, Andrews PW. Hybrids of pluripotent and nullipotent human embryonal carcinoma cells: partial retention of a pluripotent phenotype. *Int J Cancer.* 2001 Aug 1;93(3):324-32.
- Earnshaw WC, Honda BM, Laskey RA, Thomas JO. (1980) Assembly of nucleosomes: the reaction involving *X. laevis* nucleoplasmin. *Cell.* Sep;21(2):373-83.
- Eggan, K., Akutsu, H., Hochedlinger, K., Rideout, W., Yanagimachi, R., and Jaenisch, R. X-Chromosome inactivation in cloned mouse embryos. *Science* 2000. 290, 1578-1581.
- Eggan, K., Akutsu, H., Loring, J., Jackson-Grusby, L., Klemm, M., Rideout, W. M., 3rd, Yanagimachi, R., and Jaenisch, R. Hybrid vigor, fetal overgrowth, and viability of mice derived by nuclear cloning and tetraploid embryo complementation. *Proc Natl Acad Sci U S A.* 2001. 98, 6209-6214.
- Eggan, K., Rode, A., Jentsch, I., Samuel, C., Hennek, T., Tintrup, H., Zevnik, B., Erwin, J., Loring, J., Jackson-Grusby, L., et al.. Male and female mice derived from the same embryonic stem cell clone by tetraploid embryo complementation. *Nat Biotechnol* 2002 20, 455-459.
- Ekker M, Ye F, Joly L, Tellis P, Chevrette M. Zebrafish/mouse somatic cell hybrids for the characterization of the zebrafish genome. *Methods Cell Biol.* 1999 60:303-21.



Ekker M, Speevak MD, Martin CC, Joly L, Giroux G, Chevrette M Stable transfer of zebrafish chromosome segments into mouse cells. *Genomics*. 1996 Apr 1;33(1):57-64.

Englen MD, Finnell RH. Strain differences in expression of the murine heat shock response: implications for abnormal neural development. *Results Probl Cell Differ*. 1991 17:71-82.

Evans MJ, Kaufman MH. Establishment in culture of pluripotential cells from mouse embryos. *Nature*. 1981 Jul 9;292(5819):154-6.

Eyestone WH, Campbell KH. Nuclear transfer from somatic cells: applications in farm animal species. *J Reprod Fertil Suppl* 1999 54:489.

Fan Y, Sirotkin A, Russell RG, Ayala J, Skoultchi AI. Individual somatic H1 subtypes are dispensable for mouse development even in mice lacking the H1(0) replacement subtype. *Mol Cell Biol*. 2001 Dec;21(23):7933-43.

Finaz C, Lefevre A, Teissie J Electrofusion. A new, highly efficient technique for generating somatic cell hybrids. *Exp Cell Res*. 1984 Feb;150(2):477-82.

Finch BW, Ephrussi B. Retention of multiple developmental potentialities by cells of a mouse testicular teratocarcinomas during prolonged culture in vitro and their extinction upon hybridization with cells of permanent cell lines. *Proc. Mat. Acad. Sci. (USA)*, 1967 Mar 15, 57(3): 615-621.

Fedorov LM, Haegel-Kronenberger H, Hirchenhain J.A comparison of the germline potential of differently aged ES cell lines and their transfected descendants. *Transgenic Res* 1997 May;6(3):223-31.

Feil R, Khosla S. Genomic imprinting in mammals: an interplay between chromatin and DNA methylation? *Trends Genet*. 1999 Nov;15(11):431-5. Review.

Feinberg MR, Bhaskar AG, Bourne P. Differential diagnosis of malignant lymphomas by imprint cytology. *Acta Cytol*. 1980 24(1):16-25.

Fowlkes BJ, Pardoll DM. Molecular and cellular events of T cell development. *Adv Immunol*. 1989;44:207-64.

Freshney R I .*Culture of Animal Cells* 2nd Edition 1987 Pub. Alan R. Liss, Inc., New York P324.

Fu G, Ghadam P, Sirotkin A, Khochbin S, Skoultchi AI, Clarke HJ. Mouse oocytes and early embryos express multiple histone h1 subtypes. *Biol Reprod*. 2003 May;68(5):1569-76.

Fulka J Jr, First NL, Moor RM. Nuclear transplantation in mammals: remodelling of transplanted nuclei under the influence of maturation promoting factor. *Bioessays*. 1996 Oct;18(10):835-40.

Funderburgh JL, Funderburgh ML, Mann MM, Corpuz L, Roth MR. Proteoglycan expression during transforming growth factor beta -induced keratocyte-myofibroblast transdifferentiation. *J Biol Chem*. 2001 276(47):44173-8.

Furth PA, St Onge L, Boger H, Gruss P, Gossen M, Kistner A, Bujard H, Hennighausen L. Temporal control of gene expression in transgenic mice by a tetracycline-responsive promoter. *Proc Natl Acad Sci U S A*. 1994 Sep 27;91(20):9302-6.

Galand P, Degraef C Cyclin/PCNA immunostaining as an alternative to tritiated thymidine pulse labelling for marking S phase cells in paraffin sections from animal and human tissues. *Cell Tissue Kinet* 1989 22(5):383-92.

Galli C, Lagutina I, Crotti G, Colleoni S, Turini P, Ponderato N, Duchi R, Lazzari G. Pregnancy: a cloned horse born to its dam twin. *Nature*. 2003 Aug 7;424(6949):635.

Gao S, McGarry M, Ferrier T, Pallante B, Gasparrini B, Fletcher J, Harkness L, De Sousa P, McWhir J, Wilmut I. Effect of cell confluence on production of cloned mice using an inbred embryonic stem cell line. *Biol Reprod* 2003 Feb;68(2):595-603

Garrido C, Ottavi P, Fromentin A, Hammann A, Arrigo AP, Chauffert B, Mehlen P. HSP27 as a mediator of confluence-dependent resistance to cell death induced by anticancer drugs. *Cancer Res*. 1997 Jul 1;57(13):2661-7.

Gautier J, Minshull J, Lohka M, Glotzer M, Hunt T, Maller JL. Cyclin is a component of maturation-promoting factor from *Xenopus*. *Cell*. 1990 Feb 9;60(3):487-94.

Geiger H, Sick S, Bonifer C, Muller AM. Globin gene expression is reprogrammed in chimeras generated by injecting adult hematopoietic cells into mouse blastocysts. *Cell*. 1998 Jun 12;93(6):1055-65.

Gilbert SF (Editor) *Developmental Biology* 4<sup>th</sup> Ed. 1997 Sinauer Associates Inc. Publishers Part 1 Principles of Development in Biology.

Girard F, Strausfeld U, Fernandez A, Lamb NJ. Cyclin A is required for the onset of DNA replication in mammalian fibroblasts. *Cell*. 1991 Dec 20;67(6):1169-79.

Giles RE, Ruddle FH. Production of Sendai virus for cell fusion. *In Vitro* 1973 9:103-7

Ginsburg M, Snow MH, McLaren A. Primordial germ cells in the mouse embryo during gastrulation. *Development*. 1990 Oct;110(2):521-8.

- Glotzer M, Murray AW, Kirschner MW. Cyclin is degraded by the ubiquitin pathway. *Nature*. 1991 Jan 10;349(6305):132-8.
- Gomez MC, Jenkins JA, Giraldo A, Harris RF, King A, Dresser BL, Pope CE. Nuclear transfer of synchronized african wild cat somatic cells into enucleated domestic cat oocytes. *Biol Reprod*. 2003 Sep;69(3):1032-41.
- Gossen M, Freundlieb S, Bender G, Muller G, Hillen W, Bujard H. Transcriptional activation by tetracyclines in mammalian cells. *Science*. 1995 Jun 23;268(5218):1766-9.
- Gossen M, Bujard H. Tight control of gene expression in mammalian cells by tetracycline-responsive promoters. *Proc Natl Acad Sci U S A*. 1992 Jun 15;89(12):5547-51.
- Graves JA, Gartler SM. Mammalian X chromosome inactivation: testing the hypothesis of transcriptional control. *Somat Cell Mol Genet*. 1986 May;12(3):275-80.
- Gurdon JB. Adult frogs derived from the nuclei of single somatic cells. *Dev Biol*. 1962 Apr; 4: 256-73.
- Gurdon JB. The cytoplasmic control of gene activity. *Endeavour*. 1966 May;25(95):95-9.
- Gurdon, J. B. Changes in somatic cell nuclei inserted into growing and maturing amphibian oocytes. *J. Embryol. Exp. Morphol*. 1968 20: 401- 414.
- Gurdon JB. Molecular biology in a living cell. *Nature*. 1974 Apr 26;248(451):772-6.
- Gurdon, JB and Brown, DD. Cytoplasmic regulation of RNA synthesis and nucleolus formation in developing embryos of *Xenopus laevis*. *J. Mol. Biol*. 1965 12, 27-35.
- Gurdon JB, Byrne JA. The first half-century of nuclear transplantation. *Proc Natl Acad Sci U S A*. 2003 Jul 8;100(14):8048-52.
- Gurdon JB, Laskey RA, Reeves OR. The developmental capacity of nuclei transplanted from keratinized skin cells of adult frogs. *J Embryol Exp Morphol*. 1975 Aug;34(1):93-112.
- Gurdon JB, Uehlinger V. "Fertile" intestine nuclei. *Nature*. 1966 Jun 18;210(42):1240-1.
- Haig D. Multiple paternity and genomic imprinting. *Genetics* 1999 151:1229

Hajkova P, Erhardt S, Lane N, Haaf T, El-Maarri O, Reik W, Walter J, Surani MA. Epigenetic reprogramming in mouse primordial germ cells. *Mech Dev.* 2002 Sep;117(1-2):15-23.

Hakelien AM, Landsverk HB, Robl JM, Skalhegg BS, Collas P. Reprogramming fibroblasts to express T-cell functions using cell extracts. *Nat Biotechnol.* 2002 20(5):460-6

Hall JG. How imprinting is relevant to human disease. *Dev Suppl.* 1990 12:141-8. Review.

Hark AT, Schoenherr CJ, Katz DJ, Ingram RS, Levorse JM, Tilghman SM. CTCF mediates methylation-sensitive enhancer-blocking activity at the H19/Igf2 locus. *Nature.* 2000 May 25;405(6785):486-9.

Harley CB. Telomere loss: mitotic clock or genetic time bomb? *Mutat Res.* 1991 Mar-Nov;256(2-6):271-82. Review.

Harris H, Watkins JF. Hybrid cells derived from mouse and man: artificial heterokaryons of mammalian cells from different species. *Nature.* 1965 Feb 13; 205: 640-6.

Harris H, Watkins JF, Campbell GL, Evans EP, Ford CE Mitosis in hybrid cells derived from mouse and man. *Nature* 1965 207(997):606-8.

Hart IR Tumor cell hybridization and neoplastic progression. *Symp Fundam Cancer Res* 1983 36:133

Hartwell Cell cycle control (Eds. Hutchison & Glover) 1995 IRL Press Chapter 1 Introduction to cell cycle control.

Hatada I, Mukai T. Genomic imprinting and human disease--toward the elucidation of the imprinting mechanism. *Seikagaku.* 1997 Dec;69(12):1378-84. Review.

Helmbrecht K, Zeise E, Rensing L. Chaperones in cell cycle regulation and mitogenic signal transduction: a review. *Cell Prolif.* 2000 Dec;33(6):341-65.

Henderson JK, Draper JS, Baillie HS, Fishel S, Thomson JA, Moore H, Andrews PW. Preimplantation human embryos and embryonic stem cells show comparable expression of stage-specific embryonic antigens. *Stem Cells.* 2002;20(4):329-37.

Herr W, Sturm RA, Clerc RG, Corcoran LM, Baltimore D, Sharp PA, Ingraham HA, Rosenfeld MG, Finney M, Ruvkun G, et al. The POU domain: a large conserved region in the mammalian pit-1, oct-1, oct-2, and *Caenorhabditis elegans* unc-86 gene products. *Genes Dev.* 1988 Dec;2(12A):1513-6.

Hightower LE. Cultured animal cells exposed to amino acid analogues or puromycin rapidly synthesize several polypeptides. *Cell Physiol.* 1980 Mar;102(3):407-27.

Hill DA. Influence of linker histone H1 on chromatin remodeling. *Biochem Cell Biol.* 2001;79(3):317-24.

Hirata R, Chamberlain J, Dong R, Russell DW. Targeted transgene insertion into human chromosomes by adeno-associated virus vectors. *Nat Biotechnol.* 2002 Jul;20(7):735-8.

Hiyama K, Hirai Y, Kyoizumi S, Akiyama M, Hiyama E, Piatyszek MA, Shay JW, Ishioka S, Yamakido M. Activation of telomerase in human lymphocytes and hematopoietic progenitor cells. *J Immunol.* 1995 Oct 15;155(8):3711-5.

Hochedlinger K, Jaenisch R. Monoclonal mice generated by nuclear transfer from mature B and T donor cells. *Nature.* 2002 Feb 28;415(6875):1035-8.

Hoess RH, Abremski K. Interaction of the bacteriophage P1 recombinase Cre with the recombining site loxP. *Proc Natl Acad Sci U S A.* 81(4):1026-9.

Hogan BL. Changes in the behaviour of teratocarcinoma cells cultivated in vitro. *Nature.* 1976 Sep 9;263(5573):136-7.

Holliday R, Pugh JE. DNA modification mechanisms and gene activity during development. *Science.* 1975 Jan 24;187(4173):226-32.

Homma M, Tashiro M. Cell fusion by hemagglutinating virus of Japan *Nippon Saikingaku Zasshi.* 1979 Nov;34(6):779-95.

Hooper M L "Embryonal stem cells: introducing planned changes into the animal germline" 1992 Harwood Academic Publishers. Chapter 2

Hope RM, Graves JA. Fusion and hybridization of marsupial and eutherian cells. V. Development of selective systems. *Aust J Biol Sci.* 1978 Jun;31(3):293-301.

Hu E, Tontonoz P, Spiegelman BM. Transdifferentiation of myoblasts by the adipogenic transcription factors PPAR gamma and C/EBP. *Proc Natl Acad Sci USA* 1995 92(21):9856-60

Huang S, Ingber DE. The structural and mechanical complexity of cell-growth control. *Nat Cell Biol.* 1999 Sep;1(5):E131-8. Review.

Ianus A, Holz GG, Theise ND, Hussain MA. In vivo derivation of glucose-competent pancreatic endocrine cells from bone marrow without evidence of cell fusion. *J Clin Invest.* 2003 Mar;111(6):843-50.

Iliakis GE, Pantelias GE. Effects of hyperthermia on chromatin condensation and nucleoli disintegration as visualized by induction of premature chromosome condensation in interphase mammalian cells. *Cancer Res.* 1989 Mar 1;49(5):1254-60.

Illmensee K, Hoppe PC. (1981) Nuclear transplantation in *Mus musculus*: developmental potential of nuclei from preimplantation embryos. *Cell*. Jan;23(1):9-18.

Iwata K, Hozumi K, Iihara A, Nomizu M, Sakairi N, Nishi N. Mechanism of salmon sperm decondensation by nucleoplasmin. *Int J Biol Macromol*. 1999 Nov;26(2-3):95-101.

Itagaki H, Doi H, Ohkohchi N, Satomi S. Development of new cell fusion technique by laser device and application to bio-medical field *Nippon Rinsho*. 1997 Oct;55(10):2780-7. Review.

Itskovitz-Eldor J, Schuldiner M, Karsenti D, Eden A, Yanuka O, Amit M, Soreq H, Benvenisty N. (2000) Differentiation of human embryonic stem cells into embryoid bodies compromising the three embryonic germ layers. *Mol Med*. Feb;6(2):88-95.

James RM, Klerkx AH, Keighren M, Flockhart JH, West JD. (1995) Restricted distribution of tetraploid cells in mouse tetraploid $\leftrightarrow$ diploid chimaeras. *Dev Biol*. 167(1):213-26.

Jarozeski MJ, Gilbert R, Heller R. (1994) Flow cytometric detection and quantitation of cell-cell electrofusion products. *Methods Mol Biol*. 91:149-56.

Jahn R, Grubmuller H. Membrane fusion. *Curr Opin Cell Biol*. 2002 Aug;14(4):488-95. Review.

Jeppesen P, Turner BM. The inactive X chromosome in female mammals is distinguished by a lack of histone H4 acetylation, a cytogenetic marker for gene expression. *Cell*. 1993 Jul 30;74(2):281-9.

Johnson RT, Rao PN. (1970) Mammalian cell fusion: induction of premature chromosome condensation in interphase nuclei. *Nature*. May 23;226(247):717-22.

Johnson RT, Rao PN. Nucleo-cytoplasmic interactions in the achievement of nuclear synchrony in DNA synthesis and mitosis in multinucleate cells. *Biol Rev Camb Philos Soc*. 1971 Feb;46(1):97-155. Review.

Johnston LH, Game JC. Mutants of yeast with depressed DNA synthesis. *Mol Gen Genet*. 1978 May 3;161(2):205-14.

Jornot L, Mirault ME, Junod AF. Differential expression of hsp70 stress proteins in human endothelial cells exposed to heat shock and hydrogen peroxide. *Am J Respir Cell Mol Biol*. 1991 Sep;5(3):265-75.

Jones DO, Cowell IG, Singh PB. Mammalian chromodomain proteins: their role in genome organisation and expression. *Bioessays*. 2000 Feb;22(2):124-37. Review.



- Jones KA, Kadonaga JT. (2000) Exploring the transcription-chromatin interface. *Genes Dev.* Aug 15;14(16):1992-6.
- Kafri T, Ariel M, Brandeis M, Shemer R, Urven L, McCarrey J, Cedar H, Razin A. Developmental pattern of gene-specific DNA methylation in the mouse embryo and germ line. *Genes Dev.* 1992 May;6(5):705-14.
- Kalinich JF, McClain DE. Rapid isolation of nuclear transport-competent *Xenopus* nucleoplasm produced in *Escherichia coli* strain BL21(DE3). *Protein Expr Purif.* 1994 Aug;5(4):324-30.
- Kalinich JF, Douglas MG. In vitro translocation through the yeast nuclear envelope. Signal-dependent transport requires ATP and calcium. *J Biol Chem.* 1989 Oct 25;264(30):17979-89.
- Kanamori H, Siegel JN. Induction of erythroid gene expression by microcell fusion. *Exp Cell Res.* 1997 Apr 10;232(1):90-6.
- Kass SU, Wolffe AP. DNA methylation, nucleosomes and the inheritance of chromatin structure and function. *Novartis Found Symp.* 1998 214:22-35. Review.
- Kato Y, Tani T, Sotomaru Y, Kurokawa K, Kato J, Doguchi H, Yasue H, Tsunoda Y 1998 *Science* 282:2095.
- Kelly SJ. Studies of the developmental potential of 4- and 8-cell stage mouse blastomeres. *J Exp Zool.* 1977 Jun;200(3):365-76.
- Khochbin S. Histone H1 diversity: bridging regulatory signals to linker histone function. *Gene.* 2001 Jun 13;271(1):1-12.
- Khochbin S, Wolffe AP. Developmentally regulated expression of linker-histone variants in vertebrates. *Eur J Biochem.* 1994 Oct 15;225(2):501-10.
- Kikyo N, Wolffe AP. Reprogramming nuclei: insights from cloning, nuclear transfer and heterokaryons. *J Cell Sci.* 2000 Jan;113 ( Pt 1):11-20. Review.
- Kilby NJ, Snaith MR, Murray JA. Site-specific recombinases: tools for genome engineering. *Trends Genet.* 1993 9(12):413-21. Review.
- Kill IR, Bridger JM, Campbell KH, Maldonado-Codina G, Hutchison CJ. The timing of the formation and usage of replicase clusters in S-phase nuclei of human diploid fibroblasts. *J Cell Sci.* 1991 100:869-76.
- Kimura M, Takatsuki A, Yamaguchi I. Blasticidin S deaminase gene from *Aspergillus terreus* (BSD): a new drug resistance gene for transfection of mammalian cells. *Biochim Biophys Acta.* 1994 Nov 22;1219(3):653-9.

- Kingston RE, Narlikar GJ. ATP-dependent remodeling and acetylation as regulators of chromatin fluidity. *Genes Dev.* 1999 Sep 15;13(18):2339-52.
- Kleinsmith LJ, Pierce GB (1964) Multipotentiality of single embryonal carcinoma cells. *Cancer Res.* 24, 1544-1549.
- Korn LJ, Gurdon JB, Price J. (1982) Oocyte extracts reactivate developmentally inert *Xenopus* 5S genes in somatic nuclei. *Nature.* Nov 25;300(5890):354-5.
- Kornberg RD, Lorch Y. Chromatin and transcription: where do we go from here. *Curr Opin Genet Dev.* 2002 Apr;12(2):249-51.
- Kouzarides T. Histone methylation in transcriptional control. *Curr Opin Genet Dev.* 2002 Apr;12(2):198-209.
- Krishan A. Rapid flow cytofluorometric analysis of mammalian cell cycle by propidium iodide staining. *J Cell Biol.* 1975 Jul;66(1):188-93.
- Krohne G, Franke WW. A major soluble acidic protein located in nuclei of diverse vertebrate species. *Exp Cell Res.* 1980 Sep;129(1):167-89.
- Lange, K., Uckert, W., Blankenstein, T., Nadrowitz, R., Bittner, C., Renaud, J.C., van Snick, J., Feller, A.C. and Merz, H. Overexpression of NPM-ALK induces different types of malignant lymphomas in IL-9 transgenic mice. *Oncogene* 2003; 22 (4), 517-527.
- Langst G, Becker PB. Nucleosome mobilization and positioning by ISWI-containing chromatin-remodeling factors. *J Cell Sci.* 2001 Jul;114(Pt 14):2561-8.
- Lanza RP, Cibelli JB, Blackwell C, Cristofalo VJ, Francis MK, Baerlocher GM, Mak J, Schertzer M, Chavez EA, Sawyer N, Lansdorp PM, West MD. Extension of cell life-span and telomere length in animals cloned from senescent somatic cells. *Science.* 2000 Apr 28;288(5466):665-9.
- Laskey RA, Honda BM, Mills AD, Finch JT. Nucleosomes are assembled by an acidic protein which binds histones and transfers them to DNA. *Nature.* 1978 Oct 5;275(5679):416-20.
- Lebkowski, J.S., Gold, J., Xu, C., Funk, W., Chiu, C.P., Carpenter, M.K. Human embryonic stem cells: culture, differentiation, and genetic modification for regenerative medicine applications. 2001 *Cancer J. Suppl.*, 2: S83-93.
- Lefebvre L, Viville S, Barton SC, Ishino F, Keverne EB, Surani MA. Abnormal maternal behaviour and growth retardation associated with loss of the imprinted gene *Mest*. *Nat Genet.* 1998 Oct;20(2):163-9.
- Lee J, Inoue K, Ono R, Ogonuki N, Kohda T, Kaneko-Ishino T, Ogura A, Ishino F. Erasing genomic imprinting memory in mouse clone embryos produced from day 11.5 primordial germ cells. *Development.* 2002 Apr;129(8):1807-17.

- Lee JT, Jaenisch R. Long-range cis effects of ectopic X-inactivation centres on a mouse autosome. *Nature*. 1997 Mar 20;386(6622):275-9.
- Lee G, Saito I. Role of nucleotide sequences of loxP spacer region in Cre-mediated recombination. 1998 *Gene*. 216(1):55-65.
- Lenardo MJ, Staudt L, Robbins P, Kuang A, Mulligan RC, Baltimore D. (1989) Repression of the IgH enhancer in teratocarcinoma cells associated with a novel octamer factor. *Science*. Jan 27;243(4890):544-6.
- Leno GH, Mills AD, Philpott A, Laskey RA. (1996) Hyperphosphorylation of nucleoplasmin facilitates *Xenopus* sperm decondensation at fertilization. *J Biol Chem*. Mar 29;271(13):7253-6.
- Levy MZ, Allsopp RC, Futcher AB, Greider CW, Harley CB. Telomere end-replication problem and cell aging. *J Mol Biol*. 1992 Jun 20;225(4):951-60.
- Li E, Beard C, Jaenisch R. Role for DNA methylation in genomic imprinting. *Nature*. 1993 Nov 25;366(6453):362-5.
- Li GC, Laszlo A. Amino acid analogs while inducing heat shock proteins sensitize CHO cells to thermal damage. *J Cell Physiol*. 1985 Jan;122(1):91-7.
- Li GC, Werb Z. Correlation between synthesis of heat shock proteins and development of thermotolerance in Chinese hamster fibroblasts. 1982 *PNAS* 79:3218-3222.
- Lindsey J, McGill NI, Lindsey LA, Green DK, Cooke HJ. In vivo loss of telomeric repeats with age in humans. 1991 *Mutat Res*. 256(1):45-8.
- Lindquist S, Craig EA. The heat-shock proteins. (1988) *Annu Rev Genet*. 22:631-77. Review.
- Lo AW, Sprung CN, Fouladi B, Pedram M, Sabatier L, Ricoul M, Reynolds GE, Murnane JP. Chromosome instability as a result of double-strand breaks near telomeres in mouse embryonic stem cells. *Mol Cell Biol*. 2002 Jul;22(13):4836-50.
- Lohka MJ, Masui Y. 1984 Roles of cytosol and cytoplasmic particles in nuclear envelope assembly and sperm pronuclear formation in cell-free preparations from amphibian eggs. *J Cell Biol*. Apr;98(4):1222-30.
- Lohka MJ, Hayes MK, Maller JL. Purification of maturation-promoting factor, an intracellular regulator of early mitotic events. *Proc Natl Acad Sci U S A*. 1988 May;85(9):3009-13.
- Lohka MJ, Masui Y. Roles of cytosol and cytoplasmic particles in nuclear envelope assembly and sperm pronuclear formation in cell-free preparations from amphibian eggs. *J Cell Biol*. 1984 Apr;98(4):1222-30.

Loi P, Clinton M, Barboni B, Fulka J Jr, Cappai P, Feil R, Moor RM, Ptak G. Nuclei of nonviable ovine somatic cells develop into lambs after nuclear transplantation. *Biol Reprod.* 2002 Jul;67(1):126-32.

Longo L, Bygrave A, Grosveld FG, Pandolfi PP. The chromosome make-up of mouse embryonic stem cells is predictive of somatic and germ cell chimaerism. *Transgenic Res* 1997 Sep;6(5):321-8.

Lu ZH, Xu H, Leno GH. (1999) DNA replication in quiescent cell nuclei: regulation by the nuclear envelope and chromatin structure. *Mol Biol Cell.* Dec;10(12):4091-106.

Ludwig T, Eggenschwiler J, Fisher P, D'Ercole AJ, Davenport ML, Efstratiadis A. Mouse mutants lacking the type 2 IGF receptor (IGF2R) are rescued from perinatal lethality in *Igf2* and *Igf1r* null backgrounds. *Dev Biol.* 1996 Aug 1;177(2):517-35.

MacArthur, C.A. and Shackleford, G.M. *Npm3*: a novel, widely expressed gene encoding a protein related to the molecular chaperones nucleoplasmin and nucleophosmin. *Genomics* 1997; 42 (1), 137-140.

Mack A, Sauer B, Abremski K, Hoess R. Stoichiometry of the Cre recombinase bound to the lox recombining site. *Nucleic Acids Res.* 1992 20(17):4451-5.

Magin TM, McEwan C, Milne M, Pow AM, Selfridge J, Melton DW. A position- and orientation-dependent element in the first intron is required for expression of the mouse *hprt* gene in embryonic stem cells. *Gene.* 1992 Dec 15;122(2):289-96.

Martin GR. (1981) Isolation of a pluripotent cell line from early mouse embryos cultured in medium conditioned by stem cells. *Proc Natl Acad Sci U S A.* Dec;78(12):7634-8.

Martin GR, Evans MJ. Differentiation of clonal lines of teratocarcinoma cells: formation of embryoid bodies in vitro. *Proc Natl Acad Sci U S A.* 1975 Apr;72(4):1441-5.

Mathew A, Shi Y, Jolly C, Morimoto RI. Analysis of the mammalian heat-shock response. Inducible gene expression and heat-shock factor activity. *Methods Mol Biol.* 2000;99:217-55. Review.

Masui Y, Markert CL. Cytoplasmic control of nuclear behavior during meiotic maturation of frog oocytes. *J Exp Zool.* 1971 Jun;177(2):129-45.

Matsui Y, Zsebo K, Hogan BL. Derivation of pluripotential embryonic stem cells from murine primordial germ cells in culture. *Cell.* 1992 Sep 4;70(5):841-7.

Mattson MP. Emerging neuroprotective strategies for Alzheimer's disease: dietary restriction, telomerase activation, and stem cell therapy. *Exp Gerontol.* 2000 Jul;35(4):489-502.

Matveeva NM, Shilov AG, Kaftanovskaya EM, Maximovsky LP, Zhelezova AI, Golubitsa AN, Bayborodin SI, Fokina MM, Serov OL. In vitro and in vivo study of pluripotency in intraspecific hybrid cells obtained by fusion of murine embryonic stem cells with splenocytes. *Mol Reprod Dev.* 1998 Jun;50(2):128-38.

Mayer W, Niveleau A, Walter J, Fundele R, Haaf T. Demethylation of the zygotic paternal genome. *Nature.* 2000 Feb 3;403(6769):501-2.

McAteer JA, Douglas WHJ, Jakoby, Cell Culture. *Methods in Enzymology Volume LVIII.* Academic Press, New York. Eds. W. B. and Pastan, I. H. 1979. Chapter 10: Monolayer Culture Techniques pp132-134.

McBurney MW, Mai T, Yang X, Jardine K. Evidence for repeat-induced gene silencing in cultured Mammalian cells: inactivation of tandem repeats of transfected genes. *Exp Cell Res.* 2002; 274(1):1-8.

McGrath J, Solter D. Inability of mouse blastomere nuclei transferred to enucleated zygotes to support development in vitro. *Science.* 1984 Dec 14;226(4680):1317-9.

McWhir J, Schnieke AE, Ansell R, Wallace H, Colman A, Scott AR, Kind AJ. Selective ablation of differentiated cells permits isolation of embryonic stem cell lines from murine embryos with a non-permissive genetic background. *Nat Genet.* 1996 Oct;14(2):223-6.

Mermoud JE, Costanzi C, Pehrson JR, Brockdorff N. Histone macroH2A1.2 relocates to the inactive X chromosome after initiation and propagation of X-inactivation. *J Cell Biol.* 1999 Dec 27;147(7):1399-408.

Metzger D, Feil R. Engineering the mouse genome by site-specific recombination. *Curr Opin Biotechnol.* 1999 Oct;10(5):470-6. Review.

Mohler WA, Blau HM. Membrane-bound neomycin phosphotransferase confers drug-resistance in mammalian cells: a marker for high-efficiency targeting of genes encoding secreted and cell-surface proteins. *Somat Cell Mol Genet.* 1994 May;20(3):153-62.

Monk M. Methylation and the X chromosome. *Bioessays.* 1986 May;4(5):204-8.

Monk M, Boubelik M, Lehnert S. Temporal and regional changes in DNA methylation in the embryonic, extraembryonic and germ cell lineages during mouse embryo development. *Development.* 1987 Mar;99(3):371-82.



- Moore T. Genetic conflict, genomic imprinting and establishment of the epigenotype in relation to growth. *Reproduction*. 2001 122(2):185-93. Review.
- Moore T, Constancia M, Zubair M, Bailleul B, Feil R, Sasaki H, Reik W. Multiple imprinted sense and antisense transcripts, differential methylation and tandem repeats in a putative imprinting control region upstream of mouse *Igf2*. 1997 *Proc Natl Acad Sci U S A*. 94(23):12509-14.
- Moore T, Haig D. Genomic imprinting in mammalian development: a parental tug-of-war. *Trends Genet*. 1991 7(2):45-9. Review.
- Moreau N, Angelier N, Bonnanfant-Jais ML, Gounon P, Kubisz P. Association of nucleoplasmin with transcription products as revealed by immunolocalization in the amphibian oocyte. *J Cell Biol*. 1986 Sep;103(3):683-90.
- Morrison SJ. Stem cell potential: can anything make anything? *Curr Biol*. 2001; 11(1):R7-9
- Monk M. Methylation and the X chromosome. *Bioessays*. 1986 May;4(5):204-8.
- Monk M, Boubelik M, Lehnert S. Temporal and regional changes in DNA methylation in the embryonic, extraembryonic and germ cell lineages during mouse embryo development. *Development*. 1987 Mar;99(3):371-82.
- Muller C, Leutz A. Chromatin remodeling in development and differentiation. *Curr Opin Genet Dev*. 2001 Apr;11(2):167-74.
- Munro S, Pelham H. What turns on heat shock genes? *Nature*. 1985 Oct 10-16;317(6037):477-8.
- Murray A, Hunt T The cell cycle: an introduction. Oxford University Press, Inc (1993) ISBN 0-19-509529-4
- Murray AW, Solomon MJ, Kirschner MW. The role of cyclin synthesis and degradation in the control of maturation promoting factor activity. *Nature*. 1989 339(6222):280-6.
- Neuer A, Spandorfer SD, Giraldo P, Dieterle S, Rosenwaks Z, Witkin SS. The role of heat shock proteins in reproduction. *Hum Reprod Update*. 2000 Mar-Apr;6(2):149-59. Review.
- Nichols J, Zevnik B, Anastassiadis K, Niwa H, Klewe-Nebenius D, Chambers I, Scholer H, Smith A. Formation of pluripotent stem cells in the mammalian embryo depends on the POU transcription factor Oct4. *Cell*. 1998 Oct 30;95(3):379-91.
- Ning Y, Pereira-Smith OM. Molecular genetic approaches to the study of cellular senescence. *Mutat Res*. 1991 Mar-Nov;256(2-6):303-10.



Niwa H, Miyazaki J, Smith AG. 2000 Quantitative expression of Oct-3/4 defines differentiation, dedifferentiation or self-renewal of ES cells. *Nat Genet.* Apr;24(4):372-6.

Nover L. HSFs and HSPs--a stressful program on transcription factors and chaperones. *Stress Proteins and the Heat Shock Response.* New Biol. 1991; Sep;3(9):855-9.

Okano M, Bell DW, Haber DA, Li E. DNA methyltransferases Dnmt3a and Dnmt3b are essential for de novo methylation and mammalian development. *Cell.* 1999 Oct 29;99(3):247-57.

Okamoto K, Okazawa H, Okuda A, Sakai M, Muramatsu M, Hamada H A novel octamer binding transcription factor is differentially expressed in mouse embryonic cells. 1990 *Cell* 60:461-72.

Okazawa H, Okamoto K, Ishino F, Ishino-Kaneko T, Takeda S, Toyoda Y, Muramatsu M, Hamada H The oct3 gene, a gene for an embryonic transcription factor, is controlled by a retinoic acid repressible enhancer. *EMBO J.* 1991; 10:2997-3005

Olovnikov AM. A theory of marginotomy. The incomplete copying of template margin in enzymic synthesis of polynucleotides and biological significance of the phenomenon. *J Theor Biol.* 1973 Sep 14;41(1):181-90.

O'Neill RJ, O'Neill MJ, Graves JA. Undermethylation associated with retroelement activation and chromosome remodelling in an interspecific mammalian hybrid. (1998) *Nature.* 393(6680):68-72.

Oswald J, Engemann S, Lane N, Mayer W, Olek A, Fundele R, Dean W, Reik W, Walter J. Active demethylation of the paternal genome in the mouse zygote. *Curr Biol.* 2000 Apr 20;10(8):475-8.

Pagano M, Pepperkok R, Verde F, Ansorge W, Draetta G. Cyclin A is required at two points in the human cell cycle. *EMBO J.* 1992 Mar;11(3):961-71.

Pallante B Effect of quiescence on development and epigenetic status of cloned embryos. 2002 University of Edinburgh PhD Thesis.

Palmieri SL, Peter W, Hess H, Schöler HR. Oct-4 transcription factor is differentially expressed in the mouse embryo during establishment of the first two extraembryonic cell lineages involved in implantation. *Dev Biol.* 1994 Nov;166(1):259-67.

Pan GJ, Chang ZY, Schöler HR, Pei D. Stem cell pluripotency and transcription factor Oct4. *Cell Res.* 2002 Dec;12(5-6):321-9.

Parseghian MH, Hamkalo BA. A compendium of the histone H1 family of somatic subtypes: an elusive cast of characters and their characteristics. *Biochem Cell Biol.* 2001;79(3):289-304.

Pells S, Di Domenico AI, Callagher EJ, McWhir J. Multipotentiality of neuronal cells after spontaneous fusion with embryonic stem cells and nuclear reprogramming in vitro. *Cloning Stem Cells*. 2002;4(4):331-8.

Perreault SD. Chromatin remodeling in mammalian zygotes. *Mutat Res* 1992 Dec; 296(1-2):43-55. Review.

Pesce M, Gross MK, Schöler HR. In line with our ancestors: Oct-4 and the mammalian germ. *Bioessays*. 1998 Sep;20(9):722-32. Review.

Pesce M, Anastassiadis K, Schöler HR. Oct-4: lessons of totipotency from embryonic stem cells. *Cells Tissues Organs*. 1999 165(3-4):144-52. Review.

Pesce M, Schöler HR. Oct-4: control of totipotency and germline determination. *Mol Reprod Dev*. 2000; 55(4):452-7.

Pesce M, Schöler HR. Oct-4: gatekeeper in the beginnings of mammalian development. *Stem Cells*. 2001;19(4):271-8.

Peterson JA, Weiss MC. Expression of differentiated functions in hepatoma cell hybrids: induction of mouse albumin production in rat hepatoma-mouse fibroblast hybrids. *Proc Natl Acad Sci U S A*. 1972 69(3):571-5.

Pikarsky E, Sharir H, Ben-Shushan E, Bergman Y. Retinoic acid represses Oct-3/4 gene expression through several retinoic acid-responsive elements located in the promoter-enhancer region. *1994 Mol Cell Biol*. Feb;14(2):1026-38.

Pines J, Hunter T. The differential localization of human cyclins A and B is due to a cytoplasmic retention signal in cyclin B. *EMBO J*. 1994; 13(16):3772-81.

Pines J, Hunter T. Isolation of a human cyclin cDNA: evidence for cyclin mRNA and protein regulation in the cell cycle and for interaction with p34cdc2. *Cell*. 1989 58(5):833-46.

Pines J. Cyclins and cyclin-dependent kinases: take your partners. *Trends Biochem Sci*. 1993 Jun;18(6):195-7.

Piper J, Granum E. On Fully Automatic Feature Measurement for Banded Chromosome Classification. *Cytometry*. 1989; 10: 242-255.

Pells S, Di Domenico AI, Callagher EJ, McWhir J. Multipotentiality of neuronal cells after spontaneous fusion with embryonic stem cells and nuclear reprogramming in vitro. *Cloning Stem Cells*. 2002;4(4):331-8.

Pikarsky E, Sharir H, Ben-Shushan E, Bergman Y. Retinoic acid represses Oct-3/4 gene expression through several retinoic acid-responsive elements located in the promoter-enhancer region. *Mol Cell Biol*. 1994 Feb;14(2):1026-38.

Polejaeva IA, Chen SH, Vaught TD, Page RL, Mullins J, Ball S, Dai Y, Boone J, Walker S, Ayares DL, Colman A, Campbell KH. Cloned pigs produced by nuclear transfer from adult somatic cells. *Nature*. 2000 Sep 7;407(6800):86-90.

Pontecorvo G. Production of mammalian somatic cell hybrids by means of polyethylene glycol treatment. *Somatic Cell Genet*. 1975 Oct; 1(4): 397-400.

Ohno-Shosaku T, Okada Y. Facilitation of electrofusion of mouse lymphoma cells by the proteolytic action of proteases. *Biochem Biophys Res Commun*. 1984 Apr 16;120(1):138-43.

Ratnam S, Mertineit C, Ding F, Howell CY, Clarke HJ, Bestor TH, Chaillet JR, Trasler JM. Dynamics of Dnmt1 methyltransferase expression and intracellular localization during oogenesis and preimplantation development. *Dev Biol*. 2002 May 15;245(2):304-14.

Razin A, Shemer R. DNA methylation in early development. *Hum Mol Genet*. 1995; 4:1751-5. Review.

Rao PN, Johnson RT. Mammalian cell fusion: studies on the regulation of DNA synthesis and mitosis. *Nature*. 1970 Jan 10;225(228):159-64.

Rao PN, Johnson RT. Mammalian cell fusion. IV. Regulation of chromosome formation from interphase nuclei by various chemical compounds. *J Cell Physiol*. 1971 Oct;78(2):217-23.

Reik W, Dean W, Walter J. Epigenetic reprogramming in mammalian development. *Science*. 2001 Aug 10;293(5532):1089-93. Review.

Reik W, Kelsey G, Walter J. Dissecting de novo methylation. *Nat Genet*. 1999 Dec;23(4):380-2.

Reik W, Surani MA. Cancer genetics. Genomic imprinting and embryonal tumours. *Nature*. 1989 338(6211):112-3.

Reik W, Walter J. Imprinting mechanisms in mammals. *Curr Opin Genet Dev*. 1998 8(2):154-64. Review.

Reik W, Maher ER. Imprinting in clusters: lessons from Beckwith-Wiedemann syndrome. *Trends Genet*. 1997 Aug;13(8):330-4. Review.

Renard JP, Barra J, Babinet C. Action of the paternal genome at the beginning of embryonic development. *Reprod Nutr Dev*. 1988;28(6B):1541-54.

Reubinoff BE, Pera MF, Fong CY, Trounson A, Bongso A. Embryonic stem cell lines from human blastocysts: somatic differentiation in vitro. *Nat Biotechnol*. 2000 Apr;18(4):399-404.

Rideout WM 3rd, Wakayama T, Wutz A, Eggan K, Jackson-Grusby L, Dausman J, Yanagimachi R, Jaenisch R. Generation of mice from wild-type and targeted ES cells by nuclear cloning. *Nat Genet.* 2000 Feb;24(2):109-10.

Richards M, Fong CY, Chan WK, Wong PC, Bongso A. Human feeders support prolonged undifferentiated growth of human inner cell masses and embryonic stem cells. *Nat Biotechnol.* 2002 Sep;20(9):933-6.

Riggs AD. X inactivation, differentiation, and DNA methylation. *Cytogenet Cell Genet.* 1975;14(1):9-25. Review.

Ritossa, F. A new puffing pattern induced by temperature shock and DNP in *Drosophila*. *Experientia* 1962 13:571-573.

Robertson KD, Jones PA. Dynamic interrelationships between DNA replication, methylation, and repair. *Am J Hum Genet.* 1997 Dec;61(6):1220-4. Review.

Rosner MH, Vigano MA, Ozato K, Timmons PM, Poirier F, Rigby PW, Staudt LM. A POU-domain transcription factor in early stem cells and germ cells of the mammalian embryo. *Nature* 1990 Jun 21;345 (6277):686-92.

Rousset JP, Dubois P, Lasserre C, Aviles D, Fellous M, Jami J. Phenotype and surface antigens of mouse teratocarcinoma x fibroblast cell hybrids. *Somatic Cell Genet.* 1979 Nov;5(6):739-52.

Reyes JC, Barra J, Muchardt C, Camus A, Babinet C, Yaniv M. Altered control of cellular proliferation in the absence of mammalian brahma (SNF2alpha). *EMBO J.* 1998 Dec 1;17(23):6979-91.

Santos F, Hendrich B, Reik W, Dean W. Dynamic reprogramming of DNA methylation in the early mouse embryo. *Dev Biol.* 2002 Jan 1;241(1):172-82.

Sathananthan H, Pera M, Trounson A. The fine structure of human embryonic stem cells. *Reprod Biomed Online.* 2002 Jan-Feb;4(1):56-61.

Sauer B. Inducible gene targeting in mice using the Cre/lox system. *Methods.* 1998 14(4):381-92. Review.

Savatier P, Huang S, Szekely L, Wiman KG, Samarut J. Contrasting patterns of retinoblastoma protein expression in mouse embryonic stem cells and embryonic fibroblasts. *Oncogene.* 1994 Mar;9(3):809-18.

Scherthan H, Weich S, Schwegler H, Heyting C, Harle M, Cremer T. Centromere and telomere movements during early meiotic prophase of mouse and man are associated with the onset of chromosome pairing. *J Cell Biol.* 1996 Sep;134(5):1109-25.

Schmidhauser, C., Casperson, G.F., Myers, C.A., Sanzo, K.T., Bolten, S., and Bissell, M.J. 1992. A novel transcriptional enhancer is involved in the prolactin- and

- extracellular matrix-dependent regulation of  $\beta$ -casein gene expression. *Mol. Biol. Cell.* 3:699-709
- Schmidt EE, Taylor DS, Prigge JR, Barnett S, Capecchi MR. Illegitimate Cre-dependent chromosome rearrangements in transgenic mouse spermatids. *Proc Natl Acad Sci U S A.* 2000 97(25):13702-7.
- Schnaider T, Oikarinen J, Ishiwatari-Hayasaka H, Yahara I, Csermely P. Interactions of Hsp90 with histones and related peptides. *Life Sci.* 1999;65(22):2417-26.
- Schöler HR, Ruppert S, Suzuki N, Chowdhury K, Gruss P. New type of POU domain in germ line-specific protein Oct-4. *Nature.* 1990 Mar 29;344(6265):435-9.
- Schöler HR, Balling R, Hatzopoulos AK, Suzuki N, Gruss P. Octamer binding proteins confer transcriptional activity in early mouse embryogenesis. *EMBO J.* 1989 Sep;8(9):2551-7.
- Schoorlemmer J, van Puijenbroek A, van Den Eijnden M, Jonk L, Pals C, Kruijer W. Characterization of a negative retinoic acid response element in the murine Oct4 promoter. *Mol Cell Biol.* 1994 Feb;14(2):1122-36.
- Scott-Taylor TH, Pettengell R, Clarke I, Stuhler G, La Barthe MC, Walden P, Dalglish AG. Human tumour and dendritic cell hybrids generated by electrofusion: potential for cancer vaccines. *Biochim Biophys Acta.* 2000 Mar 17;1500(3):265-79.
- Scherthan H, Weich S, Schwegler H, Heyting C, Harle M, Cremer T. Centromere and telomere movements during early meiotic prophase of mouse and man are associated with the onset of chromosome pairing. *J Cell Biol.* 1996 Sep;134(5):1109-25.
- Schultz RM, Davis W Jr, Stein P, Svoboda P. Reprogramming of gene expression during preimplantation development. *J Exp Zool.* 1999; Oct 15;285(3):276-82. Review.
- Selfridge J, Pow AM, McWhir J, Magin TM, Melton DW. Gene targeting using a mouse HPRT minigene/HPRT-deficient embryonic stem cell system: inactivation of the mouse ERCC-1 gene. *Somat Cell Mol Genet.* 1992; 18(4):325-36.
- Serov O, Matveeva N, Kuznetsov S, Kaftanovskaya E, Mittmann J. Embryonic hybrid cells: a powerful tool for studying pluripotency and reprogramming of the differentiated cell chromosomes. *An Acad Bras Cienc.* 2001 Dec;73(4):561-8. Review.
- Sambrook J., Fritsch E. F. and Maniatis T. *Molecular Cloning: A Laboratory Manual.* 2<sup>nd</sup> Edn. 1989 Cold Spring Harbor Laboratory Press, Cold Spring Harbor, New York, NY.

- Shemer G, Podbilewicz B. The story of cell fusion: big lessons from little worms. *Bioessays*. 2003 Jul;25(7):672-82.
- Shen CN, Slack JM, Tosh D. Molecular basis of transdifferentiation of pancreas to liver. *Nat Cell Biol*. 2000; 2(12):879-87
- Sherman JM, Pillus L. An uncertain silence. *Trends Genet*. 1997 Aug;13(8):308-13. Review.
- Shi W, Haaf T. Aberrant methylation patterns at the two-cell stage as an indicator of early developmental failure. *Mol Reprod Dev*. 2002 Nov;63(3):329-34.
- Shi W, Zakhartchenko V, Wolf E. Epigenetic reprogramming in mammalian nuclear transfer. *Differentiation*. 2003 Mar;71(2):91-113.
- Shibata H, Yoshino K, Sunahara S, Gondo Y, Katsuki M, Ueda T, Kamiya M, Muramatsu M, Murakami Y, Kalcheva I, Plass C, Chapman VM, Hayashizaki Y. Inactive allele-specific methylation and chromatin structure of the imprinted gene *U2af1-rs1* on chromosome 11. *Genomics*. 1996 35(1):248-52.
- Shih TY, Lake RS. Studies on the structure of metaphase and interphase chromatin of Chinese hamster cells by circular dichroism and thermal denaturation. *Biochemistry*. 1972 Dec 5;11(25):4811-7.
- Shimazaki T, Okazawa H, Fujii H, Ikeda M, Tamai K, McKay RD, Muramatsu M, Hamada H. Hybrid cell extinction and re-expression of Oct-3 function correlates with differentiation potential. *EMBO J*. 1993 Dec;12(12):4489-98.
- Shirahata S, Katakura Y, Teruya K. Cell hybridization, hybridomas, and human hybridomas. *Methods Cell Biol*. 1998;57:111-45.
- Siegel S and Castellan NJ. *Nonparametric Statistics for the Behavioural Sciences* (2nd edn), McGraw-Hill, New York, 1988. pp. 177-178
- Singh P (2000) Roslin Institute Edinburgh Annual Report 1998-1999 p. 53.
- Siroky J, Cervenka J. Hybridization frequencies of different mammalian cell types by electrofusion. *Gen Physiol Biophys*. 1990 Oct;9(5):489-99.
- Sirotkin AM, Edelmann W, Cheng G, Klein-Szanto A, Kucherlapati R, Skoultchi AI. Mice develop normally without the H1(0) linker histone. *Proc Natl Acad Sci U S A*. 1995 Jul 3;92(14):6434-8.
- Smith AG. Embryo-derived stem cells: of mice and men. *Annu Rev Cell Dev Biol*. 2001;17:435-62.
- Smith AG. Cell therapy: in search of pluripotency. *Curr Biol*. 1998 Nov 5;8(22):R802-4. Review.



Smith AG, Hooper ML. Buffalo rat liver cells produce a diffusible activity which inhibits the differentiation of murine embryonal carcinoma and embryonic stem cells. *Dev Biol*. 1987 May;121(1):1-9.

Smith-Arica JR, Thomson AJ, Ansell R, Chiorini J, Davidson B, McWhir J. Infection efficiency of human and mouse embryonic stem cells using adenoviral and adeno-associated viral vectors. *Cloning Stem Cells*. 2003;5(1):51-62.

Sorger PK. Heat shock factor and the heat shock response. *Cell*. 1991 May 3;65(3):363-6.

Sowers AE. A long-lived fusogenic state is induced in erythrocyte ghosts by electric pulses. *J Cell Biol*. 1986 Apr;102(4):1358-62. Sowers AE (1986) *J Cell Biol* 102:1358

Solter D. Differential imprinting and expression of maternal and paternal genomes. *Annu Rev Genet*. 1988;22:127-46. Review.

Sorger PK. Heat shock factor and the heat shock response. *Cell*. 1991 May 3;65(3):363-6. Review.

Sowers AE. (1986) A long-lived fusogenic state is induced in erythrocyte ghosts by electric pulses. *J Cell Biol*. 102(4):1358-62.

Spemann H (1938) *Embryonic Development and Induction*. (Hafner Publishing Company, New York.).

Stanbridge EJ. Genetic analysis of human malignancy using somatic cell hybrids and monochromosome transfer. *Cancer Surv*. 1988;7(2):317-24.

Steffler C. Aspects of biochemical effects by hyperthermia. *Natl Cancer Inst Monogr*. 1982 Jun;61:11-7.

Strickland S, Mahdavi V. The induction of differentiation in teratocarcinoma stem cells by retinoic acid. *Cell*. 1978 Oct; 15(2): 393-403.

Strickland S, Smith, KK, Marotti KR. Hormonal induction of differentiation in teratocarcinoma stem cells: generation of parietal endoderm by retinoic acid and dibutyryl cAMP. *Cell*. 1980 Sep; 21, 347-355.

Stein A, Whitlock JP Jr, Bina M. Acidic polypeptides can assemble both histones and chromatin in vitro at physiological ionic strength. *Proc Natl Acad Sci U S A*. 1979 Oct;76(10):5000-4.

Sternberg N. Demonstration and analysis of P1 site-specific recombination using lambda-P1 hybrid phages constructed in vitro. *Cold Spring Harb Symp Quant Biol*. 1979;43 Pt 2:1143-6.

Sternberg N, Sauer B, Hoess R, Abremski K. Bacteriophage P1 cre gene and its regulatory region. Evidence for multiple promoters and for regulation by DNA methylation. *J Mol Biol.* 1986 Jan 20;187(2):197-212.

Stewart TA, Mintz B. Successive generations of mice produced from an established culture line of euploid teratocarcinoma cells. *Proc Natl Acad Sci U S A.* 1981 Oct;78(10):6314-8.

Streffer C. (1982) Aspects of biochemical effects by hyperthermia. *Natl Cancer Inst Monogr.* 61:11-7.

Surani MA. Reprogramming a somatic nucleus by trans-modification activity in germ cells. *Semin Cell Dev Biol.* 1999 Jun;10(3):273-7. Review.

Surani MA. Reprogramming of genome function through epigenetic inheritance. *Nature.* 2001 Nov 1; 414(6859): 122-8. Review.

Surani MA, Barton SC, Norris ML. Nuclear transplantation in the mouse: heritable differences between parental genomes after activation of the embryonic genome. *Cell.* 1986 Apr 11;45(1):127-36.

Sun FL, Dean WL, Kelsey G, Allen ND, Reik W. Transactivation of *Igf2* in a mouse model of Beckwith-Wiedemann syndrome. (1997) *Nature.* 389(6653):809-15.

Szebeni, A., Hingorani, K., Negi, S. and Olson, M.O. Role of protein kinase CK2 phosphorylation in the molecular chaperone activity of nucleolar protein b23. *J. Biol. Chem.* 278 (11), 9107-9115 (2003).

Tada M, Morizane A, Kimura H, Kawasaki H, Ainscough JF, Sasai Y, Nakatsuji N, Tada T. Pluripotency of reprogrammed somatic genomes in embryonic stem hybrid cells. *Dev Dyn.* 2003 Aug;227(4):504-10.

Tada T, Tada M. (2001) Toti-/pluripotential stem cells and epigenetic modifications. *Cell Struct Funct.* 26(3):149-60.

Tada M, Tada T, Lefebvre L, Barton SC, Surani MA. Embryonic germ cells induce epigenetic reprogramming of somatic nucleus in hybrid cells. *EMBO J.* 1997 Nov 3;16(21):6510-20.

Tada T, Takagi N. Early development and X-chromosome inactivation in mouse parthenogenetic embryos. *Mol Reprod Dev.* 1992 Jan;31(1):20-7.

Tada M, Takahama Y, Abe K, Nakatsuji N, Tada T. Nuclear reprogramming of somatic cells by in vitro hybridization with ES cells. *Curr Biol.* 2001; 11(19):1553-8.

Takagi N, Oshimura M. Fluorescence and Giemsa banding studies of the allocyclic X chromosome in embryonic and adult mouse cells. *Exp Cell Res.* 1973 Mar 30;78(1):127-35.

Takagi N, Yoshida MA, Sugawara O, Sasaki M. Reversal of X-inactivation in female mouse somatic cells hybridized with murine teratocarcinoma stem cells in vitro. *Cell.* 1983 Oct;34(3):1053-62.

Takeda K, Takahashi S, Onishi A, Goto Y, Miyazawa A, Imai H (1999) Dominant distribution of mitochondrial DNA from recipient oocytes in bovine embryos and offspring after nuclear transfer. *J Reprod Fertil* 116:253

Tani T, Kato Y, Tsunoda Y. Reprogramming of Bovine Somatic Cell Nuclei Is not Directly Regulated by Maturation Promoting Factor or Mitogen-Activated Protein Kinase Activity. *Biol Reprod.* 2003 Aug 6 [Epub ahead of print].

Teisse J, Rols MP. Fusion of mammalian cells in culture is obtained by creating the contact between cells after their electroporation. *Biochem Biophys Res Commun.* 1986; 140:258

Terada N, Hamazaki T, Oka M, Hoki M, Mastalerz DM, Nakano Y, Meyer EM, Morel L, Petersen BE, Scott EW. Bone marrow cells adopt the phenotype of other cells by spontaneous cell fusion. *Nature.* 2002; 416:542-5.

Tersaril J, Nagy ZP, Mendoza C, Greco E. Chemically and mechanically induced membrane fusion: non-activating methods for nuclear transfer in mature human oocytes. *Hum Reprod.* 2000; 15:1149

Thaete LG, Ahnen DJ, Malkinson AM. Proliferating cell nuclear antigen (PCNA/cyclin) immunocytochemistry as a labeling index in mouse lung tissues. *Cell Tissue Res;* 1989 Apr;256(1):167-73

Theise ND, Nimmakayalu M, Gardner R, Illei PB, Morgan G, Teperman L, Henegariu O, Krause DS. Liver from bone marrow in humans. *Hepatology.* 2000 Jul;32(1):11-6.

Thomson JA, Itskovitz-Eldor J, Shapiro SS, Waknitz MA, Swiergiel JJ, Marshall VS, Jones JM. 1998 Embryonic stem cell lines derived from human blastocysts. *Science.* Nov 6;282(5391):1145-7.

Thyagarajan B, Guimaraes MJ, Groth AC, Calos MP. (2000) Mammalian genomes contain active recombinase recognition sites. *Gene.* 244(1-2):47-54.

Tian XC, Xu J, Yang X. Normal telomere lengths found in cloned cattle. *Nat Genet.* 2000 Nov;26(3):272-3.

Tilghman SM. The sins of the fathers and mothers: genomic imprinting in mammalian development. *Cell.* 1999 Jan 22;96(2):185-93. Review.

Tsunoda Y, Kato Y. Nuclear transplantation of embryonic stem cells in mice. *J Reprod Fertil.* 1993 Jul;98(2):537-40.

Tsunoda Y, Yasui T, Shioda Y, Nakamura K, Uchida T, Sugie T. Full-term development of mouse blastomere nuclei transplanted into enucleated two-cell embryos. *J Exp Zool.* 1987 May;242(2):147-51.

Turner BM. Cellular memory and the histone code. *Cell.* 2002 Nov 1;111(3):285-91.

Turner BM. Histone acetylation and an epigenetic code. *Bioessays.* 2000 Sep;22(9):836-4.

Ungewickell E. The 70-kd mammalian heat shock proteins are structurally and functionally related to the uncoating protein that releases clathrin triskelia from coated vesicles. *EMBO J.* 1985 Dec 16;4(13A):3385-91.

Vaziri H, Dragowska W, Allsopp RC, Thomas TE, Harley CB, Lansdorp PM. Evidence for a mitotic clock in human hematopoietic stem cells: loss of telomeric DNA with age. *Proc Natl Acad Sci U S A.* 1994 Oct 11;91(21):9857-60.

Varmuza S, Mann M. Genomic imprinting--defusing the ovarian time bomb. *Trends Genet.* 1994 Apr;10(4):118-23.

Vienken J, Zimmermann U. Electric field-induced fusion: electro-hydraulic procedure for production of heterokaryon cells in high yield. *FEBS Lett.* 1982 Jan 11;137(1):11-3.

Wade PA, Kikyo N. Chromatin remodeling in nuclear cloning. *Eur J Biochem.* 2002 May;269(9):2284-7.

Wakayama T, Perry AC, Zuccotti M, Johnson KR, Yanagimachi R. Full-term development of mice from enucleated oocytes injected with cumulus cell nuclei. *Nature.* 1998 Jul 23;394(6691):369-74.

Walsh D, Li K, Crowther C, Marsh D, Edwards M. Thermotolerance and heat shock response during early development of the mammalian embryo. *Results Probl Cell Differ.* 1991;17:58-70.

Wang ZQ, Fung MR, Barlow DP, Wagner EF. Regulation of embryonic growth and lysosomal targeting by the imprinted *Igf2/Mpr* gene. *Nature.* 1994 Dec 1;372(6505):464-7.

Wang ZF, Sirotkin AM, Buchold GM, Skoultschi AI, Marzluff WF. The mouse histone H1 genes: gene organization and differential regulation. *J Mol Biol.* 1997 Aug 8;271(1):124-38.

Wangh LJ, DeGrace D, Sanchez JA, Gold A, Yeghiazarians Y, Wiedemann K, Daniels S. Efficient reactivation of *Xenopus* erythrocyte nuclei in *Xenopus* egg extracts. *J Cell Sci.* 1995 Jun;108 ( Pt 6):2187-96.

Watanabe M, Suzuki K, Kodama S, Sugahara T. Normal human cells at confluence get heat resistance by efficient accumulation of hsp72 in nucleus. *Carcinogenesis.* 1995 Oct;16(10):2373-80.

Weismann A. *The Germ-Plasm: A Theory of Heredity* Walter Scott Ltd., London. 1893

Weiss MC, Chaplain M. Expression of differentiated functions in hepatoma cell hybrids: reappearance of tyrosine aminotransferase inducibility after the loss of chromosomes. *Proc Natl Acad Sci U S A.* 1971 Dec;68(12):3026-30.

Weiss A, Keshet I, Razin A, Cedar H. DNA demethylation in vitro: involvement of RNA. *Cell.* 1996 86(5):709-18.

Wells DN. Factors affecting murine ES cell isolation. PhD Thesis. University of Edinburgh.

Williams RL, Hilton DJ, Pease S, Willson TA, Stewart CL, Gearing DP, Wagner EF, Metcalf D, Nicola NA, Gough NM. Myeloid leukaemia inhibitory factor maintains the developmental potential of embryonic stem cells. *Nature.* 1988 Dec 15;336(6200):684-7.

Wilmut I, Schnieke AE, McWhir J, Kind AJ, Campbell KH. Viable offspring derived from fetal and adult mammalian cells. *Nature.* 1997 Feb 27;385(6619):810-3.

Wilmut I, Campbell KH. Quiescence in nuclear transfer. *Science.* 1998 Sep 11;281(5383):1611.

Wilson CJ, Chao DM, Imbalzano AN, Schnitzler GR, Kingston RE, Young RA. (1996) RNA polymerase II holoenzyme contains SWI/SNF regulators involved in chromatin remodeling. *Cell.* 84(2):235-44.

Winston F, Allis CD. The bromodomain: a chromatin-targeting module? *Nat Struct Biol.* 1999 Jul;6(7):601-4.

Wolffe AP. Chromatin and gene regulation at the onset of embryonic development. *Reprod Nutr Dev.* 1996 36(6):581-606.

Wolffe AP, Matzke MA. Epigenetics: regulation through repression. *Science.* 1999 Oct 15;286(5439):481-6.

Woods GL, White KL, Vanderwall DK, Li GP, Aston KI, Bunch TD, Meerdo LN, Pate BJ. A mule cloned from fetal cells by nuclear transfer. *Science.* 2003 Aug 22;301(5636):1063.

Wrenzycki C, Lucas-Hahn A, Herrmann D, Lemme E, Korsawe K, Niemann H. In vitro production and nuclear transfer affect dosage compensation of the X-linked gene transcripts G6PD, PGK, and Xist in preimplantation bovine embryos. *Biol Reprod.* 2002 Jan;66(1):127-34.

Wright WE, Brasiskyte D, Piatyszek MA, Shay JW Experimental elongation of telomeres extends the lifespan of immortal x normal cell hybrids. *EMBO J* 1996 15:1734.

Wutz A, Smrzka OW, Schweifer N, Schellander K, Wagner EF, Barlow DP. Imprinted expression of the *Igf2r* gene depends on an intronic CpG island. *Nature.* 1997 Oct 16;389(6652):745-9.

Xu C, Inokuma MS, Denham J, Golds K, Kundu P, Gold JD, Carpenter MK. (2001) Feeder-free growth of undifferentiated human embryonic stem cells. *Nat Biotechnol* 19(10):971-4.

Xue F, Tian XC, Du F, Kubota C, Taneja M, Dinnyes A, Dai Y, Levine H, Pereira LV, Yang X. Aberrant patterns of X chromosome inactivation in bovine clones. *Nat Genet.* 2002 Jun;31(2):216-20.

Yanagimachi R. Cloning: experience from the mouse and other animals. *Mol Cell Endocrinol.* 2002 Feb 22;187(1-2):241-8. Review.

Yeom YI, Ha HS, Balling R, Schöler HR, Artzt K. Structure, expression and chromosomal location of the Oct-4 gene. *Mech Dev.* 1991 Nov;35(3):171-9.

Yeom YI, Fuhrmann G, Ovitt CE, Brehm A, Ohbo K, Gross M, Hubner K, Scholer HR. Germline regulatory element of Oct-4 specific for the totipotent cycle of embryonal cells. *Development.* 1996 Mar;122(3):881-94.

Ying QL, Nichols J, Evans EP, Smith AG. Changing potency by spontaneous fusion. *Nature.* 2002; 416(6880):545-8.

Young LE, Fernandes K, McEvoy TG, Butterwith SC, Gutierrez CG, Carolan C, Broadbent PJ, Robinson JJ, Wilmut I, Sinclair KD. Epigenetic change in *IGF2R* is associated with fetal overgrowth after sheep embryo culture. *Nat Genet.* 2001 Feb;27(2):153-4.

Zheng C, Hayes JJ. Structures and interactions of the core histone tail domains. *Biopolymers.* 2003 Apr;68(4):539-46.

Zhou Q, Jouneau A, Brochard V, Adenot P, Renard JP. Developmental potential of mouse embryos reconstructed from metaphase embryonic stem cell nuclei. *Biol Reprod.* 2001 Aug;65(2):412-9.



Zimmermann U, Pilwat G, Riemann F. Preparation of erythrocyte ghosts by dielectric breakdown of the cell membrane. *Biochim Biophys Acta*. 1975 Jan 28;375(2):209-19.

Zlatanova J, Leuba SH. Chromatin fibers, one-at-a-time. *J Mol Biol*. 2003 Aug 1;331(1):1-19.

Zwaka TP, Thomson JA. *Nat Biotechnol*. 2003 Mar;21(3):319-21. Homologous recombination in human embryonic stem cells.

## [12] Appendices

### [12.1] MEDIA AND STOCK SOLUTIONS

#### [12.1.1] TISSUE CULTURE STOCK SOLUTIONS

**PBS:** 8g NaCl, 0.2g KCl, 1.44g Na<sub>2</sub>HPO<sub>4</sub> and 0.24g KH<sub>2</sub>PO<sub>4</sub> were dissolved in 800ml distilled H<sub>2</sub>O. The pH was adjusted to 7.4 with HCl and the volume was made up to 1L with H<sub>2</sub>O.

**10x HBS:** was made up by dissolving 16g NaCl, 0.74g KCl, 0.252g Na<sub>2</sub>HPO<sub>4</sub>.2H<sub>2</sub>O, 2.0g Dextrose, and 10g HEPES in 180ml sterile double distilled water, and adjusting pH to 7.2 before making the volume up to 200ml.

**10x TBS:** 1.5M NaCl in 0.1M Tris buffer (pH 7.5).

**TEG:** 92.7mM NaCl, 0.845mM Na<sub>2</sub>HPO<sub>4</sub>, 1.58mM KH<sub>2</sub>PO<sub>4</sub>, 4.46mM KCl, 5mM D-glucose, 22.28mM Tris, 0.0009% phenol red, 0.25% trypsin, 1.05mM EGTA and 0.000105% polyvinyl alcohol. The pH was then adjusted to 7.6 and made up to final volume with distilled water after all the components were dissolved.

#### [12.1.2] ROUTINE CULTURE MEDIA

**Murine ES medium:** GMEM [2mM L-glutamine freshly added to 'GMEM w/o L-glutamine' (Life Technologies)] was supplemented with 5% FCS, 5% NBCS, 50µM β-mercaptoethanol, 0.1mM mM sodium pyruvate, 1% non-essential amino acids (Life Technologies), 400-1,000U/ml recombinant murine Leukaemia Inhibitory Factor (ESGRO-LIF, Life Technologies).

**Human ES medium:** 20% SR Serum Replacement (Life Technologies), 1% non-essential amino acids, 1mM L-glutamine, 0.1mM β-mercaptoethanol, 4ng/ml human

recombinant basic fibroblast growth factor (Life Technologies) in Knockout Dulbecco's modified Eagle's medium (KO DMEM, GIBCO/BRL-Life Technologies).

**Complete PEF medium:** 5% FCS, 5% NBCS, 2mM L-glutamine, and 1% NEAA in DMEM.

**Serum starvation PEF medium:** 0.5% FCS, 2mM L-glutamine, and 1% NEAA in DMEM.

**Murine embryoid body medium:** 10% NBCS, 0.1mM mM sodium pyruvate in GMEM (1mM L-glutamate freshly added to 'GMEM w/o glutamine').

**Murine cardiogenesis differentiation medium:** 20% FCS, 1% NEAA, 2mM L-glutamate, 50 $\mu$ M  $\beta$ -mercaptoethanol in DMEM.

**Murine myogenesis differentiation medium:** 15% DCC FCS, 1% NEAA, 2mM L-glutamate, 50 $\mu$ M  $\beta$ -mercaptoethanol, 10 $\mu$ g/ml human transferrin, 7.5% BSA in DMEM.

**Murine neurogenesis differentiation medium:** 20% FCS, 1% NEAA, 2mM L-glutamate, 50 $\mu$ M  $\beta$ -mercaptoethanol, 10 $\mu$ g/ml human transferrin, 7.5% BSA, 0.1nM RA in DMEM.

### [12.1.3] KARYOTYPING

**2x SSC:** 300mM NaCl, 30mM sodium citrate pH 7.2. This was dispensed into aliquots before autoclaving in a glass Coplin staining jar.

#### [12.1.4] GENOMIC DNA EXTRACTION

**Lysis buffer:** Lysis buffer was prepared by mixing 100mM Tris HCl pH 8.5 (50 ml from 1M Tris pH 8.5 stock), 5mM EDTA pH 8.4 (5ml from 0.5M EDTA stock) and 200mM NaCl (33.3ml from 3M NaCl stock), for a total volume of 490ml in distilled water. This solution was autoclaved and then supplemented with 10 ml of 10 % SDS (final concentration 0.2 %) and proteinase K (100µg / ml) just before use.

#### [12.1.5] EXTRACTION OF PLASMID DNA FROM BACTERIA

**Low salt LB medium for zeomycin selection:** 10g tryptone, 5g yeast extract, 5g NaCl was mixed in 1 litre of deionised, distilled water. The pH was adjusted to 7.5 with 1M NaOH to prevent zeomycin being inactivated at higher salt concentrations. The medium was autoclaved and allowed to cool before the drug (25µg / ml final concentration) was added.

#### [12.1.6] DNA PURIFICATION

**TE buffer:** 10 mM Tris-HCl, 1 mM EDTA pH to 8.

#### [12.1.7] RNA PURIFICATION

**10x running buffer:** (RB) 4.18 g MOPS (200 mM), 0.372g EDTA (10 mM) and 0.410g sodium acetate (50 mM) in 100 ml of DEPC-treated distilled water. pH was adjusted to 7.0 with 5M NaOH. Formaldehyde agarose gels (0.8-1.2%) were prepared by melting the appropriate amount of agarose in 10ml RB (1x), 72.1ml DEPC-water and 17.9 ml of 38% formaldehyde.

**0.2% DEPC:** 2ml DEPC per litre.

### [12.1.8] WESTERN BLOTTING

**2x SDS loading buffer:** 100mM Tris pH6.8, 200mM DTT, 4%SDS, 0.2% Bromophenol blue, 20% glycerol. The solution was made without DTT and kept at RT. DTT was added to the stock before use.

**10x Tris-Glycine Running Buffer:** 30.2g Tris base, 188g glycine, 50ml 20% SDS were weighed out and made up to 1 litre with dH<sub>2</sub>O.

**10x Western Transfer buffer:** 60g Tris base and 288g glycine were added to 500ml H<sub>2</sub>O and the pH was adjusted to 8.3 with concHCl. This was then made up to 2 litres with more water. 20% methanol was added to this 1x Running Buffer prior to use.

**Blocking solution:** 5% marvel powered milk, 1% BSA, 1% FCS in PBS.

**Wash solution:** 0.1% Tween 20, 1% FCS in PBS.

**4% paraformaldehyde:** 4% paraformaldehyde in PBS. The solution was heated and stirred until the solution had gone clear and was left to cool before use.

### [12.1.9] IMMUNOSTAINING FOR FACS ANALYSIS

**Staining buffer:** 10ml Foetal Calf Serum, 0.3722g EDTA Sigma E-5134 in 490ml PBS. The solution can be stored for up to two months at 4°C.

**Blocking buffer:** 6ml staining buffer and 4ml heat inactivated rabbit serum (Jackson immunosystems) are mixed and stored at 4°C for up to 2 months.

### [12.1.10] PROPIDIUM IODIDE STAINING

**Propidium Iodide (PI) Stock Solution:** 1x PBS was supplemented with 0.1% (w/v)  $\text{NaN}_3$  and filtered using a  $0.22\mu\text{m}$  filter. PI powder (P4170 Sigma) was dissolved in this solution to a final concentration of 1mg / ml. 1 ml aliquots of this solution were wrapped in tin foil and stored at  $-20^\circ\text{C}$ .

**RNase A Stock Solution:** Ribonuclease A (R5000 Sigma) was diluted to a final concentration of 1 mg/ml with  $0.22\mu\text{m}$  filtered 1xPBS. 1ml aliquots of this solution were stored at  $-20^\circ\text{C}$ .

### [12.1.11] FISH ANALYSIS

**20x SSC:** 80.6g NaCl and 44.1g Na Citrate were dissolved in 500ml distilled  $\text{H}_2\text{O}$  and the pH was adjusted to 7.4 with concentrated HCl. This stock solution was autoclaved and stored at  $4^\circ\text{C}$ .

**1x SSC:** 25ml 20x SSC stock solution was added to 475ml  $\text{dH}_2\text{O}$  and mixed well.

**2x SSC:** 50ml 20x SSC stock solution was added to 450 ml  $\text{dH}_2\text{O}$  and mixed well.

**Denaturation Solution:** 70 ml deionised formamide was added to 30ml 2x SSC and mixed well.

**Stringency Wash Solution:** 50ml deionised formamide was added to 50ml 1x SSC and mixed well.

**Detergent Wash Solution:** 125ml 20 x SSC and 250 ml Tween-20 was added to 125ml  $\text{dH}_2\text{O}$ .



**[12.1.12] *LacZ* STAINING**

**Fixing solution:** 1x PBS with 0.5% glutaraldehyde

**Washing solution:** 1mM MgCl<sub>2</sub> in 1xPBS

**Staining solution:** 250µl 20mM K<sub>4</sub>Fe(CN)<sub>6</sub>.3H<sub>2</sub>O/PBS, 250µl 20mM K<sub>3</sub>Fe(CN)<sub>6</sub>/1x PBS, 1µl 1M MgCl<sub>2</sub> and 50µl 2% X-gal in dimethylformamide (DMF) made up to 1 ml with 1xPBS.

## [12.2] OPTIMISING INSTRUMENT ELECTRONICS FOR FACS ANALYSIS

Full details of optimising instrument settings for FACS analysis is given in DB Biosciences Software Users Guide Chapter 4. A brief summary is presented here to help readers unfamiliar with FACS analysis understand how the graphs and histograms in the text were generated.

### ADJUSTMENT OF FORWARD SCATTER (FSC) AND SIDE SCATTER (SSC) SETTINGS

First the FSC Amp gain, SSC Voltage were adjusted so the scatter properties of the sample are clearly displayed. In any cell sample there will be two populations: living cells will be seen as large grouping of cells with a varied cell size and complexity. Dead cells will be a smaller less complex population. This is done by adjusting the FSC AMP gain and SSC voltage settings.

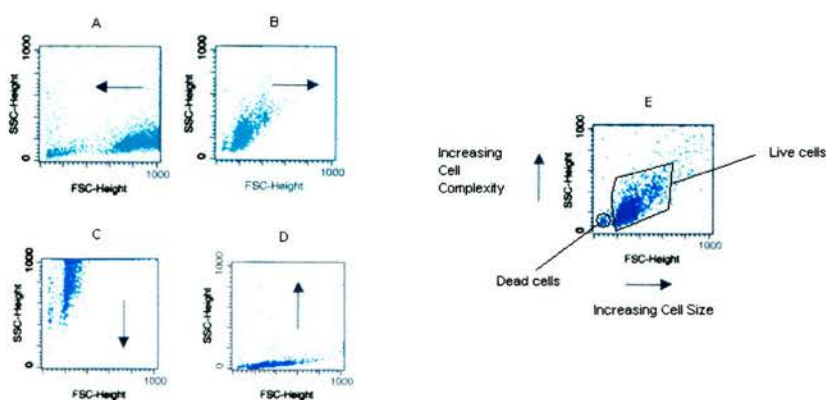


**Fig 12.1 Forward Scatter (FSC) Amp gain, Side Scatter (SSC) Voltage adjustment allows gating of live cells from dead cells**

In **A**, the FSC AMP gain is set too high, in **B** it is set too low. Decreasing the AMP gain moves the cells to the right and increasing it moves it to the left. In **C** SSC voltage is set to low and in **D** it is set too high. Decreasing the SSC voltage is too high and in **D** it is too low. Decreasing the SSC voltage moves the cells down and increasing them up. **E** shows a properly adjusted FSC/SSC plot.

## ADJUSTMENT OF FLUORESCENCE DETECTORS

In order to insure that the FACS machine can register fluorescent cells, its important that the fluorescence peaks of non-fluorescent controls lie just above the minimum fluorescent limit that the FACS machine registers. This is done by adjusting the voltage setting for fluorescent channels.

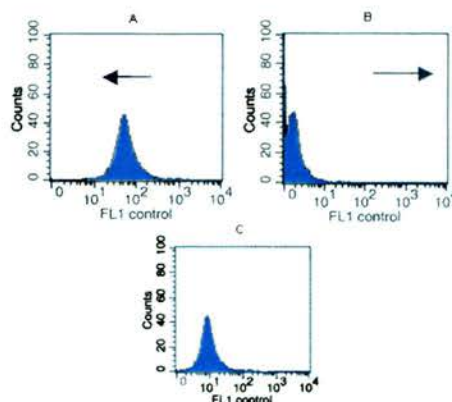


**Fig 12.2 Forward Scatter (FSC) adjustment of the fluorescence detectors**

A shows FL1 voltage set too high, and B shows it too low. Decreasing FL1 voltage will move the peak to the left and increasing it will move the peak to the right. C shows a properly adjusted histogram for negatively control cells. The FACS machine will be able to register cells up to a 1000 times greater than the negatively controlled cells while still registering unstained cells.

## ADJUSTING FLUORESCENCE COMPENSATION

Compensation are used to adjust for spectral overlap. For 2-dye FACS analysis, mixtures of stained but unpulsed cells were used to insure that CMTMR stained cells were misidentified as CMFDA stained cells. The FL1-%FL2 setting was increased until both populations of stained cells were clearly distinct from each other and in each fluorescence spectrum peaks were distinct from each other. If the cells are not properly compensated, CMFDA cells can be misidentified as CMTMR cells due to spectral overlap. If cells are properly compensated, mixtures of stained cells

appear as two distinct cell populations on FL1/FL2 histograms (See Fig 12.3).

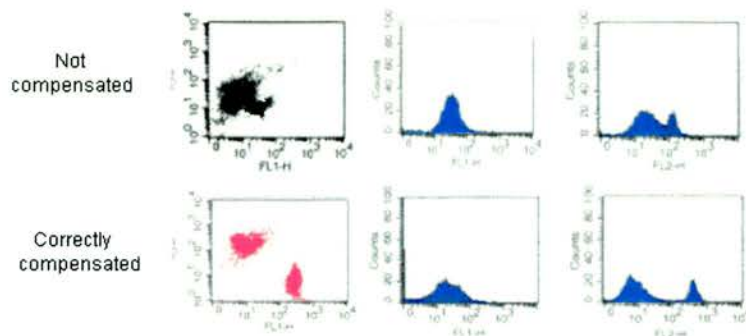


**Fig 12.3 Compensation prevents spectral overlap, allowing CMTMR stained to be distinguished from CMFDA stained cells**

### [12.3] CLONING STRATEGIES USED FOR PLASMID CONSTRUCTION

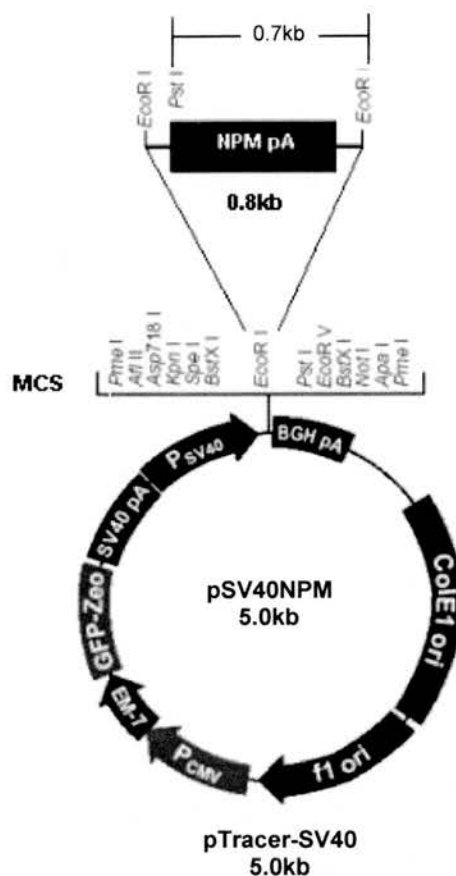
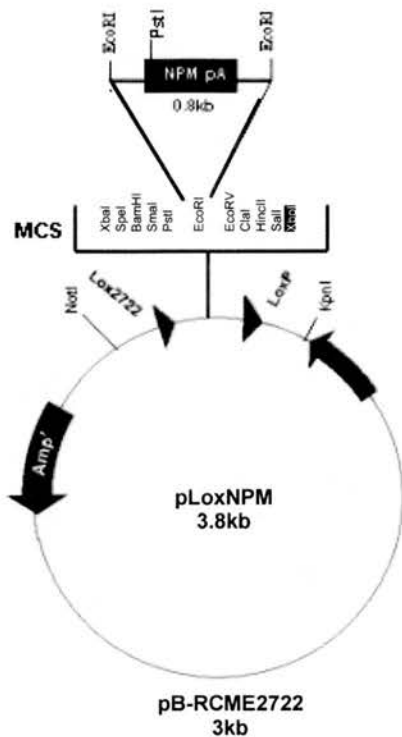


**Fig 12.4 Construction of pSV40NPM**

The expression vector pSV40NPM was generated by the following series of steps using standard recombinant DNA techniques [Subsection 2.5.5]. A 0.8kb *EcoR*I fragment, containing the complete nucleoplasmin coding sequence, was excised from pUCNPM and cloned into the *EcoR*I site in the multiple cloning site (MCS) of pTracerSV40 (Invitrogen). pUCNPM was a gift from Prof. Ron Laskey, Cambridge. Correct orientation of the insert was confirmed by *Pst*I. Descriptions of pUCNPM and pTracerSV40 are given in Subsection [2.3.5].

A



B

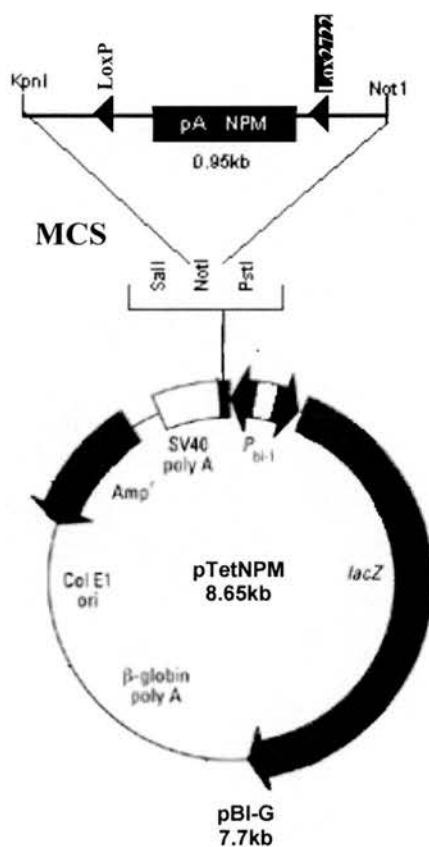


**Fig 12.5 Construction of plasmid pTetNPM**

The expression vector pTetNPM was generated by the following series of steps using standard recombinant DNA techniques [Section 2.5.5]. *Panel A* A 0.8kb fragment



was removed from pUCNPM using an *EcoRI* digest and inserted into the *EcoRI* site within the multiple cloning site of pB-RCME2722 generating plasmid pLoxNPM. pUCNPM and pB-RCME2722 were gifts from Prof. Ron Laskey and Dr. Andreas Kolb respectively. Correct orientation of the insert was confirmed by *PstI*. **Panel B** pLoxNPM was then linearised with *KpnI*. This linearised DNA fragment was then blunted with Klenow fragment. This linear DNA was then digested with *NotI*. The 0.95kb band was extracted and cloned into the *NotI* site within the multiple cloning site of pBI-G (Clontech). The 8.65kb fragment then blunted with Klenow fragment and ligated to generate pTetNPM. Descriptions of pUCNPM, pB-RCME2772 and pBI-G are given in **Subsection [2.3.5]**.

#### [12.4] ANTIBODIES

IgG3 *Sigma Cat No 3645 (1:100)*

IgM *Sigma Cat No M3759 (1:100)*

SSEA1 *Development Studies Hybridoma Bank (DSHB) Cat No MC-480 (1:100)*

SSEA4 *(DSHB) Cat No MC-813-70 (1:100)*

FITC conjugated hyaluronan binding protein *(DSHB) Cat No 12/21/1-C-6 (1:100)*

FITC conjugated CD90 *(sc-18914 FITC Santa Cruz) (1:100)*

FITC conjugated control rat immunoglobulin *(sc-2340 Santa Cruz) (1:250)*

Ectoderm Monoclonal anti-beta-tubulin isotype III-HPR *(Sigma Cat No T8660) (1:100)*

Mesoderm Monoclonal anti-troponin T *cardiac isoform (Research Diagnostics Cat No RDI-4T19) (1:100)*

Goat anti mouse IgG3-FITC *(Southern Biotechnologies Cat No 1022-02) (1:500)*

Goat anti mouse IgM-PE *(Southern Biotechnologies Cat No 1022-09) (1:500)*